Western Australian School of Mines - Minerals, Energy and Chemical Engineering

Corrosion Inhibition of Deposited Steels in the Presence of Bacteria

Erika M. Suarez-Rodriguez

This thesis is presented for the Degree of Doctor of Philosophy of Curtin University

November 2019

Declaration

To the best of my knowledge and belief, this thesis contains no material previously published by any another person except where due acknowledgment has been made.

This thesis contains no material which has been accepted for the award of any other degree or diploma in any university.

Signature: …………………………………………

Date: …………………………………………

Abstract

The concomitant presence of deposits and microorganisms at internal pipeline surfaces has been the cause of many operation corrosion failures in the oil and gas industry. This complex phenomenon defined as under-deposit microbial corrosion (UDMC) refers to a combination of electrochemical, physical and microbiological processes compromising pipeline integrity. However, to date, this combination of investigation fields is limited in the published literature. In this research project, complex corrosion phenomena such as microbiologically influenced corrosion (MIC), under-deposit corrosion (UDC) and corrosion inhibition under these scenarios have been investigated.

Phase I of this project focused on the identification and integration of existing methods and approaches to study UDC and MIC. The integration of these corrosion phenomena or under-deposit microbial corrosion (UDMC) led to the selection of two setups for conducting experiments in the consequent phases.

Phase II comprised the evaluation of corrosion inhibitors in the presence of different types of mineral deposits in a CO_2-saturated brine. Two film-forming corrosion inhibitors, a surfactant molecule, 1-dodecylpyridinium chloride hydrate (DPC) and a smaller, non-surfactant molecule, 2-mercaptopyrimidine (MPY) were selected for UDC studies. Inhibitor adsorption measurements on mineral deposits (Al_2O_3, SiO_2 and $CaCO_3$) using UV spectroscopy, revealed that DPC showed minimal adsorption on all deposits, but it exhibited insufficient performance to inhibit corrosion. Conversely, MPY performed efficiently in preventing UDC with the three mineral deposits investigated despite its relatively high adsorption on $CaCO_3$. The performance of DPC and MPY inhibitors was assessed using a wire beam electrode (WBE) array and silica sand as a deposit. Characteristic small potential differences and galvanic currents between sand deposited and non-deposited steel areas were detected in the WBE distribution maps. MPY demonstrated the best performance, which was related to the molecular structure of this film-forming inhibitor. Thus, proposing that the size of this small non-surfactant molecule (4 carbon atoms) allows a better penetration capacity through the sand layers. These molecular characteristics could be used for selecting efficient corrosion inhibitors to prevent UDC.

In phase III, UDMC was investigated using both a bacterial isolate *Shewanella oneidensis* MR-1 and a microbial consortium from an Australian oilfield. Corrosion on carbon steel surfaces by *S.oneidensis* was investigated using electrochemical measurements and surface analytical methods. For this investigation, two sets of test conditions were applied: 1) artificial seawater (ASW) contained a high lactate concentration (59 mM). Steel samples in the biotic test had lower corrosion rates compared to the abiotic counterpart. This finding was related to the formation of copious biofilms and non-corrosive metabolites deposited at steel surface. Both biofilms and metabolites had a positive effect on mitigating corrosion compared to the abiotic control test; 2) Sand-deposited and sand-free samples were immersed in ASW with low concentrations of lactate (5 mM) to stimulate corrosion via direct electron transfer by the bacterium as in electrical MIC (EMIC). Results showed that sand-free samples suffered more significant corrosion than sand-deposited steel surfaces. Results confirmed a barrier-effect frequently cited in corrosion studies and exerted by artificial sand deposits in CO_2 environments. However, sand-deposited samples still suffered localised corrosion in the presence of *S.oneidensis*, which indicated that the bacterium surpassed this barrier effect to some extent. Field-emission scanning electron microscopy (FESEM) images of cross-sectioned corroded samples evidenced biofilm formation beneath and between sand grains. Additional methods and experiments are needed to complement this test methodology to study the EMIC mechanism and its connection to deposits.

The second part of phase III comprised the evaluation of localised corrosion at deposited-carbon steel surfaces in the presence of a thermophilic oilfield microbial consortium. The predominant microbial populations identified in the consortium via 16S rRNA gene sequencing corresponded to methanogenic archaea, fermenting bacteria and sulphidogenic microorganisms. The activity of this microbial consortium resulted in severe MIC and increased localised corrosion, with maximum pitting depth of 220 µm and 207 µm for sand-free and sand-deposited steel surfaces, respectively. The trend of average corrosion rates corresponded with those of localised corrosion values. Differences in the composition of the microbial community and stratification of corrosion products were found between sand-deposited and sand-free steels. In correlation with findings from the first part of this phase, this work demonstrated that microbial activity could surpass the barrier effect posed by sand deposit under abiotic

CO_2 conditions. This investigation is relevant to industrial applications, demonstrating the aggressiveness of multispecies biofilms against carbon steel.

Finally, phase IV of the project involved research on UDMC and corrosion inhibitor performance in the presence of bacteria. The research in this phase innovatively used a modified WBE system to visualise dissimilar corrosion events such as self-corrosion, galvanic effects and corrosion potentials at specific locations of the metal surface. Apart from the WBE system, the test methodology included surface analysis and microbiological monitoring. A bacterium *Enterobacter roggenkampii* recovered from deposits associated with a corrosion failure in an oil production facility caused UDMC. The bacterium led UDMC via iron oxidation coupled to nitrate reduction under anaerobic conditions, formating and precipitating iron oxides on the metal surface. Linear polarisation (LP) measurements were performed at each wire of the WBE surface to create corrosion rate distribution maps. This information, combined with surface analysis, allowed to visualise localised corrosion initiation and evolution in the presence of microorganisms.

The corrosion inhibitor, 2-mercaptopyrimidine (MPY), was found to be ineffective at preventing localised corrosion by the bacterium. The results indicated that microbial activity caused damage to the inhibitor film on the steel surface, and consequent UDMC took place on the affected areas. These findings provided insights into the potential of microorganisms to compromise corrosion inhibitor efficiency in steel pipelines, highlighting the importance of incorporating a microbial component when assessing corrosion inhibitor performance. In the present research, the developed test methodology, comprising a multidisciplinary scientific approach, contributed to the understanding of UDMC and its mitigation. This information is of considerable significance for extending the life of carbon steel equipment and pipelines in the oil and gas industry.

Acknowledgements

Publications

This thesis is assembled by peer-reviewed journal publications, either published, accepted, submitted or in preparation which forms the individual chapters listed below:

Chapter II:

E.M. Suarez, L.L. Machuca, K. Lepková, The Role of Bacteria in Under-deposit Corrosion in Oil and Gas Facilities: A Review of Mechanisms, Test Methods and Corrosion Inhibition, Corrosion and Materials, 44 (2019) 80-87.

Chapter III:

E.M. Suarez, L.L. Machuca, B. Kinsella, K. Lepková, CO_2 Corrosion Inhibitors Performance at Deposited-Carbon Steel and Their Adsorption on Different Deposits, Corrosion Journal, 75, 9 (2019) 1118-1127.

Chapter IV:

E.M. Suarez, L.L. Machuca, M.Y. Tan, B. Kinsella, M. Forsyth, K. Lepková, Molecular Characteristics Affecting the Efficiency of Corrosion Inhibitors at Sand-Deposit Carbon Steel: A New Approach Using a Multi-Electrode Array. Manuscript submitted.

Chapter V:

E.M. Suarez, K. Lepková, L.L. Machuca, Evaluating Under-Deposit Microbial Corrosion Using a Bacterial Isolate, *Shewanella oneidensis* MR-1. Manuscript version to be submitted.

Chapter VI:

E.M. Suarez, K. Lepková, B. Kinsella, L.L. Machuca, Aggressive Corrosion of Steel by a Thermophilic Microbial Consortium in the Presence and Absence of Sand, International Biodeterioration & Biodegradation, 137 (2019) 137-146.

Chapter VII:

E.M. Suarez, K. Lepková, M. Forsyth, M.Y. Tan, B. Kinsella, L.L. Machuca, *In situ* Investigation of Under-Deposit Microbial Corrosion and Its Inhibition Using a Multi-Electrode Array. Manuscript submitted.

I warrant that I have obtained, where necessary, permission from the copyright owners to use any third-party copyright material reproduced in the thesis or to use any of my own published work in which the copyright is held by another party.

Statement of Contribution of Others

I, Erika M. Suarez-Rodriguez, as the first author of the publications comprising this thesis was primarily involved in planning, conducting the experiments, data analysis, interpretation and manuscript preparation. Contributions by the co-authors are mentioned below, and the written statements from the co-authors are included in Appendix 5.

Dr Kateřina Lepková significantly contributed supervising the progress of the project, design of all experiments, data interpretation related to under-deposit corrosion and corrosion inhibition as well as the preparation and critical review of the manuscripts.

Dr Laura L Machuca-Suarez provided fully accompaniment of the progress of the project, design of all experiments, especially the ones that involved microbiologically influenced corrosion. Dr Laura Machuca actively contributed to the preparation and revision of the manuscripts.

Prof. Brian Kinsella provided invaluable ideas for the design of experiments, actively participated in data analysis, interpretation, preparation and, critical revision of the manuscripts.

Prof. Maria Forsyth and Prof. Mike Yongjun Tan assisted with the training in the wire beam electrode (WBE) system and use of the facilities in the institute for frontiers materials (IFM) at Deakin University. They also contributed to the revision of manuscripts that involved the use of a multi-electrode array system.

The experiments were conducted at the Curtin Corrosion Centre (CCC), Western Australian School of Mines-Minerals, Energy and Chemical Engineering (WASM-MECE) of Curtin University.

Financial support for this research was provided by Curtin International Postgraduate Research Scholarship (CIPRS). The MIC cost centre through Dr Laura Machuca also provided financial support for the purchase of specialised equipment, parts and, consumables.

List of Abbreviations

UDC	Under-deposit corrosion
UDMC	Under-deposit microbial corrosion
ASW	ASW
WBE	Wire-beam electrode
MPY	2-mercaptopyrimidine
DPC	1-dodecylpiridinium chloride hydrate
S°RB	Sulphur-reducing bacteria
TRB	Thiosulphate-reducing bacteria
SRP	Sulphate-reducing prokaryotes
IOB	Iron-oxidising bacteria
IRB	Iron-reducing bacteria
MRB	Manganese-reducing bacteria
ATP	Adenosine triphosphate
OCP	Open circuit potential
LPR	Linear polarisation resistance
EIS	Electrochemical impedance spectroscopy
EFM	Electrochemical frequency modulation
EDS	Energy-dispersive X-ray spectroscopy
FESEM	Field-Emission Scanning Electron Microscopy
DNA	Deoxyribonucleic acid
RNA	Ribonucleic acid

Table of Contents

Chapter I

Introduction and overview

1.1. Literature Review

1.1.1. CO_2 Under-Deposit Corrosion (UDC)

Corrosion represents a critical engineering and economic problem that significantly impacts many sectors, including the oil and gas industry. The global cost of corrosion estimated by a NACE International study was US\$2.5 trillion in 2013. It is approximately 3.4% of the global gross domestic product (GDP) [1]. Corrosion refers to metallic degradation by interaction with a corrosive environment. Corrosive species such as carbon dioxide (CO_2), hydrogen sulphide (H_2S) and, organic acids are often produced along with oil, gas and water in the underground rock formation. These species dissolved in water can compromise inner surfaces of pipelines. Despite the advances in the development of corrosion-resistant alloys, carbon steel is still the most cost-effective pipeline material for oil and gas transmission and distribution [2]. Therefore, the industry has made significant efforts to expand the lifetime of existent carbon steel infrastructure.

CO_2 corrosion involves dissolution of iron that leads to deterioration of steel surfaces by an electrochemical oxidation process. Simultaneously, cathodic hydrogen evolution reaction provides the required electron sink for iron dissolution to progress. The hydrogen evolution reaction comprises several cathodic reactions involving the reduction of H^+, H_2CO_3, HCO_3^-, and H_2O with molecular hydrogen as their product.

The widely known electrochemical reactions related to acidic CO_2 corrosion of carbon steel corrosion are as follows [2-5]:

Cathodic reactions:
$$H^+_{(aq)} = e^- \leftrightharpoons \frac{1}{2}H_{2(g)}$$
$$H_2O_{(1)} + e^- \leftrightharpoons OH^-_{(aq)} = \frac{1}{2}H_{2(g)}$$
$$H_2CO_{3(aq)} + e^- \leftrightharpoons HCO_3^- + \frac{1}{2}H_{2(g)}$$
$$HCO^-_{3(aq)} + e^- \leftrightharpoons CO^{2-}_{3(aq)} + \frac{1}{2}H_{2(g)}$$
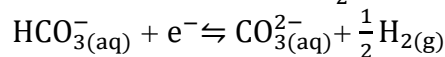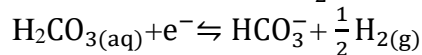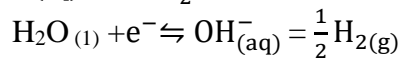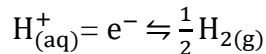
Anodic reaction:
$$Fe^{2+}_{(aq)} + 2e^- \leftrightharpoons Fe_{(s)}$$
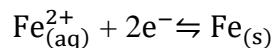
In addition to the CO_2 corrosion damage towards carbon steel surfaces, the presence of deposits in pipelines represents an additional threat to pipeline integrity.

This corrosion phenomenon called under-deposit corrosion (UDC) refers to corrosion damage beneath deposit layers. UDC can take place at sub-sea injection [6], transmission [7], well-fluid pipelines and, also in cooling water systems [8]. Deposits tend to accumulate usually at 6 o'clock position of the pipelines and inclined sections such as elbows and sometimes during shutdowns. UDC takes place in diverse stratified flow regime in which the different phases are separated. Lighter fluids can move across the top, and heavier phases and solids are moved along and settling at the bottom of the pipeline as a result of the lack of turbulence [9].

In partially covered-steels, electrochemical differences are formed between the bare and deposited-steel surface. Surface heterogeneities can drive galvanic effects which may lead to localised corrosion underneath the deposit [10-12]. Zhang *et al.* [11] stated that galvanic corrosion occurs when two dissimilar conducting materials in electrical contact and immersed in an electrolyte generate a galvanic current which flows between both materials. The authors also found that a mixed deposit containing sand, clay, ferrous carbonate, ferrous sulphide, and elemental sulphur acted as a cathode while the bare steel behaved as an anode at room temperature in a partially covered steel electrode. However, this polarity reversed at a temperature of $60^{\circ}C$ [10]. Apart from the galvanic effects, researches have established models to study UDC at deposit covered-steel surfaces. For instance, Pandarinathan *et al.* [13] evaluated three mineral deposits commonly present in oil and gas pipelines. Alumina was the most corrosive deposit followed by calcite and silica sand. The authors also suggested that deposit characteristics influenced the UDC processes.

UDC mechanisms are challenging to define due to the diverse aspects that can impact the UDC occurrence. These aspects include, nature of the deposits, elemental composition and metallurgy of the steel material [14]. Also, the presence and type of corrosive species such as oxygen and hydrogen ions, carbon dioxide, hydrogen sulphide, among others, can influence the UDC processes [14]. Deposits of diverse nature are present in oil and gas production, transportation and, processing facilities. For instance, silica sand is an inorganic deposit commonly found in production facilities. This deposit is transported from the underground rock formation where the oil, gas or water is produced. Other inorganic deposits such as corrosion products e.g. iron sulphides, oxides and carbonates can be also present in these systems [9, 15].

Furthermore, some deposits found in these facilities have an organic nature. Examples of these organic deposits are asphaltene; wax precipitated from crude oil and biofilms attached to steel surfaces, amongst others [14]. Also, mixed deposits such as schmoo, which consists of a mixture of organic and inorganic compounds, is commonly found in production facilities. An alternative mixture is the presence of biofilms embedded in mineral deposits which are often present in oil and gas systems [16-18]. Previous studies have shown how the nature of deposit can influence and determine the type of UDC. For instance, Standlee *et al.* [9] demonstrated more significant corrosion damage of API X-65 pipeline deposited with hydrogen sulphide than the steel surface deposited with inert silica sand. Similarly, Alanazi *et al.* [19] found that a sludge deposit caused higher general and localised corrosion of a multi-electrode array sensor compared to the non-deposited sensor.

The dimension of pipelines has also been mentioned as a contributor to UDC at different locations. This as a result of the variations in the fluid dynamics, resulting in quantity and structure differences of deposit layers between large and small diameter pipelines [20]. Another possible influencing factor for UDC can be the size of the deposit particles. Previous work proved that large sand particles were more corrosive than particles with smaller sizes in the presence of a corrosion inhibitor. The authors suggested that larger sand particles have a higher porosity than smaller sand particles. Thus, when the inhibitor penetrates the deposit of larger sand particles, it would have fewer but larger cathodic areas, i.e. inhibited surface in between sand particles. Conversely, small sand particles; it would have numerous, small and cathodic areas on the surface [21]. A similar study demonstrated that a deposit with low porosity and/or a thick deposit slows down the diffusion of corrosive species, resulting in a lower corrosion rate of carbon steel under CO_2 conditions. [22]

1.1.1.1. *Methods of UDC Study and its Inhibition*

This section presents an overview of various testing methods commonly used to evaluate UDC and its inhibition. Some of these methods are listed in the NACE technical committee report (TG) 380 [23]. It is worth mentioning that the methods are

different in nature and design, thus evaluate UDC and UDC inhibition in different ways.

UDC Test Method

This test methodology has been developed and applied in the Curtin Corrosion Centre and used in this research for UDC, UDC inhibition, and MIC investigation at the deposit covered-steel samples [13, 24-29]. The methodology consists of electrochemical measurements, mass loss and, surface analysis conducted in a three-electrode test cell setup. The steel samples are set as working electrodes by soldering wire for electrical connection. Then, the samples are arranged at the bottom of the test cell in a face-up position and fully covered by the deposit. This setup has also been adapted to work with microorganisms but using electrochemical cells of larger volume capacity. The steel samples are placed in glass holders and fully covered with the deposit. The cells can also be adapted to work in different flow modes such as batch (no flow), semi-batch and, as a continuous flow reactor.

Under-Deposit Corrosion Method

Commonly, the reservoirs are monitored to identify the presence and deposition of sand using this method. The inhibitor is added before or after sand addition to cover both scenarios in the reservoir. The setup involves a glass cell with a circular holder containing two samples in its outer part. A pipe is connected to the cell lid to introduce sand, and the holder rotates to spread the sand uniformly. Three steel samples are moulded together with a reference electrode in epoxy. One sand-deposited sample is galvanic connected to a sand-free sample. The second sand-deposited samples are not galvanically coupled [23]. Finally, galvanic current densities, potential and corrosion rate are measured and monitored through the experimental period [30].

UDC Autoclave Method

This UDC test is performed simulating pipeline conditions such as temperature and partial gas pressure. It is also designed to test both conductive and non-conductive deposits. The pressure vessels are made of glass or corrosion-resistant alloys (CRAs) with double wall to heat or cool the vessel. It can be adapted with an additional vessel

for partitioning purposes. The vessel also contains a three-finger probe and an additional flat sample in a holder like-cup to place the deposits. This flat sample also has a counter and reference electrode for electrochemical measurements, which enables comparison between deposit and non-deposited sample. Linear polarisation resistance (LPR), mass loss, and pitting depth are measured using this configuration [31].

Bubble Test Method

Considering that some inhibitors can adsorb onto deposits, this test method aims to evaluate inhibitor performance in the presence of deposits. The test cell operates at ambient pressure, and the cell lid is designed to fit a reference, working and counter electrodes. LPR measurements are performed before and after corrosion inhibitor addition. [32]

Artificial Pit Test Method

The purpose of this method is to evaluate the ability of a corrosion inhibitor to restrain a localised corrosion process propagating at a known rate. An artificial pit electrode is connected to a counter electrode of the same material but the larger area (ratio 1 to 1000). These electrodes are connected to a zero-resistance ammeter (ZRA) to measure currents and potentials at the coupled electrodes. Also, LPR measurements and final polarisation curves at individual electrodes provide corrosion rate information for the experiments [33].

Iron Sulphide Method in Inhibited Systems

This test assesses the effect of iron sulphide (FeS) film on corrosion inhibitor efficiency. The film is formed *in situ* when iron chloride ($FeCl_2$) reacts with hydrogen sulphide (H_2S) sparged in the solution. Alternatively, the steel probe can be pre-corroded in an H_2S environment without a corrosion inhibitor. The setup consists of a reservoir that feeds the testing cell using a pump. Also, the deoxygenated-$FeCl_2$ solution is pumped to the cell to form a FeS film. Afterwards, the inhibitor is injected

into the system containing two electrical resistance (ER) probes, one suspended in the brine and the other located at the bottom of the testing cells. Linear polarisation resistance (LPR) and mass loss measurements are performed in this method. [34]

Multi-Electrode Array Systems

Multi-electrode arrays provide information about local corrosion events in a deposited system and the efficiency of corrosion inhibitors under these conditions. Currently, there are variants of configurations for this system. For instance, Turnbull and Hinds [35-37] have used multi-electrode array sensors of 24 carbon steel wires to evaluate UDC inhibition under sour (H_2S) and sweet conditions (CO_2). Individual electrodes can be selected and pre-corroded to different depths, using a potentiostat in galvanostatic mode. Galvanic corrosion rates are calculated if the difference between corrosion potentials of the anode and the mixed galvanic potentials is above 100 mV. Tan *et al*. [38] used a multi-electrode array system, namely wire beam electrode (WBE) to study UDC and its inhibition, but this time the sensor contains 100 wires. The WBE surface was partially covered with the deposit using an O-ring, aiming to visualise electrochemical differences between covered and uncovered electrodes. Local corrosion potential and galvanic currents can be measured between one electrode and the remaining 99 in the array. Zhang *et al.* [10] has also worked with a WBE system but using a synthetic deposit simulating the composition of deposits recovered from sour gas fields.

1.1.1.2 UDC Mitigation

One of the most common and effective methods of protection against UDC is mechanical cleaning, e.g. brushing, water jets, pipeline inspection gauge (PIG) amongst others. Mechanical cleaning is implemented in a system to remove sludge, scale, encrustations and biofilms embedded in these deposits [39]. Nonetheless, mechanical cleaning is not sufficient by itself; it should be complemented with chemical treatment regimes.

Corrosion inhibitors have been routinely used to protect infrastructure carrying oil and gas as an economical and efficient mitigation strategy against carbon steel corrosion. An appropriate inhibitor should be compatible with the system, low cost, environmentally safe and, active at low concentrations [40].

Numerous test methods have been used to evaluate inhibitor performance. For instance, the standard guide for evaluating and qualifying oilfield and refinery corrosion inhibitors in CO_2 or H_2S environment, ASTM G170 [41] recommends some methodologies. The methods include flow loop, rotating cylinder electrode (RCE), rotating cage (RC), and, jet impingement cell (JIC) to evaluate the inhibitor performance. The standard also suggests an evaluation of secondary inhibitor properties, e.g., oil-water partitioning, solubility, foaming/emulsification tendency and toxicity, amongst others. However, other mitigation challenges associated with ageing pipelines such as UDC, galvanic corrosion, top-of-the-line (TLC), preferential weld corrosion (PWC) [42] and, MIC [43] are not considered in this document.

Approximately 80% of inhibitors are organic compounds that protect inner steel surfaces by either physical adsorption, chemisorption, or film formation [44]. Film-forming corrosion inhibitors are routinely applied to protect carbon steel pipelines in CO_2 and H_2S ambience, including crude oil export lines, wet gas pipelines, and flow lines amongst others [45, 46]. The protection mechanism starts with the reaction of the inhibitor with the metal surface forming films which can grow and create an adherent, hydrophobic and protective films [44]. Typically, these organic compounds contain nitrogen, phosphorus, oxygen, and sulphur. The functional groups of film-forming inhibitors are amide/imidazoline; amide/imidazoline + quaternary compounds; alkyl morpholines; amine; amide; amine salts; pyridine salt + quaternary compounds; quaternary ammonium salts; sulfonate amongst others [46].

The role of film-forming inhibitors in UDC mitigation is an important research topic for both industry and academia. The presence of deposits can affect corrosion inhibitor performance in different ways. For instance, some inhibitors can adsorb onto deposits leading to the ineffectiveness of the chemical treatment underneath deposit layers [47, 48]. Pandarinathan *et al*. [28] compared two groups of corrosion inhibitors for their adsorption affinity to silica sand. The group of cationic-surfactant inhibitors studied were cetylpyridinium chloride monohydrate (CPC) and 1-dodecylpyridinium

chloride hydrate (DPC). The group of sulphur-containing inhibitors included 2-mercaptopyrimidine (MPY) and thiobenzamide (TB). It was found that sulphur-containing organic compounds were less adsorbed on sand than surfactants and had the highest inhibition performance at the sand-deposited steel. It was stated that corrosion inhibitor adsorption on the deposits affected their performance. This relation adsorption-inhibition performance was established by the high adsorption of CPC on silica sand and the low performance of this surfactant on sand-deposited-carbon steels. In a different study was suggested that the inhibition efficiency on deposited-steels depends on the chemical nature of the corrosion inhibitor. [13].

Sulphur-containing compounds such as pyrimidines derivatives have been reported as highly efficient in preventing CO_2 corrosion [49] and also in the presence of deposits [24, 27, 28]. Thus, formulation with these molecules represents appropriate candidates to prevent and mitigate UDC. The integrity of pipeline structures relies on appropriate corrosion inhibition programs to select suitable inhibitors for specific environments. Research efforts and field applications of film-forming inhibitors through the last decade have provided understating of corrosion inhibition to some extent. However, there are still unclear aspects, such inhibitor effectiveness in the presence of biofilms and mineral deposits.

1.1.2 Microbiologically Influenced Corrosion (MIC)

The contact of biofilm with the metal can facilitate, initiate or accelerate corrosion processes in different ways as a result of electrochemical changes at the metal-solution interface. This microbiologically influenced corrosion (MIC) phenomenon is widely known for causing severe corrosion problems and for being difficult and expensive to mitigate. In general, microorganisms can cause corrosion by different mechanisms, e.g. through corrosive metabolites that they produce, a mechanism known as chemical-MIC (CMIC). Microorganisms can also enhance corrosion by extracting electrons directly from the metal surface, a MIC mechanism named electrical-MIC (EMIC).

Chemical MIC (CMIC)

The following microbial metabolic groups are frequently cited in the literature as CMIC-related microorganisms often recovered from deposits:

1) Sulfidogenic microorganisms: microorganisms of the sulphur cycle include, 1) sulphate-reducing microorganisms (SRM). Bacteria and archaea of this group reduce sulphate to sulphide and this in turn to iron sulphide (FeS) which can be corrosive under certain conditions [50-52]; 2) Sulphur-reducing bacteria (S°RB) reduce elemental sulphur (S°) to hydrogen sulphide (H_2S), and this can form iron sulphide when Fe ions are available. Some species of *Thermovirga* sp. frequently isolated from oil production facilities have the metabolic capability of reducing elemental sulphur (S^0) [53]. *Thermovirga* species have been pointed as high-risk MIC microorganisms associated with failures in the presence of deposits [54]; 3) Thiosulphate-reducing bacteria (TRB) group has been linked to MIC occurrence in association with field deposits [25]. A notable TRB representative is *Thermoanaerobacter* sp. frequently recovered from oil and gas facilities experiencing MIC problems [53, 55-57].

2) Fermentative microorganisms: fermentation is a form of anaerobic catabolism in which an organic compound is both an electron donor and an electron acceptor [58]. Fermenters play a vital role in MIC due to their capability of oxidising a wide range of substrates and producing corrosive, volatile fatty acids such as acetate, formic and lactic acids. In oil and gas facilities, acetogenic bacteria represent a MIC threat since they can ferment carbohydrates and oil hydrocarbons producing acetic acid. The produced acid can precipitate on steel surfaces, creating a local acid environment and thus leading to corrosion [59]. Fermenters can also play a dual corrosion role using inorganic sulphur compounds such thiosulphate as an electron sink during glucose and xylose oxidation with acetate as end product [60, 61]. Scully *et al.* [62] demonstrated the catabolism of several amino acids by *Thermoanaerobacter* strain AK90 under two electron-scavenging systems (either the presence of methanogens or thiosulphate) with acetate as the primary end product. In addition to the corrosion effects on the steel surface exerted by biogenic organic acids, some of these organics produced by fermentation processes can also be used by other microbial metabolic groups establishing metabolic associations [63].

3) Iron/Manganese-Oxidising Bacteria (FeOB/MnOB): these groups of metal-depositing bacteria, oxidise, e.g., ferrous iron (Fe^{2+}) to ferric iron (Fe^{3+}) which

precipitate as ferric oxides or hydroxides [64]. In a previous study, localised corrosion occurred in the presence of FeOB, suggesting a crevice effect caused by biogenic ferric oxides deposited on stainless steel surfaces [65]. Another research proposed an aerobic corrosion mechanism by FeOB, where the areas beneath colonies of microorganism behave as anodes; while the areas outside of the colonies with oxygen concentrations are relatively higher, support the cathodic reaction [66]. Moreover, some FeOB can oxidise iron coupled to nitrate reduction in the absence of oxygen. This sub-group is known as iron-oxidising/nitrate-reducing (FeONRB), which use ferrous iron (Fe^{2+}) as electron donor and nitrate (NO_3^-) as electron acceptor [67]. The end products can be either nitrite (NO_2^-) or can be reduced further to dinitrogen gas (N_2) in a well-known microbial process called denitrification [58]. Under certain conditions, the ferric iron (Fe^{3+}) produced can precipitate at the steel surface, forming ochre-like deposits [68]. The corrosion mechanism of this particular metabolic group remains uncertain. Straub *et al.* [69] found that some of these neutrophilic anaerobic FeONRB also grows mixotrophically using organic acids such as acetate as co-substrates for the synthesis of cell components. The authors stated that for these mixotrophs, it is unclear whether Fe^{2+} oxidation supports cell growth or it is oxidised in an undefined side reaction [70].

4) Iron/manganese-reducing bacteria (FeRB/MnRB): there are controversial studies about the effect of this metabolic group on corrosion [71, 72]. However, it is reasonable to link these metal-reducing microorganisms with UDC occurrence. FeRB/MnRB reduce solid Fe^{3+} and Mn^{4+} oxides to soluble Fe^{2+} and Mn^{2+} ions. This removal of passivating oxides layers allows direct contact of small exposed steel areas with corrosive species. Therefore, electrochemical differences between deposited and non-deposited areas can lead to localised corrosion [73, 74]. *Geobacter* and S*hewanella* genera are model iron reducers able to use ferric iron (Fe^{3+}) as a terminal electron acceptor in anaerobic respiration. However, little work has been done to study the contribution of FeRB to corrosion.

5) Methanogens: methanogenic archaea are attracting the attention of the MIC specialists because this group is frequently recovered from corroded oil and gas facilities. Methanogens use molecular hydrogen (H_2) to reduce CO_2 and produce methane (CH_4) [75]. The contribution of these hydrogenotrophic microorganisms to corrosion is through their capability to consume hydrogen leading to cathodic depolarisation of the steel and hence corrosion of steel surfaces [76].

<u>Electrical-MIC (EMIC)</u>

Considerable research advances have been achieved in the study of extracellular electron transfer (ETT) applied to diverse bioelectrochemical systems [77-81]. However, the understanding of the role of electrochemically active biofilms in corrosion processes remains limited. Likewise, to the best of our knowledge, the interactions of such biofilms with deposits have not been investigated. Kato *et al*. [82] defined "ETT as the metabolism that enables efficient electron transfer between microbial cells and extracellular solid materials". Previous MIC studies have pointed out that different diverse metabolic groups were able to cause corrosion via their EET metabolisms. The commonly cited metabolic groups are sulfidogenic microorganisms [83, 84], methanogens [85, 86], acetogens, nitrate-reducing bacteria (NRB) and, metal bacteria like *Shewanella* and *Geobacter* [87, 88].

To date, the effect of deposits on the EMIC processes remains unclear. However, it is acknowledged that some mineral deposits, e.g., silica, can create a mass transfer barrier for corrosive species to the metal surface in sterile conditions [12, 13]. Therefore, it is reasonable to suggest that inert deposits could interfere with EET. Another EMIC research gap related to deposits, is the possibility that conductive or semi-conductive deposits may facilitate EET mechanisms. For instance, electrochemically active iron sulphides such as Mackinawite [15] can be formed by sulphidogenic microorganisms which are well-known for forming electroactive biofilms [83, 89]. Enning *et al*. [84] found that marine sulphate-reducing bacteria in the presence of an electro-conductive mineral crust corroded up to 72% of the steel samples within five months of exposure. The mineral crust consisted of FeS, $FeCO_3$, and $Mg/CaCO_3$, which exhibited an electrical conductivity of 50 Sm^{-1}. This conductivity maintained electron flow from the metal through semi-conductive sulphides to the sulphate-reducing bacteria.

1.1.2.1. *MIC methods of study*

MIC studies typically aim to find corrosion-related microorganisms in the bulk solution, in biofilms attached to steel or coupons or within corrosion products. Supportive methods focus on determining cumulative corrosion damage, monitor

corrosion and identify corrosion products chemistry consistent with a MIC mechanism. This section presents an overview of the different methods that have been applied to assess MIC and others that can be adapted to conduct UDMC research.

Identification of MIC-related microorganisms

The main methods to detect, estimate and, quantify causative corrosion microorganisms are optical and fluorescence microscopy, adenosine triphosphate (ATP), microbial culture testing and molecular microbiological methods [90-92].

Epi-fluorescence microscopy has been successfully applied to detect biofilm attached to metal surfaces. However, some specimens can emit a secondary fluorescence under optical epi-fluorescence microscopes. This often occurs through the excited volume and obscures resolution of features that lie in the objective focal plane. The problem is due to the thickness of specimens (above 2 µm), which usually exhibit a high degree of fluorescence emission losing most of the fine detail.

The measurement of adenosine triphosphate (ATP) molecule is a direct indicator of total living biomass. Currently, some ATP kits are designed to measure ATP from biofilms attached to metal surfaces and also from corrosion products. Therefore, results from this method indicate the presence and activity of potential MIC-related microorganisms. ATP analysis is widely used to monitor biomass on field and laboratory. However, these kits possess some limitations related to samples collection, storage, and processing times. Following the kit instructions and field protocols can improve these limitations providing vital information related to biological content present in deposits.

Culture-dependent techniques have been historically used for enumeration of MIC-related microbes. Despite some inherent limitations of the techniques related to the low percentage of cultivable microorganisms, cultures represent the primary tool to recover and isolate bacterial species from bulk and deposits collected from oilfield facilities.

Molecular microbiological methods such as next-generation sequencing (NGS) of the 16S rRNA gene represent an essential tool for MIC studies. NGS is a culture-independent method that enables analysis of the entire microbial community within a

sample. A previous MIC used NGS to demonstrate that environmental conditions such as temperature impacted both the structure of the microbial population and the corrosion process of carbon steel [93]. A combination of NGS method and surfaces analysis indicated that microbial populations from locally-generated aerosols colonised and corroded steel surfaces exposed to an atmospheric environment. In the present research, differences in the microbial community composition between sand-deposited and sand-free samples were identified using 16S rRNA sequencing [94].

It is worth mentioning that most of the above methods require biological content viability or integrity of molecules for an accurate diagnosis. It is essential to follow specific sampling and storage protocols to collect products of corrosion or affected steel. It is also necessary to identify the corrosion mechanism in order to target causative microorganisms related to that environment. Finally, the cumulative investigations allow the association of these microorganisms with the corrosion problem.

In addition, the NACE standard TM0194-2014 [91] mentions commercially available culture media that are used for the detection of specific bacterial groups. Also, there are test kits offered for bacterial activity measurements. These kits include hydrogenase measurement, radiorespirometry and APS-reductase test amongst others. However, it is advised to evaluate the suitability of these commercial culture media and test kits for particular systems.

Omics-based techniques

Omics refers to the use of a group of technologies to study roles and relationships of cell molecules such as deoxyribonucleic acid (DNA), ribonucleic acid (RNA), proteins and metabolites. Specifically, metagenomics identifies and characterise the entire microbial population present in a sample. Also, complementary techniques such as transcriptomics provide information about population activity in terms of gene expression. Proteomics and metabolomics study protein and metabolites production by microbial communities in a sample [95-97]. These techniques offer information about MIC biofilm communities at their compositional and functional levels. The study of functional genes involved in metabolic pathways is essential when aiming to link microbial diversity with specific functions related to corrosion. These techniques could

offer a potential approach to the understanding of UDMC. For instance, transcriptomics could serve to establish differences in metabolic pathways of microorganisms present in systems containing deposits.

Similarly, metagenomics would provide differences in microbial composition on steels with and without mineral deposits. Apart from the potential benefits of omics-based techniques on UDMC research, it is crucial to consider the sensitivity of microbial molecules to degradation and changes. Therefore, the successful application of these methods would require strict sampling and preservation guidelines for accurate detection and quantification of cell molecules. Experiments should be designed to control critical aspects such as temperatures, sample replicates, adequate manipulation of the samples, use of preservation solutions, and processing times to generate reliable data.

Corrosion product identification

Elemental composition of corrosion products connects the microbiological component to corrosion processes at the metal surfaces. Spectroscopy methods provide qualitative and semi-quantitative information on corrosion products deposited at the steel surfaces [98]. The list of these surface chemical analysis techniques used for MIC studies includes X-ray diffraction (XRD); energy dispersive X-ray analysis (EDS); attenuated total reflectance/Fourier transform infrared spectroscopy (ATR/FTIR); time-of-flight secondary ion mass spectrometry (TOF-SIMS), among others [99-104].

Biofilm studies by microscopy

Microscopy allows imaging microbial cell, colonies morphology and biofilm distribution, as well as the presence of extracellular polymeric substances (EPS) and the nature of corrosion products. For instance, confocal scanning laser microscopy (CLSM), time-of-flight secondary ionisation mass spectrometry (TOF-SIMS) provides *in situ* molecular imaging of biofilm and its matrix, biofilm development, thickness, and viability [100, 105, 106]. Field-emission scanning electron microscopy (FESEM) and transmission electron microscopy (TEM) are essential tools in the study of biofilm development, composition, distribution and biofilm-metal interaction [107].

Also, atomic force microscopy (AFM) offers information about biofilm formation and EPS production [108-112].

Localised corrosion evaluation

Surface profilometry analysis is often applied to MIC studies, providing cumulative localised corrosion information after corrosion products removal. Measurements such as average and maximum pit depths and surface roughness are key parameters to determine the extent of corrosion after the immersion period [25, 94, 113].

Corrosion measurements

Electrochemical techniques (EC) have played an essential role in the understanding of corrosion processes. EC techniques are frequently used to measure and monitor MIC. A significant limitation in MIC monitoring is the inability to relate microbial events to corrosion in real-time. Some techniques can detect a specific modification in the system due to the presence and activities of microorganisms (e.g., heat transfer resistance, fluid friction resistance, galvanic current) and relate this to corrosion processes. Other methods measure electrochemical parameters such as polarisation resistance, electrochemical noise and correlate these results with microbial activity on the metal surface. Therefore, the combined use of EC techniques and microbiological-related methods is useful to monitor corrosion connecting the corrosion process with a specific biological activity.

The following group of EC techniques are frequently used in MIC investigations [107] [23]: open circuit potential (OCP); electrochemical noise (ECN) [114, 115]. Also, linear polarisation resistance (LPR); electrochemical impedance spectroscopy (EIS) [116-118]; electrochemical frequency modulation (EFM) [119]; potentiodynamic and potentiostatic polarisation measurements [120, 121].

1.1.2.2 MIC Mitigation

As mentioned in the UDC section, mechanical cleaning like pigging has shown to be a useful tool in removing all type of deposits, including biomass mixed with

mineral deposits, sludge, scales and, encrustations [39]. However, pigging is an expensive procedure, and not all facilities are accessible to this type of mechanical cleaning. Alternatively, physical methods like filtration and UV-radiation have been applied to mitigate MIC and to prevent biofouling [122, 123].

Biocides are the most common chemical treatments used to prevent and control MIC in new and ageing assets. Biocides are single or mixtures of compounds able to kill or inhibit microorganisms. The efficiency of the biocides is governed by the type of microorganisms and specific operating conditions of the system. Thus, it is recommended to perform biocide screening in the laboratory and further trials on the field, before including the selected chemical treatment to existing mitigation programs. Specifically, for industrial waters, the vast list of biocides include oxidising biocides and non-oxidising biocides. However, non-oxidising biocides such as glutaraldehyde [124-126], quaternary ammonium compounds (QUATS) [127] and Tetrakis hydroxyl methyl phosphonium (THPs) [128, 129] are preferentially applied for MIC mitigation.

Non-oxidising biocides are broad-spectrum, pH-independent and highly persistent after application. Currently, several studies have developed complementary agents for biocides treatments, i.e. biocides enhancers such as D-amino acids, chelators [130-133] and biofilm dispersants [134]. Another alternative is the use of bacteriophages to prevent biofilm formation on surfaces [135-137]. To date, only a few studies have investigated multifunctional compounds capable of acting as both corrosion inhibitors and biocides. Pound *et al*. [138] evaluated quaternary phosphonium compounds as corrosion inhibitors with biocidal properties in low alloy steel. Nevertheless, the compounds were effective against acid-producing bacteria or sulphate-reducing bacteria, but not against both.

1.1.3. Under-deposit microbial corrosion (UDMC)

In addition to the potential UDC occurrence by mineral deposits settled in the pipelines, microorganisms represent an additional threat to carbon steel surfaces. In general, microorganisms are widespread in oil and gas facilities; under some conditions, they are capable of actively colonise internal pipeline surfaces establishing biofilms [139]. Likewise, deposits are known to be preferential sites for bacteria

settlement and proliferation. The combination of MIC/UDC occurrence or UDMC can be defined as "electrochemical, physical and microbiological processes compromising pipeline integrity" [140].

The interaction of microorganisms with deposits and their relation with corrosion processes is a topic that remains unexplored. However, MIC-related microorganisms are expected to influence, initiate or accelerate UDC processes. In real industry scenarios, microbial consortia and deposits are frequently recovered from facilities experiencing corrosion problems. Some studies have correlated corrosion at steel surfaces with the presence of deposits and microorganisms. For instance, microbial activities occurring within sludge deposits were pointed as responsible for localised corrosion attack at metal surfaces [141]. Likewise, previous research under stagnant seawater conditions showed severe corrosion affectation when both microorganisms and mixed deposits (magnetite, calcium carbonate and sea sand) were present. The corrosion products comprised a mixture of iron oxides (magnetite), iron sulphides, sulphated green rust and Ca-based minerals. The authors postulated a synergism between MIC and UDC [18]. Case studies have also postulated the combination of microorganisms and deposits as responsible for pipelines failures in production facilities [7] and injection systems [6].

Another relevant aspect to consider is the existence of syntrophic relationships among microbial metabolic groups in deposited environments. Microorganisms isolated from oil and gas facilities usually comprise complex consortia of hundreds of species displaying different metabolic capabilities. These species frequently work together, establishing beneficial partnerships. In these associations, microorganisms can transfer reducing agents such as hydrogen or formate [142-144]. Furthermore, they can exchange electrons, organic, sulphur and, nitrogen compounds and also remove toxic microbial agents [145, 146]. Previous MIC research works have linked corrosion problems with the presence of different microbial metabolic groups, possibly establishing cross-feeding associations in natural environments containing deposits [57, 147-149].

The presence of microorganisms may influence or induce UDC in different ways. For example, biofilms can represent a UDC threat by modifying cathodic and anodic reactions at the metal surfaces as a result of microbial activity within biofilm [150]. Similarly, biofilms and settled mineral deposits can form complex deposit mixtures

in the inner pipeline surfaces. Thus, microorganisms can thrive within solid particles via uptake of nutrients accumulated in these areas. This environment could also favour microbial growth by protecting microbes from external threats. Another possible microbial effect towards UDMC occurrence is related to biomineralisation processes. Some microorganisms involved in geological processes are capable of mediating iron oxidation and reduction reactions under different environments [73, 151-155]. Thus, metal-depositing bacteria can lead to UDMC by the formation and precipitation of iron oxides/hydroxides on the metal surface, creating electrochemical differences between areas underneath and outside deposits [156]. Conversely, metal-reducing bacteria can dissolve accumulated metal oxides on the surface, creating electrochemical differences across the surface [157].

1.1.3.1.   UDMC methods of study: current state and challenges

Currently, several methods have been described to assess MIC, UDC and UDC inhibition separately [23, 90]. Nonetheless, their integration to study and address UDMC has not been adopted as an industry standard or a recommended practice. An interdisciplinary approach is crucial to design a laboratory test methodology to investigate UDMC. This section contains the methodology used to study UDMC and highlights some field and laboratory challenges associated with these analyses.

Characterisation of corrosion products on carbon steel surfaces represents a critical source of information of this type of corrosion. Energy-dispersive X-ray analysis (EDS) is used to determine the elemental composition of corrosion products formed on carbon steel surfaces. These corrosion products can be associated with organic oilfield deposit [25], mineral deposits such as silica sand as well as microorganisms [94]. Elemental composition analysis required an extra effort to preserve corrosion products. Not adequate corrosion products handling, e.g. oxygen exposure can result in changes in their composition and hence not reliable results. It is also worth mentioning that to help diagnose MIC as part of UDC, the deposits collected for identification must also be processed and manipulated for microbial analysis.

The combined use of 3D-imaging X-ray micro-computed tomography (X-ray µCT), fourier transform infrared spectroscopy (FTIR), Raman spectroscopy and X-ray diffraction (XRD) allow to determine the spatial distribution and composition of

corrosion products of shipwrecks [158,159-163]. For instance, Albahri *et al*. [158] identified goethite as the primary corrosion phase in deep-water shipwrecks. In addition, mineralised microbial structures were present within the layer of deposits demonstrating the suitability of this set of techniques to analyse corrosion-mineralised products with biological content.

Confocal laser scanning microscopy (CLSM) offers several advantages over conventional wide-field optical microscopy. The advantages include the ability to control depth of field, reducing background information from the focal plane. CLSM can also collect serial optical sections from relatively thick biofilms. In the present investigation, the presence of thick layers of deposits on steel surfaces made it challenging to visualise microbial cells in direct contact with the metal surface. Another limitation of this method is that some MIC studies based on confocal microscopy often rely on imagining live/dead microbial cells, thus representing a critical issue when targeting anaerobic microorganisms. Optimisation of confocal imaging protocols for UDMC would be crucial to minimise these limitations imparted by the presence of mineral deposits and anaerobes settled on the metal base.

Field-emission scanning electron microscopy (FESEM) represents an essential tool for UDMC studies. However, one of the requirements of FESEM on biological samples is that the specimens need to be completely dry due to high vacuum conditions of the mounting chamber. Thus, biofilms covering metal samples must follow strict protocols to be chemically fixed with glutaraldehyde or formaldehyde to preserve their structure. In this research project, FESEM from cross-sectioned corroded steel specimens revealed features of the damage from the top to bottom (metal base) [94].

Previous studies determined corrosion inhibitor adsorption on minerals deposits by UV-Visible spectrophotometry and high-performance liquid chromatography (HPLC). [28, 29, 47, 164]. The application of this method in measuring inhibitors residuals after contact with mineral deposits could also provide information on the inhibitor depletion after exposure with biofilms. Likewise, quantification of organic substrates after deposit contact represents a vital parameter to determine the depletion of electron sources by deposits. In the current project, sodium lactate depletion by silica sand was determined using fourier-transform infrared spectroscopy (FTIR).

Surface profilometry analysis represents one of the primary tools to reveal localised corrosion of the steel surfaces in the presence of deposits and microorganisms [18]. The combination of surface analysis and corrosion monitoring techniques such as electrochemical measurements (EC) provides local and general corrosion information about UDMC process [25, 94]. EC measurements on one-piece working electrodes or corrosion coupons are excellent sources of corrosion information in deposited systems when they are monitored continuously. However, EC techniques applied to one-piece electrodes can mix and average electrochemical parameters, e.g. corrosion potential and corrosion rate recorded at the entire surface [165].

Multi-electrode array systems, namely wire beam electrode (WBE) measure local electrochemical parameters such as corrosion potential and galvanic currents, thus providing spatial and temporal information of localised corrosion processes. WBE systems have demonstrated to be a suitable tool for studying different corrosion topics such as general and localised corrosion [166-168]; erosion-corrosion studies [169, 170]; coatings evaluation [171-173]; UDC and UDC inhibition [10, 35, 36, 38, 174]. The system has been applied to water line corrosion investigation [175], crevice corrosion [176] and ennoblement research [177]. In addition, the WBE system has been used in combination with electrochemical noise (ECN) resistance measurements [178, 179] and scanning reference electrode technique (SRET) [180]. The system has also been tested at temperatures above 100°C [181] and recently applied to MIC studies [115, 182, 183].

1.2. Objectives

This research investigates corrosion inhibition of deposited steels in the presence of bacteria. The specific objectives of this work are as follows:

- Identify existent methods and approaches used for investigating MIC, UDC and corrosion inhibition to integrate these research fields.

- Evaluate the efficiency of corrosion inhibitors to mitigate corrosion on carbon steel in the presence of different types of mineral deposits.

- Investigate under-deposit microbial corrosion (UDMC) in the presence of both a bacterial isolate and an oilfield microbial consortium.

- Develop a multidisciplinary approach to study UDMC and to evaluate the performance of corrosion inhibitors in the presence of bacteria.

1.3. Significance of this research

Root cause analyses usually associate the presence of microorganisms and deposits with devastating corrosion-related failures of pipelines. MIC alone represents approximately 20% of the total cost of corrosion [184]. Hence, controlling under-deposit microbial corrosion (UDMC) constitute an economic and technological challenge for the oil and gas industry.

Several methods are used to identify problems associated with MIC and UDC in different environments. The lack of integration of both corrosion phenomena has led to inaccurate diagnoses and underestimation of this type of corrosion. Consequently, this study aims to develop a suitable test methodology, including different corrosion disciplines, to study this phenomenon. To date, the interactions between MIC and UDC remain unclear. Thus, this information will assist the oil and gas industry needs to address this problem and hence, to preserve existent and new assets.

This research project contributes to the understanding of UDMC of carbon steel and the performance of corrosion inhibitors in the presence of microorganisms. The objectives were achieved through the development of a multidisciplinary approach to study this complex type of corrosion. Results from this research will provide valuable information for assessing integrity management based on chemical treatments. Incorrect selection of chemical treatments can be costly and result in insufficient corrosion protection leading to premature equipment failure and potential environmental damage.

1.4. Thesis outline

This thesis is assembled as a hybrid of peer-reviewed publications, submitted manuscripts and manuscripts in preparation as follows:

Chapter II Identifies existent methods and approaches to address the UDMC research field. The chapter gives a detailed literature review of concepts, testing methods and monitoring techniques for UDC and MIC, and discusses MIC mitigation strategies. This review highlights the importance of addressing knowledge gaps related to these topics. These gaps include the effect of the microorganisms on inhibitor efficiency and inhibitor performance in the presence of biofilms and deposits. This publication also suggests strengthening MIC research on syntrophic relationship mechanism related to corrosion. Also, it recommends reinforcing investigation of specific interactions between deposits and microorganisms and their relation with corrosion of metals.

Chapter III presents an evaluation of inhibitor performance in preventing under deposit corrosion of carbon steel and their adsorption on aluminium oxide (Al_2O_3), calcium carbonate $CaCO_3$, and silica sand (SiO_2) deposit, using electrochemical measurements and UV-Visible spectroscopy. The film-forming inhibitors tested were a sulphur-containing compound, 2-mercaptopyrimidine (MPY) and a cationic surfactant 1-dodecylpiridinium chloride (DPC). Despite the relatively high percentage adsorption of MPY on $CaCO_3$, this corrosion inhibitor provided the highest protection

at both deposited and non-deposited steel surfaces. Conversely, DPC showed minimal adsorption on all deposits, but it exhibited insufficient performance. This work proposed that inhibitors adsorption tend to be related to the type of inhibitor and not to the physical properties of the deposits.

Chapter IV proposes a new approach to evaluate and identify corrosion inhibitors for preventing under-deposit corrosion. This study investigated corrosion inhibition of a steel wire beam electrode (WBE) partially deposited with silica sand in CO_2 ambience. This work shows that both organic filming corrosion inhibitors, MPY and DPC created differences in potential resulting in galvanic corrosion currents on the carbon steel surface. The smaller non-surfactant MPY molecule was more effective than DPC in penetrating the silica sand deposit and preventing under deposit corrosion. DPC did not perform efficiently underneath sand layers. In this study, the MPY effectiveness is related to its molecular structure that allows its high penetration capacity through the sand layer. These molecular characteristics could be used for selecting effective molecules as corrosion inhibitors to prevent under deposit corrosion. The WBE system demonstrated to be a suitable method for visualising specific electrochemical events related to under-deposit corrosion and corrosion inhibitor performance, including their rate and effectiveness of penetration through deposits in CO_2 conditions.

Chapter V shows an under-deposit microbial corrosion (UDMC) study using a bacterial isolate, *Shewanella Oneidensis* MR-1. Corrosion effects on carbon steel surfaces by this isolate were investigated using electrochemical measurements, surface analysis and analytical methods. This UDMC investigation was conducted in two different environments; in artificial seawater (ASW) containing an excess of soluble electron donor (lactate) and in ASW at low lactate concentration. The test condition at low lactate concentration would stimulate *S.oneidensis* metabolisms to extract the electrons directly from steel surfaces. Biotic test with high lactate concentration of 59 mM lactate showed lower corrosion damage than the abiotic counterpart. These results proposed that non-corrosive metabolic by-products produced by biofilms were deposited on the steel, exerting a barrier effect against corrosive species in the solution.

Sand-free samples immersed in biotic conditions with 5 mM lactate had more considerable corrosion damage than sand-deposited samples. However, sand-deposited samples were affected to some extent, suggesting that *S.oneidensis* could impact steel surfaces even in the presence of thick sand deposit layer. FESEM images of cross-sectioned corroded samples evidenced biofilm formation underneath and between sand grains. This methodology provided valuable information about differences in corrosion effects exerted by this bacterial isolate.

Chapter VI presents a study of an aggressive microbial attack on carbon steel surfaces covered and uncovered with a sand deposit using surface analysis techniques and 16S rRNA gene sequencing. The thermophilic microbial consortium was recovered from an oilfield facility in Western Australia. The consortium consisted of methanogens, fermenting and sulphidogenic microorganisms which significantly increased average and localised corrosion at both sand-deposited and sand-free samples. Microbial metabolisms and syntrophy partnerships within the consortium seemed to contribute to metallic corrosion. Also, electrochemical reactions were discussed based on the layers of corrosion products settled on the steel surface. The structure of the microbial community and corrosion products stratification were different between sand-free and sand-deposited samples. These results highlighted the importance of conducting tests for under deposit corrosion, including native microbial consortia to have a better approximation to the field environment.

Chapter VII demonstrates the use of methodology developed in this project to study UDMC. This work merges different UDMC components such as biofilms, biogenic deposits and, corrosion inhibition under this environment using a wire beam electrode (WBE) system. Local corrosion rates, galvanic currents, corrosion potentials and, profilometry analysis, were measured to assess UDMC information. The results showed that a marine bacterium, *Enterobacter roggenkampii* caused localised corrosion under biogenic deposits through its capability to oxidise iron coupled to nitrate reduction in anaerobic conditions. Localised corrosion initiation and evolution reactions were discussed based on local electrochemistry. The organic film-forming inhibitor, 2-mercaptopyrimidine (MPY) inhibited average corrosion but was not

efficient in preventing localised corrosion. The ability of the WBE to locally measure self-corrosion processes, galvanic effects and, corrosion potentials across the steel surface demonstrated its suitability to detect, evaluate and monitor the UDMC and its inhibition. This research highlights the importance of incorporating the microbial component to corrosion inhibitors evaluation to ensure chemical effectiveness in the likely scenario of deposit formation and microbial contamination in oil and gas production equipment.

1.5. Overview of research design

This research used several methods to study and integrate under-deposit microbial corrosion UDMC phenomenon. The basic experimental design of the tests consisted of exposing the deposited and non-deposited steel samples to the test solutions either containing microorganisms (biotic tests) or in sterile conditions (abiotic tests). Sample preparation and sterilisation procedures varied according to the requirements of each experiment (details are presented in each chapter, and Appendix 1). Similarly, test solution composition, test materials, deposits type, configuration for electrochemical measurements, varied according to the experimental conditions for each test. In general, all the tests solutions were sparged with specific gasses for 2 h before the experiments. The oxygen-free test solutions were transferred to the deaerated test cells using a peristaltic pump and elastic tubing with low oxygen permeability. The gas was continuously sparged throughout the test period to ensure anaerobic environment.

1.5.1. Test methods for investigating UDMC in the present research

Corrosion rates evaluation

Corrosion monitoring techniques were applied to evaluate UDMC and the performance of corrosion inhibitors. Methods were conducted as per the ASTM standard procedures [185, 186] using a three-electrode cell setup. The techniques used were corrosion potentials, linear polarisation resistance (LPR), and potentiodynamic polarisation. A wire beam electrode (WBE) system was used to measure local

electrochemical events such as galvanic currents, corrosion potentials and, corrosion rates in the study of UDMC and its inhibition. Both configurations, the three-electrode test cells setup, and the WBE were suitable to evaluate UDC, UDMC and corrosion inhibitor performance under these scenarios. Mass loss measurements complemented the corrosion monitoring techniques and provided cumulative corrosion information by calculating metal mass loss after the immersion tests.

Microbial evaluation

Biofilm population differences recovered from carbon steel surfaces with and without sand deposit were identified using 16S next-generation sequencing. Direct phase-contrast microscopy, adenosine triphosphate (ATP) measurements and culture-independent analysis were the main microbiological tools to detect, quantify, isolate and monitor microbial activity in the different experiments for this research project.

Post-surface analysis

Surface analysis such as X-ray-spectroscopy (EDS) generated elemental composition maps from corrosion products formed at deposited and non-deposited steel surfaces. Similarly, field-emission scanning electron microscopy (FESEM) allowed visualisation of biofilms covering steel surfaces. Cross-sectional features of the damage such as corrosion products stratification from top to the metal base were identified by high-resolution microscopy. 3D-profilometry of steel surfaces was used to assess localised corrosion. This evaluation consisted of the visualisation of localised corrosion, e.g. pit morphology/profile and calculation of pitting rate.

1.6. References

1.   Koch, G.; Varney, J.; Thompson, N.; Moghissi, O.; Gould, M.; Payer, J. *International measures of prevention, application and economics of corrosion technologies study (impact)*; Technical Report, NACE International: 2016.

2.   Kahyarian, A.; Achour, M.; Nesic, S., CO_2 corrosion of mild steel. In *Trends in Oil and Gas Corrosion Research and Technologies*, **2017**; pp 149-190.

3.   Kahyarian, A.; Brown, B.; Nesic, S., *Mechanism of CO$_2$ Corrosion of Mild Steel: a New Narrative*. 2018.

4.   Frankel, G., Fundamentals of corrosion kinetics. In *Active Protective Coatings*, Springer: **2016**; pp 17-32.

5.   Nešić, S., Carbon Dioxide Corrosion of Mild Steel. In *Uhlig's Corrosion Handbook*, John Wiley & Sons, Inc.: **2011**; pp 229-245.

6.   Shukla, P. K.; Naraian, S., Under-Deposit Corrosion in a Sub-Sea Water Injection Pipeline—A Case Study. NACE International: 2017.

7.   Esan, T.; Kapusta, S. D.; Simon-Thomas, M. J. J., Case Study: Extreme Corrosion of a 20" Oil Pipeline in the Niger Delta Region. In *NACE International*, NACE International: 2001.

8.   Yang, B., Method for On-Line Determination of Underdeposit Corrosion Rates in Cooling Water Systems. *Corrosion* **1995**, 75(2):153-165.

9.   Standlee, S.; Efird, K. D.; Spiller, D., Under Deposit Corrosion From Iron Sulfide. In *Conference & Expo*, NACE International: 2011.

10.   Zhang, G. A.; Yu, N.; Yang, L. Y.; Guo, X. P., Galvanic corrosion behavior of deposit-covered and uncovered carbon steel. *Corrosion Science* **2014,** *86*, 202-212.

11.   Zhang, X. G., Galvanic Corrosion. In *Uhlig's Corrosion Handbook*, John Wiley & Sons, Inc.: **2011**; pp 123-143.

12.   Huang, J.; Brown, B.; Choi, Y.-S.; Ne; ic, S., Prediction of Uniform CO$_2$ Corrosion of Mild Steel Under Inert Solid Deposits. NACE International: 2011.

13.   Pandarinathan, V.; Lepková, K.; Bailey, S. I.; Gubner, R., Impact of Mineral Deposits on CO$_2$ Corrosion of Carbon Steel. NACE International: Houston, TX, 2013.

14.   Vera, J. R.; Daniels, D.; Achour, M. H., Under Deposit Corrosion (UDC) In The Oil And Gas Industry: A Review Of Mechanisms, Testing And Mitigation. NACE International: Houston, TX, 2012.

15.   Zhang, Y.; Moloney, J., Corrosion Monitoring Under Iron Sulfide Deposit: Testing Method Development. NACE International: 2014.

16.   Crozier, B.; Been, J.; Tsaprailis, H.; Place, T. D., Long Term Evaluation of Microbial Induced Corrosion Contribution to Underdeposit Sludge Corrosivity in a Heavy Crude Oil Pipeline. NACE International: 2013.

17.   Païssé, S.; Ghiglione, J.-f.; Marty, F.; Abbas, B.; Gueuné, H.; Amaya, J. M.; Sanchez; Muyzer, G.; Quillet, L., Sulfate-reducing bacteria inhabiting natural

corrosion deposits from marine steel structures. *Applied microbiology and biotechnology* **2013,** *97* (16), 7493-504.

18.   Wang, X.; Melchers, R. E., Corrosion of carbon steel in presence of mixed deposits under stagnant seawater conditions. *Journal of Loss Prevention in the Process Industries* **2017,** *45*, 29-42.

19.   Alanazi, N. M., Investigation of Under-Deposit Corrosion on X-60 using Multielcetrode System. NACE International: 2017.

20.   Been, J.; Place, T. D.; Crozier, B.; Mosher, M.; Ignacz, T.; Soderberg, J.; Cathrea, C.; Holm, M.; Archibald, D., Development Of A Test Protocol For The Evaluation Of Underdeposit Corrosion Inhibitors In Large Diameter Crude Oil Pipelines. In *NACE International Corrosion Conference Series*, NACE International: 2011.

21.   Hassani, S.; Huang, J.; Victor, A. C.; Brown, B.; Singer, M., Inhibited Under-Deposit CO2 Corrosion: Small Particle Silica Sand and Eicosane Paraffin Deposits. In *NACE - International Corrosion Conference Series*, NACE International: New Orleans, Louisiana, USA, 2017; Vol. 4, pp 2340-2351.

22.   Huang, J.; Brown, B.; Jiang, X.; Kinsella, B.; Nesic, S., Internal CO2 Corrosion Of Mild Steel Pipelines Under Inert Solid Deposits. In *NACE - International Corrosion Conference Series*, NACE International: San Antonio, TX, 2010.

23.   NACE 61114 (TG) 380. Underdeposit Corrosion (UDC) Testing and Mitigation Methods in the Oil and Gas Industry. In NACE International: 2014.

24.   Pandarinathan, V.; Lepková, K.; Gubner, R., Inhibition Of CO_2 Corrosion Of 1030 Carbon Steel Beneath Sand-Deposits. In *Conference & Expo*, NACE International: 2011.

25.   Machuca, L. L.; Lepkova, K.; Petroski, A., Corrosion of carbon steel in the presence of oilfield deposit and thiosulphate-reducing bacteria in CO_2 environment. *Corrosion Science* **2017,** *129*, 18-25.

26.   Pandarinathan, V.; Lepková, K.; Bailey, S. I.; Becker, T.; Gubner, R., Adsorption of Corrosion Inhibitor 1-Dodecylpyridinium Chloride on Carbon Steel Studied byin Situ AFM and Electrochemical Methods. *Industrial & Engineering Chemistry Research* **2014,** *53* (14), 5858-5865.

27.   Pandarinathan, V.; Lepkova, K.; Bailey, S. I.; Gubner, R., Inhibition of Under-Deposit Corrosion of Carbon Steel by Thiobenzamide. *Journal of the Electrochemical Society* **2013,** *160* (9), C432-C440.

28.   Pandarinathan, V.; Lepková, K.; Bailey, S. I.; Gubner, R., Evaluation of corrosion inhibition at sand-deposited carbon steel in CO_2-saturated brine. *Corrosion Science* **2013,** *72*, 108-117.

29.   Suarez, E. M.; Machuca, L. L.; Kinsella, B.; Lepkova, K., CO_2 Corrosion Inhibitors Performance at Deposited-Carbon Steel and their Adsorption in Different Deposits. *CORROSION* **2019,** *75* (9), 118-1127.

30.   Nyborg, R.; Foss, M., Experience With An Under Deposit Corrosion Test Method With Galvanic Current Measurements. In *conference & expo*, NACE International: 2011.

31.   De Reus, H.; Hendriksen, L. J. A.; Wilms, M.; Al-Habsi, Y. N.; Durnie, W.; Gough, M. Test Methodologies and Field Verification of Corrosion Inhibitors to Address under Deposit Corrosion in Oil and Gas Production Systems. NACE International: Houston, TX, 2005.

32.   Papavinasam, S.; Revie, R. W.; Bartos, M., Testing Methods and Standards for Oilfield Corrosion Inhibitors. In *CORROSION 2004*, NACE International: New Orleans, Louisiana, 2004; p 12.

33.   Palmer, J. W.; Marsh, J.; Newman, R. C., Evaluation of Inhibitor Performance for Protection against Localized Corrosion. In *CORROSION 2002*, NACE International: Denver, Colorado, 2002; p 16.

34.   Achour, M.; Kolts, J.; Humble, P.; Hudgins, R., Experimental Evaluation Of Corrosion Inhibitor Performance In Presence Of Iron Sulfide In CO_2/H_2S Environment. In *CORROSION 2008*, NACE International: New Orleans, Louisiana, 2008; p 11.

35.   Turnbull, A.; Hinds, G.; Cooling, P.; Zhou, S., A Multi-Electrode Approach To Evaluating Inhibition Of Underdeposit Corrosion In CO_2 Environments. NACE International: 2009.

36.   Hinds, G.; Turnbull, A., Novel Multi-Electrode Test Method for Evaluating Inhibition of Underdeposit Corrosion—Part 1: Sweet Conditions. *Corrosion* **2010,** *66* (4), 046001-046001-10.

37.   Hinds, G.; Turnbull, A., Novel Multi-Electrode Test Method for Evaluating Inhibition of Underdeposit Corrosion-Part 2: Sour Conditions. *Corrosion* **2010,** *66* (5), E1-E6.

38.   Tan, Y.; Fwu, Y.; Bhardwaj, K., Electrochemical evaluation of under-deposit corrosion and its inhibition using the wire beam electrode method. *Corrosion Science* **2011,** *53* (4), 1254-1261.

39.   Videla, H. A., Prevention and control of biocorrosion. *International Biodeterioration & Biodegradation* **2002,** *49* (4), 259-270.

40.   Dariva, C. G.; Galio, A. F., Corrosion inhibitors–principles, mechanisms and applications. In *Developments in corrosion protection*, InTech: **2014**.

41.   ASTM G170-06, Standard Guide for Evaluating and Qualifying Oilfield and Refinery Corrosion Inhibitors in the Laboratory. In ASTM international: 2012.

42.   SPE-169615-MS Jenkins, A., The Challenges Associated with the Development and Application of Oil and Gas Corrosion Inhibitors. In Society of Petroleum Engineers; 2014.

43.   Videla, H. A.; Guiawet, P. S.; Gomez Saravia, S. G.; Allegreti, P.; Furlong, J., Microbial Degradation of Film Forming Inhibitors and Its Possible Effects on Corrosion Inhibition Performance. In *Corrosion 2000*, NACE International: Orlando, Florida, 2000; p 10.

44.   Papavinasam, S., Corrosion Inhibitors. In *Uhlig's Corrosion Handbook*, John Wiley & Sons, Inc.: 2011; pp 1021-1032.

45.   Palmer, J. W., Corrosion Control by Film Forming Inhibitors. In *CORROSION 2006*, NACE International: San Diego, California, 2006; p 12.

46.   Achour, M.; Kolts, J., Corrosion Control by Inhibition Part I: Corrosion Control by Film Forming Inhibitors. In *CORROSION 2015*, NACE International: Dallas, Texas, 2015; p 15.

47.   Binks, B. P.; Fletcher, P. D. I.; Salama, I. E.; Horsup, D. I.; Moore, J. A., Quantitative Prediction of the Reduction of Corrosion Inhibitor Effectiveness Due to Parasitic Adsorption onto a Competitor Surface. *Langmuir* **2011,** *27* (1), 469-473.

48.   Horsup, D. I.; Clark, J. C.; Binks, B. P.; Fletcher, P. D. I.; Hicks, J. T., "I Put It In, But Where Does It Go- The Fate Of Corrosion Inhibitors In Multiphase Systems. In *CORROSION 2007*, NACE International: Nashville, Tennessee, 2007.

49.   Reznik, V. S.; Akamsin, V. D.; Khodyrev, Y. P.; Galiakberov, R. M.; Efremov, Y. Y.; Tiwari, L., Mercaptopyrimidines as inhibitors of carbon dioxide corrosion of iron. *Corrosion Science* **2008,** *50* (2), 392-403.

50.   Beech, I. B.; Gaylarde, C. C., Recent advances in the study of biocorrosion: an overview. *Journal of Microbiology* **1999,** *30*, 117-190.

51.	Javed, M. A.; Neil, W. C.; McAdam, G.; Wade, S. A., Effect of sulphate-reducing bacteria on the microbiologically influenced corrosion of ten different metals using constant test conditions. *International Biodeterioration & Biodegradation* **2017,** *125*, 73-85.

52.	AlAbbas, F. M.; Williamson, C.; Bhola, S. M.; Spear, J. R.; Olson, D. L.; Mishra, B.; Kakpovbia, A. E., Influence of sulfate reducing bacterial biofilm on corrosion behavior of low-alloy, high-strength steel (API-5L X80). *International Biodeterioration & Biodegradation* **2013,** *78*, 34-42.

53.	Stevenson, B. S.; Drilling, H. S.; Lawson, P. A.; Duncan, K. E.; Parisi, V. A.; Suflita, J. M., Microbial communities in bulk fluids and biofilms of an oil facility have similar composition but different structure. *Environmental Microbiology* **2011,** *13* (4), 1078-1090.

54.	Skovhus, T. L.; Caffrey, S. M.; Hubert, C. R. J., *Applications of Molecular Microbiological Methods*. Caister Academic Press: **2014**.

55.	Lan, G.; Hong, H.; Qing, D.; Wu, Y.; Tan, H., Identification and bio-corrosion behavior of Thermoanaerobacter CF1, a thiosulfate reducing bacterium isolated from Dagang oil field. *African Journal of Microbiology Research* **2012,** *6* (12), 3065-3071.

56.	Lenhart, T. R.; Duncan, K. E.; Beech, I. B.; Sunner, J. A.; Smith, W.; Bonifay, V.; Biri, B.; Suflita, J. M., Identification and characterization of microbial biofilm communities associated with corroded oil pipeline surfaces. *Biofouling* **2014,** *30* (7), 823-835.

57.	Duncan, K. E., Biocorrosive Thermophilic Microbial Communities in Alaskan North Slope Oil Facilities. *Environmental Science & Technology* **2010,** *43* (20), 7977–7984.

58.	Madigan, M. T.; Martinko, J. M.; Bender, K. S.; Buckley, D. H.; Stahl, D. A., *Brock biology of microorganisms (14th edition)*. **2014**.

59.	Kato, S.; Yumoto, I.; Kamagata, Y., Isolation of Acetogenic Bacteria That Induce Biocorrosion by Utilizing Metallic Iron as the Sole Electron Donor. *Applied and environmental microbiology* **2015,** *81* (1), 67-73.

60.	Fardeau, M.-L.; Faudon, C.; Cayol, J.-L.; Magot, M.; Patel, B.; Ollivier, B., Effect of thiosulphate as electron acceptor on glucose and xylose oxidation by *Thermoanaerobacter finnii* and a *Thermoanaerobacter sp*. isolated from oil field water. *Research in Microbiology* **1996,** *147* (3), 159-165.

61.   Etchebehere, C.; Muxí, L., Thiosulfate reduction and alanine production in glucose fermentation by members of the genus Coprothermobacter. *Antonie van Leeuwenhoek* **2000,** *77* (4), 321-327.

62.   Scully, S. M.; Orlygsson, J., Amino acid metabolism of Thermoanaerobacter strain AK90: the role of electron-scavenging systems in end product formation. *Journal of amino acids* **2015,** *2015*.

63.   Ollivier, B.; Cayol, J.-L., Fermentative, iron-reducing, and nitrate-reducing microorganisms. In *Petroleum Microbiology*, American Society of Microbiology: 2005; pp 71-88.

64.   Starosvetsky, D.; Armon, R.; Yahalom, J.; Starosvetsky, J., Pitting corrosion of carbon steel caused by iron bacteria. *International Biodeterioration & Biodegradation* **2001,** *47* (2), 79-87.

65.   Starosvetsky, J.; Starosvetsky, D.; Pokroy, B.; Hilel, T.; Armon, R., Electrochemical behaviour of stainless steels in media containing iron-oxidizing bacteria (IOB) by corrosion process modeling. *Corrosion Science* **2008,** *50* (2), 540-547.

66.   Little, B.; Wagner, P.; Mansfeld, F., An overview of microbiologically influenced corrosion. *Electrochimica Acta* **1992,** *37* (12), 2185-2194.

67.   Straub, K. L.; Schönhuber, W. A.; Buchholz-Cleven, B. E.; Schink, B., Diversity of ferrous iron-oxidizing, nitrate-reducing bacteria and their involvement in oxygen-independent iron cycling. *Geomicrobiology Journal* **2004,** *21* (6), 371-378.

68.   Hedrich, S.; Schlömann, M.; Johnson, D. B., The iron-oxidizing proteobacteria. *Microbiology* **2011,** *157* (6), 1551-1564.

69.   Straub, K. L.; Benz, M.; Schink, B., Iron metabolism in anoxic environments at near neutral pH. *FEMS microbiology ecology* **2001,** *34* (3), 181-186.

70.   Straub, K. L., Fe(II)-Oxidizing prokaryotes. In *Encyclopedia of Earth Sciences Series*, 2011; pp 367-370.

71.   Herrera, L. K.; Videla, H. A., Role of iron-reducing bacteria in corrosion and protection of carbon steel. *International Biodeterioration & Biodegradation* **2009,** *63* (7), 891-895.

72.   Cote, C.; Rosas, O.; Basseguy, R., Geobacter sulfurreducens: An iron reducing bacterium that can protect carbon steel against corrosion? *Corrosion Science* **2015,** *94*, 104-113.

73.   Lee, A. K.; Newman, D. K., Microbial iron respiration: impacts on corrosion processes. *Applied microbiology and biotechnology* **2003,** *62* (2), 134-139.

74.   Schütz, M. K.; Libert, M.; Schlegel, M. L.; Lartigue, J.-E.; Bildstein, O., Dissimilatory Iron Reduction in the Presence of Hydrogen: A Case Study of Microbial Activity and Nuclear Waste Disposal. *Procedia Earth and Planetary Science* **2013,** *7*, 409-412.

75.   Ozuolmez, D.; Na, H.; Lever, M. A.; Kjeldsen, K. U.; Jørgensen, B. B.; Plugge, C. M., Methanogenic archaea and sulfate reducing bacteria co-cultured on acetate: teamwork or coexistence? *Frontiers in Microbiology* **2015,** *6*, 492.

76.   Davidova, I. A.; Duncan, K. E.; Perez-Ibarra, B. M.; Suflita, J. M., Involvement of thermophilic archaea in the biocorrosion of oil pipelines. *Environmental Microbiology* **2012,** *14* (7), 1762-1771.

77.   Dulon, S.; Parot, S.; Delia, M.-L.; Bergel, A., Electroactive biofilms: new means for electrochemistry. *Journal of Applied Electrochemistry* **2007,** *37* (1), 173-179.

78.   Sydow, A.; Krieg, T.; Mayer, F.; Schrader, J.; Holtmann, D., Electroactive bacteria—molecular mechanisms and genetic tools. *Applied microbiology and biotechnology* **2014,** *98* (20), 8481-8495.

79.   Strycharz-Glaven, S. M.; Snider, R. M.; Guiseppi-Elie, A.; Tender, L. M., On the electrical conductivity of microbial nanowires and biofilms. *Energy & Environmental Science* **2011,** *4* (11), 4366-4379.

80.   Lovley, D. R., Electromicrobiology. *Annual Review of Microbiology* **2012,** *66* (1), 391-409.

81.   Babauta, J.; Renslow, R.; Lewandowski, Z.; Beyenal, H., Electrochemically active biofilms: facts and fiction. A review. *Biofouling* **2012,** *28* (8), 789-812.

82.   Kato, S., Microbial extracellular electron transfer and its relevance to iron corrosion. *Microbial Biotechnology* **2016,** *9* (2), 141-148.

83.   Cordas, C. M.; Guerra, L. T.; Xavier, C.; Moura, J. J. G., Electroactive biofilms of sulphate reducing bacteria. *Electrochimica Acta* **2008,** *54* (1), 29-34.

84.   Enning, D.; Venzlaff, H.; Garrelfs, J.; Dinh, H. T.; Meyer, V.; Mayrhofer, K.; Hassel, A. W.; Stratmann, M.; Widdel, F., Marine sulfate-reducing bacteria cause serious corrosion of iron under electroconductive biogenic mineral crust. *Environmental Microbiology* **2012,** *14* (7), 1772-1787.

85.   Deutzmann, J. S.; Sahin, M.; Spormann, A. M., Extracellular enzymes facilitate electron uptake in biocorrosion and bioelectrosynthesis. *MBio* **2015,** *6* (2), e00496-15.

86.   Hara, M.; Onaka, Y.; Kobayashi, H.; Fu, Q.; Kawaguchi, H.; Vilcaez, J.; Sato, K., Mechanism of Electromethanogenic Reduction of CO2 by a Thermophilic Methanogen. *Energy Procedia* **2013,** *37* (Supplement C), 7021-7028.

87.   Doyle, L. E.; Marsili, E., Methods for enrichment of novel electrochemically-active microorganisms. *Bioresource Technology* **2015,** *195*, 273-282.

88.   Dumas, C.; Basseguy, R.; Bergel, A., Microbial electrocatalysis with Geobacter sulfurreducens biofilm on stainless steel cathodes. *Electrochimica Acta* **2008,** *53* (5), 2494-2500.

89.   Cordas, C. M.; Moura, J. J. G., Sulphate reducing bacteria - electroactive biofilm formation. *International Journal of Medical and Biological Frontiers* **2011,** *17* (4/5), 295-312.

90.   International, N., Detection, Testing, and Evaluation of Microbiologically Influenced Corrosion on Internal Surfaces of Pipelines. NACE International: 2018.

91.   International, N., Field Monitoring of Bacterial Growth in Oil and Gas Systems. NACE International: 2014.

92.   Dockens, K.; Demeter, M.; Johnston, S.; Leong, S. In *Comparison of Planktonic and Sessile Bacteria Counts using ATP and DNA Based Methods*, CORROSION 2017, NACE International: 2017.

93.   Salgar-Chaparro, S. J.; Machuca, L. L.; Lepkova, K.; Pojtanabuntoeng, T.; Darwin, A., Investigating the Effect of Temperature in the Community Structure of an Oilfield Microbial Consortium, and Its Impact on Corrosion of Carbon Steel. In *Corrosion 2019*, NACE International: Nashville, Tennessee, USA, 2019; p 16.

94.   Suarez, E. M.; Lepkova, K.; Kinsella, B.; Machuca, L. L., Aggressive corrosion of steel by a thermophilic microbial consortium in the presence and absence of sand. *International Biodeterioration & Biodegradation* **2019,** *137*, 137-146.

95.   Beale, D. J.; Dunn, M. S.; Marney, D., Application of GC–MS metabolic profiling to 'blue-green water' from microbial influenced corrosion in copper pipes. *Corrosion Science* **2010,** *52* (9), 3140-3145.

96.   Beale, D. J.; Dunn, M. S.; Morrison, P. D.; Porter, N. A.; Marlow, D. R., Characterisation of bulk water samples from copper pipes undergoing microbially

influenced corrosion by diagnostic metabolomic profiling. *Corrosion Science* **2012,** *55*, 272-279.

97.   Beale, D. J.; Karpe, A. V.; Jadhav, S.; Muster, T. H.; Palombo, E. A., Omics-based approaches and their use in the assessment of microbial-influenced corrosion of metals. *Corrosion Reviews* **2016,** *34* (1-2), 1-15.

98.   Beech, I. B., Corrosion of technical materials in the presence of biofilms—current understanding and state-of-the art methods of study. *International Biodeterioration & Biodegradation* **2004,** *53* (3), 177-183.

99.   Boxer, S. G.; Kraft, M. L.; Weber, P. K., Advances in imaging secondary ion mass spectrometry for biological samples. *Annual review of biophysics* **2009,** *38*, 53-74.

100.   Ding, Y.; Zhou, Y.; Yao, J.; Szymanski, C.; Fredrickson, J.; Shi, L.; Cao, B.; Zhu, Z.; Yu, X.-Y., In Situ Molecular Imaging of the Biofilm and Its Matrix. *Analytical Chemistry* **2016,** *88* (22), 11244-11252.

101.   Seyeux, A.; Zanna, S.; Marcus, P., 8 - Surface analysis techniques for investigating biocorrosion. In *Understanding Biocorrosion*, Woodhead Publishing: Oxford, 2014; pp 197-212.

102.   Tuccitto, N.; Marletta, G.; Carnazza, S.; Grasso, L.; Caratozzolo, M.; Guglielmino, S.; Licciardello, A., ToF-SIMS imaging of surface self-organized fractal patterns of bacteria. *Surface and Interface Analysis* **2011,** *43* (1-2), 370-375.

103.   Seyeux, A.; Zanna, S.; Allion, A.; Marcus, P., The fate of the protective oxide film on stainless steel upon early stage growth of a biofilm. *Corrosion Science* **2015,** *91*, 352-356.

104.   Seyeux, A.; Marcus, P., Analysis of the chemical or bacterial origin of iron sulfides on steel by time of flight secondary ion mass spectrometry (ToF-SIMS). *Corrosion Science* **2016,** *112*, 728-733.

105.   Wikieł, A. J.; Datsenko, I.; Vera, M.; Sand, W., Impact of Desulfovibrio alaskensis biofilms on corrosion behaviour of carbon steel in marine environment. *Bioelectrochemistry* **2014,** *97*, 52-60.

106.   Chen, Y.; Tang, Q.; Senko, J. M.; Cheng, G.; Zhang Newby, B.-m.; Castaneda, H.; Ju, L.-K., Long-term survival of *Desulfovibrio vulgaris* on carbon steel and associated pitting corrosion. *Corrosion Science* **2015,** *90*, 89-100.

107. Little, B. J.; Ray, R. I.; Lee, J. S., Diagnosing, Measuring, and Monitoring Microbiologically Influenced Corrosion. In *Uhlig's Corrosion Handbook*, John Wiley & Sons, Inc.: **2011**; pp 1203-1216.

108. Beech, I. B.; Smith, J. R.; Steele, A. A.; Penegar, I.; Campbell, S. A., The use of atomic force microscopy for studying interactions of bacterial biofilms with surfaces. *Colloids and Surfaces B: Biointerfaces* **2002,** *23* (2–3), 231-247.

109. Sheng, X.; Ting, Y. P.; Pehkonen, S. O., Force measurements of bacterial adhesion on metals using a cell probe atomic force microscope. *Journal of Colloid and Interface Science* **2007,** *310* (2), 661-669.

110. Dufrêne, Y. F., Atomic force microscopy, a powerful tool in microbiology. *Journal of bacteriology* **2002,** *184* (19), 5205-5213.

111. Xu, L.-C.; Chan, K.-Y.; Fang, H. H. P., Application of atomic force microscopy in the study of microbiologically influenced corrosion. *Materials Characterization* **2002,** *48* (2–3), 195-203.

112. Fang, H. H. P.; Chan, K.-Y.; Xu, L.-C., Quantification of bacterial adhesion forces using atomic force microscopy (AFM). *Journal of Microbiological Methods* **2000,** *40* (1), 89-97.

113. Machuca, L. L.; Jeffrey, R.; Melchers, R. E., Microorganisms associated with corrosion of structural steel in diverse atmospheres. *International Biodeterioration and Biodegradation* **2016,** *114*, 234-243.

114. Hou, Y. Corrosion Monitoring Based on Recurrence Quantification Analysis of Electrochemical Noise and Machine Learning Methods. 2018.

115. Dong, Z. H.; Shi, W.; Ruan, H. M.; Zhang, G. A., Heterogeneous corrosion of mild steel under SRB-biofilm characterised by electrochemical mapping technique. *Corrosion Science* **2011,** *53* (9), 2978-2987.

116. Kim, T.; Kang, J.; Lee, J.-H.; Yoon, J., Influence of attached bacteria and biofilm on double-layer capacitance during biofilm monitoring by electrochemical impedance spectroscopy. *Water Research* **2011,** *45* (15), 4615-4622.

117. Bayoudh, S.; Othmane, A.; Ponsonnet, L.; Ouada, H. B., Electrical detection and characterization of bacterial adhesion using electrochemical impedance spectroscopy-based flow chamber. *Colloids and Surfaces A: physicochemical and engineering aspects* **2008,** *318* (1), 291-300.

118.   Ben-Yoav, H.; Freeman, A.; Sternheim, M.; Shacham-Diamand, Y., An electrochemical impedance model for integrated bacterial biofilms. *Electrochimica Acta* **2011,** *56* (23), 7780-7786.

119.   Beese, P.; Venzlaff, H.; Srinivasan, J.; Garrelfs, J.; Stratmann, M.; Mayrhofer, K. J. J., Monitoring of anaerobic microbially influenced corrosion via electrochemical frequency modulation. *Electrochimica Acta* **2013,** *105*, 239-247.

120.   Kang, J.; Kim, T.; Tak, Y.; Lee, J.-H.; Yoon, J., Cyclic voltammetry for monitoring bacterial attachment and biofilm formation. *Journal of Industrial and Engineering Chemistry* **2012,** *18* (2), 800-807.

121.   MacHuca, L. L.; Bailey, S. I.; Gubner, R., Microbial corrosion resistance of stainless steels for marine energy installations. In *Advanced Materials Research*, **2012**; Vol. 347-353, pp 3591-3596.

122.   Machuca, L. L.; Jeffrey, R.; Bailey, S. I.; Gubner, R.; Watkin, E. L. J.; Ginige, M. P.; Kaksonen, A. H.; Heidersbach, K., Filtration-UV irradiation as an option for mitigating the risk of microbiologically influenced corrosion of subsea construction alloys in seawater. *Corrosion Science* **2014,** *79*, 89-99.

123.   Mansouri, J.; Harrisson, S.; Chen, V., Strategies for controlling biofouling in membrane filtration systems: challenges and opportunities. *Journal of Materials Chemistry* **2010,** *20* (22), 4567-4586.

124.   Ganzer, G.; McIlwaine, D.; Diemer, J.; Freid, M.; Russo, M., Applications of Glutaraldehyde in the Control of MIC. In *CORROSION 2001*, NACE International: Houston, Texas, 2001.

125.   Wen, J.; Zhao, K.; Gu, T.; Raad, I. I., A green biocide enhancer for the treatment of sulfate-reducing bacteria (SRB) biofilms on carbon steel surfaces using glutaraldehyde. *International Biodeterioration & Biodegradation* **2009,** *63* (8), 1102-1106.

126.   Greene, E. A.; Brunelle, V.; Jenneman, G. E.; Voordouw, G., Synergistic Inhibition of Microbial Sulfide Production by Combinations of the Metabolic Inhibitor Nitrite and Biocides. *Applied and environmental microbiology* **2006,** *72* (12), 7897-7901.

127.   Cloete, T. E.; Jacobs, L.; Broezel, V. S., The chemical control of biofouling in industrial water systems. *Biodegradation* **1998,** *9* (1), 23-37.

128. Talbot, R. E.; Larsen, J.; Sanders, P. F., Experience With the Use of Tetrakishydroxymethylphosphonium Sulfate (THPS) for the Control of Downhole Hydrogen Sulfide. In *Corrosion 2000*, NACE International: Orlando, Florida, 2000.

129. Wen, J.; Xu, D.; Gu, T.; Raad, I., A green triple biocide cocktail consisting of a biocide, EDDS and methanol for the mitigation of planktonic and sessile sulfate-reducing bacteria. *World journal of microbiology & biotechnology* **2012,** *28* (2), 431-5.

130. Kolodkin-Gal, I.; Romero, D.; Cao, S.; Clardy, J.; Kolter, R.; Losick, R., D-Amino Acids Trigger Biofilm Disassembly. *Science* **2010,** *328* (5978), 627-629.

131. Xu, D.; Wen, J.; Gu, T.; Raad, I., Biocide cocktail consisting of glutaraldehyde, ethylene diamine disuccinate (EDDS), and methanol for the mitigation of souring and biocorrosion. *Corrosion* **2012,** *68* (11), 994-1002.

132. Xu, D.; Li, Y.; Gu, T., A synergistic d-tyrosine and tetrakis hydroxymethyl phosphonium sulfate biocide combination for the mitigation of an SRB biofilm. *World Journal of Microbiology & Biotechnology* **2012,** *28* (10), 3067-3074.

133. Jia, R.; Yang, D.; Li, Y.; Xu, D.; Gu, T., Mitigation of the Desulfovibrio vulgaris biofilm using alkyldimethylbenzylammonium chloride enhanced by D-amino acids. *International Biodeterioration & Biodegradation* **2017,** *117*, 97-104.

134. Hobley, L.; Kim, S. H.; Maezato, Y.; Wyllie, S.; Fairlamb, A. H.; Stanley-Wall, N. R.; Michael, A. J., Norspermidine is not a self-produced trigger for biofilm disassembly. *Cell* **2014,** *156* (4), 844-854.

135. Gutiérrez, D.; Rodríguez-Rubio, L.; Martínez, B.; Rodríguez, A.; García, P., Bacteriophages as weapons against bacterial biofilms in the food industry. *Frontiers in microbiology* **2016,** *7*, 825.

136. Eydal, H. S.; Jägevall, S.; Hermansson, M.; Pedersen, K., Bacteriophage lytic to Desulfovibrio aespoeensis isolated from deep groundwater. *The ISME journal* **2009,** *3* (10), 1139.

137. Motlagh, A. M.; Bhattacharjee, A. S.; Goel, R., Biofilm control with natural and genetically-modified phages. *World Journal of Microbiology and Biotechnology* **2016,** *32* (4), 67.

138. Pound, B. G.; Cox, P.; Mortelmans, K. E., The Use of Quaternary Phosphonium Compounds as Antibacterial Corrosion Inhibitors for Low-Alloy Steel. *Corrosion* **2018,** *74* (6), 694-704.

139. AlAbbas, F. M.; Spear, J. R.; Kakpovbia, A.; Balhareth, N. M.; Olson, D. L.; Mishra, B., Bacterial attachment to metal substrate and its effects on microbiologically-influenced corrosion in transporting hydrocarbon pipelines. *Journal of Pipeline Engineering* **2012,** *11* (1), 63.

140. Suarez, E. M.; Machuca, L. L.; Lepkova, K., The role of bacteria in under-deposit corrosion in oil and gas facilities: A review of mechanisms, test methods and corrosion inhibition. *Corrosion and Materials* **2019,** *44* (1), 80-87.

141. Mosher, W.; Mosher, M.; Lam, T.; Cabrera, Y.; Oliver, A.; Tsaprailis, H., Methodology for Accelerated Microbiologically Influenced Corrosion in Under Deposits from Crude Oil Transmission Pipelines. NACE International: 2014.

142. Stams, A. J.; Plugge, C. M., Electron transfer in syntrophic communities of anaerobic bacteria and archaea. *Nature Reviews Microbiology* **2009,** *7* (8), 568-577.

143. Stolyar, S.; Van Dien, S.; Hillesland, K. L.; Pinel, N.; Lie, T. J.; Leigh, J. A.; Stahl, D. A., Metabolic modeling of a mutualistic microbial community. *Molecular Systems Biology* **2007,** *3*, 92-92.

144. Valentine, D. L., Thermodynamic Ecology of Hydrogen-Based Syntrophy. In *Symbiosis: Mechanisms and Model Systems*, Seckbach, J., Ed. Springer Netherlands: Dordrecht, 2002; pp 147-161.

145. Morris, B. E. L.; Henneberger, R.; Huber, H.; Moissl-Eichinger, C., Microbial syntrophy: interaction for the common good. *FEMS Microbiology Reviews* **2013,** *37* (3), 384-406.

146. Warikoo, V.; McInerney, M. J.; Robinson, J. A.; Suflita, J. M., Interspecies acetate transfer influences the extent of anaerobic benzoate degradation by syntrophic consortia. *Applied and environmental microbiology* **1996,** *62* (1), 26-32.

147. Zhang, T.; Fang, H.; Ko, B., Methanogen population in a marine biofilm corrosive to mild steel. *Applied microbiology and biotechnology* **2003,** *63* (1), 101-106.

148. Mand, J.; Park, H. S.; Jack, T. R.; Voordouw, G., The role of acetogens in microbially influenced corrosion of steel. *Frontiers in Microbiology* **2014,** *5* (268).

149. Li, X.-X.; Yang, T.; Mbadinga, S. M.; Liu, J.-F.; Yang, S.-Z.; Gu, J.-D.; Mu, B.-Z., Responses of Microbial Community Composition to Temperature Gradient and Carbon Steel Corrosion in Production Water of Petroleum Reservoir. *Frontiers in Microbiology* **2017,** *8* (2379).

150.   Beech, I. B.; Sunner, J., Biocorrosion: towards understanding interactions between biofilms and metals. *Curr Opin Biotechnol* **2004,** *15* (3), 181-6.

151.   Kappler, A.; Straub, K. L., Geomicrobiological cycling of iron. *Reviews in Mineralogy and Geochemistry* **2005,** *59* (1), 85-108.

152.   Perez-Gonzalez, T.; Jimenez-Lopez, C.; Neal, A. L.; Rull-Perez, F.; Rodriguez-Navarro, A.; Fernandez-Vivas, A.; Iañez-Pareja, E., Magnetite biomineralization induced by Shewanella oneidensis. *Geochimica et Cosmochimica Acta* **2010,** *74* (3), 967-979.

153.   Vali, H.; Weiss, B.; Li, Y.-L.; Sears, S. K.; Kim, S. S.; Kirschvink, J. L.; Zhang, C. L., Formation of tabular single-domain magnetite induced by Geobacter metallireducens GS-15. *Proceedings of the National Academy of Sciences of the United States of America* **2004,** *101* (46), 16121-16126.

154.   Wu, W.; Li, B.; Hu, J.; Li, J.; Wang, F.; Pan, Y., Iron reduction and magnetite biomineralization mediated by a deep-sea iron-reducing bacterium *Shewanella piezotolerans* WP3. *Journal of Geophysical Research. Biogeosciences* **2011,** *116* (4).

155.   Weber, K. A.; Achenbach, L. A.; Coates, J. D., Microorganisms pumping iron: anaerobic microbial iron oxidation and reduction. *Nature reviews. Microbiology* **2006,** *4* (10), 752-64.

156.   Gu, J. D.; Ford, T. E.; Mitchell, R., Microbiological Corrosion of Metallic Materials. In *Uhlig's Corrosion Handbook*, John Wiley & Sons, Inc.: 2011; pp 549-557.

157.   Little, B.; Wagner, P.; Hart, K.; Ray, R.; Lavoie, D.; Nealson, K.; Aguilar, C., The role of biomineralization in microbiologically influenced corrosion. *Biodegradation* **1998,** *9* (1), 1-10.

158.   Albahri, M.; Barifcani, A.; Dwivedi, D.; Iglauer, S.; Lebedev, M.; MacLeod, I. D.; Machuca, L. L., X-ray micro-computed tomography analysis of accumulated corrosion products in deep-water shipwrecks. *Materials and Corrosion* **2019**, *70* (11), 1977-1998 .

159.   MacLeod, I., Monitoring, modelling and prediction of corrosion rates of historical iron shipwrecks. In *Corrosion and Conservation of Cultural Heritage Metallic Artefacts* **2013**; pp 466-477.

160.   MacLeod, I. D., Corrosion and Conservation Management of the Submarine HMAS AE2 (1915) in the Sea of Marmara, Turkey. *Heritage* **2019,** *2* (1), 868-883.

161.   MacLeod, I. D., In-situ corrosion measurements of WWII shipwrecks in Chuuk Lagoon, quantification of decay mechanisms and rates of deterioration. *Frontiers in Marine Science* **2016,** *3*, 38.

162.   MacLeod, I. D., Corrosion products and site formation processes. *Site formation processes of submerged shipwrecks. Gainesville: University Press of Florida* **2016**.

163.   MacLeod, I. D.; Selman, A.; Selman, C., Assessing the impact of typhoons on historic iron shipwrecks in Chuuk Lagoon through changes in the corrosion microenvironment. *Conservation and Management of Archaeological Sites* **2017,** *19* (4), 269-287.

164.   Doležal, D.; Bolanca, T.; Stefanović, Š. C., Development of UV/VIS spectrometric methodology for corrosion inhibitor residuals monitoring in oilfield brine. Entwicklung von UV/VIS-spektrometrischen Methoden zur Überwachung von Korrosionsinhibitoren im Ölfeld Salzwasser. *Materialwissenschaft und Werkstofftechnik* **2011,** *42* (3), 229-233.

165.   Tan, Y. M.; Revie, R. W., *Heterogeneous electrode processes and localized corrosion*. John Wiley & Sons: **2012**; Vol. 13.

166.   Tan, Y., Understanding the effects of electrode inhomogeneity and electrochemical heterogeneity on pitting corrosion initiation on bare electrode surfaces. *Corrosion Science* **2011,** *53* (5), 1845-1864.

167.   Yang, L.; Chiang, K.-T. K.; Shukla, P. K.; Shiratori, N., Internal Current Effects On Localized Corrosion Rate Measurements Using Coupled Multielectrode Array Sensors. NACE International: 2009.

168.   Yang, L.; Sun, X.; Barnes, R.; Griego, R., Evaluation of Coupled Multielectrode Array Sensor for Monitoring General Corrosion. NACE International: 2015.

169.   Xu, Y.; Tan, M. Y., Probing the initiation and propagation processes of flow accelerated corrosion and erosion corrosion under simulated turbulent flow conditions. *Corrosion Science* **2019,** *151*, 163-174.

170.   Xu, Y.; Tan, M. Y., Visualising the dynamic processes of flow accelerated corrosion and erosion corrosion using an electrochemically integrated electrode array. *Corrosion Science* **2018,** *139*, 438-443.

171. Tan, Y., An overview of techniques for characterizing inhomogeneities in organic surface films and underfilm localized corrosion. *Progress in Organic Coatings* **2013,** *76* (5), 791-803.

172. Varela, F.; Tan, M. Y.; Forsyth, M., Electrochemical Method for Studying Localized Corrosion beneath Disbonded Coatings under Cathodic Protection. *Journal of The Electrochemical Society* **2015,** *162* (10), C515-C527.

173. Tan, M. Y.; Varela, F.; Huo, Y.; Mahdavi, F.; Forsyth, M.; Hinton, B., Monitoring Dynamic Corrosion and Coating Failure on Buried Steel Using an Multi-Electrode Array. In *Corrosion 2017*, NACE International: New Orleans, Louisiana, USA, 2017.

174. Tan, Y., Experimental methods designed for measuring corrosion in highly resistive and inhomogeneous media. *Corrosion Science* **2011,** *53* (4), 1145-1155.

175. Tan, Y.-J.; Bailey, S.; Kinsella, B., Mapping non-uniform corrosion using the wire beam electrode method. III. Water-line corrosion. *Corrosion Science* **2001,** *43* (10), 1931-1937.

176. Tan, Y.-J.; Bailey, S.; Kinsella, B., Mapping non-uniform corrosion using the wire beam electrode method. II. Crevice corrosion and crevice corrosion exemption. *Corrosion Science* **2001,** *43* (10), 1919-1929.

177. Zhang, X.; Wang, W.; Wang, J., A novel device for the wire beam electrode method and its application in the ennoblement study. *Corrosion Science* **2009,** *51* (6), 1475-1479.

178. Tan, Y.-J., An experimental comparison of three wire beam electrode based methods for determining corrosion rates and patterns. *Corrosion Science* **2005,** *47* (7), 1653-1665.

179. Tan, Y. J.; Bailey, S.; Kinsella, B.; Lowe, A., Mapping Corrosion Kinetics Using the Wire Beam Electrode in Conjunction with Electrochemical Noise Resistance Measurements. *Journal of The Electrochemical Society* **2000,** *147* (2), 530-539.

180. Tan, Y.; Aung, N. N.; Liu, T., Evaluating localised corrosion intensity using the wire beam electrode. *Corrosion Science* **2012,** *63*, 379-386.

181. Tsan, K.; Chiang, K.; Yang, L., A Coupled Multielectrode Array Sensor For Corrosion Monitoring At High Temperatures. NACE International: 2008.

182. Wang, W.; Zhang, X.; Wang, J., The influence of local glucose oxidase activity on the potential/current distribution on stainless steel: a study by the wire beam electrode method. *Electrochimica Acta* **2009,** *54* (23), 5598-5604.

183. Liu, H.; Meng, G.; Li, W.; Gu, T.; Liu, H., Microbiologically Influenced Corrosion of Carbon Steel Beneath a Deposit in CO_2-Saturated Formation Water Containing *Desulfotomaculum nigrificans*. *Frontiers in microbiology* **2019,** *10*, 1298-1298.

184. Dall'Agnol, L. T.; Moura, J. J. G., 4 - Sulphate-reducing bacteria (SRB) and biocorrosion. In *Understanding Biocorrosion*, Liengen, T.; Féron, D.; Basséguy, R.; Beech, I. B., Eds. Woodhead Publishing: Oxford, **2014**; pp 77-106.

185. ASTM G59-97. Standard Test Method for Conducting Potentiodynamic Polarization Resistance Measurements. in ASTM International: 2014.

186. ASTM G31 Standard Guide for Laboratory Immersion Corrosion Testing of Metals. in ASTM International: 2012.

187. Venkateswaran, K.; Moser, D. P.; Dollhopf, M. E.; Lies, D. P.; Saffarini, D. A.; MacGregor, B. J.; Ringelberg, D. B.; White, D. C.; Nishijima, M.; Sano, H.; Burghardt, J.; Stackebrandt, E.; Nealson, K. H., Polyphasic taxonomy of the genus Shewanella and description of Shewanella oneidensis sp. nov. *International Journal of Systematic and Evolutionary Microbiology* **1999,** *49* (2), 705-724.

Chapter II

E.M. Suarez, L.L. Machuca, Kateřina Lepková.

The Role of Bacteria in Under-Deposit Corrosion in Oil and Gas Facilities: A review of Mechanisms, Test Methods and Corrosion Inhibition.

An original reprint of the publication is shown in Appendix 2

Chapter III

E.M. Suarez, L.L. Machuca, B. Kinsella, Kateřina Lepková.

CO₂ Corrosion Inhibitors Performance at Deposited-Carbon Steel and Their Adsorption on Different Deposits.

An original reprint of the publication is shown in appendix 3.

Detailed information about the setup is provided in Appendix 1, sub-section 1.2.

Chapter IV:

E.M. Suarez, L.L. Machuca, M.Y. Tan, M. Forsyth, B. Kinsella, Kateřina Lepková.

Molecular characteristics affecting the efficiency of corrosion inhibitors at sand-deposited carbon steel: A new approach using a multi-electrode array.

Manuscript submitted.

Detailed information about the setup is provided in Appendix 1, sub-section 1.3.

Molecular characteristics affecting the efficiency of corrosion inhibitors at sand-deposited carbon steel: A new approach using a multi-electrode array.

Erika M. Suarez [1,z], Laura L. Machuca [1], Maria Forsyth [2], Mike Yongjun Tan [2], Brian Kinsella [1], Kateřina Lepková [1,z].

[1] *Curtin Corrosion Centre (CCC), Western Australia School of Mines: Minerals, Energy and Chemical Engineering (WASM-MECE), Curtin University, WA 6102, Australia.*

[2] *Institute for Frontier Materials and School of Engineering, Deakin University, VIC 3216, Australia.*

Abstract

CO_2 corrosion inhibition of carbon steel deposited with silica sand was investigated using a wire beam electrode (WBE) array. Different behaviours were observed from two film-forming inhibitors with different molecular characteristics: a larger surfactant molecule with a long chain structure containing both hydrophobic and hydrophilic groups, 1-dodecylpyridinium chloride hydrate (DPC) and a smaller, non-surfactant molecule, 2-mercaptopyrimidine (MPY). MPY suppressed galvanic currents flowing between anodic and cathodic areas at both deposited and non-deposited regions. Contrary, the cationic surfactant inhibitor DPC demonstrated poor performance in reducing galvanic currents even after 96 h contact time. The ineffectiveness of DPC and the effectiveness of MPY are clearly shown by the small potential differences between sand deposited and non-deposited areas and small galvanic currents in the WBE distribution maps. The good performance of MPY is related to its molecular structure that allows its high penetration capacity through the sand layer. These molecular characteristics could be used for selecting efficient molecules as corrosion inhibitors to prevent under deposit corrosion.

4.1. Introduction

Under deposit corrosion (UDC) has been reported to cause equipment failure in oil and gas production and transportation facilities where the accumulation and deposition of solid particles occur in sections with low flow velocities or inclined areas.

UDC cannot be described as a single mechanism since several factors can influence and determine the type and severity of its occurrence. Those factors include the nature of the deposits (either inorganic, organic or mixed), the elemental composition and metallurgy of the steel material, and the presence of corrosive species such as oxygen, hydrogen ions, carbon dioxide, hydrogen sulphide, among others [1-2]. The inorganic deposits can be inert, e.g., silica sand or an active semiconductor material like magnetite, which can support cathodic reactions. Sand deposit is usually transported from the underground rock formation where oil, gas or water are produced. Corrosion products can also have inorganic nature; they are often originated in the system as a result of the metal deterioration. In addition, inorganic materials such as scales can precipitate from water, representing a common problem for the integrity of the assets. Organic deposits can include wax and asphaltene that precipitate from the oil as well as biofilms formed by microbial attachment and further colonisation of the metal surface. Also, deposits can comprise mixtures of organic and inorganic compounds such as biofilms embedded in silica sand, which can lead to microbiologically influenced corrosion (MIC) and UDC [3-6].

Silica sand (SiO_2) is usually present in large quantities in pipelines and typically provide a physical barrier restricting the mass transfer of corrosive species, thus reducing general corrosion. However, the accumulation of sand particles can still cause localised corrosion in CO_2 environments [7-10]. Chemical treatments using corrosion inhibitors is one of the most cost-effective methods to mitigate internal corrosion of carbon steel pipelines [11]. Several compounds have been used as corrosion inhibitors in a CO_2 environment. For instance, nitrogen-based organic surfactants, such as imidazoline amides, imidazoline amidoamines, and their derivatives, have been proven to be effective at reducing corrosion rates by inhibiting CO_2 corrosion [12-15]. However, different studies reported poor performance of imidazoline compounds against localised corrosion [16-17]. Rare earth 4-hydroxycinnamate compounds have also been applied to protect steel surfaces against CO_2 corrosion of mild steel by forming protective inhibiting deposits at the active electrochemical corrosion sites [18-20].

Despite corrosion inhibitors effectiveness in CO_2 ambience, deposits are known to impact the efficiency of corrosion inhibitors [21-22]. Even if an inhibitor compound provides excellent protection to the non-deposited steel, this does not necessarily imply

that the inhibitor will provide corrosion protection to the steel in the presence of deposits.

Different factors are known to affect corrosion inhibition when deposits are present in a system. For instance, the nature of the deposit (whether organic or inorganic) and the thickness of the surface layers can affect the performance of corrosion inhibitors. Also, the porosity, surface area, surface charge, inhibitor type and, the presence of hydrocarbons can impact the corrosion inhibition process [23]. Some inhibitors can also adsorb onto deposits leading to ineffective corrosion mitigation beneath deposit layers. Binks *et al.* and Pandarinathan *et al.* [21-22] demonstrated that inhibitor species adsorbed onto sand deposit, which reduced its availability to protect the metal surfaces. For these reasons, the criteria for selecting inhibitors for preventing under-deposit corrosion can be somewhat different from those used for preventing more usual forms of corrosion. Therefore there are precise needs for convenient methods and selection criteria for under-deposition inhibitors.

Film-forming inhibitors have been postulated as promising candidates for preventing carbon steel corrosion in the presence of different deposits. For instance, 2-mercaptopyrimidine (MPY) demonstrated to provide higher corrosion protection at sand-deposited steel surfaces compare to cationic surfactants such as 1-dodecylpyridinium chloride hydrate (DPC) [21]. Both MPY and DPC have exhibited different properties in terms of performance and adsorption to sand, aluminium oxide and calcium carbonate [7, 24].

This work is designed to study potential methods and selection criteria for under-deposition inhibitors. Multi-electrode array sensors, namely wire beam electrode (WBE) systems, have been used to study different corrosion topics such as erosion-corrosion [25-26], localised corrosion [27], UDC [28-29], and corrosion inhibition [32,38], among others. Particularly for UDC phenomenon, WBE allows visualisation of local variations in corrosion activity such as galvanic effects between deposited and non-deposited areas on the metal surface [28-32].

This study aimed to use the WBE system to evaluate the selected corrosion inhibitors DPC and MPY in the presence of a sand deposit. A better understanding of the electrochemical processes occurring beneath and outside a deposit when inhibitors are applied should assist in selecting a chemical treatment under these conditions.

4.2. Materials and methods

Test materials
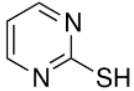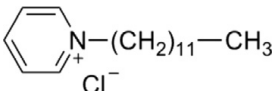
The brine consisted of 3% sodium chloride (NaCl; Chem-Supply analytical reagent, 99.9%) and 0.01% sodium hydrogen carbonate ($NaHCO_3$; Chem-Supply, 99.7%). The brine was prepared in ultra-pure water (Milli-Q system with resistivity 18.5 MΩ cm). The deposited was acid-washed silica sand of analytical reagent grade supplied from Sigma-Aldrich. The properties of the silica sand used in this work were determined in previous studies. These properties included grain size of ~300 μm [21], bulk density 1.42 g/cm^3 and, porosity 27% [24]. The performance of the two corrosion inhibitors (CI), from Sigma-Aldrich, were evaluated at a concentration of 0.892 mM, which is above the critical micelle concentration (CMC) reported elsewhere [24, 33]. Their chemical formula and molecular structures are shown in Table 1. A wire beam electrode (WBE) system, purchased from CPE systems Pty Ltd, was used to measure local galvanic currents and potentials. The WBE was fabricated with 100 tightly packed but electrically isolated steel electrodes, each 2.44 mm x 2.44 mm (0.0595 cm^2) of API X65 pipeline steel with a total surface area of 5.95 cm^2. All the electrodes were arranged as a 10 x 10 square array and embedded in epoxy resin separated at an interval of 0.2 mm from each other [31]. The WBE surface was polished to 1200 grit finish (SiC paper), washed with absolute ethanol and dried with N_2 gas. The reference electrode was a single junction Ag/AgCl reference electrode (placed into a lugging capillary filled with 3% agar and 1.5% 3M KCl). A platinum-coated titanium mesh was used as a counter electrode. The holder used to contain the sand deposit was 1 cm height allowing a sand layer of the same thickness to sit on top of the metal surface. This holder covered approximately 16 wires leading to a 5:1 ratio area (cm^2) of non-deposited and deposited-WBE surface, respectively.

Experimental Setup

The brine (2L) was saturated with CO_2 by sparging it for two hours. The prepared WBE was mounted face-up inside a custom-made glass cell, as shown in Fig. 1. Subsequently, the assembled cell was deoxygenated using CO_2 gas for 15 minutes before pumping the CO_2-saturated brine into the cell. All terminals of the WBE were connected to the WBE measurement instrument. Thus, electrons could move freely

between electrodes, in a similar way as would occur with a single electrode of comparable surface area. Electrochemical measurements were carried out during 24 h of exposure. After completing these measurements, 10 mL of the brine was taken from the cell and mixed with 1.5 g of sand. The mixture was then sparged with CO_2 gas for 30 minutes and injected into the cell directly to a plastic holder placed on one corner of the WBE surface to simulate the under-deposited environment (Fig. 1).

Table 1. Names, chemical formulas and, molecular structures of corrosion inhibitors.

Inhibitor	Chemical formula	Molecular structure
2-mercaptopyrimidine- 98%	$C_4H_4N_2S$	
1-dodecylpiridinium chloride hydrate -98%	$C_{17}H_{30}ClN \cdot xH_2O$	

Electrochemical monitoring across the WBE was again performed during 48 h in the partially covered WBE to study electrochemical differences between non-deposited and sand-deposited steel. After this period, 200 mL of the solution was pumped out from the cell to dissolve the corrosion inhibitor. The solution containing the inhibitor was then sparged with CO_2 gas for 30 minutes and pumped back into the testing cell. Electrochemical measurements were recorded for 96 h to visualise the changes as a result of inhibitor contact to both non-deposited and sand-deposited steel areas. The tests were conducted at 30 ± 5 °C, maintaining CO_2 flow for a total period of 192 h of immersion.

Test methods

Electrochemical tests were performed by coupling all the electrodes in the WBE together, thus simulating a large one-piece working electrode (entire metal surface). In this operational mode, mode 1 (red dashed lines in Fig.1), the WBE system was used

in conjunction with an external potentiostat Gamry reference +600 ™. The 100 electrodes in the array were connected to the auto-switch device and the potentiostat using a three-electrode configuration. Linear polarisation (LP) measurements were performed by applying a potential perturbation of ±10 mV vs OCP at a scan rate of 0.1 mV/s.

Local potentials and galvanic currents measurements were conducted, as shown in mode 2 (blue dashed lines in Fig.1). In this operational mode, the WBE was connected to a pre-programmed auto-switch device and, an ACM AutoZRA (WBE instrument). Corrosion potential distribution maps were obtained by measuring the potential difference between the Ag/AgCl reference electrode and each electrode in the array, i.e., one at the time sequentially. In this voltage mode, all inputs were disconnected; the first electrode was selected and connected to the internal voltmeter and the potential measured. The next electrode in the sequence was then selected, and the voltage measured, as per the first measurement. These steps were repeated for each electrode until the voltage at all electrodes had been measured.

Current distribution maps were obtained by performing sequential measurements between each electrode and the remaining 99 electrodes shorted together. In this current mode, all inputs were connected to a 16-bit analogue-to-digital converter (ADC); the selected electrode was then connected to the terminal of the ZRA. Then the next electrode in the sequence was selected and current measured as per the first measurement. These steps were repeated for each electrode to complete the current measurements across the surface of the WBE. A total of 100 potential and 100 current measurements were performed, and both sets of measurements were plotted using OriginPro® 2019 to obtain potential and current distribution mapping across the WBE surface.

4.3. Results and discussion

Electrochemical measurements at the coupled steel WBE (Operation mode 1)

Fig. 2 shows corrosion potentials and corrosion rates from LP measurements monitored at the coupled WBE sensor following the same stages of events described

in section 2.2. In this mode, the WBE system is connected to the potentiostat to perform electrochemical measurements connecting all-steel electrodes of the sensor
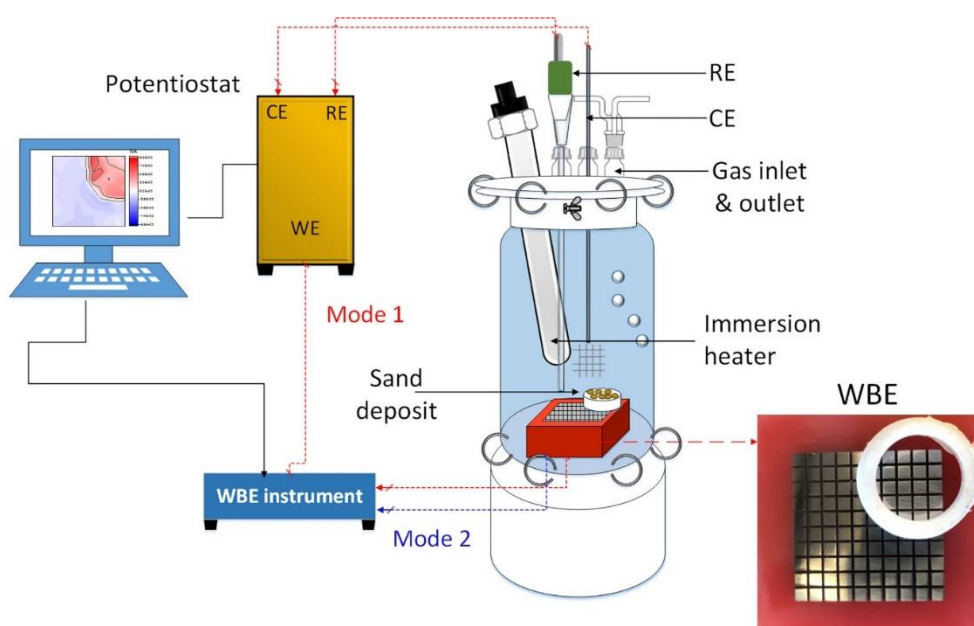
Figure 1. Schematic diagram of the experimental setup of UDC testing and its inhibition in a partially covered WBE.

and thus, working as a one-piece electrode. It can be seen in Fig. 2a that from 12 h to 24 h of immersion in the brine solution, the potentials shifted positively by ~10 mV. After sand addition and during 48 h the corrosion potentials remained steady.

After inhibitor addition, the potentials shifted again more positively by +45 mV and +23 mV to values of -645 mV and -665 mV for MPY and DPC, respectively. Maximum values of -635 mV for MPY and -656 mV for DPC were obtained after 24 h contact with these inhibitors (120 h total immersion). This positive shift indicated that both corrosion inhibitors penetrated and influenced the steel surface. A similar observation was previously reported in at carbon steel surfaces fully covered with a sand deposit where MPY caused corrosion potential to shift positively by + 40 mV compared to the sand-free surfaces [24].

Fig. 2b indicated a decrease of corrosion rates from ~1.4 mmpy at 24 h immersion in brine to 1.0 mmpy after sand addition. The corrosion rates further decreased after inhibitors addition. This was particularly noticeable with MPY where the corrosion rates dropped to 0.1 and 0.04 mmpy after 5 and 96 hours respectively.

Contrary, after 5 hours addition of DPC, the recorded corrosion rate was still high at 1.1 mmpy. A reasonable level of protection achieved by this cationic surfactant was not evident until after 24 h contact, where the corrosion rates were 0.3 and 0.2 mmpy respectively after 24 h and 96 h.

Local corrosion potential measurements at steel WBE (Operation mode 2)

Fig. 3 shows potential distribution maps, following the same order of the sequence mentioned at the beginning of this section. In general, the potential maps are in agreement with galvanic current maps for both tests, which will be discussed in the following section, Section 3.3.

Typically, when a galvanic reaction takes place without an external polarisation, the areas of relatively negative potential behave as the anodes where the oxidation of iron takes place, and the areas of greater positive potential behave as cathodes supporting the hydrogen evolution reaction by reduction of the dissociated hydrogen ions (H+).
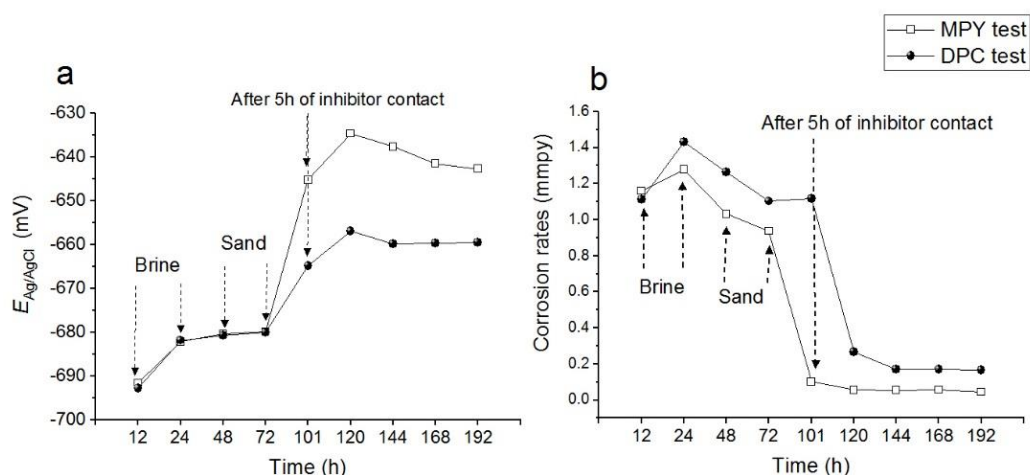
Figure 2. **a)** Open circuit potential and **b)** corrosion rates from linear polarisation resistance measurements recorded at the coupled WBE immersed in CO_2-saturated brine at 30ºC for 192 h. Sequence: 24 h in brine, followed by 48 h in the partially covered WBE with sand and, 96 h corrosion monitoring after inhibitor addition.

The possible overall reactions can be as follows [34-36]:

Anodic reaction: [Eq. 1]

Fe → Fe^{2+} + 2e^-
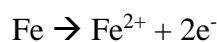
Cathodic reaction: [Eq. 2]

$$2H^+ + 2e^- \rightarrow H_2$$
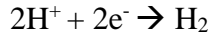
It can be seen in Fig. 3b-c differences in local corrosion potentials between the sand-deposited area and non-deposited steel (between 20-30 mV approximately). Even though these differences were not so marked, they could be easily detected on the maps by measuring local corrosion potentials (operation mode 2 in Fig. 1).
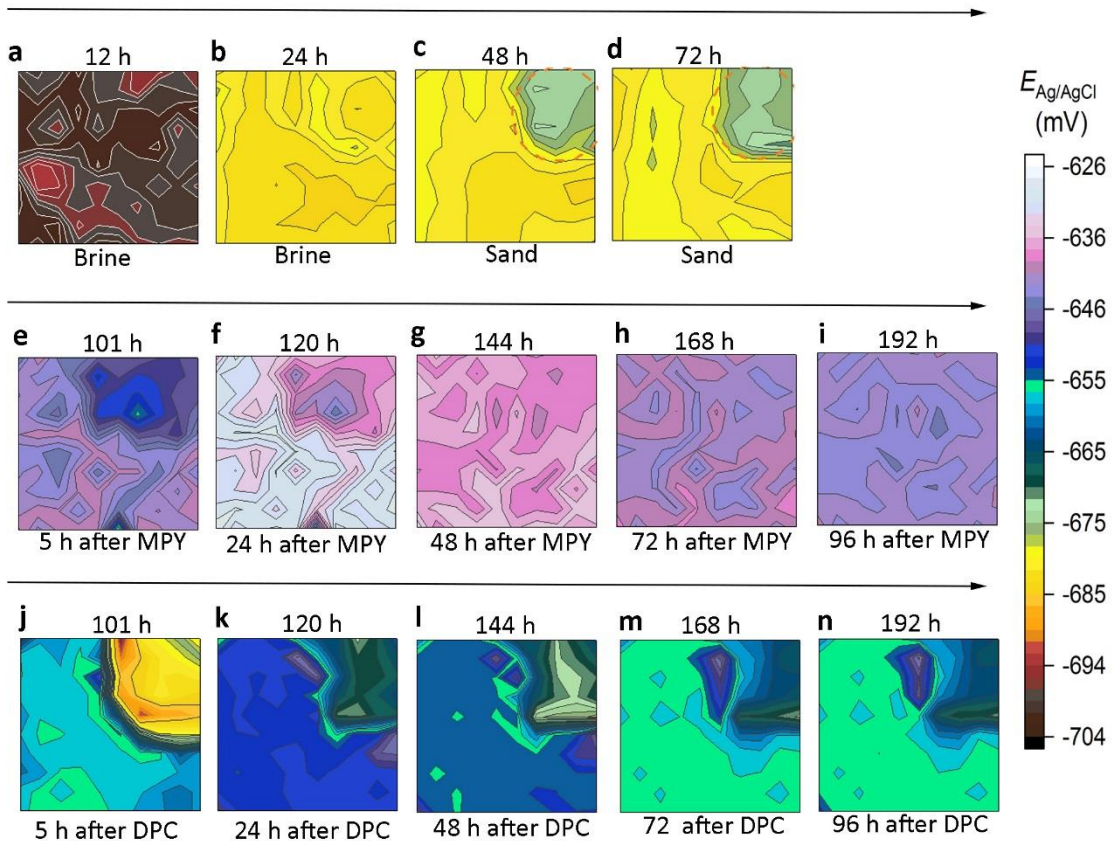
Figure 3. Potential distribution maps of X65 WBE immersed in CO_2-saturated brine. Sequence: **a-b)** immerse in brine; **c-d)** maps after silica sand addition on the top right corner of the electrode array (4X4 electrodes delimitated inside the orange dashed line); **e-i)** maps after MPY addition (0.892mM); **j-n)** maps after DPC addition (0.892mM).

In contrast, when the electrodes in the WBE sensor were coupled (operation mode 1 in Fig. 1) to measure the average corrosion potential at the interphase, the change in the OCP after sand addition was negligible (Fig. 2a). This demonstrates the power of the WBE to monitor areas of localised potential and localised corrosion taking place as opposed to a single metal electrode of similar surface area. As stated by Tan *et al.*,[31] measuring the corrosion potential of the entire metal surface (one-piece electrode) does not allow to visualise heterogeneous electrochemical processes.

MPY shifted the potential to more positive values in both deposited and non-deposited areas of the electrode (Fig. 3e-i). DPC also caused the corrosion potential to shift positively but not that noticeable and only in the non-deposited area of steel. The area beneath the sand, on the contrary, shifted to more negative values. Corrosion potentials between -685 mV and -740 mV were still measured underneath the sand deposit 5h after addition of DPC (Fig. 3j). This shift in potential towards more negative values at the sand-deposited area was again not noticeable when corrosion potential measurements were performed at the coupled electrodes (Fig. 2a).

After 5h addition of DPC addition, i.e., from 24 h to 96 h, corrosion potentials under the deposit gradually shifted more positively to reach similar values to those at the uncovered steel surface (Fig. 3k-3n). This more uniform distribution of potential, reached after 96 h exposure, likely corresponds to the gradual transport of the DPC through the sand to the steel surface. This uniform distribution of potentials is in agreement with Fig. 2 showing a low corrosion rate value recorded after 96 hours of DPC addition.

Local galvanic current measurements at steel WBE (Operation mode 2)

In general, the galvanic currents maps recorded after inhibitors contact are in agreement with their respective potential distribution maps (Fig. 3).

Fig. 4 displays galvanic currents distribution maps across the WBE immersed in CO_2-saturated brine. It can be seen that in Fig. 4a, at 12 h immersion with no sand present, various anodic and cathodic sites are shown across the steel surface due to the heterogeneous nature of the corrosion process. These areas continued to vary in time and space, as shown in Fig. 4b at 24 h immersion. However, after sand addition (Fig. 4c), the area under sand deposit exhibits net cathodic galvanic current behaviour due to the reduction of mass transfer of corroding species, H^+ and H_2CO_3. Non-deposited areas of steel outside of deposit show areas of anodic and cathodic behaviour due to general and heterogeneous nature of the corrosion process. Seventy-two (72) hours of immersion and 24 h after sand addition (Fig. 4d), the area underneath the sand layers continued to show cathodic current behaviour, while areas adjacent to the deposit supported anodic current reactions. Other areas across the non-deposited steel surface

continued to demonstrate anodic and cathodic behaviour due to heterogeneous general corrosion.

Figure 4.Galvanic current distribution maps of X65 WBE immerse in CO_2-saturated brine. The range of reds and blues represent anodic and cathodic areas, respectively. Sequence: **a-b)** immerse in brine; **c-d)** maps after silica sand addition on the top right corner of the electrode array (4X4 electrodes delimitated inside the orange dashed line); **e-j)** maps after MPY addition (0.892mM). Inset: maximum anodic and cathodic current in red and blue type, respectively

Ninety-six (96) hours of immersion, 48 h after sand addition and, 1 minute after MPY addition (Fig. 4e) there was almost an immediate reversal of galvanic currents. The area under the sand reverted to anodic current behaviour due to the sand reducing inhibitor mass transfer to the steel surface. Areas outside the deposit exhibit general cathodic behaviour. After 101 h immersion and, 5 h after MPY addition (Fig. 4f), the anodic current generated under the sand reduced in intensity due to the MPY penetrating the sand and filming the steel surface. The magnitude of the galvanic currents was reduced substantially. After 120-192 h immersion and 24-96 h after inhibitor addition (Fig. 4g-j) sees a continuing development in time and space of anode and cathode current regions. Nevertheless, the magnitude of these currents is substantially lower, demonstrating the good performance of MPY as a corrosion inhibitor. The small magnitude anodic and cathodic current areas illustrate a more uniform and low corrosion process, which may be related to the rapid and robust surface complexes that pyrimidine derivatives form on the metal changing both cathodic and anodic reactions across the surfaces [37]. This superior protection exhibited

by MPY even after 96 h of addition suggests a strong film persistency of this sulphur containing molecules. The performance of this pyrimidine derivative compound has been tested and reported as highly protective against CO_2 corrosion of carbon steel fully covered with silica sand, aluminium oxide and calcium carbonate deposit [21, 24]. Reznik et al. [37] stated that mercaptopyrimidines form stable complexes with steel surfaces modifying both anodic and cathodic reactions under CO_2 conditions. In the present study, MPY provided fast, effective and prolonged corrosion protection by suppressing galvanic currents flowing between anodic and cathodic areas at the non-deposited and sand-deposited steel. The effectiveness of MPY reflected in small galvanic currents and potential differences recorded across the WBE surface can potentially be used for investigating under deposit corrosion (UDC) and also for selecting and investigating the efficiency of corrosion inhibitors to prevent this type of corrosion.

In the current distribution maps recorded for evaluating DPC inhibitor (Fig. 5), the first 72 h of immersion without inhibitor (Fig. 5a-d) followed the same pattern as the MPY test. However, after 1 min addition of this cationic surfactant compound (Fig. 5e), the anodic and cathodic currents reached relatively high values of 6856 nA and, -2350 nA respectively. This current reversal was more marked than those recorded after MPY addition (Fig. 5e). It can be seen in Fig. 5f that after 5 h of DPC being added, the anodic currents continued to increase. After 24 h (Fig. 5g), galvanic currents had decreased to some extent but not sufficient to provide adequate corrosion protection in the sand-deposited area during this contact period. In fact, after 96 h DPC exposure, the WBE exhibited areas with higher galvanic currents than the non-deposited WBE initially immersed in the uninhibited brine (Fig. 5a-c).

A similar observation was made by Suarez et al. [24] in fully covered carbon steels with silica sand where this cationic surfactant was not effective in reducing corrosion under CO_2 conditions. It is possible that DPC adsorption on silica sand led to a loss of inhibitor and thus, impacting the performance of this surfactant. Binks et al. [22] demonstrated inhibitors ineffectiveness, as a result of their parasitic adsorption onto competitor surfaces like sand. Pandarinathan et al. [21] reported that DPC had higher adsorption on silica sand (0.14 mg/g of sand) than MPY on this mineral deposit (<0.02 mg/g of sand) after 72 h contact under CO_2 conditions. The author also suggested that

the hydrophilic quaternary ammonium head of the surfactant is attracted by the acquired negative charges at the sand grains.
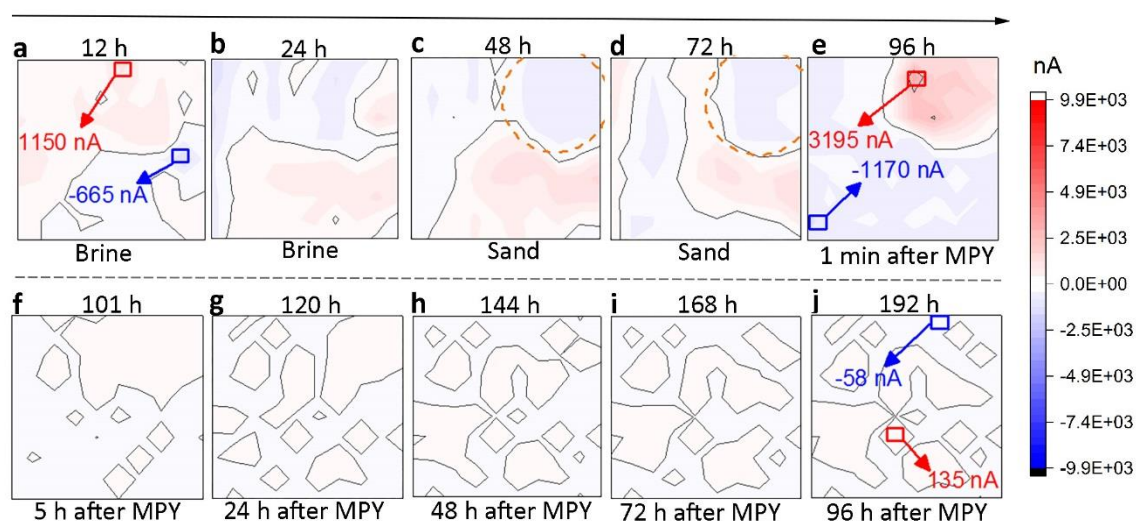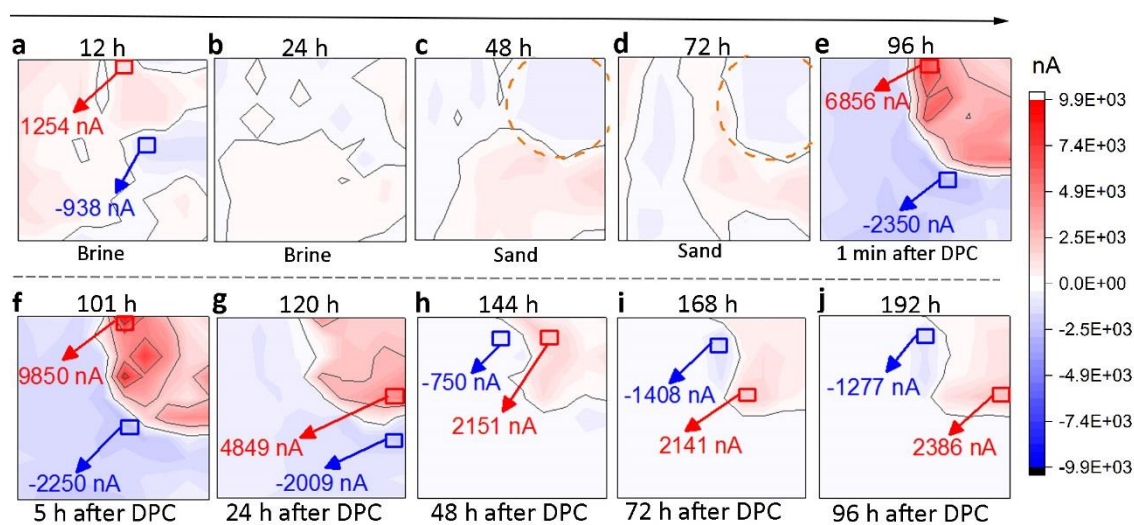

Figure 5. Galvanic current distribution maps of X65 WBE immerse in CO_2-saturated brine. The range of reds and blues represent anodic and cathodic areas, respectively. Sequence**: a-b)** immerse in brine; **c-d)** maps after silica sand addition on the top right corner of the electrode array (4X4 electrodes delimitated for the orange dashed line); **e-j)** maps after DPC addition (0.892mM). Inset: maximum anodic and cathodic currents in red and blue type, respectively.

Another possible explanation for the inhibition ineffectiveness of this surfactant could be related to the low penetration capability due to its larger and long alkyl chain molecule as well as its stronger adsorption at silica sand. DPC molecules can agglomerate to form relatively large micelles. These micelles, when formed in solution, may have difficulty penetrating the sand layer. The concentration of DPC used of 0.892 mM is above the CMC of 0.211 mM [24, 33]. Based on these results, it can be suggested to avoid large and long alkyl chain molecules with high tendency to preferentially adsorb on a sand deposit as an essential criterion for selecting corrosion inhibitors for preventing under deposit corrosion (UDC).

In real case scenarios, the presence of deposits in a pipeline and treatment with this or an incorrect inhibitor formulation could create higher galvanic currents and more susceptibility to localised corrosion attack. For instance, Tan *et al*. [28] demonstrated that imidazoline initiated under-deposit corrosion on a wire beam

electrode. Thus, leading to an opposite effect to what is expected from a corrosion inhibitor.

4.4. Conclusions

• A new approach to evaluate and discover inhibitors for preventing under-deposit corrosion have been proposed and assessed through experiments. The WBE system was proven to be a suitable method for visualising specific electrochemical events related to under-deposit corrosion inhibitor performance, including their rate and effectiveness of penetration through deposits in a CO_2 environment.

• It was shown that the organic filming corrosion inhibitors, 2-mercaptopyrimidine (MPY) and 1-dodecylpyridinium chloride (DPC) were able to create differences in potential (anodic and cathodic areas) resulting in galvanic corrosion currents on the surface of carbon steel. The smaller non-surfactant MPY molecule was shown to be more effective in penetrating a silica sand deposit and preventing under deposit corrosion.

• DPC did not perform efficiently underneath sand layers. The galvanic currents decreased to some extent but remained higher than the currents recorded at the non-deposited WBE sensor immersed in the uninhibited brine solution.

• The ineffectiveness of DPC and the effectiveness of MPY are clearly shown by the characteristically small potential differences between sand deposited, non-deposited areas, and minimal galvanic currents in the WBE distribution maps.

• The good performance of MPY is related to its molecular structure that allows its high penetration capacity through the sand layer. These molecular characteristics have been proposed as a new inhibitor selection criterion for selecting efficient molecules as corrosion inhibitors to prevent under deposit corrosion.

4.5. References

1.   Vera, J. R.; Daniels, D.; Achour, M. H., Under Deposit Corrosion (UDC) In The Oil And Gas Industry: A Review Of Mechanisms, Testing And Mitigation. NACE International: 2012; Vol. 4, pp 3028-3040.

2.   Ly, K. T.; Blumer, D. J.; Bohon, W. M.; Chan, A., Novel Chemical Dispersant for Removal of Organic/Inorganic "Schmoo" Scale in Produced Water Injection Systems. NACE International: 1998.

3.   Suarez, E. M.; Lepková, K.; Kinsella, B.; Machuca, L. L., Aggressive Corrosion of Steel by a Thermophilic Microbial Consortium in the Presence and Absence of sand. *International Biodeterioration & Biodegradation* **2019,** *137*, 137-146.

4.   Suarez, E. M; Machuca, L.; Lepková, K., The Role of Bacteria in Under-Deposit Corrosion in Oil and Gas Facilities: A Review of Mechanisms, Test Methods and Corrosion Inhibition. *Corrosion and Materials* **2019,** *44* (1), 80-87.

5.   Machuca, L. L.; Lepková, K.; Petroski, A., Corrosion of Carbon Steel in the Presence of Oilfield Deposit and Thiosulphate-Reducing Bacteria in CO_2 Environment. *Corrosion Science* **2017,** *129*, 18-25.

6.   Machuca, L. L., Understanding and Addressing Microbiologically Influence Corrosion (MIC). *Corrosion and Materials* **2019,** *44* (1), 88-96.

7.   Pandarinathan, V.; Lepková, K.; Bailey, S. I.; Gubner, R., Impact of Mineral Deposits on CO_2 Corrosion of Carbon Steel. NACE International: Houston, TX, 2013.

8.   Hou, Y.; Aldrich, C.; Lepková, K.; Kinsella, B., Detection of Under Deposit Corrosion in a CO_2 Environment by Using Electrochemical Noise and Recurrence Quantification Analysis. *Electrochimica Acta* **2018,** *274*, 160-169.

9.   Pandarinathan, V.; Lepková, K.; van Bronswijk, W., Chukanovite $(Fe_2(OH)2CO_3)$ Identified as a Corrosion Product at Sand-Deposited Carbon Steel in CO_2-Saturated Brine. *Corrosion Science* **2014,** *85*, 26-32.

10.   Huang, J.; Brown, B.; Jiang, X.; Kinsella, B.; Nesic, S., Internal CO_2 Corrosion Of Mild Steel Pipelines Under Inert Solid Deposits. In *NACE - International Corrosion Conference Series*, NACE International: San Antonio, TX, 2010.

11.   Papavinasam, S., Corrosion Inhibitors. In *Uhlig's Corrosion Handbook*, John Wiley & Sons, Inc. 2011; pp 1021-1032.

12.   Jovancicevic, V.; Ramachandran, S.; Prince, P., Inhibition of Carbon Dioxide Corrosion of Mild Steel by Imidazolines and their Precursors. *Corrosion* **1999,** *55* (5), 449-455.

13.   Zhang, X.; Wang, F.; He, Y.; Du, Y., Study of the Inhibition Mechanism of Imidazoline Amide on CO_2 Corrosion of Armco iron. *Corrosion Science* **2001,** *43* (8), 1417-1431.

14.   Edwards, A.; Osborne, C.; Webster, S.; Klenerman, D.; Joseph, M.; Ostovar, P.; Doyle, M., Mechanistic Studies of the Corrosion Inhibitor oleic Imidazoline. *Corrosion Science* **1994,** *36* (2), 315-325.

15.   Pandarinathan, V.; Lepková, K.; Bailey, S. I.; Gubner, R., Inhibition of Under-Deposit Corrosion of Carbon Steel by Thiobenzamide. *Journal of the Electrochemical Society* **2013,** *160* (9), C432-C440.

16.   Tan, M.Y.J; Mocerino, M.; Paterson, T., Organic Molecules Showing the Characteristics of Localised Corrosion Aggravation and Inhibition. *Corrosion Science* **2011,** *53* (5), 2041-2045.

17.   Liu, X.; Okafor, P.; Zheng, Y., The Inhibition of CO_2 Corrosion of N80 Mild Steel in Single Liquid Phase and Liquid/Particle Two-Phase Flow by Aminoethyl Imidazoline Derivatives. *Corrosion Science* **2009,** *51* (4), 744-751.

18.   Nam, N. D.; Mathesh, M.; Hinton, B.; Tan, M. Y. J; Forsyth, M., Rare Earth 4-Hydroxycinnamate Compounds as Carbon Dioxide Corrosion Inhibitors for Steel in Sodium Chloride Solution. *Journal of The Electrochemical Society* **2014,** *161* (12), C527-C534.

19.   Nam, N. D.; Somers, A.; Mathesh, M.; Seter, M.; Hinton, B.; Forsyth, M.; Tan, M. Y. J., The Behaviour of Praseodymium 4-hydroxycinnamate as an Inhibitor For Carbon Dioxide Corrosion and Oxygen Corrosion of Steel in NaCl Solutions. *Corrosion Science* **2014,** *80*, 128-138.

20.   Nam, N. D.; Panaitescu, C.; Tan, M. Y. J.; Forsyth, M.; Hinton, B., An Interaction between Praseodymium 4-Hydroxycinnamate with AS1020 and X65 Steel Microstructures in Carbon Dioxide Environment. *Journal of The Electrochemical Society* **2018,** *165* (2), C50-C59.

21.   Pandarinathan, V.; Lepková, K.; Bailey, S. I.; Gubner, R., Evaluation of corrosion inhibition at sand-deposited carbon steel in CO_2-Saturated Brine. *Corrosion Science* **2013,** *72*, 108-117.

22.   Binks, B. P.; Fletcher, P. D. I.; Salama, I. E.; Horsup, D. I.; Moore, J. A., Quantitative Prediction of the Reduction of Corrosion Inhibitor Effectiveness Due to Parasitic Adsorption onto a Competitor Surface. *Langmuir: the ACS journal of surfaces and colloids* **2011,** *27* (1), 469-473.

23.   De Reus, H.; Hendriksen, L. J. A.; Wilms, M.; Al-Habsi, Y. N.; Durnie, W.; Gough, M., Test Methodologies and Field Verification of Corrosion Inhibitors to Address under Deposit Corrosion in Oil and Gas Production Systems. NACE International: Houston, TX, 2005.

24.   Suarez, E. M.; Machuca, L. L.; Kinsella, B.; Lepková, K., CO_2 Corrosion Inhibitors Performance at Deposit-Covered Carbon Steel and Their Adsorption on Different Deposits. *CORROSION* **2019,** *75* (9), 1118-1127.

25.   Xu, Y.; Tan, M. Y. J, Probing The Initiation and Propagation Processes of Flow Accelerated Corrosion and Erosion Corrosion Under Simulated Turbulent Flow Conditions. *Corrosion Science* **2019,** *151*, 163-174.

26.   Xu, Y.; Tan, M. Y. J, Visualising the Dynamic Processes of Flow Accelerated Corrosion and Erosion Corrosion Using an Electrochemically Integrated Electrode Array. *Corrosion Science* **2018,** *139*, 438-443.

27.   Tan, M.Y. J. Understanding the Effects of Electrode Inhomogeneity and Electrochemical Heterogeneity on Pitting Corrosion Initiation on Bare Electrode Surfaces. *Corrosion Science* **2011,** *53* (5), 1845-1864.

28.   Tan, Y.; Fwu, Y.; Bhardwaj, K., Electrochemical Evaluation of Under-Deposit Corrosion and its Inhibition Using the Wire Beam Electrode Method. *Corrosion Science* **2011,** *53* (4), 1254-1261.

29.   Zhang, G. A.; Yu, N.; Yang, L. Y.; Guo, X. P., Galvanic Corrosion Behavior of Deposit-Covered and Uncovered Carbon Steel. *Corrosion Science* **2014,** *86*, 202-212.

30.   Tan, M.Y. J, Experimental Methods Designed for Measuring Corrosion in Highly Resistive and Inhomogeneous Media. *Corrosion Science* **2011,** *53* (4), 1145-1155.

31.   Tan, M.Y. J; Revie, R. W., *Heterogeneous electrode processes and localized corrosion*. John Wiley & Sons: 2012; Vol. 13.

32.   Hinds, G.; Turnbull, A., Novel Multi-Electrode Test Method for Evaluating Inhibition of Underdeposit Corrosion—Part 1: Sweet Conditions. *CORROSION* **2010,** *66* (4), 046001-046001-10.

33.   Pandarinathan, V.; Lepková, K.; Bailey, S. I.; Becker, T.; Gubner, R., Adsorption of Corrosion Inhibitor 1-Dodecylpyridinium Chloride on Carbon Steel Studied by in Situ AFM and Electrochemical Methods. *Industrial & Engineering Chemistry Research* **2014,** *53* (14), 5858-5865.

34.   Kahyarian, A.; Achour, M.; Nesic, S., CO_2 Corrosion of Mild Steel. In *Trends in Oil and Gas Corrosion Research and Technologies*, 2017; pp 149-190.

35.   Kahyarian, A.; Brown, B.; Nesic, S., *Mechanism of CO_2 Corrosion of Mild Steel: a New Narrative*. 2018.

36.   Nešić, S., Carbon Dioxide Corrosion of Mild Steel. In *Uhlig's Corrosion Handbook*, John Wiley & Sons, Inc.: 2011; pp 229-245.

37.   Reznik, V. S.; Akamsin, V. D.; Khodyrev, Y. P.; Galiakberov, R. M.; Efremov, Y. Y.; Tiwari, L., Mercaptopyrimidines as Inhibitors of Carbon Dioxide Corrosion of Iron. *Corrosion Science* **2008,** *50* (2), 392-403.

38. Muster, T. H.; Hughes, A. E.; Furman, S. A.; Harvey, T.; Sherman, N.; Hardin, S.; Corrigan, P.; Lau, D.; Scholes, F. H.; White, P. A.; Glenn, M.; Mardel, J.; Garcia, S. J.; Mol, J. M. C., A rapid screening multi-electrode method for the evaluation of corrosion inhibitors. *Electrochimica Acta* **2009**, 54 (12), 3402-3411.

Chapter V

Evaluating Under-deposit Microbial Corrosion using a Bacterial Isolate, Shewanella oneidensis MR-1.

This chapter represents test procedures and observations during and after immersion tests.

Detailed information about the setup is provided in Appendix 1, sub-section 1.4.

Evaluating Under-deposit Microbial Corrosion Using a Bacterial Isolate, *Shewanella oneidensis* **MR-1**

Abstract

Carbon steel corrosion by *Shewanella oneidensis* MR-1 was investigated using electrochemical measurements and surface analytical methods. This under-deposit microbial corrosion (UDMC) study was conducted in different environments, with high and low soluble electron donor (lactate) concentration in which case this bacterium accesses electrons from steel. Biotic test with lactate 59 mM showed lower corrosion damage than the abiotic counterpart. Sand-free samples of biotic test with 5 mM lactate were more corroded than sand-deposited ones. However, sand-deposited samples were affected to some extent, suggesting that this bacterium could surpass the barrier effect generally observed by a sand deposit in abiotic CO_2 anaerobic conditions. FESEM images of cross-sectioned corroded samples evidenced the formation of biofilm underneath and between sand grains. This work highlights the relevance of conducting UDMC studies using single species to gain insights into the understanding of specific microbial mechanisms and their relation to mineral deposits towards steel surfaces integrity.

5.1. Introduction

Shewanella oneidensis MR-1 is an electroactive microorganism which in anaerobic conditions can reduce insoluble iron and manganese oxides. This bacterium can also reduce an extensive list of other compounds such as thiosulphate; nitrate; nitrite; fumarate dimethyl sulfoxide; trimethylamine N-oxide; uranium; sulphur; sulphite and vanadate [1-3]. One of the most cited and controversial metabolism of *Shewanella* sp. associated with corrosion is its ability to reduce iron oxides. In this metabolism, *S.oneidensis* reduces Fe^{3+} protective corrosion products leaving some parts of the steel surface exposed to corrosive species in the solution [4-8]. Conversely, a previous study showed that this metabolism could inhibit corrosion on steel surfaces by the formation of protective iron phosphate layers [9]. Other authors have demonstrated that *S.oneidensis* altered the protective corrosion products layers

composed of magnetite and H_2 as electron donor reactivating the corrosion process developed under this environment [10-12].

Besides the reduction of iron oxides, *S.oneidensis* can perform extracellular electron transfer (EET) by extracting electrons directly from steel surfaces [13-15]. The increasing search for renewable and clean energy to replace conventional fossil fuel sources has contributed to biofilm/metal interaction knowledge. These research areas include bioelectricity production by microbial fuel cells (MFCs) [16-17] and biohydrogen production by microbial electrolysis cells (MECs) [18-19]. The link of MECs research with electrical-microbiologically influenced corrosion (EMIC) is because of microbial activities in biocathodes resemble those activities involved in corrosion. In biocathodes, electrogenic bacteria consume electrons from the electrode to reduce the electron acceptors present in solution [20]. Similarly, in the EMIC mechanism, microorganisms directly utilise zero-valent metallic iron as an electron donor via EET which lead to corrosion under anaerobic conditions [21].

In a microbial electrocatalysis study, *Geobacter Sulfurreducens* used fumarate as an electron acceptor, and in the absence of an electron donor, this bacterium used stainless steel (biocathode) as an electron source. *G. Sulfurreducens* was found responsible for the electrocatalysis of fumarate reduction resulting in significant-high current densities [22]

Previous UDC studies have proven a barrier effect exerted by sand deposits on corrosion of carbon steel surfaces. Sand layers showed to decrease general corrosion under the deposit by reducing the mass transfer of corrosive species to the metal surface [23-25]. However, this blocking effect of deposit layers to corrosive species may present different results in the presence of microorganisms. The occurrence of UDC-MIC or under-deposit microbial corrosion (UDMC) was defined as the combination of electrochemical, physical and microbiological processes compromising pipeline integrity [26].

A previous study demonstrated that a thermophilic microbial consortium corroded sand-deposited steel surfaces suggesting not marked barrier effect exerted by sand when microbes are present. Therefore, in this research was hypothesised that sand layers would affect the corrosion process when the bacterial metabolism relies on the direct contact to the steel surface, i.e. EMIC by using the metallic surface as an electron

source. It was expected that the use of one bacterial species, *S.oneidensis* would facilitate the understanding of UDMC mechanism, which is more difficult to achieve when several metabolic groups are conforming a microbial consortium.

This study aims to evaluate under-deposit microbial corrosion exerted by *Shewanella oneidensis* MR-1 in an environment with an excess of electron donor (lactate) and acceptor (fumarate) and, also in a scenario lacking lactate. Thus, creating suitable conditions for the bacterium to take the electrons from steel surfaces. Investigating the effect of this electroactive bacterium on corrosion of carbon steel beneath sand deposits will contribute to the understanding of the UDMC which is essential to improve control strategies in scenarios where microbes and mineral deposits are present.

5.2. Materials and Methods

5.2.1. Test solutions.

Enriched artificial seawater (ASW) 2.6% salinity was used to maintain *S.oneidensis* isolate as well as test solution of experiments. ASW composition was as follows: sea salts; ammonium chloride (NH_4Cl) 28 mM; sodium lactate as the electron donor (Table 1); sodium fumarate as the electron acceptor (Table 1) and 1 L of ultrapure water (Milli-Q system, resistivity 18.4 MΩ cm). The compounds were mixed and sterilised by autoclave. Then, 20 mL of vitamin solution and 1 mL of trace elements were added to the sterile solution [27]. Final pH was adjusted to pH 7.2 ±0.2 using deoxygenated sodium bicarbonate ($NaHCO_3$) solution 59 mM. The solution was sparged with a gas mixture of CO_2/N_2 for 2 h before transfer to the deoxygenated reactor.

5.2.2. Metal samples and test setup.

Carbon steel coupons (AISI 1030) of 6.2 cm^2 exposed surface area were prepared as working electrodes. Their chemical composition was (wt. %): C (0.37), Mn (0.80), Si (0.282), P (0.012), S (0.001), Cr (0.089), Ni (0.012), Mo (0.004), Sn (0.004), Al (0.01), and Fe (balance). The steel samples were coated with Powercron 6000cx and wet ground up to 600 grit finish. Afterwards, the samples were immersed in ethanol

70% for 5 min, dried with nitrogen and finally exposed to ultraviolet (UV) radiation for 15 minutes each side. The reference electrode was a single junction Ag/AgCl electrode with a lugging capillary filled with sterile 3M KCl. The ceramic tip of the capillary was placed near the steel surface in order to minimise the IR drop. The counter electrode was a platinum-coated mesh.

Table. 1 shows the four immersion tests named as "systems": abiotic reactor containing lactate 59 mM (**I**); biotic reactor containing lactate 59 mM (**II**); biotic reactor containing lactate 5 mM and sand-deposited samples (**III**); 4) biotic reactor containing lactate 5 mM and sand-free samples (**IV**). Systems I and II were supplemented with 59 mM of lactate (electron donor) to facilitate *S.oneidensis* growth by providing an excess of soluble electron donor. It is well known that most of the microorganisms tend to prefer soluble electron donors over the no-soluble ones, e.g. metallic iron. Therefore, it is unlikely that *S.oneidensis* extracted the electrons directly from the metal surface, having an excess of lactate. In systems III and IV, the concentration of lactate, a soluble electron donor, was reduced more than ten times in order to help initiate biofilm establishment. Under this nutrition depletion, it is expected *S.oneidensis* to switch its metabolism once the lactate is consumed. The biofilm is forced to use no-soluble electron donor (metallic iron) from the steel surfaces, hence leading electrical-MIC (EMIC).

All the materials for the test set-up were sterilised by autoclaving, followed by UV radiation before testing. Steel coupons were placed horizontally in glass holders as described elsewhere [28]. For the test with sand, silica sand (Sigma-Aldrich) with a mean particle size of 300μm [23] was used to cover the steel surfaces in systems III and IV. First, the sand was acid-washed and dried before testing [24]. Then, the samples were placed on glass holders and fully covered by the sand deposit of approximately 5 mm thickness.

The reactors were sealed and sparged with a gas mixture of 20% CO_2 in 80% N_2 followed by temperature and stirring adjustment at 30 ± 2 °C, and 200 rpm using a digital hotplate (IKA RTC) with a thermocouple control. A CO_2/N_2 gas blanket was maintained throughout the experimental period. Then, the reactors were dismantled inside an anaerobic (N_2) glove box to avoid steel samples contact with oxygen. All samples were processed in duplicate for the analyses described in the following sections.

Table 1. Different concentrations of the ASW components according to test conditions (System I-IV).

System	Electron donor Sodium DL-lactate (mM)	Electron acceptor Sodium fumarate (mM)	Sea salts (g/L)	Immersion period (days)
I- abiotic test	59	None	23	8
II-biotic tests	59	25	22	10
III-biotic test-sand	5	25	23.8	16
IV-biotic test-no sand	5	25	23.8	16

5.2.3. Bacterial cultures.

Shewanella oneidensis Venkateswaran was purchased from American Type Culture Collection (ATCC® 700550™)[187]. This bacterium was first gradually adapted to high salinity concentration solutions and maintained at 30°C in anaerobic glass vials. The test solution composition varied according to the test condition (section 2.1 and Table 1). Before testing, the bacterial isolate was inoculated at 10% into anaerobic test solution and incubated at 30°C for 48 h (exponential phase ~ 10^8 cell/mL). Bacterial cells were harvested by centrifugation (3,600 x g, 30 min at 30° temperature) to remove metabolic by-products formed by microbial activity in the culture. The supernatant was discarded and, the pellet was suspended in 1 mL of the respective sterile test solution. This suspension was then inoculated into the reactor.

Analytical methods

5.2.4. Bacterial enumeration and pH monitoring.

An aliquot of test solution was collected from each reactor to estimate *S.oneidensis* cells using a Neubauer chamber and, a Nikon Eclipse Ci-L phase-contrast microscope, Nikon Inc. The pH in the solution was monitored using the Thermo Scientific Orion ™ Star A221 pH portable meter using the same aliquot of the test solution.

5.2.5. Test solution chemistry.

Ferrous iron (Fe^{2+}) and total iron (FeT) concentrations of the artificial seawater were measured by spectrophotometer (Hatch, DR3900). The method for determination of Fe^{2+} was 1, 10-phenanthroline method and for total iron was USEPA1 FerroVer® method-2. Ferric iron (Fe^{3+}) was then calculated by deducting Fe^{2+} from FeT values.

5.2.6. *Lactate depletion by silica sand deposit.*

Fourier-transform infrared spectroscopy (FTIR) was used to determine sodium lactate depletion after contact with silica sand deposit. Initially, a calibration curve was created using different lactate solutions (250, 500, 1000, 2000, and 4000 mM) at a maximum absorbance of 1123 nm. Lactate depletion was performed by mixing 8 g of silica sand with 100 mL of lactate solutions (1000 mM) in glass bottles. The bottles were then sparged with CO_2/N_2 for 2 h, capped and kept at 30°C with agitation for 24 h or 48 h (in duplicate for each contact period).

Stirring and temperature were controlled at 150 rpm and 30°C using a Ratek orbital shaker-incubator. After each contact period, the total content was centrifuged at $3260\times$ g for 30 min to remove sand grains from the solution before FTIR analysis. The absorbances were recorded at a wavelength range from 600 nm to 4000 nm using a PerkinElmer 100 FT-IR spectrophotometer. The amount of lactate depleted after each contact time with sand deposit was determined from the calibration curve. The reduction of lactate concentration corresponded to the amount of lactate depleted in mg/g (q_{ads}) on silica sand and was calculated using the following equation [24]:

$$q_{ads} = \frac{(c_i - c_f) \times V}{m} \quad (1)$$

Where C_i corresponds to the lactate concentration before deposit addition in mM = 1000, C_f is the final lactate concentration in the solution after contact with deposits, V is the volume of the test solution in litres = 0.1 L and m is the mass of the deposit (silica sand) in grams = 8 g.

Electrochemical measurements

Electrochemical measurements were carried out using a Gamry reference 600+ potentiostat (Gamry Instruments, Inc.). Linear polarisation resistance (LPR)

measurements were recorded daily within the immersion period using a potential perturbation of ± 10 mV vs. OCP and a scan rate of 0.1667 mV/s. Electrochemical impedance spectroscopy (EIS) measurements were conducted, allowing a stabilisation period of 30 min at OCP before EIS measurements. The AC excitation amplitude of 10 mV over a frequency range of 0.01 Hz to 10 kHz at 10 points per decade was applied. The impedance spectra were analysed using ZView software (Scribner Associates Inc, USA). Potentiodynamic curves were recorded at the end of the experimental period at the potential range of +/- 250 mV vs. OCP at a scan rate of 0.1667 mV/s. The stabilisation period before potentiodynamic measurements was 30 min.

Post-immersion analysis

5.2.7. Microscopy and surface analysis.

Field-emission scanning electron microscopy (FESEM) was carried out to reveal cross-sectional features from the top of the surface layers to the metal base. At the end of the experimental period, one coupon from each reactor was placed in a sealed glass cell under continuous injection of N_2 for one week to ensure complete drying of the sample before surface analysis. After drying, samples were mounted in Epofix® resin and cut to reveal the cross-section profile of the corroded steel. Biofilm-coated coupons were removed from the reactors and fixed in glutaraldehyde and dehydrated with ethanol following a procedure described elsewhere [29]. Then, dried coupons were sputter-coated with platinum (5 nm thickness) for FESEM imaging (Zeiss NEON) of biofilms and deposits on steel surfaces. The microscope was coupled with an energy dispersive X-ray detector for EDS analysis. The EDS-mapping analysis was used to determine the distribution of the elements within surface layers and at specific points at the surfaces. EDS data were analysed using Aztec® 3.0 software (Oxford Instruments NanoAnalysis).

5.2.8. Mass loss measurements and 3D-profilometry.

After the immersion period,   three samples were ultrasonically cleaned using Clarke's solution according to the standard chemical cleaning procedure for the corrosion product removal [30]. Afterwards, corrosion rates from the mass loss of

triplicate steel samples were calculated following the standard ASTM G1 procedure [31]. Two of the cleaned steel samples were used for surface examination to determine the average and the maximum pit depth at each sample using a 3D optical profilometer (Alicona imaging infinite focus microscope IFM G4 3.5). The average pit depth was obtained using the 10 deepest pits measured on each sample. Pitting rate was calculated using the maximum pit depth as described in NACE SP-0075 standard practice [37]. The pitting rate equation is as follows:

$$PR \ (mmpy) = \frac{Depth \ of \ deepest \ pit \ (mm)}{exposure \ time \ (days)} \times 365$$

5.3. Results and discussion

5.3.1. Sodium lactate depletion by silica sand deposit

Fig. 1 gives the FTIR spectra of lactate solutions (250, 500, 1000, 2000, and 4000 mM), and artificial seawater (ASW) containing 1000 mM of lactate after contact with silica sand. From the complete IR wavelength range of the lactate solutions (Fig 1.a), the wavelength range from approximately 1050 to 1150 nm was selected for analysis. Fig. 1b shows the IR spectra of the lactate solutions at a wavelength of 1123 nm of maximum absorbance values (λ max). The correlation coefficient (r) of the linear fit calibration plots was above 0.99, indicating an acceptable calibration.

Fig 1.c displays the IR absorbance spectra of ASW containing 1000 mM of lactate and after 24 and 48 h contact with 8 grams of silica sand. The absorbance intensities (A) at the marked wavelength (λ max) of 1123 nm were used to determine the final lactate concentration (C_f). It can be seen in this figure and Table. 2 that sand deposit reduced lactate concentration by 7.2 % and 9.5% after 24 and 48 h, respectively. This minimum lactate depletion by silica sand indicates no affinity of the deposit for this organic compound. Therefore, lactate could be available for bacterial utilisation, even underneath deposit layers.

5.3.2. Bacterial and pH monitoring:

Fig.2 shows growth monitoring of planktonic *S.oneidensis* cells by direct counting (bacteria/mL) and pH monitoring of the test solution. It can be observed in

Fig.2a that the pH in the system II remained close to 7.2 during the first eight days of immersion and then, decreased by almost 0.2 pH units perhaps due to the metabolic by-products accumulation after one week of immersion.

Table 2. Lactate depletion by silica sand after 24 and 48 h assessed by IR spectrophotometry.

Sand+ Lactate 1000 mM	Absorbance λmax	Concentration Cf*mM	Inhibitor absorbed qads* mM	Reduction %
Sand 24 hours	0.0059	928.4 ± 19.8	0.90	7.2
Sand 48 hours	0.0057	904.8 ± 21.9	1.19	9.5

C_i initial lactate concentration (1000 mM), C_f final lactate concentration
q_{ads} amount of lactate absorbed (mM) on silica sand. Equation 1
V= volume of test solution in L, m= mass of mineral (8 grams)
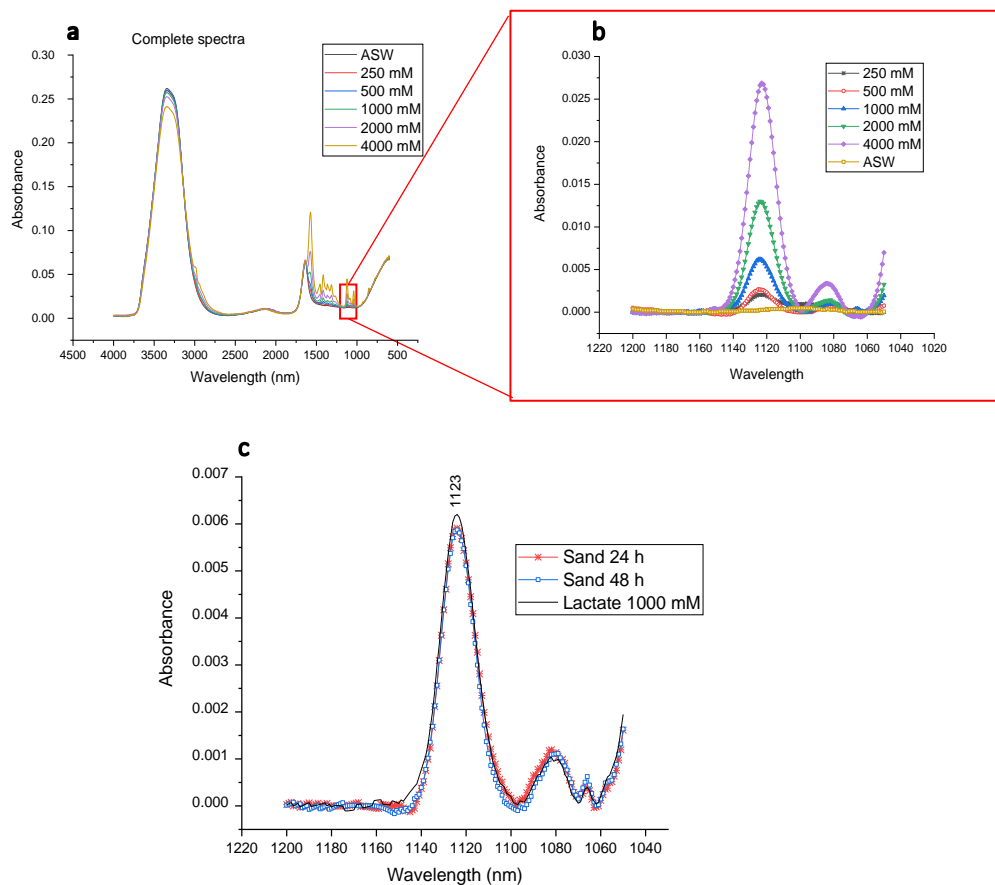
Figure 1. a) FTIR Spectra of the lactate solutions in the complete IR wavelength range; **b)** close-up at the organics IF region; **c)** Absorbance spectra of CO_2/N_2 sparged artificial seawater (ASW) containing 1000 mM of lactate and after 24 and 48 h contact with silica sand (8 grams).

The bacterial enumeration indicated a gradual increase in cell numbers in test solution from 10^7 to 10^8 cells/mL from day 1 to day 5 of immersion. At this time, the cell numbers dropped probably due to a high-speed consumption of nutrients in the solution.

System III (Fig.2b) and IV (Fig.2c) had a similar trend of this bacterial numbers throughout experimental. The high numbers and visible solution turbidity at initial stages indicated favourable bacterial growth conditions even at low soluble electron donor concentration. Therefore, these results indirectly suggest a metal iron utilisation as an electron donor for bacterial metabolism when the soluble source of electrons (lactate) is scarce. Regarding pH in these tests (Fig. 2b-c), it can be seen an increase of one and two units from day 4th to 6th, time in which the values dropped and remained close to 7.
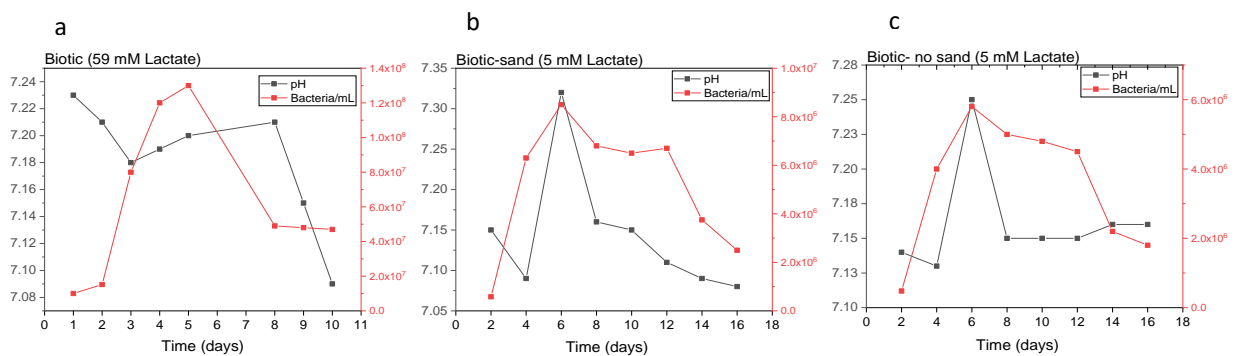
Figure 2. Bacterial and pH monitoring of biotic tests. Right Y-axis: growth monitoring of planktonic *S.oneidensis* cells by direct counting (bacteria/mL) and left Y-axis: pH monitoring. **a)** System II; **b)** III and, **c)** IV.

5.3.3. *Corrosion rate monitoring by linear polarisation resistance (LPR) measurements*

Fig. 3 provides the average corrosion rates calculated from LPR measurements. Steel samples in system II recorded lower corrosion rates than the abiotic counterpart (system I). Fig.3a showed that corrosion rates in the abiotic test (system I) progressively decreased from 0.7 mmpy at day 1 to 0.45 mmpy on day 8. Corrosion rate values on system II were lower than system I and varied through experimental reaching a value of 0.25 mmpy at the end of the immersion period.

Sand-deposited samples in system III had low corrosion rates throughout the exposure (Fig.3b). This result suggests that the sand diminished the corrosion effects on the steel surface. It can be attributed to barrier effect exerted by sand layers impeding direct metal contact to corrosive species in the solution. Previous work demonstrated that sand deposit exerted a diffusion barrier on carbon steel samples under abiotic conditions [23]. Differently, sand-free samples in system IV recorded the highest average corrosion rate (0.53 mmpy) calculated from potentiodynamic scans. These results coincided with corrosion rates (0.51 mmpy) calculated from LPR measurements at the last experimental day. However, it is important to clarify that during corrosion monitoring (Fig. 3b), higher corrosion values (1.0 mmpy) were recorded at day 13th of the immersion period. These results suggest that average corrosion of sand-free samples reached high values until later iron oxides deposition on the metal surface, which could decrease the corrosion process the last days of immersion.
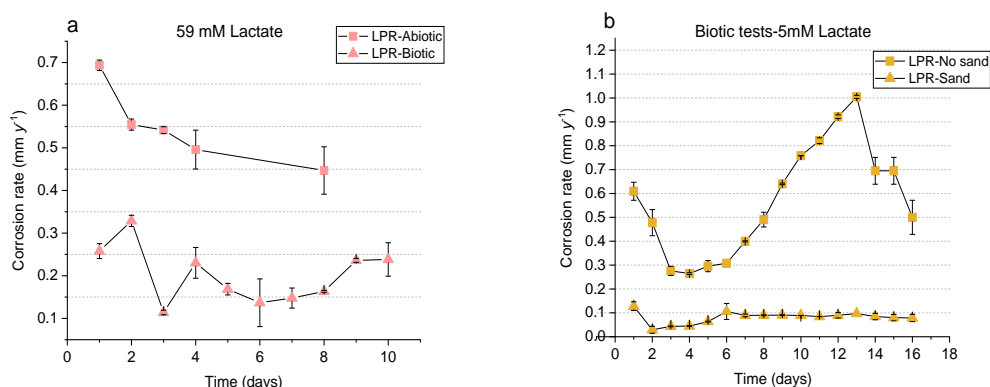
Figure 3. Average corrosion rates calculated from LPR measurements of carbon steel samples immersed in sparged CO_2/N_2 artificial seawater. **a)** Systems I-II and, **b)** Systems III-IV.

5.3.4.   Corrosion rate monitoring by electrochemical impedance spectroscopy (EIS).

Fig. 4 shows the Nyquist plots and Bode plots of samples in the system I and II containing lactate 59 mM under abiotic and biotic conditions, respectively. Insets on figures contain the Randel's equivalent circuits used to fit impedance data. Single semicircles equivalent to charge transfer resistance (R_{ct}) are observed for all test conditions suggesting that the corrosion reactions are charge transfer controlled. The

components of these circuits were described in a previous bacterial adhesion study [32]. R_s represents the solution resistance; Q_1 corresponds to the double-layer capacitance biofilm/electrode; Q_2 double-layer capacitance electrode/electrolyte; R_1 is the resistance biofilm/electrode and, R_{ct} is the resistance of electrode/electrolyte (charge-transfer resistance related to the leakage current). Table 3 summarises fitting results from the EIS analysis of the samples immersed in these systems. The low error percentages (Error %) of R_{ct} and low Chi-squared (X^2) values indicated an acceptable data fitting for all test conditions. For the system I, R_{ct} values gradually increased from 71.43 Ω cm^2 at day 1 to 106.2 Ω cm^2 in the last experimental day (8th day). Differently, R_{ct} values in system II fluctuated through experimental, reaching a value of 169 Ω cm^2 at the end of the immersion period (10th day).Correspondingly, both Nyquist and Bode plots from the system I showed a gradual increase in the impedance magnitude.

Similarly, the plots in system II revealed variations of impedance in the presence of *S.oneidensis* (Fig.4). Biological metabolic reactions are active processes which are influenced by the consumption of nutrients and gradual deposition of metabolic by-products on the steels. Thus, it can be suggested that a non-uniform biofilm and corrosion products deposition happened on metal surfaces, resulting in a marked impedance magnitude fluctuations under the present experimental conditions. For both systems, a shift was observed at the high-frequency domain of Bode phase plots when compared the first immersion day with the last one. This indicates that corrosion products and/or biofilm deposited protected the underlying steel surface reflected at the end of the immersion period.

Fig. 5 and Table 3 present corrosion rates values, derivated from EIS analysis of systems I and II. Corrosion rates recorded at samples immersed in the system I progressively decreased from 0.66 mmpy to 0.45 mmpy suggesting final general corrosion protection exerted by corrosion products formed on steels immersed in the sterile ASW. Samples on system II, on the other hand, had lower corrosion rates compared with the system I, which indicate that biofilm, metabolites and corrosion products deposited, reduced general corrosion effects observed in the abiotic environment [35]. These corrosion rate values are in agreement with the ones obtained from LPR measurements (Fig. 3a).
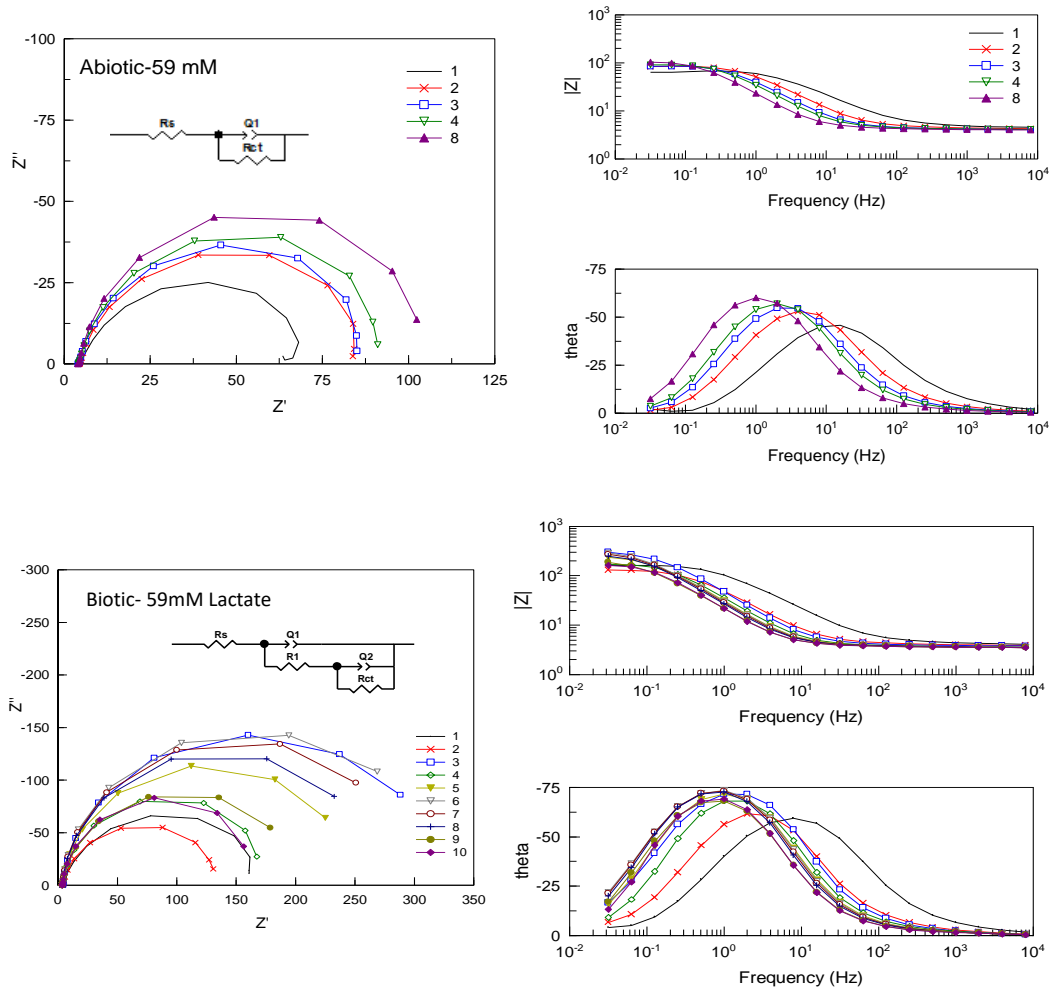
Figure 4. Impedance spectra of carbon steel samples immersed in CO_2/N_2-artificial seawater containing lactate 59 mM. Nyquist (left) and Bode plots (right). Fig. Inset: equivalent circuit model used to fit impedance data at top panels: abiotic test (system I); bottom panels: biotic test (system II).

Table 3. Estimated corrosion parameters from the EIS analysis of carbon steel samples. Top table: system I (abiotic); bottom table: system II (biotic).

Day	Rs $(\Omega\ cm^2)$	Q_{1-T}	Q_{1-p}	Rct $(\Omega\ cm^2)$	Error (%)	X^2	$i_{corr}=B/R_{ct}$ $(\mu A/cm^2)$	CR $(mm\ y^{-1})$
1	4.62	1.9E-03	7.7E-01	71.43	0.86	6.7E-04	57.1	0.66
2	4.43	3.0E-03	8.5E-01	84.30	0.97	2.9E-03	48.3	0.56
3	4.25	4.4E-03	8.7E-01	85.88	1.04	3.2E-03	47.5	0.55
4	4.27	5.3E-03	8.9E-01	92.13	1.18	3.6E-03	44.2	0.51
8	4.17	8.3E-03	9.0E-01	106.20	1.63	4.7E-03	38.4	0.45

Day	Rs $(\Omega\ cm^2)$	Q_{1-T}	Q_{1-p}	R_1 $(\Omega\ cm^2)$	Q_{2-Q}	Q_{2-n}	Rct $(\Omega\ cm^2)$	Error (%)	X^2	$i_{corr}=B/R_{ct}$ $(\mu A/cm^2)$	CR $(mm\ y^{-1})$
1	4.11	6.9E-04	8.5E-01	1.13	2.0E-04	8.5E-01	165.3	0.94	8.4E-04	24.7	0.29
2	3.93	2.0E-03	8.8E-01	1.35	9.7E-04	9.3E-01	131.3	0.38	1.9E-04	31.0	0.36
3	3.82	3.2E-03	8.8E-01	2.55	1.2E-03	1.1E+00	322.9	1.01	8.8E-04	12.6	0.15
4	3.62	1.7E-03	9.6E-01	0.79	2.3E-03	9.5E-01	174.9	0.61	5.3E-04	23.3	0.27
5	3.60	2.0E-03	9.6E-01	0.71	2.7E-03	9.5E-01	245.6	0.41	2.1E-04	16.6	0.19
6	3.59	2.9E-03	9.2E-01	0.84	2.6E-03	9.7E-01	318.1	0.67	3.3E-04	12.8	0.15
7	3.58	2.1E-03	9.6E-01	0.65	3.1E-03	9.5E-01	295.6	0.57	3.3E-04	13.8	0.16
8	3.59	2.2E-03	9.7E-01	0.66	3.3E-03	9.5E-01	268.8	0.58	3.6E-04	15.2	0.18
9	3.54	2.6E-03	9.5E-01	0.54	4.1E-03	9.3E-01	196.2	0.95	9.9E-04	20.8	0.24
10	3.57	3.6E-03	9.8E-01	1.12	3.5E-03	9.5E-01	169.0	1.35	1.8E-03	24.1	0.28
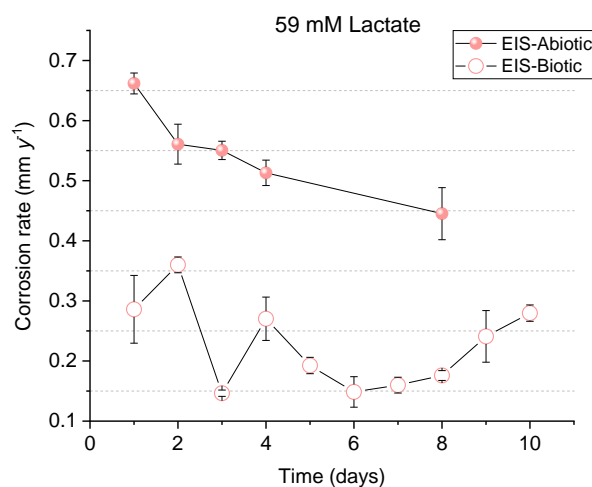
Figure 5. Average corrosion rates calculated from EIS measurements of carbon steel samples immersed in CO_2/N_2 artificial seawater containing 59 mM of lactate (systems I and II)

Fig. 6 shows nyquist, and Bode plots of the system III and system IV. The samples were immersed in ASW containing lactate 5 mM and in the presence of *S.oneidensis*. Table 4 showed low error percentages (Error %) of R_{ct} and low Chi-squared (X^2) values which denote an acceptable data fitting for systems III-IV. The Nyquist plots of system III differed to those observed in system IV. Although semicircles for both systems seem to be charge transfer controlled, in the presence of silica sand, these semicircles are incomplete in comparison with the ones without sand. The impedance magnitude was also different between the two systems, displaying considerably higher impedances on sand-deposited samples than the sand-free steel surfaces (Fig. 6).

The results indicate resistance to corrosion or a certain degree of protection exerted by the sand layers when microorganisms are present. R_{ct} values of sand-

deposited samples (system III) started with 383 Ω cm^2 on day 1 followed with a sharp increase to 2885 Ω cm^2 on day 2 of immersion. Subsequently, R_{ct} values slightly fluctuated exhibiting a trend towards lower values through experimental, reaching a value of 784 Ω cm^2 at the end of the immersion period. Notably, R_{ct} values of the sand-free samples (system IV) gradually increased, from 69.3 Ω cm^2 on day 1, to 158 Ω cm^2 on day 6 suggesting a level of corrosion protection by biofilm and/or corrosion products deposited on the steel surface. It may occur due to the availability at that stage of soluble electron donor (lactate), hence no need of taking electrons from the steel. Afterwards, the charge-transfer resistance trend reversed to smaller values reaching 37.4 Ω cm^2 on day 14 of immersion which indicates an active corrosion process in that period. However, the last two days R_{ct} values reversed again recording values of 65.4 Ω cm^2 on day 15 and 95.1 Ω cm^2 on last experimental day (16th day). Presumably, iron oxides films formed during the two weeks started reducing the corrosion process towards the steel surfaces in the last stage of the immersion period.

Fig. 7 and Table 4 displays average corrosion rates values derivated from EIS analysis of systems III and IV. Corrosion rates at sand-deposited samples (system III) recorded a value of 0.12 mmpy on day 1. Then, corrosion rate values slightly fluctuated remaining below 0.1 mmpy during the experimental time. These results indicate minimal general corrosion when sand layers are covering steel surfaces and in the presence of bacteria growing with a low concentration of soluble electron donor.
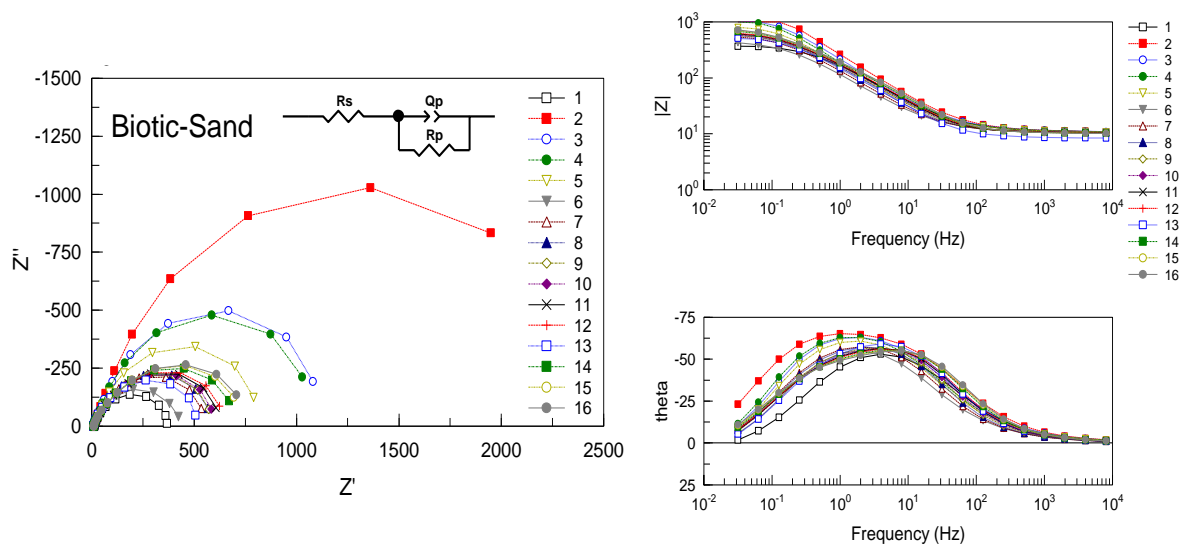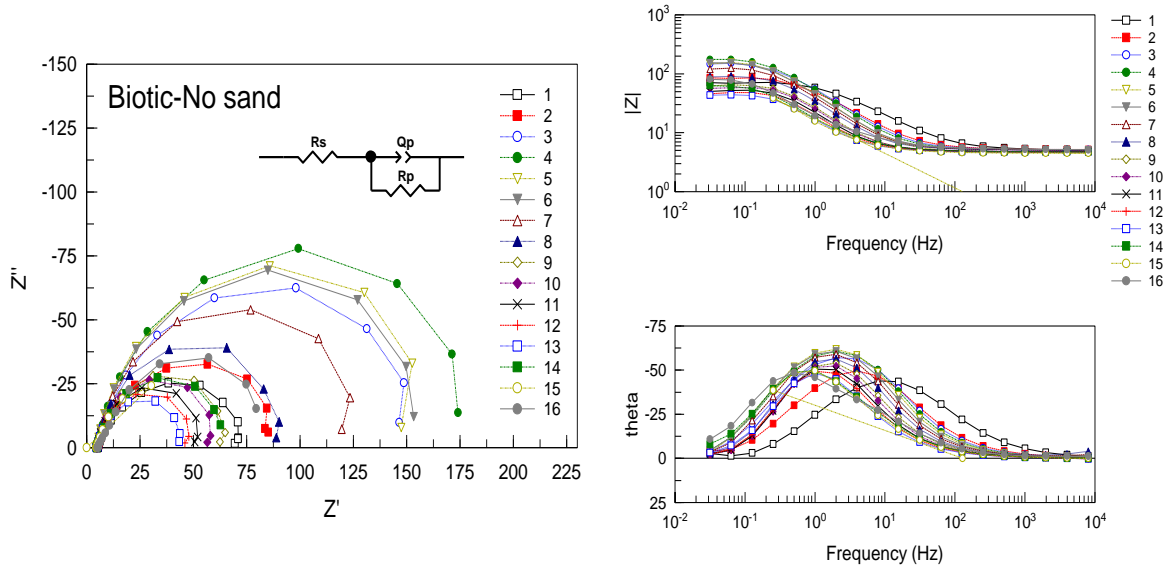
Figure 6. Impedance spectra of sand-deposited carbon steel samples in CO_2/N_2-artificial seawater containing 5 mM lactate and in the presence of *S.oneidensis* during 16 days. Nyquist (left) and Bode plots (right); Inset: equivalent circuit model used to fit impedance data at the top panels: system III; bottom panels: system IV.

It can be suggested that sand deposit provide a physical barrier to corrosive metabolites in the solution formed by bacterial activity. Sand-free samples, on the other hand, recorded variable corrosion rate values starting with 0.71 mmpy on day 1 and gradually. This is probably due to a level of corrosion protection in the first week of immersion as a result of initial lactate availability in the solution. Therefore, *S.oneidensis* would tend to use this electron donor rather than the electrons from the metal surface. After day 7 corrosion rates values gradually increased, recording a maximum corrosion rate value of 1.21 on day 14. Subsequently, corrosion rates suddenly dropped to 0.55 mmpy on the last day of the experiment, probably due to iron oxides film formation, which decreased general corrosion processes on the metal surface. Corrosion rate values from EIS measurements were in agreement with the ones obtained from LPR measurements (Fig. 3a).

Table 4. Estimated corrosion parameters from EIS analysis of carbon steel-top table: system IV (No sand); bottom table: system III (sand).

Day	Rs (Ω cm^2)	Q_{1-T}	Q_{1-p}	Rct (Ω cm^2)	Error (%)	X^2	$i_{corr}=B/R_{ct}$ ($\mu A/cm^2$)	CR (mm y^{-1})
				No sand				
1	5.12	2.1E-03	7.8E-01	69.3	1.04	2.3E-03	61.1	0.71
2	5.20	3.5E-03	8.3E-01	85.3	0.91	1.7E-03	46.4	0.54
3	5.20	3.4E-03	8.6E-01	153.5	1.04	1.8E-03	36.2	0.42
4	5.18	3.5E-03	8.8E-01	181.9	1.11	2.1E-03	21.9	0.25
5	4.65	4.0E-03	9.0E-01	159.6	1.61	4.9E-03	25.1	0.29
6	5.16	4.1E-03	8.9E-01	158.4	1.22	2.9E-03	24.6	0.29
7	5.16	4.5E-03	9.0E-01	124.4	1.53	5.2E-03	32.6	0.38
8	5.14	5.1E-03	9.1E-01	88.7	1.69	7.7E-03	47.2	0.55
9	4.68	6.4E-03	9.3E-01	62.0	1.51	7.1E-03	63.0	0.73
10	4.91	6.8E-03	9.3E-01	55.8	1.66	9.4E-03	70.4	0.82
11	4.86	7.9E-03	9.3E-01	49.5	1.77	1.1E-02	79.2	0.92
12	4.82	9.1E-03	9.3E-01	45.0	1.76	1.1E-02	90.6	1.05
13	4.77	1.1E-02	9.1E-01	41.3	1.59	8.0E-03	94.5	1.10
14	4.52	1.3E-02	9.1E-01	37.4	1.58	8.1E-03	104.4	1.21
15	4.81	1.2E-02	8.4E-01	65.4	2.33	9.4E-03	59.6	0.69
16	5.26	1.3E-02	7.6E-01	95.1	4.35	1.5E-02	47.1	0.55
				Sand				
1	10.99	1.2E-03	7.8E-01	383	1.43	2.4E-03	9.9	0.12
2	11.14	8.4E-04	8.0E-01	2885	2.74	2.5E-03	2.3	0.03
3	11.40	9.7E-04	8.1E-01	1293	3.08	6.1E-03	3.3	0.04
4	11.39	1.1E-03	8.1E-01	1247	3.34	6.9E-03	3.5	0.04
5	11.39	1.1E-03	8.1E-01	1247	3.34	6.9E-03	3.5	0.04
6	11.28	1.3E-03	8.0E-01	918	2.99	6.3E-03	4.7	0.05
7	10.85	1.9E-03	7.9E-01	448	2.10	4.1E-03	7.5	0.09
8	10.66	1.6E-03	8.0E-01	589	1.40	1.7E-03	6.6	0.08
9	10.53	1.5E-03	8.0E-01	617	1.31	1.5E-03	6.6	0.08
10	10.42	1.4E-03	7.9E-01	618	1.35	1.6E-03	6.7	0.08
11	10.31	1.3E-03	7.8E-01	630	1.47	1.9E-03	6.6	0.08
12	10.31	1.3E-03	7.8E-01	630	1.47	1.9E-03	6.4	0.07
13	10.21	1.2E-03	7.8E-01	653	1.62	2.2E-03	6.1	0.07
14	10.10	1.2E-03	7.7E-01	674	1.78	2.5E-03	6.7	0.08
15	8.05	1.3E-03	7.9E-01	570	1.75	2.7E-03	7.0	0.08
16	9.74	1.2E-03	7.4E-01	784	2.67	4.6E-03	6.0	0.07

5.3.5. Potentiodynamic polarisation measurements (Tafel plots)

Fig. 8 gives potentiodynamic curves recorded after at the end of the immersion period for each experimental condition. It can be noticed that in system II, biofilm and corrosion products deposited at steel surfaces had a favourable effect on reducing i_{corr} and the average corrosion rate recording 0.17 ± 0.05.). Also, biofilm and corrosion products shifted the corrosion potential to more positive values in the order of +35 mV(Table 5).
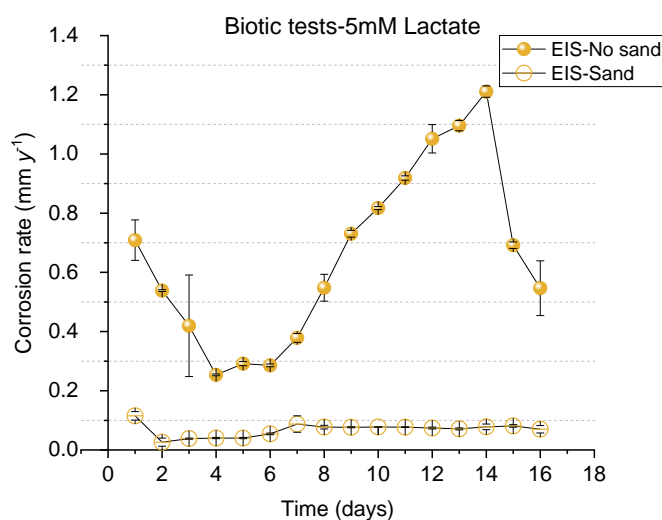
Figure 7. Average corrosion rates calculated from EIS measurements of carbon steel samples immersed in CO_2/N_2 artificial seawater containing 5 mM of lactate under biotic conditions (systems III and IV)

In the presence of bacteria, there was a slight change in the shape of the cathodic curve associated with a reduction in corrosion rate. Differently, the system I (abiotic test) recorded 0.44 ± 0.014 mmpy (Table 5)

Drawing a comparison between systems III and IV, it was evident that silica sand reduced i_{corr} and average corrosion rate. Corrosion rate decreased from 0.53 ± 0.06 mmpy to 0.1 ± 0.02 mmpy when the sand deposit was present (Table 5). Overall, the shapes of the anodic and cathodic curves of the sand-free samples in system IV remained similar to sand-deposit samples in system III. However, silica sand caused the corrosion potential to shift negatively. The corrosion potential changed from -0.66 V to -0.75 ± 0.4 V or 87 mV (Table 5). These results are in general agreement with the deposits having a blocking effect in reducing the rate of mass transfer of corroding species to the steel surface [23, 25]. Differently, sand-free samples in system IV recorded the highest average corrosion rate (0.53 mmpy) from potentiodynamic measurement. These results coincided with corrosion rates (0.51 mmpy) calculated from LPR measurements at the last experimental day. However, it is important to clarify that during corrosion monitoring (Fig. 3b) higher corrosion values (1.0 mmpy) were recorded at day 13th of the immersion period. This is likely due to an active corrosion process by *S.oneidensis* at these immersion days, followed by iron oxidates deposition, reducing corrosion rates the last two days of immersion.

Thus, low corrosion rates were recorded at the end of the experimental time.
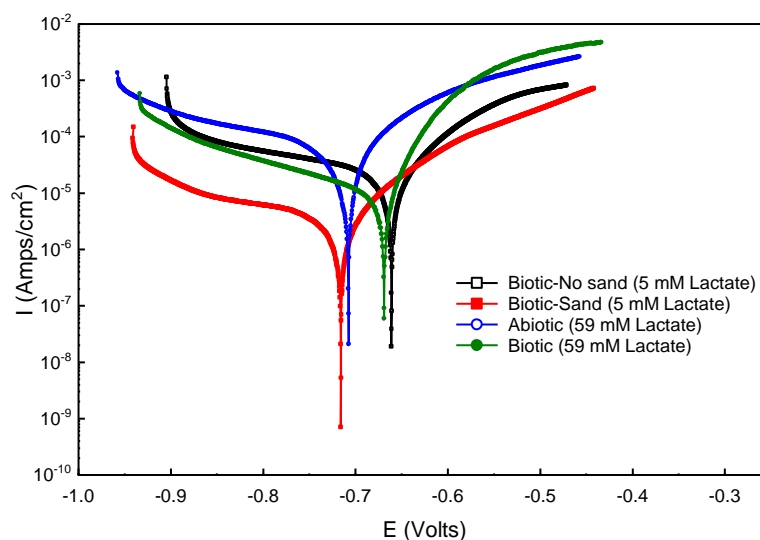
Figure 8. Potentiodynamic curves of carbon steel samples immersed in CO_2/N_2-artificial seawater for all test conditions (systems I-IV)

Table 5. Electrochemical parameters of the carbon steel derived from potentiodynamic polarisation curves (Fig. 8)

Experiment	Sample	βa V dec^{-1}	βc V dec^{-1}	E_{corr} V vs.Ag/AgCl	i_{corr} (μA/cm^2)	CR (mm y^{-1})
Biotic (59 mM Lactate)	1	0.06	0.56	-0.669	17.88	0.21
	2	0.06	0.34	-0.673	38.54	0.13
Abiotic (59 mM Lactate)	1	0.09	0.21	-0.707	38.54	0.45
	2	0.09	0.23	-0.705	37.18	0.43
Biotic- No sand (5 mM Lactate)	1	0.12	0.12	-0.661	41.76	0.49
	2	0.11	0.83	0.661	48.93	0.57
Biotic- Sand (5 mM Lactate)	1	0.12	1.73	-0.715	6.83	0.08
	2	0.12	4.97	-0.781	9.71	0.11

5.3.6. Cumulative corrosion information from mass loss measurements

Fig.9 shows average corrosion rates calculated from mass loss measurements on carbon steel samples from all test conditions (systems I-IV). Average corrosion rates from steel samples immersed in the system I (abiotic conditions) were considerably

higher when compared to the test with system II (biotic conditions). Sand-free samples in system IV had higher average corrosion rates when compared to the values obtained from the sand-deposited samples in system III. This cumulative corrosion information from mass loss is in total accordance with data recorded from LPR, EIS and potentiodynamic measurements in the last immersion day for all systems.
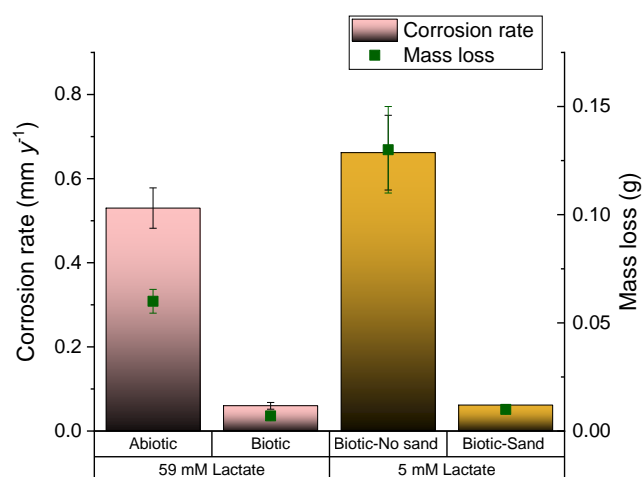
Figure 9. Average corrosion rates (left Y-axis) calculated from mass loss measurements (right axis) of carbon steel samples immersed in sparged CO_2/N_2 artificial seawater for all systems (I-IV)

5.3.7. Assessment of localised corrosion.

Fig. 10 displays the average pitting and maximum depths from visible light 3D profilometry on the carbon steel samples. Samples in system II had lower average and maximum pitting compared to the abiotic counterpart (system I) with values of 9 μm and 14 μm, respectively (Fig. 10a). It can be attributed to biofilm and or/metabolites deposited at metal surface reducing local corrosion attack compared to the system I. Based on these results; it is suggested that *S.oneidensis* does not affect the steel surface when lactate is in high concentration. It may also be possible that the metabolic by-products formed under these conditions have no corrosive nature.

Localised corrosion results for systems III-IV are presented in Fig. 10b. Sand-free samples in system IV had higher localised corrosion with maximum pitting depth of 31 μm compared to sand-deposited samples (system III) with only 10 μm of maximum pitting depth. These results are in agreement with general corrosion information by LPR (Fig. 3b) and EIS (Fig 7) as well as potentiodynamic measurements (Fig. 8 and Table 5). As mentioned earlier in the corrosion monitoring

sections (3.3-3.5), sand deposit seems to have a positive effect on carbon steel surfaces decreasing corrosion processes in the presence of *S. oneidensis* with low lactate concentration in the solution.
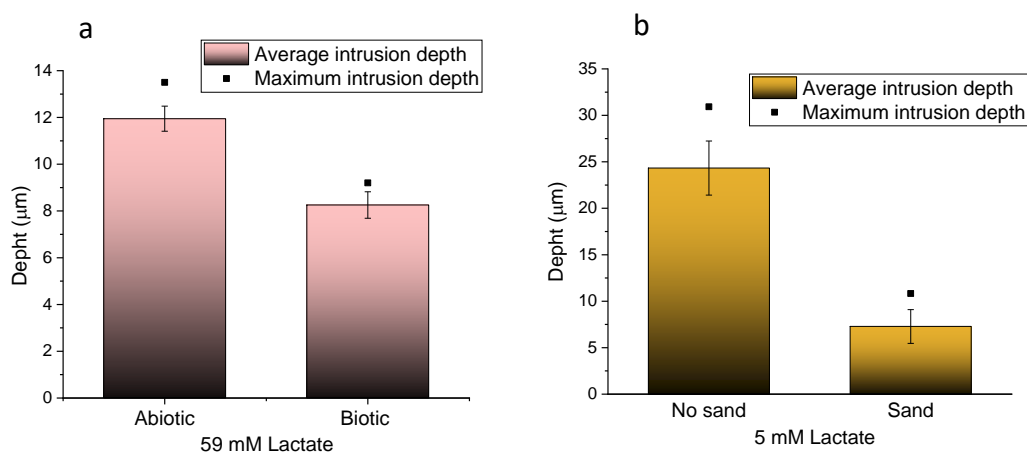
Figure 10. Average and maximum pitting depths by visible light 3D profilometry of carbon steel samples immersed in CO_2/N_2-artificial seawater for all systems (I-IV). The average pitting depth was obtained using the 10 deepest points measured on each sample. Left: system I (abiotic test) and II (biotic test). Right: system III (sand-deposited samples) and IV (sand-free samples).

5.3.8. *Summary of general and localised corrosion.*

Fig. 11 provides an overview of general and localised corrosion information obtained by different methods. Pitting rates were calculated from maximum pitting depth values assuming that the localised corrosion measured over the total immersion period initiated from the 1st day and propagated at the same rate throughout testing. Overall, localised and general corrosion information followed a similar trend for all test conditions. Also, results in Fig. 11 are in agreement with corrosion monitoring (LPR and EIS measurements) recorded on the last testing day. Corrosion rates from pitting rate (IR) across all tests had higher values than their respective values from potentiodynamic and mass loss measurements. It is expected that localised corrosion information may differ to some extent from general corrosion data. However, methods for assessing average corrosion rates tended to underestimate the local corrosion attack under the present experimental conditions.
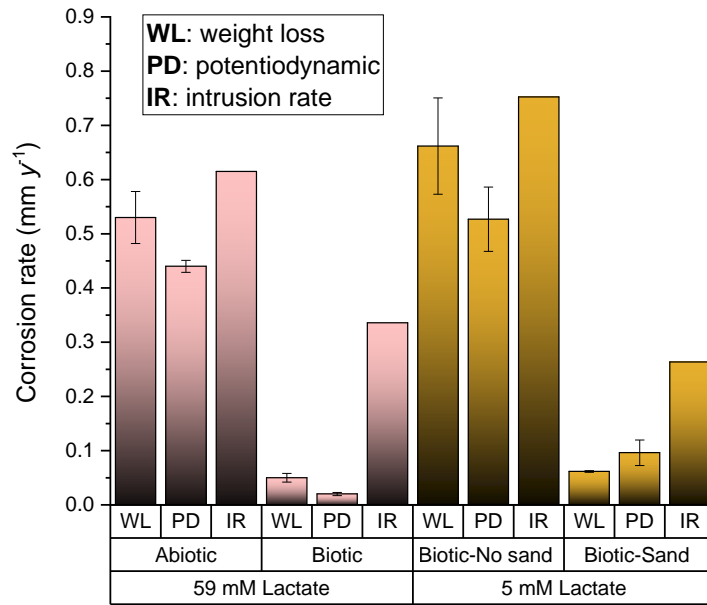
Figure 11. Corrosion rates calculated from mass loss measurements, potentiodynamic curves and pitting depths (from maximum pitting depth measurements) of carbon steel samples immersed in CO_2/N_2 sparged artificial seawater under abiotic (sterile) and biotic conditions (in the presence of *S.oneidensis*).

5.3.9. Test solution chemistry.

Fig. 12 presents total iron (FeT), ferrous (Fe^{2+}) and ferric iron (Fe^{3+}) results from the systems III and IV. Note the differences in scales between systems III and IV (Fig. 12a and 12b). FeT concentration gradually increased from 1.7 mg/L on day 1 to 28.5 mg/L on day 16 in the solution of the deposited system (III) (Fig. 12a). Similar FeT trend was observed in the absence of sand deposit (system IV). However, sand-free steel samples in system IV exhibited a considerably higher iron dissolution starting with 17 mg/L on day 1 and progressively increase until day 10 with a value of 82.5 mg/L. Then, the system abruptly increased FeT concentration reaching a value of 1100 mg/L after 16 days of immersion (Fig. 12b). This active iron dissolution in system IV coincided with the active general corrosion process shown by LPR (Fig. 3b) and EIS (Fig. 7) measurements at that period.

5.3.10. Visual observations:

Fig.13 shows the experimental three-electrode setup of UDMC using the bacterial isolate *S.oneidensis* in ASW containing different electron donors and acceptors in CO_2-N_2 environment at 30°C (Table 1)
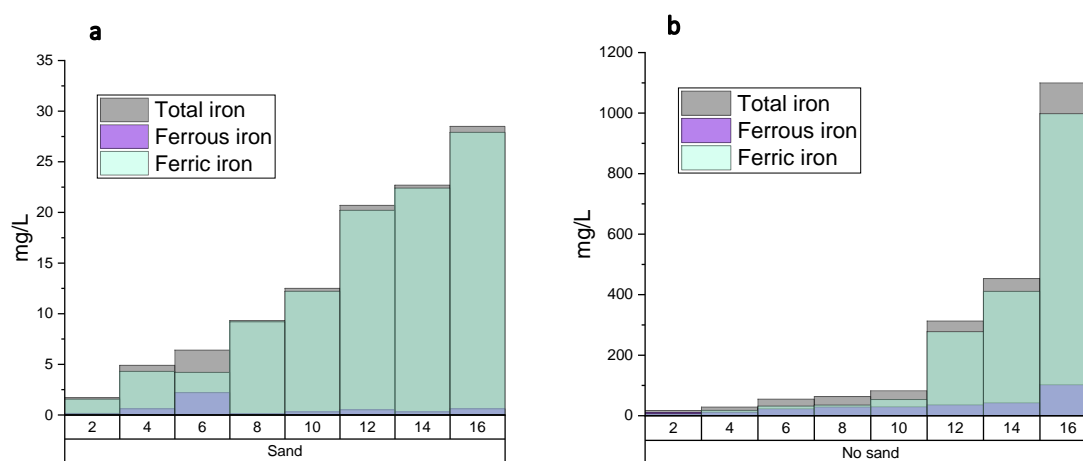
Figure 12. Total, ferrous and ferric iron monitoring during 16 days of immersion of carbon steel samples in CO_2/N_2 -artificial seawater containing 5mM of lactate and *S.oneidensis*. **a)** sand-free samples (system III) and **b)** sand-deposited samples (system IV). Note the differences in scales between systems III and IV.

The reactor in the system I, the ASW remained clear and colourless during testing, indicating no microbial activity or cross-contamination in the reactor (Fig. 13a). The solution in system II exhibited a marked pink colour and turbidity a few days after bacterial inoculation (Fig. 13b). *Shewanella oneidensis* possesses a high content of cytochromes, which confers bacterial cells a characteristic pink or red colour. The high content of cytochrome is suggestive of high demand for iron since iron is a co-factor of heme groups in the cytochromes [33]. Tetraheme cytochrome c (CymA), is usually located in the periplasmic side of the cytoplasmic membrane and represents a branch point in the electron transport chain for reduction of a variety of substrates, including Fe-citrate, MnO_2, nitrate, and fumarate [34, 36]. As expected, the developed pink colour suggests an efficient fumarate reduction accompanied by the high lactate concentration in the ASW.

Regarding systems III and IV containing lower lactate concentration (5 mM), the ASW turned from colourless to yellow colour (Fig. 13c-d). The yellow colour can be attributed to metal sample oxidation which correlated with the high dissolved iron concentration in the solution (Fig. 12). The solution in system IV (Fig. 13d) developed

a stronger yellow colour and turbidity compared to the solution in system III (Fig. 13c). This differences in colour intensity also are in agreement with results from FeT content dissolved in the solution (Fig. 12).
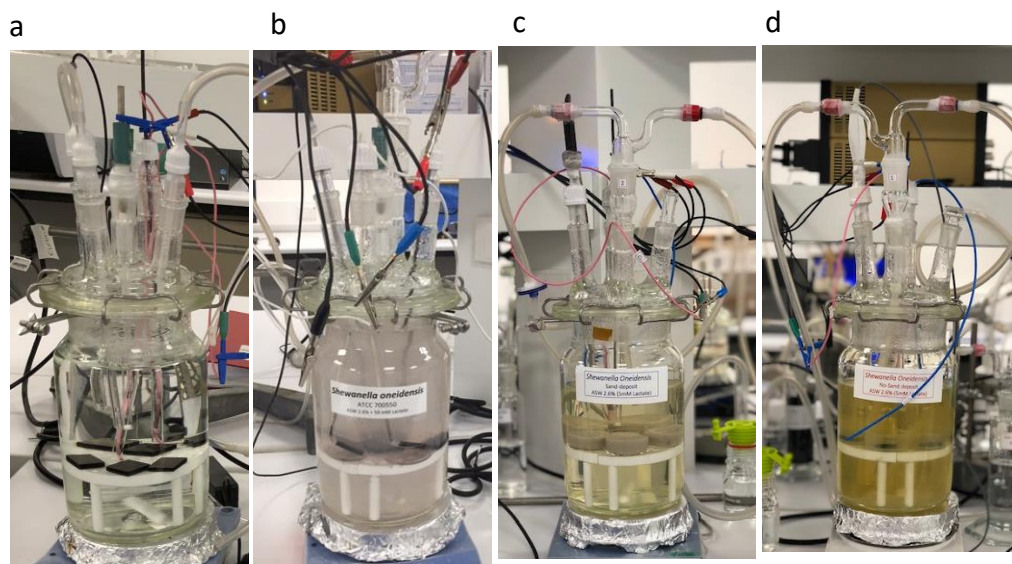
Figure 13. Experimental three-electrode setup of UDMC. *S.oneidensis* in ASW containing different electron donors and acceptors in CO_2-N_2 environment. **a)** system I (abiotic test) **b)** system II (biotic test); **b)** system III (sand-deposited samples); **c)** system IV (sand-free samples).

5.3.11. *Microscopy.*
Abiotic and biotic tests in ASW supplemented with 59 mM of lactate.

Fig. 14-15 show FESEM top images of carbon steel samples of systems I and II, respectively. It can be seen in Fig. 15 that the excess of electron acceptor and donor concentrations stimulated the formation of a copious *S.oneidensis* biofilm. This enriched environment also favoured the formation of metabolic by-products and corrosion products, which precipitated, forming a thick layer on the steel surfaces. The cracks observed on the surface layers are likely due to the drying process. The FIBSEM image in Fig 15 (right bottom) shows structures like-microbial colonies protrude from the surface. The cross-sectioned profile of these structures evidenced the presence of different compacted layers covering the steel surface. These layers or accumulation of metabolites was not evident under abiotic conditions in the system I (Fig. 14).

Fig.16 shows EDS-mapping of the structures like-colonies revealed a marked presence of carbon, which is indicative of biological content such as extracellular polymeric substances (EPS) conforming these colonies. Sodium and chlorine elements were located outside of the colony, maybe due to precipitation of the ASW components. Iron and oxygen were concentrated in the top centre of the colony, which could indicate an iron oxide on this area.

It is possible that with an excess of electron acceptors and donors for its metabolism, this bacterium excreted a large amount of non-corrosive metabolites which were deposited on steel surface protecting the steel from corrosive species in the solution, e.g. CO_2 gas. These results are supported by general and localised corrosion information that revealed more considerable corrosion damage of samples in the abiotic test (system I) that the ones exposed to this bacterial isolate (system II).
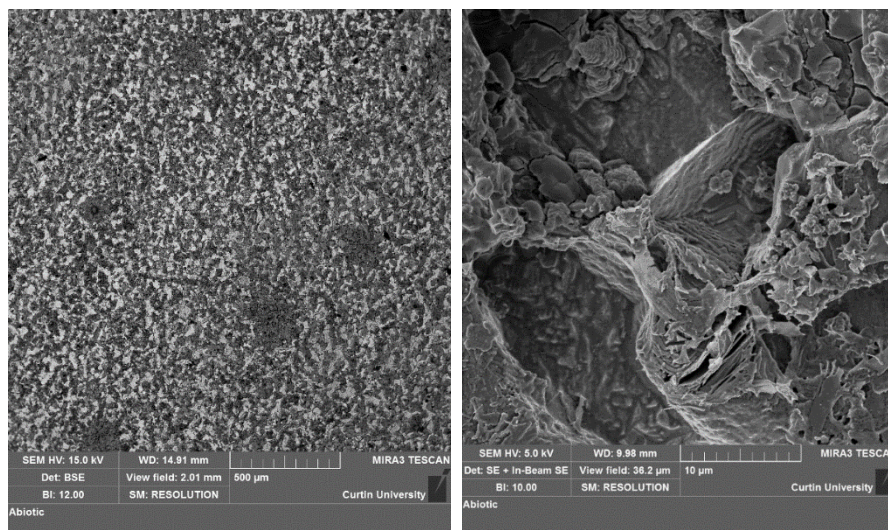
Figure 14. FESEM top images of carbon steel immersed in artificial seawater containing lactate 59 mM for 8 days under abiotic conditions (system I).
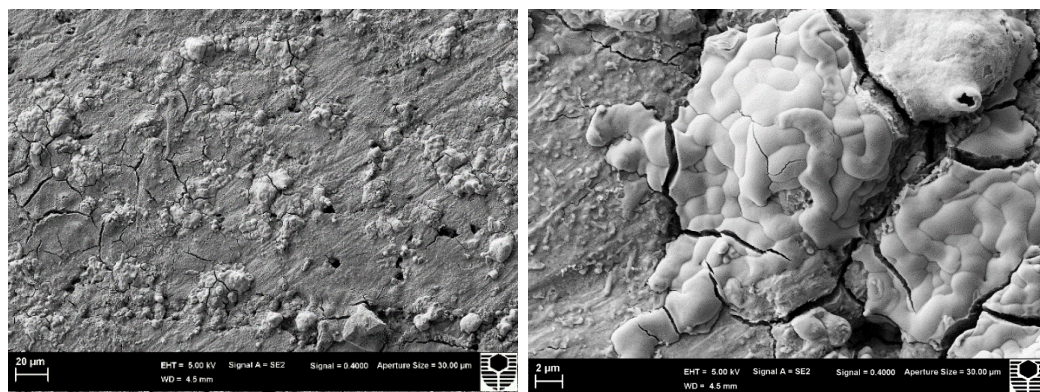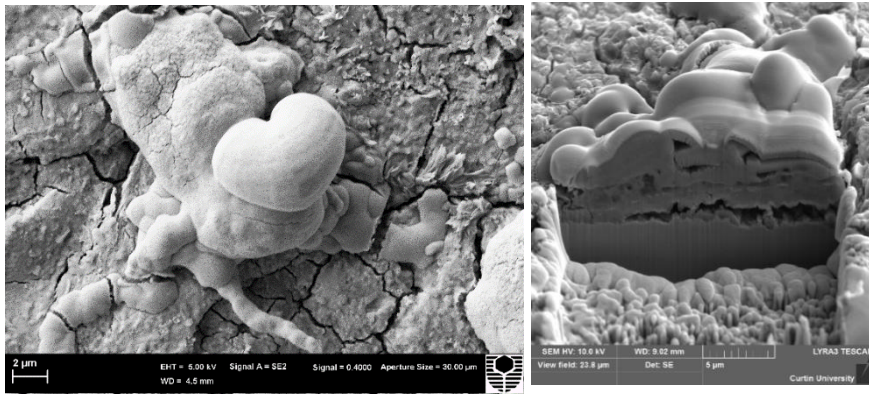
Figure 15. FESEM top images of carbon steel immersed in artificial seawater containing lactate 59 mM and in the presence of *S.oneidensis* for 10 days (system II). Focus Ion Beam scanning electron microscopy (FIB-SEM) image of structure like-microbial colony (right bottom panel).
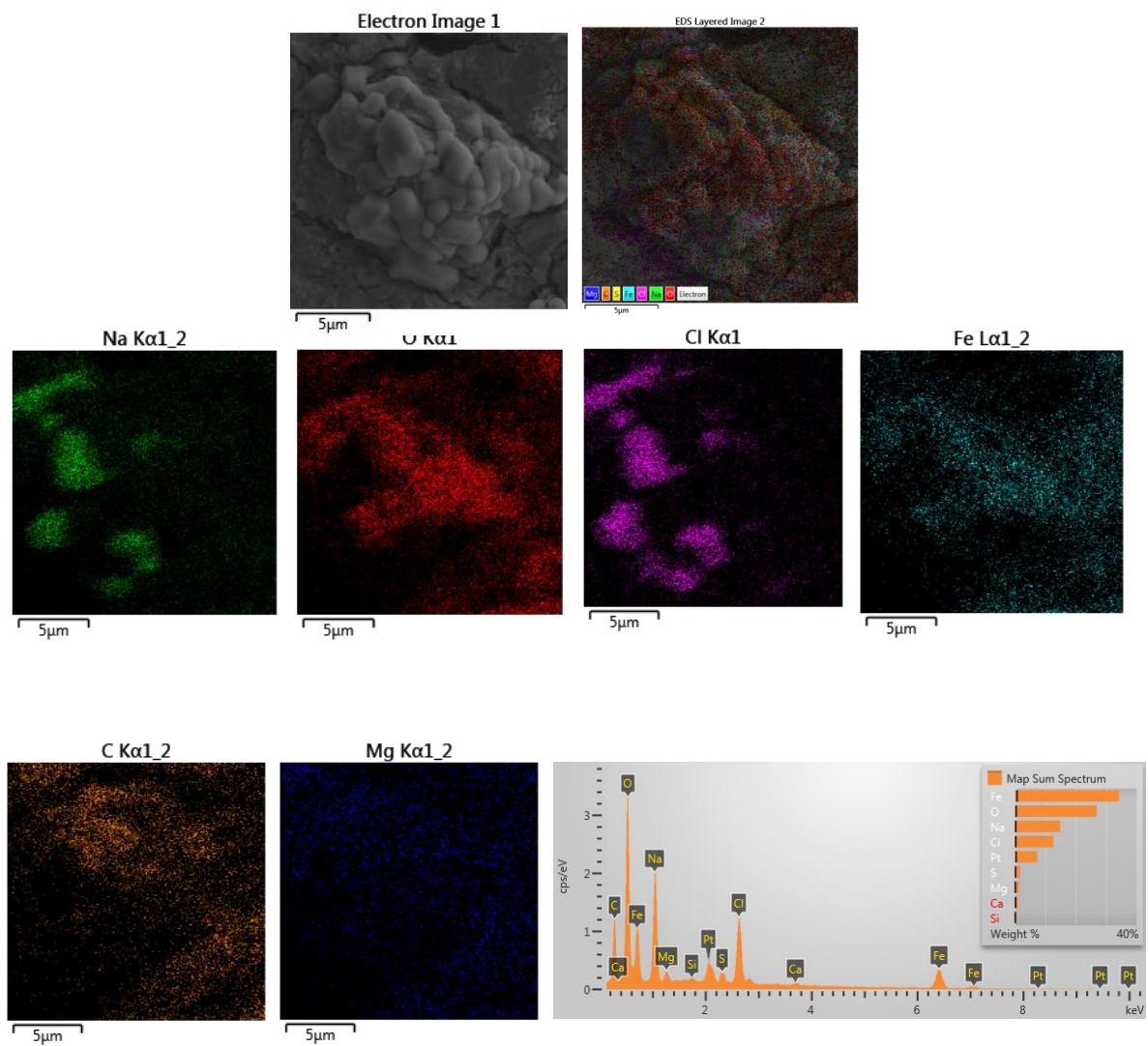
Figure 16. EDS-mapping of carbon steel immersed in artificial seawater containing lactate 59 mM and in the presence of *S.oneidensis* (system II).

5.3.12. Biotic tests in ASW supplemented with 5 mM of lactate.

Fig. 17-18 show cross-sectional features of corroded sand-deposited samples (system III) and sand-free samples (system IV), respectively. The images in Fig. 17 revealed that the biofilm was formed beneath and between sand grains. This confirms the ability of microorganisms to reach metal surfaces even in the presence of deposit layers. This observation is reasonable considering bacterial cells size (between 2-5 µm) compared to sand grain sizes (~300 µm). Although sand-deposited samples in system III were less affected by this bacterium compared to the sand-free samples in system IV, the solution in this reactor with sand (system III) also turned yellow and contained dissolved iron. Taking into account that bacterial addition to the reactor was after sand addition, the presence of biofilm in direct contact with the metal surface suggests a bacterial penetration throughout this thick deposit layers (~ 5 mm) and hence affinity for the metal surfaces.

Sand-free samples in system IV (Fig. 18) also evidenced biofilm presence on the steel surface, but this time with the greater corroded area when compared to the sand-deposited samples (Fig. 17). FESEM top images of carbon of a sand-free surface in system IV (Fig. 19) showed the formation of a significant amount of corrosion products embedded in a copious biofilm and deposited on the steel surfaces.

EDS-analysis detected iron (Fe) oxygen (O) as primary elements of the corrosion process, suggesting iron oxides formation and deposition on samples immersed under these conditions. Spectra 1 and 4 in Fig. 20 showed high content of carbon element confirming biofilm presence surrounding the iron oxides formed under these conditions. Spectra in the same EDS analysis but pointing bacterial cells recorded high content of carbon confirming biofilm presence surrounding the iron oxides formed under these conditions. FESEM images and elemental identification of iron oxides deposited on the surface correlates well with the high FeT content in the solution mainly in the form of Fe^{+3} (Fig. 12b).
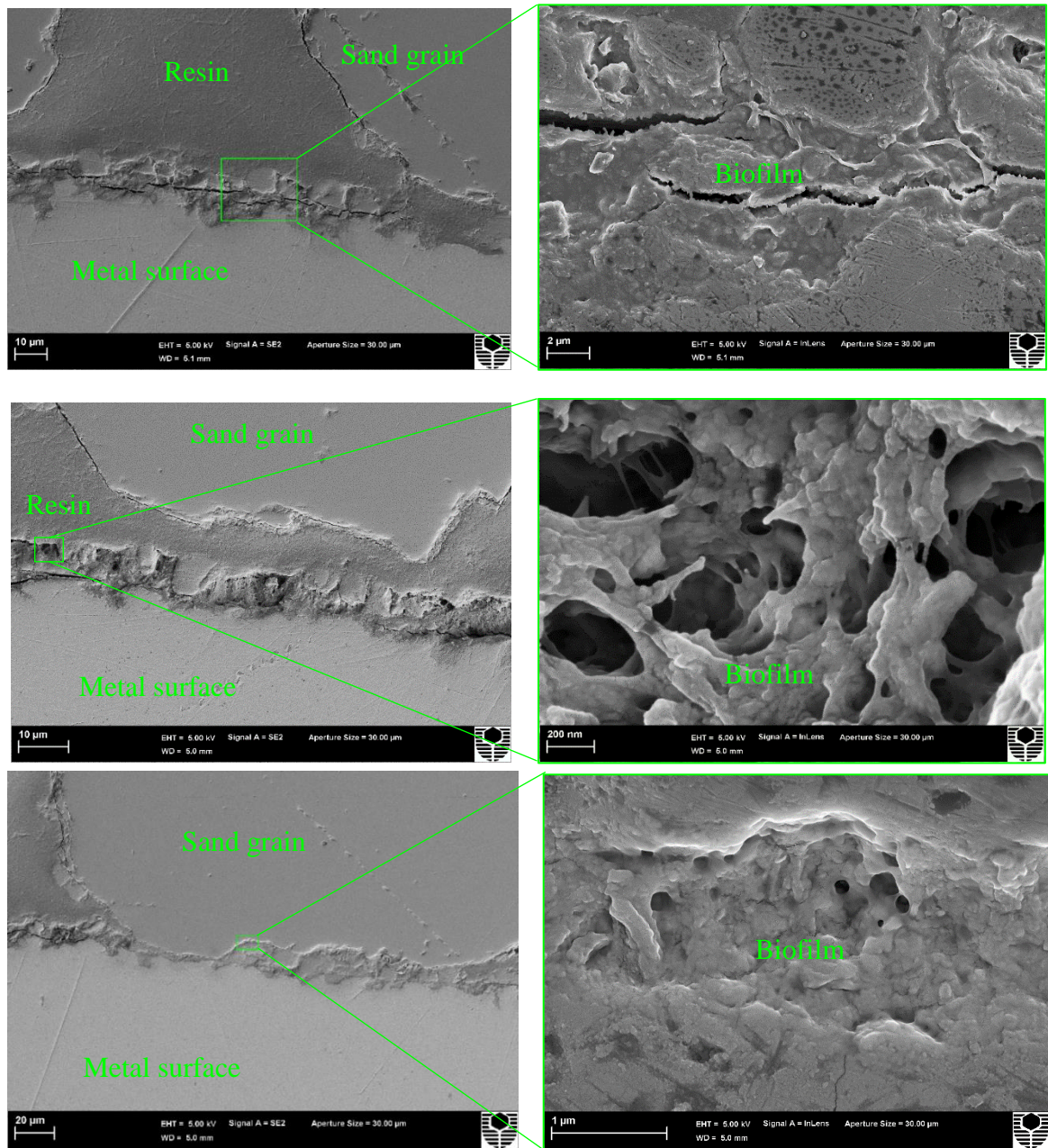
Figure 17. FESEM images from cross-sectioned sand-deposited samples immersed in CO2/N2-artificial seawater containing lactate 5 mM and in the presence of S.oneidensis for 16 days (system III). The selected area in the left image is shown at higher magnification at the right panel. The set of images revealed biofilm formation beneath and between sand grains.
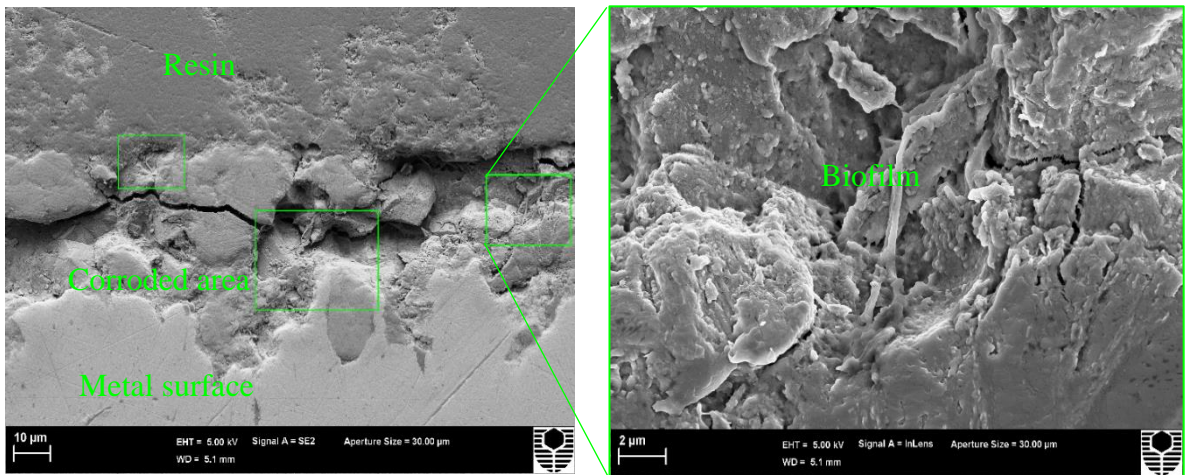
Figure 18. FESEM images from cross-sectioned sand-free samples immersed in CO_2/N_2-artificial seawater containing lactate 5 mM and in the presence of S.oneidensis for 16 days (system IV). The left panels correspond to a close up of the electron image at the right hand. The selected area in the left image is shown at higher magnification at the right panel. The image revealed biofilm formation beneath corrosion products and on top of the steel surface.
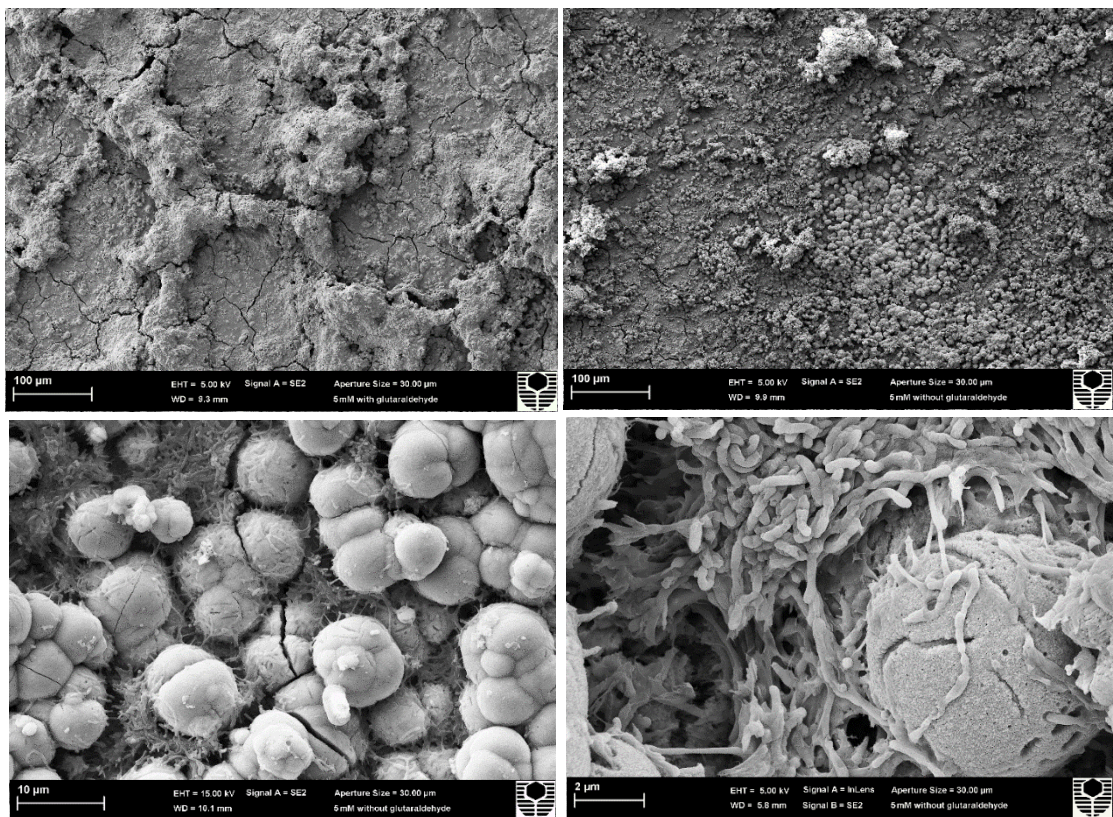
Figure 19. FESEM top images of sand-free samples immersed in CO_2/N_2 -artificial seawater containing 5 mM of lactate and in the presence of *S.oneidensis* for 16 days (system IV).

5.4. Conclusions

This study assessed carbon steel corrosion by *Shewanella oneidensis* MR-1 in a CO_2 environment with different concentration of soluble electron donor. The effects of sand deposit on steel corrosion under these conditions were also investigated using electrochemical measurements and surface analysis. The main conclusions of this work were as follows:

- The biotic test with an excess of electron donor (system II) did not show an evident average and localised corrosion. In fact, the samples in system II were less corroded than the abiotic counterpart or system I. Under these conditions *S.oneidensis* did not affect the metal surface probably due to the high lactate concentration available in the solution. The results show that this bacterium prefers a soluble source of electrons than switch its metabolism to extract electrons from the metal surface.

- FTIR analysis demonstrated that silica sand caused minimal depletion of sodium lactate from the solution. It can be concluded that this mineral deposit does not substantially interfere with the penetration of this organic compound through its layers.

- Sand-free samples in system IV exhibited greater average and localised corrosion and higher total iron content than sand-deposited samples system III.

- The oxidation of the steel samples for both systems III and IV was evident by the turn of the yellow colour of the test solution and the formation of iron oxides on the metal surface identified by EDS-analysis. These results confirmed that microbial cells and/or their activity could surpass the barrier effect commonly observed by a sand deposit in abiotic CO_2 anaerobic conditions.

- FESEM images of cross-sectioned corroded samples evidenced biofilm formation underneath and between sand grains. This direct biofilm contact with the metal surface showed that sand layers did not impede biofilm colonisation and attachment to the steel surface.

- Overall, the corrosion effects on carbon steel surfaces by *S.oneidensis* biofilm varied according to the type of metabolism stimulated. This bacterium oxidised metallic iron in an environment lacking soluble electron acceptor at a greater extent than in enriched solution containing high electron acceptor concentration.

5.5. References

1.   Carpentier, W.; De Smet, L.; Van Beeumen, J.; Brigé, A., Respiration And Growth Of *Shewanella Oneidensis* MR-1 Using Vanadate As The Sole Electron Acceptor. *Journal of bacteriology* **2005,** *187* (10), 3293-3301.

2.   Fredrickson, J. K.; Zachara, J. M.; Kennedy, D. W.; Duff, M. C.; Gorby, Y. A.; Li, S.-m. W.; Krupka, K. M., Reduction of U(VI) in goethite (α-FeOOH) Suspensions By A Dissimilatory Metal-Reducing Bacterium. *Geochimica et Cosmochimica Acta* **2000,** *64* (18), 3085-3098.

3.   DiChristina, T. J.; Bates, D. J.; Burns, J. L.; Dale, J. R.; Payne, A. N., Shewanella: Novel Strategies For Anaerobic Respiration. In *Past and Present Water Column Anoxia*, Neretin, N. L., Ed. Springer Netherlands: Dordrecht, 2006; pp 443-469.

4.   Herrera, L. K.; Videla, H. A., Role of Iron-Reducing Bacteria in Corrosion and Protection of Carbon steel. *International Biodeterioration & Biodegradation* **2009,** *63* (7), 891-895.

5.   Geesey, G. In *What is biocorrosion. Biofouling and biocorrosion in industrial water systems*, Proceedings of the International Workshop on Industrial Biofouling and Biocorrosion. Springer-Verlag, Berlin-Heidelberg, 1991.

6.   Libert, M.; Schutz, M. K.; Esnault, L.; Feron, D.; Bildstein, O., Impact Of Microbial Activity On The Radioactive Waste Disposal: Long Term Prediction Of Biocorrosion Processes. *Bioelectrochemistry* **2014,** *97*, 162-8.

7.   Schütz, M. K.; Moreira, R.; Bildstein, O.; Lartigue, J.-E.; Schlegel, M. L.; Tribollet, B.; Vivier, V.; Libert, M., Combined Geochemical And Electrochemical Methodology To Quantify Corrosion Of Carbon Steel By Bacterial Activity. *Bioelectrochemistry* **2014,** *97*, 61-68.

8.   Lee, A. K.; Newman, D. K., Microbial Iron Respiration: Impacts On Corrosion Processes. *Applied microbiology and biotechnology* **2003,** *62* (2), 134-139.

9.   Cote, C.; Rosas, O.; Basseguy, R., Geobacter sulfurreducens: An Iron Reducing Bacterium That Can Protect Carbon Steel Against Corrosion, *Corrosion Science* **2015,** *94*, 104-113.

10.   Esnault, L.; Jullien, M.; Mustin, C.; Bildstein, O.; Libert, M., Metallic Corrosion Processes Reactivation Sustained By Iron-Reducing Bacteria: Implication On Long-Term Stability Of Protective Layers. *Physics and Chemistry of the Earth, Parts A/B/C* **2011,** *36* (17–18), 1624-1629.

11.   Videla, H., Corrosion inhibition by bacteria. *Manual of biocorrosion* **1996**, 121-135.

12.   Schütz, M. K.; Libert, M.; Schlegel, M. L.; Lartigue, J.-E.; Bildstein, O., Dissimilatory Iron Reduction in the Presence of Hydrogen: A Case Study of Microbial Activity and Nuclear Waste Disposal. *Procedia Earth and Planetary Science* **2013,** *7*, 409-412.

13.   Mehanna, M.; Basseguy, R.; Delia, M.-L.; Bergel, A., Role Of Direct Microbial Electron Transfer In Corrosion Of Steels. *Electrochemistry Communications* **2009,** *11* (3), 568-571.

14.   Mehanna, M.; Basséguy, R.; Délia, M.-L.; Bergel, A., Effect Of Geobacter Sulfurreducens On The Microbial Corrosion Of Mild Steel, Ferritic And Austenitic Stainless Steels. *Corrosion Science* **2009,** *51* (11), 2596-2604.

15.   Gregory, K. B.; Bond, D. R.; Lovley, D. R., Graphite Electrodes As Electron Donors For Anaerobic Respiration. *Environmental Microbiology* **2004,** *6* (6), 596-604.

16.   Huang, L.; Regan, J. M.; Quan, X., Electron Transfer Mechanisms, New Applications, And Performance Of Biocathode Microbial Fuel Cells. *Bioresource technology* **2011,** *102* (1), 316-323.

17.   Fredrickson, J. K.; Romine, M. F.; Beliaev, A. S.; Auchtung, J. M.; Driscoll, M. E.; Gardner, T. S.; Nealson, K. H.; Osterman, A. L.; Pinchuk, G.; Reed, J. L.; Rodionov, D. A.; Rodrigues, J. L. M.; Saffarini, D. A.; Serres, M. H.; Spormann, A. M.; Zhulin, I. B.; Tiedje, J. M., Towards environmental systems biology of Shewanella. *Nature reviews. Microbiology,* **2008,** *6* (8), 592-603.

18.   Jafary, T.; Daud, W. R. W.; Ghasemi, M.; Kim, B. H.; Md Jahim, J.; Ismail, M.; Lim, S. S., Biocathode In Microbial Electrolysis Cell; Present Status And Future Prospects. *Renewable and Sustainable Energy Reviews,* **2015,** *47*, 23-33.

19.   Little, B. J.; Lee, J. S., Microbiologically Influenced Corrosion: an update. *International Materials Reviews,* **2014,** *59* (7), 384-393.

20.   Kim, B. H.; Lim, S. S.; Daud, W. R. W.; Gadd, G. M.; Chang, I. S., The Biocathode Of Microbial Electrochemical Systems And Microbially-Influenced Corrosion. *Bioresource Technology,* **2015,** *190*, 395-401.

21.   Kato, S., Microbial Extracellular Electron Transfer And Its Relevance To Iron Corrosion. *Microbial Biotechnology* **2016,** *9* (2), 141-148.

22.   Dumas, C.; Basseguy, R.; Bergel, A., Microbial Electrocatalysis With Geobacter Sulfurreducens Biofilm On Stainless Steel Cathodes. *Electrochimica Acta* **2008,** *53* (5), 2494-2500.

23.   Pandarinathan, V.; Lepková, K.; Bailey, S. I.; Gubner, R., Impact of Mineral Deposits on CO_2 Corrosion of Carbon Steel. NACE International: Houston, TX, 2013.

24.   Pandarinathan, V.; Lepková, K.; Bailey, S. I.; Gubner, R., Evaluation Of Corrosion Inhibition At Sand-Deposited Carbon Steel In Co_2-Saturated Brine. *Corrosion Science,* **2013,** *72*, 108-117.

25.   Huang, J.; Brown, B.; Jiang, X.; Kinsella, B.; Nesic, S., Internal CO_2 Corrosion of Mild Steel Pipelines Under Inert Solid Deposits. In *NACE - International Corrosion Conference Series*, NACE International: San Antonio, TX, 2010.

26.   Suarez, E. M.; Machuca, L. L.; Lepková, K., The role of bacteria in under-deposit corrosion in oil and gas facilities: A review of mechanisms, test methods and corrosion inhibition. *Corrosion and Materials,* **2019,** *44* (1), 80-87.

27.   Zinkevich, V.; Beech, I. B., Screening Of Sulfate-Reducing Bacteria In Colonoscopy Samples From Healthy And Colitic Human Gut Mucosa. *FEMS microbiology ecology,* **2000,** *34* (2), 147-155.

28.   Suarez, E. M.; Lepková, K.; Kinsella, B.; Machuca, L. L., Aggressive Corrosion Of Steel By A Thermophilic Microbial Consortium In The Presence And Absence Of Sand. *International Biodeterioration & Biodegradation,* **2019,** *137*, 137-146.

29.   Machuca, L. L.; Jeffrey, R.; Bailey, S. I.; Gubner, R.; Watkin, E. L. J.; Ginige, M. P.; Kaksonen, A. H.; Heidersbach, K., Filtration-UV Irradiation As An Option For Mitigating The Risk Of Microbiologically Influenced Corrosion Of Subsea Construction Alloys In Seawater. *Corrosion Science* **2014,** *79*, 89-99.

30.   International, A., ASTM G31 Standard Guide for Laboratory Immersion Corrosion Testing of Metals. ASTM International: 2012.

31.   ASTM, G.-. Standard Practice for Preparing, Cleaning and Evaluating Corrosion Test Specimens. 2017.

32.   Bayoudh, S.; Othmane, A.; Ponsonnet, L.; Ouada, H. B., Electrical Detection And Characterization Of Bacterial Adhesion Using Electrochemical Impedance Spectroscopy-Based Flow Chamber. *Colloids and Surfaces A: physicochemical and engineering aspects* **2008,** *318* (1), 291-300.

33.   Yang, Y.; Harris, D. P.; Luo, F.; Wu, L.; Parsons, A. B.; Palumbo, A. V.; Zhou, J., Characterization Of The Shewanella Oneidensis Fur Gene: Roles In Iron And Acid Tolerance Response. *BMC genomics* **2008,** *9 Suppl 1*, S11-S11.

34.   Heidelberg, J. F.; Paulsen, I. T.; Nelson, K. E.; Gaidos, E. J.; Nelson, W. C.; Read, T. D.; Eisen, J. A.; Seshadri, R.; Ward, N.; Methe, B.; Clayton, R. A.; Meyer, T.; Tsapin, A.; Scott, J.; Beanan, M.; Brinkac, L.; Daugherty, S.; DeBoy, R. T.; Dodson, R. J.; Durkin, A. S.; Haft, D. H.; Kolonay, J. F.; Madupu, R.; Peterson, J. D.; Umayam, L. A.; White, O.; Wolf, A. M.; Vamathevan, J.; Weidman, J.; Impraim, M.; Lee, K.; Berry, K.; Lee, C.; Mueller, J.; Khouri, H.; Gill, J.; Utterback, T. R.; McDonald, L. A.; Feldblyum, T. V.; Smith, H. O.; Venter, J. C.; Nealson, K. H.; Fraser, C. M., Genome Sequence Of The Dissimilatory Metal Ion-Reducing Bacterium *Shewanella Oneidensis*. *Nat Biotech* **2002,** *20* (11), 1118-1123.

35. Kip, N. and J. A. van Veen., The dual role of microbes in corrosion." *ISME* **2015,**J 9(3): 542-551.

36. Schwalb, C, The tetraheme cytochrome CymA is required for anaerobic respiration with dimethyl sulfoxide and nitrite in Shewanella oneidensis. *Biochemistry* **2003**, 42 (31): 9491-9497.

37. NACE SP0775, (2013). Preparation, Installation, Analysis, and Interpretation of Corrosion Coupons in Oilfield Operations in NACE International, Houston.

Chapter VI

E.M. Suarez, Kateřina Lepková, B. Kinsella, L.L. Machuca.

Aggressive Corrosion of Steel by a Thermophilic Microbial Consortium in the Presence and Absence of Sand.

An original reprint of the publication is shown in appendix 4.

Detailed information about the setup is provided in Appendix 1, sub-section 1.5.

Chapter VII

Erika M. **Suarez**, Kateřina Lepková, Maria Forsyth, Mike Yongjun Tan, Brian Kinsella, Laura L. Machuca.

In Situ Investigation of Under-Deposit Microbial Corrosion and Its Inhibition Using a Multi-Electrode Array System.

Manuscript submitted.

Detailed information about the setup is provided in Appendix 1, sub-section 1.6.

In Situ Investigation of Under-Deposit Microbial Corrosion and Its Inhibition Using A Multi-Electrode Array System

Erika M. Suarez [a], Kateřina Lepková [a], Maria Forsyth [b], Mike Yongjun Tan [b], Brian Kinsella [a], Laura L. Machuca [a]*.

[a] *Curtin Corrosion Centre (CCC), Western Australia School of Mines: Minerals, Energy and Chemical Engineering (WASM-MECE), Curtin University, WA 6102, Australia*

[b] *Institute for Frontier Materials and School of Engineering, Deakin University, VIC 3216, Australia*

Abstract

Under-deposit microbial corrosion (UDMC) and its inhibition in a CO_2 environment were investigated in real-time using a multielectrode array system. Local corrosion rates, galvanic currents and corrosion potentials were used to study the corrosion and inhibition process on carbon steel. *Enterobacter roggenkampii* caused localised corrosion underneath biogenic deposits through its capability to oxidise iron and reduce nitrate in anaerobic conditions. The initiation and evolution of localised corrosion were proposed based on corrosion rate distribution maps. A film-forming, under-deposit corrosion (UDC) inhibitor, 2-mercaptopyrimidine, inhibited average corrosion but did not prevent localised corrosion from the under-deposit microbial attack.

Keywords:

Steel

Acid inhibition

Microbiological corrosion

7.1. Introduction

Microorganisms have contributed to our planet evolution over the past 4 billion years and made it a perfectly liveable place for larger forms of life [1]. Iron-oxidising bacteria (FeOB) have played an essential role in the geochemical evolution of the earth

and nowadays continue influencing terrestrial and aquatic environments. Indeed, in a recent study, it was suggested that iron-oxidising, nitrate-reducing bacteria could exist in early Martian environments [2]. The concept of microorganisms involved in the geological process of iron oxidation was introduced early in the 19th century by Ehrenberg who discovered an iron bacteria which he named *Gaillonella ferruginea* (reviewed by Pringsheim [3]). Later, in the second half of the 19th century, Winogradsky, a founder of the modern microbiology, determined that some bacteria could oxidise iron at near-neutral pH (reviewed by Dworkin [4]). Since then, this fundamental biological process has inspired microbiologists and geoscientists to focus on the role of metal-oxidising microorganisms in the biogeochemistry of iron and other elements like manganese.

Microorganisms with these ancient metabolic capabilities are also ubiquitous in seawater and oilfield systems, and their activities have been associated with microbiologically influenced corrosion (MIC) [5-6]. Therefore, biological iron oxidation has also gained attention within the community of corrosion specialists. Particularly, because of the increasing demand for nitrate injection as a mitigation strategy against souring of reservoirs in oil and gas fields. The nitrate benefits the proliferation of nitrate-reducing bacteria (NRB) which consume organics available in the reservoir and, therefore suppress the sulphate reducing bacteria (SRB) population; this competition leads to a decrease of biogenic H_2S produced by SRB [7-10]. However, there are growing concerns about a possible undesired effect; if the injected nitrate is not entirely consumed and then transported through the pipelines, it could lead to MIC by nitrate-reducing microorganisms.

Some members of the Proteobacteria phylum can oxidise iron and reduce nitrate in anaerobic environments, instead of oxygen reduction. The iron-oxidising, nitrate-reducing bacteria species, abbreviated as FeONRB, use ferrous iron (Fe^{2+}) as electron donor and nitrate (NO_3^-) as electron acceptor with organic cosubstrates [11-13]. The final metabolic by-products of this anaerobic respiration can be either nitrite (NO_2^-), nitric oxide (NO), nitrous oxide (N_2O) or, dinitrogen gas (N_2) in a process called denitrification. Also, some FeONRB members can reduce nitrate (NO_3^-) to ammonium (NH_4^+) [14]. The electron transport pathways begin when microorganisms oxidise the electron donor ferrous iron (Fe^{2+}) inside the cell; then the electrons are channelled into respiratory chains, ultimately producing energy in the form of ATP [14]. A previous

study of anaerobic nitrate-dependant microbial oxidation found that the ratio of formed iron (Fe^{3+}) and reduced nitrate was 1: 0.22 [46].

The oxidation of ferrous iron (Fe^{2+}) to ferric iron (Fe^{3+}) can lead to Fe^{3+} precipitation and accumulation in the form of ochre-like deposits [15]. The formation of Fe^{3+} mineral deposits by bacteria was described by Kappler et al. [16] as follows:

1) The initial abiotic oxidation of Fe^{2+} form mono- and di-nuclear dissolved species of Fe^{2+} $[FeOH]^{2+}$ and $[Fe_2(OH_2)]^{4+}$.

2) The dissolved species are transformed into polymeric Fe^{3+} colloids.

3) The colloids precipitate to poorly crystalline ferrihydrite.

4) Ferrihydrite conversion to either hematite or goethite depending on the reaction conditions.

Finally, there is fast precipitation of the Fe^{3+} by-products near the microbial cells due to their low solubility at neutral pH [17].

To date, very limited work has been conducted to link the FeONRB biological process to corrosion under anaerobic conditions. Apart from the conventional concept of biological oxidation of ferrous iron (Fe^{2+}) to ferric iron (Fe^{3+}) connected to corrosion, it might also be possible that direct electron uptake from metallic iron and subsequent electrical-MIC occurs by nitrate reducers. For instance, Xu *et al.* [18] found that *Bacillus licheniformis* caused localised corrosion when conducting iron oxidation and nitrate reduction in the absence of oxygen. The authors proposed a nitrate reduction corrosion mechanism based on bioenergetics where extracellular electrons from metallic iron oxidation are transported into the NRB cytoplasm for nitrate reduction under biocatalysis. In that research, ferrous ammonium sulphate and iron nitride were identified as the main metabolic by-products. The accumulation of deposits, either biogenic or non-biogenic, on metal surfaces adds another corrosion problem, i.e., under-deposit corrosion (UDC). UDC has become recognised as a threat to the integrity of equipment and pipelines, accounting for a significant fraction of localised corrosion at otherwise non-corrosive conditions. These deposits can also provide shelter to bacteria, creating conditions that are conducive for MIC. The combined presence of deposits and microorganisms is known to result in a rather complex phenomenon recently termed as under-deposit microbial corrosion (UDMC) [19]. UDMC has been previously reported in both MIC experiments [20-22] and case studies

of pipeline failures [23-24]. However, little is known about the mechanism of UDMC on carbon steel.

In general, corrosion mitigation of carbon steel involves chemical treatment with corrosion inhibitors (CIs) and biocide chemicals. However, CI performance is known to be affected by the presence of deposits in which the chemical compounds can be adsorbed onto resulting in inhibitor depletion and therefore, insufficient level of protection to the underlying metal surface [25-28]. Additionally, biocide efficiency can be compromised in the presence of deposits where microorganisms can shield from antimicrobial compounds. Thus, the appropriate selection of a corrosion inhibitor that prevents UDC is critical and remains an industry challenge. In particular, CI efficiency in the presence of microorganisms has hardly been studied.

Electrochemical methods such as linear polarisation resistance (LPR), electrochemical impedance spectroscopy (EIS) and potentiodynamic polarisation are fast and versatile corrosion techniques commonly used to study general corrosion and inhibition mechanisms. However, they have some limitations in non-homogeneous surfaces, such as those created by biofilms and deposits, and do not offer information about local electrochemical events on the metal surface, e.g. galvanic effects [29-31]. Multi-electrode arrays, such as the wire beam electrode (WBE), can provide temporal and spatial information about potentials and galvanic effects taking place on a metal surface in a corroding environment. WBE systems have been used to study general and localised corrosion [32-35], erosion-corrosion [36-37], coating evaluation [38-40], UDC, and corrosion inhibition [29, 31, 41-43] and most recently, to study MIC [44-45].

This study investigates UDMC by *Enterobacter roggenkampii*, a FeONRB recovered and isolated from an oil production facility in Western Australia. The inhibition of UDMC was evaluated using an organic, film-forming CI, 2-mercaptopyrimidine (MPY). Local galvanic currents, corrosion potentials and, corrosion rates from the WBE system were mapped, and profilometry analysis was used to assess localised corrosion in the presence of the bacterium and the CI. Intracellular adenosine triphosphate (cATP) measurements and bacterial cell counts were also carried out to monitor bacterial growth and activity throughout the exposure. Visualising *in situ* the UDMC process in the presence and absence of a corrosion inhibitor compound will aid understanding, for the first time, the complex mechanism of UDMC and the efficiency of corrosion inhibitors under UDMC conditions. This

method has shown great promise as a reliable tool for the evaluation and selection of chemical treatments formulated to prevent localised corrosion in industrial facilities.

7.2. Materials and methods.

7.2.1. Test solution.

The test solution for both bacterial growth and corrosion studies consisted of artificial seawater (ASW) 2.45% salinity, containing ammonium nitrate as the only soluble electron acceptor for the bacteria isolate and acetate as a cosubstrate. The ASW composition was as follows: sea salts (Sigma Aldrich) 20 g/L, CH_3COONa 20 mM, NH_4NO_3 14 mM and, 0.939 L of ultrapure water (Milli-Q system, resistivity 18.5 $M\Omega.cm$). The compounds were mixed and sterilised by autoclaving. The solution was sparged with a gas mixture of 20% CO_2 in N_2 gas for 2 h, followed by addition of 10 mL of vitamins solution and, 1 mL of Wolfe's mineral elixir [46]. Finally, the pH was adjusted to 7.0 ± 0.2 using a sterile and deoxygenated $NaHCO_3$ solution 47.62 mM. For the test with CI, 2-mercaptopyrimidine (MPY) from Sigma-Aldrich was evaluated at a concentration of 0.892 mM. MPY concentration was selected according to previous work where this CI performed efficiently at deposited-carbon steel surfaces [26]. To our knowledge, this CI has not been tested in the presence of microorganisms (unknown biocidal properties). MPY was added to a separate test solution to allow the compound to dissolve before pumping into the WBE reactor.

7.2.2. Bacterium preparation.

Enterobacter roggenkampii used in the present study was provided by the Curtin Corrosion Centre (Curtin University) and maintained at 40 ^oC in anaerobic glass vials. A pre-test was performed to determine the iron oxidation and nitrate reduction capability of this isolate before the experiments. *E. roggenkampii* was grown in 100 mL glass vials containing the test solution sparged with CO_2/N_2 gas mixture (section 2.1) and 0.75 cm^2 carbon steel coupons. The test solution did not contain ferrous iron; it was strictly designed to support iron oxidation coupled to nitrate reduction under anaerobic conditions. The bacterial activity was evidenced by significant iron

oxidation and deposition on steel coupons and typical exponential curve of growth of this isolate, indicating FeONRB metabolic capability.

Before the start-up of the WBE reactor, the bacterium was inoculated at 10% into anaerobic ASW and incubated at $40^{\circ}C$ for 48 h (exponential phase ~ 10^8 cell/mL). Bacterial cells were harvested by centrifugation (3,600 x g, 30 min at room temperature) to remove metabolites formed by bacterial activity in the culture. The supernatant was discarded and, the pellet was suspended in 1 mL of sterile oxygen-free ASW. The bacterial cell suspension was then inoculated into the WBE reactor containing the anaerobic test solution.

7.2.3. Tests materials

A multielectrode array system, namely the wire beam electrode (WBE), was used to measure galvanic currents and potentials locally. Also, local corrosion rates were calculated from linear polarization (LP) measurements at each wire. The WBE system was purchased from CPE systems Pty Ltd. The WBE sensor consisted of 100 API X65 pipeline steel electrodes (0.0595 cm^2) electrically isolated and tightly packed with a total surface area of the WBE was 5.95 cm^2. Additional WBE specifications were described elsewhere [30]. Fig. 1 shows a schematic diagram of the experimental setup for UDMC testing and its inhibition using the WBE system adapted to operate in three different modes (described in section 7.2.6). The WBE reactor was a custom-made glass cell designated to operate either in a batch or a continuous flow mode. A Teflon base was also designed to mount the WBE sensor in an up-right inside position. The Teflon base, the glass reactor and the glass lid were hermetically sealed to ensure anaerobic conditions through the immersion period. The temperature was controlled using a custom-made immersion heater with an external glass sheath. A single junction Ag/AgCl reference electrode was placed into a ceramic tip capillary filled with sterile 3M KCl. The counter electrode was a platinum-coated mesh.

7.2.4. Experimental setup

The WBE surface was polished to 600 grit finish (SiC paper), washed with ethanol, dried with N$_2$ and subjected to ultraviolet germicidal irradiation (UVGI) for

15 minutes (i.e., every side of the sensor that would be in contact with the test solution was irradiated).
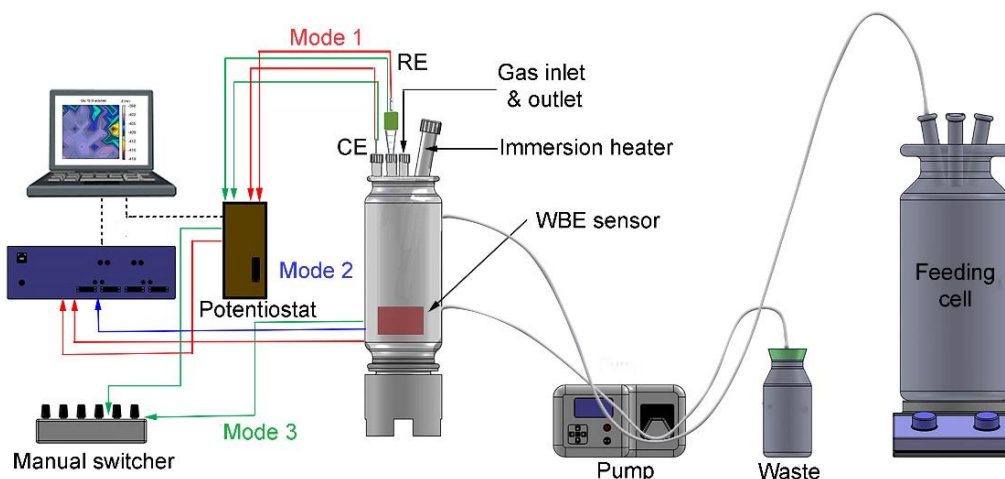
Figure 1.Schematic diagram of the experimental setup for under-deposit microbial corrosion (UDMC) testing using a WBE system adapted to operate in 3 modes. The WBE reactor is connected to a feeding cell in a continuous flow mode. The counter electrode (CE) and the reference electrode (RE).

Before setting up the WBE reactor, 2L of ASW was sparged for 2 h with a gas mixture of 20% CO_2 in N_2 in a Schott bottle sealed with a silicone stopper. All the non-autoclavable parts of the WBE system and reactor were immersed in 70% ethanol for 30 min, dried with N_2 gas and, sterilised by UV-C light exposure for a minimum of 15 minutes. The WBE surface was mounted face-up inside the reactor (Fig.1). Afterwards, the assembled reactor was de-oxygenated using CO_2/N_2 gas mixture for 15 minutes before transferring the CO_2/N_2-saturated ASW into the reactor. The ASW was then pumped into the de-aerated reactor at a flow rate of 100 rpm using a low gas permeability tubing. The WBE terminals were connected to the WBE instrument.

The test conditions were as follows:

1) abiotic test (ASW only)

2) biotic test (ASW inoculated with *E. roggenkampii*)

3) Corrosion inhibition test or CI test (MPY performance in the presence of *E. roggenkampii*).

The abiotic test was carried out in stagnant conditions through the experimental period of 12 days immersion. In the corrosion inhibition test, the steel surface of the WBE was pre-filmed with the CI for 18 h (before inoculation with *E. roggenkampii*).

For both tests (biotic and CI tests), electrochemical measurements were carried out during 6 days of exposure with bacteria with the WBE reactor set as batch mode (no flow). After this period, the WBE reactor was switched to the continuous mode (flow mode) by connecting it to a feeding cell (Fig.1) containing sterile test solution (ASW and inhibited ASW for the biotic and CI test, respectively). A catalyst™ FH100M multichannel pump was used for running the reactor under continuous mode at a flow rate of 4 rpm (~250 mL of ASW exchanged per day). This continuos mode allowed nutrients to be continuously fed into the WBE reactor and metabolic by-products (waste) removed as a continuous stream to maintain microbial activity throughout the exposure. Electrochemical monitoring across the WBE continued during 6 more days with the reactor operated under continuous mode. All the tests were conducted at $40 \pm 5^{o}C$, maintaining a CO_2/N_2 blanket for a total period of 12 days of immersion.

7.2.5. *Bacterial enumeration and cATP measurements*

Every two (2) days an aliquot of ASW was collected to estimate *E. roggenkampii* cells in the test solution using a Neubauer chamber and, a Nikon Eclipse Ci-L phase-contrast microscope, Nikon Inc. From the same aliquot, 1 mL of the solution was used to measure cellular adenosine triphosphate (cATP) as a direct indication of total living biomass in suspension using the Quench-Gone™ organic modified test kit, LuminUltra Technologies Ltd. Similarly, pH in the ASW was monitored every 2 days using the Thermo Scientific™ Orion™Star A221 pH portable meter. These analyses were performed in duplicate.

7.2.6. *Electrochemical analysis*

Fig.1 shows the schematic diagram of the WBE system setup for UDMC testing. The system was operated in three (3) different modes as follows:

Operation mode 1 (corrosion rates and corrosion potentials at the entire WBE surface).

The 100 wires or electrodes terminals in the WBE sensor were connected to the WBE instrument (auto-switch device), and this to the Gamry +600 potentiostat as shown by the red dashed lines (Fig.1). In this mode, electrochemical tests were performed by coupling all the electrodes in the WBE together, thus simulating a large one-piece working electrode. Therefore, electrochemical measurements reflected the events from the entire WBE surface. Linear polarisation (LP) was conducted by applying a potential perturbation of ± 10 mV vs OCP and a scan rate of 0.5 mV/s. The stabilisation period before LP measurements was 30 minutes, during which the OCP was continuously recorded.

Operation mode 2 (local galvanic currents).

The blue dashed lines illustrate this operation mode, where the WBE was connected to the auto switch to measure local galvanic currents. In the instrument, the 100 inputs from the WBE sensor are multiplexed to a 16-bit analogue-to-digital converter (ADC). A ZRA is used to perform current measurements; thus, no voltage is developed across the inputs. Current distribution maps were obtained by performing sequential measurements between each electrode and, the remaining 99 electrodes shorted together. A total of 100 current measurements were recorded, and the maps were plotted using OriginPro® 2019.

Operation mode 3 (local corrosion potentials and local corrosion rates).

The green dashed lines describes this operation mode. The WBE terminals were connected to a manual switcher (100 pins) and this to the potentiostat. Similar to mode 1, this mode operated as a three-electrode configuration but this time, recording electrochemical measurements at each electrode or wire in the array (one at the time). LP measurements were performed on each electrode by applying a potential perturbation of ± 10 mV vs OCP and a fast scan rate of 5 mV/s. The OCP at each electrode was recorded for 10 seconds before performing the LP measurements. It is important to mention that although LP measurements used a fast scan rate, approximately 30 minutes were needed to obtain the whole 100 measurements for plotting each map. This was due not only to the acquisition time but also to the time

required to set each measurement in the potentiostat manually. It is acknowledged that the fast scan rate will probably result in some interference due to measuring the capacitance at this faster scan rate. However, this technique was adopted in order to determine the trend in corrosion rates, and it will be demonstrated later that the measurements corresponded favourably with the potential and galvanic currents measured. Data fitting of each electrode was made using Gamry Echem Analyst, version 7.05, Gamry Instruments, and Inc. A total of 100 corrosion potentials and, 100 corrosion rates values were plotted to create each map using OriginPro®2019.

7.2.7. Surface profilometry

After the immersion period, the WBE reactor was disassembled, and the WBE sensor was washed with ASW and gauze to gently remove the outer deposit layers formed over the entire WBE surface in both biotic and CI test (supplementary material). Subsequently, the metal was cleaned with absolute ethanol and dried with N_2 gas. After this step of outer deposit layers removal, small mount-shape deposits firmly attached to the metal were exposed exhibiting a random distribution over WBE surface. Finally, these deposits were removed using Clarke's solution following the standard cleaning procedure [47]. Surface profilometry analysis was conducted by using a LaserScan profilometer, Solarius SolarScan non-contact measuring system 200NP (Solarius Inc, USA). The 3D-inspection system is equipped with Solarscan NT software version 7.4. The analysis of profiles was performed by step height measurements using the automatic method as described in ISO 5436 standard [48]. The analysis included the maximum and average pitting depths and, pitting depths density (number of depths/m^2). Pitting depths density was obtained by counting all depth points on the entire WBE surface using the 3D-image.

7.3. Results

7.3.1 Bacterial ATP and, pH monitoring

Fig.2 shows pH, bacterial cell counts and ATP measurements conducted every two (2) days during the period of immersion. It can be seen in Fig.2a that the pH in the abiotic test remained close to 7.2 for the whole experimental period. However, the pH

for the biotic test and CI test gradually decreased during the first 6 days of immersion and then, increased by almost 0.2 pH units when it was connected to the feeding cell. In this mode, pH remained constant until the end of the experiment. The bacterial enumeration in Fig.2b indicates a gradual increase in cell numbers in test solution from 10^6 to 10^8 cells/mL from day zero (0) to 6th day. At this time, the cell numbers dropped upon start-up of continuous mode due to the removal of planktonic cells from the test solution.

Similarly, a reduction of the cATP content in the solution was observed when the reactor was switched to the continuous mode in both biotic and CI tests (Fig.2c). However, after the 8th day of immersion bacteria and cATP showed exponential trends. This indicated favourable bacterial growth conditions as a result of constant nutrient replenishment and, elimination of the excess of metabolites.
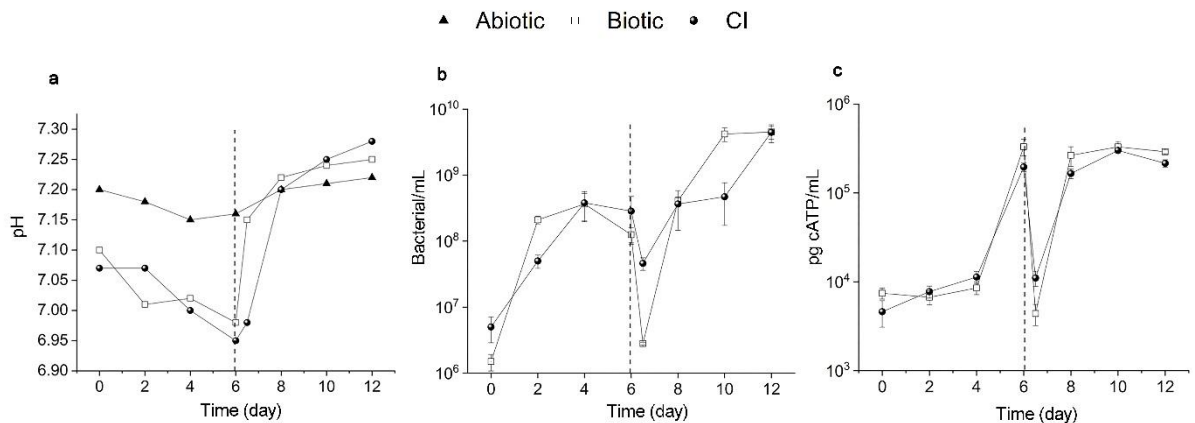
Figure 2. WBE reactor monitoring: **a)** pH; **b)** bacterial enumeration and, **c)** cATP measurements of the CO_2/N_2 saturated ASW during 12 days of immersion. The dashed line indicates the time in which the WBE reactor was switched to the continuous flow mode by connecting it to a feeding cell. The measurements after the dashed line (6.5 days) were performed after 12 hours of flow connection with approximately 125 mL of ASW exchanged.

7.3.2 Corrosion potentials and corrosion rates at the entire WBE surface

Fig.3 displays corrosion potentials and corrosion rates measurements from LP measurements recorded at the coupled WBE immersed in CO_2/N_2 saturated-ASW (operation mode 1 described in section 2.6). While the potentials in abiotic tests remained steady (-712 ± 9 mV), the potentials in the biotic test and CI test constantly

fluctuated during the immersion period (Fig. 3a). In the pre-filming period (18 h of inhibitor contact and before bacteria inoculation) a positive shift of the corrosion potentials from -675 mV to -663 mV (Fig. 3a) was observed. This positive shift on potentials after MPY addition has also been reported in previous inhibitor studies [25].

After bacteria inoculation, the corrosion potentials gradually shifted towards positive values from day zero (0) to the 5th day for biotic test and from day zero (0) to the 4th day for the corrosion inhibition test by +130 mV and +69 mV to values of -545 mV and -593 mV, respectively (Fig. 3a). Afterwards, the corrosion potentials dramatically shifted again more positively by +146 mV on the 6th day for the biotic test and by +187 mV on the 5th day for the CI test. It can also be noticed in Fig. 3a that when the reactor for the biotic test was set to continuous flow mode, the corrosion potentials recorded at the steel WBE remained steady, reaching a maximum value of -371 mV on the 9th day. Contrarily, the steel WBE at the CI test exhibited a considerable positive shift of the corrosion potential by + 229 mV to a value of -374 on the 9th day. At the 11th day of immersion, a maximum corrosion potential value of -362 mV was recorded for the CI test.

The average corrosion rates (2 readings per cycle) are shown in Fig. 3b. Regarding the biotic test (Fig. 3b), there was a gradual increase in corrosion rate during the first three (3) days of immersion with a maximum value of 0.5 mmpy recorded on the 2nd day. Then, corrosion rates progressively dropped until the last experimental day with a value of 0.1 mmpy. The abiotic control exhibited low corrosion rates throughout the exposure. On day zero (0) recorded 0.6 mmpy, then corrosion rates gradually decreased to 0.05 mmpy on the 12th day of immersion.

Fig. 3b indicated a reasonable level of protection achieved by MPY in the pre-filming period (18 h contact). The corrosion rates dropped from 0.3 mmpy on the day -1 to 0.1 mmpy on day zero (0). This inhibition performance of MPY has been previously demonstrated at fully deposited steel surfaces in a CO_2 environment at 30°C [25-26]. However, after bacteria addition corrosion rates fluctuated, reaching maximum values of 0.9 and 1.3 mmpy on the 4th and the 6th day, respectively. Upon continuous flow mode, in this CI test, the corrosion rates gradually decreased, reaching a corrosion rate value of 0.05 mmpy on day 12 of immersion. This result suggests that the continuous replenishment of fresh inhibited solution and the discharge of corrosive

metabolites from the WBE reactor diminished the corrosion effects on the steel surface. In contrast, the biotic test, the connection to the continuous flow mode was not reflected by a drop in corrosion rates at the entire WBE surface.
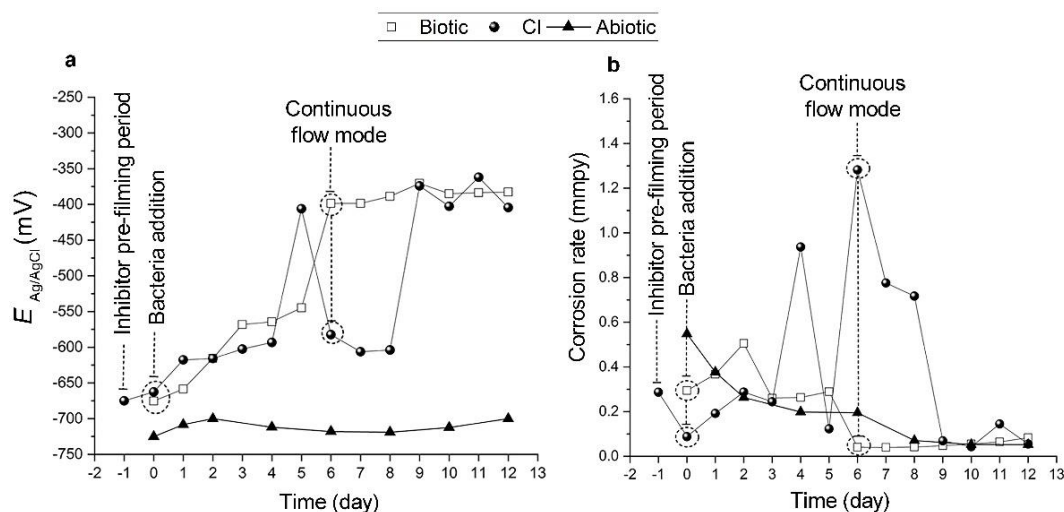
Figure 3. Open circuit potential (Fig.3a) and, corrosion rates from polarisation resistance measurements (Fig.3b) recorded at the coupled WBE (operation mode 1) immersed in CO_2/N_2 saturated-ASW at 40°C for 12 days. For the CI test, the MPY pre-filming period (~ 18 h) is represented as the day (-1) in the X-axis. From day zero (0) to the 12th day comprises the immersion period in the presence of bacteria. The dashed line on the 6th day indicates the time in which the WBE reactor was switched to the continuous flow mode by connecting it to a feeding cell.

7.3.3 Local electrochemistry- Abiotic test.

Fig.4 shows galvanic distribution maps across the WBE surface under abiotic conditions. It can be seen in Fig. 4a that on day zero (0) various cathodic and anodic areas are formed on the surface due to the heterogeneous nature of the corrosion process. These sites continued to change, showing a continuing development in time and space of anodic and cathodic areas (Fig. 4b-c). However, the magnitude of these currents is low, and the potential differences across the electrodes are small (Fig. 4f-g) indicating low corrosivity of the test solution under abiotic conditions. These results are in agreement with the 3D-image in Fig. 4d where the WBE surface looks unaffected and with no apparent signs of localised corrosion.
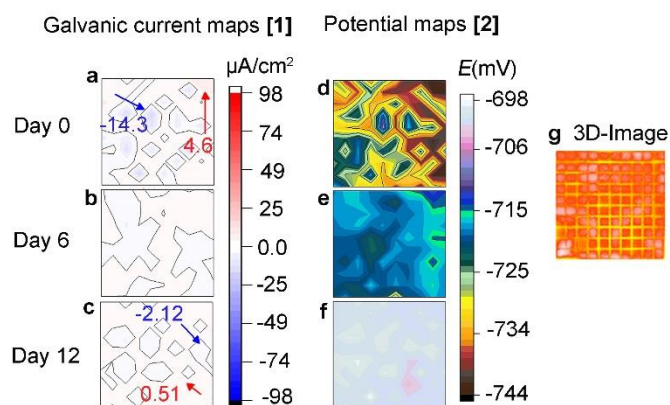
Figure 4. **a-c)** Galvanic current and **d-f)** corrosion potential distribution maps of steel WBE immersed in CO_2/N_2 saturated-ASW under abiotic or sterile conditions. Inset: maximum anodic and cathodic currents in red and, blue colour, respectively; g) 3D-image of the entire WBE surface after 12 days of immersion.

7.3.4   Local electrochemistry-Biotic test.

Fig. 5 displays distribution maps of galvanic currents (1st column), corrosion potentials (2nd column) and, corrosion rates (3rd column) across the WBE surface in the biotic test. The figure also shows photos of the WBE surface before and after the corrosion products were removed and, a 3-D image at the last row. It is noteworthy to clarify that areas of the WBE that recorded net galvanic currents with anodic and cathodic behaviour will be referred as anodic and cathodic areas through the document to facilitate the description of the current distribution maps.

The scale shown on the potential maps were set using the maximum, and minimum values recorded at each time to visualise small differences in potential. In general, the distribution of potential is in agreement with galvanic currents and corrosion rates mapped across the surface of the WBE. Sites with higher negative potentials matched the anodic areas and these, in turn, coincided with many of the areas with higher corrosion rates. Also, a general trend of the potentials to shift towards more positive values through time was observed in this biotic test. The maximum and minimum potential values were -660 mV and -641 mV on day zero (0) and -492mV and -360 mV on day 12, respectively. Based on the results shown in Fig.5, the sequence of events that describe UDMC evolution across the steel WBE are presented as follows:

Day zero (0): Net galvanic currents (Fig. 5a.1) show different anodic and cathodic areas indicating heterogeneous reactions at the early stages of biofilm adhesion. However, small differences of only -19 mV in corrosion potentials across the WBE were observed (Fig. 5a.2). Interestingly, a wide range of corrosion rates from 0.01 mmpy to 1.68 mmpy was measured through the WBE surface. These local differences in corrosion rates indicated a heterogeneous corrosion process at this initial MIC stage.

Second (2nd) day: anodic and cathodic areas continued developing in time and space, the region at the top right of the WBE exhibited higher anodic currents than the adjacent area (Fig. 5b.1). This coincided with the corrosion potential maps (Fig. 5b.2) which had more negative potentials at this region. Also, the differences in potentials were higher 51 mV at this time compared to the ones recorded on day zero (0). It can also be noticed in Fig. 5b.3 that local corrosion rates across the surface of the WBE decreased in magnitude. This observation is particularly noticeable in the regions labelled in the Figure.

Fourth (4th) day: Fig. 5c.1 shows there was a shift in current distribution across the surface of the electrode array with anodic currents developing in areas that had previously exhibited cathodic currents. Only a maximum potential difference of 24 mV was recorded at this immersion time (Fig. 5c.2). Some electrodes in Fig. 5c.3 showed higher and lower corrosion rates in respective similar areas compared to the previous map. These results could be an indication of non-linear localised corrosion evolution under these conditions.

Sixth (6th) day: a reversal in galvanic current was again observed, but this time, the anodic currents increased, reaching a maximum value of 11.89 $\mu A/cm^2$. It can be seen in Fig. 2b-c, that on this day the highest values of planktonic bacteria cell counts and ATP content. Thus, it is possible to relate this increase of anodic currents to bacteria presence, probably translated in an efficient metabolic activity leading to local corrosion products deposition. The corrosion rate distribution map followed the same trend as the previous map displaying corrosion rates fluctuations at specific locations. However, most of the areas on the WBE sensor showed lower corrosion rates than the ones recorded on previous days.

Eighth (8th) day: it can be observed in Fig.5 e.1 that there was a decrease in anodic currents across the WBE surface. At this point, approximately two days passed since the WBE reactor was set to a continuous flow mode (~ 1 L of ASW exchanged). Perhaps the reduction of excess metabolic by-products allowed better visualisation of localised events on the metal surface. For instance, electrode #35 recorded the highest anodic current, and this coincided with the more negative potential (Fig. 5e.2). This potential was 79 mV more negative than the adjacent electrode with a value of -389 mV, showing good correlation with corrosion rates measured at this electrode with a value of 0.51 mmpy (Fig. 5e.3)

Tenth (10th) day: Fig. 5f.1-2 followed the same pattern as the 8th day. However, the site with maximum anodic current and a more negative potential is in a different location (electrode # 75). Again the areas locally affected seemed to evolve differently.

Twelfth (12th) day: at this point, 6 days have passed since the reactor was connected in continuous flow mode. The anodic currents were in general, reduced reaching a maximum value of ~10 μA/cm^2 at electrode #39 (Fig. 5g.1). Potential map (Fig. 5g.2) on the other hand, had a high corrosion potential difference over 130 mV between the most positive and most negative potential, thus localised corrosion is expected. Corrosion rates of the electrodes labelled in Fig. 5g.3 increased, indicating localised corrosion propagation events. Another notable finding was the confluence of corroded areas, as indicated in the map for electrodes #39 and #49. The WBE surface photographed before corrosion products removal and after biofilm removal (Fig. 5h.1) revealed corrosion product deposition randomly across the WBE surface. The deposits had mound-shaped morphology with different sizes and located at different areas within each electrode or wire. The removal of corrosion products (Fig. 5h.2) exposed the corroded areas or pits. The pits were located precisely underneath the deposits. These observations coincided with the 3D-image which revealed locally affected areas in the form of pits (blue-black areas) in the places previously covered by deposits. These results demonstrate that under deposit localised corrosion occurred as a result of *E. roggenkampii* activity.
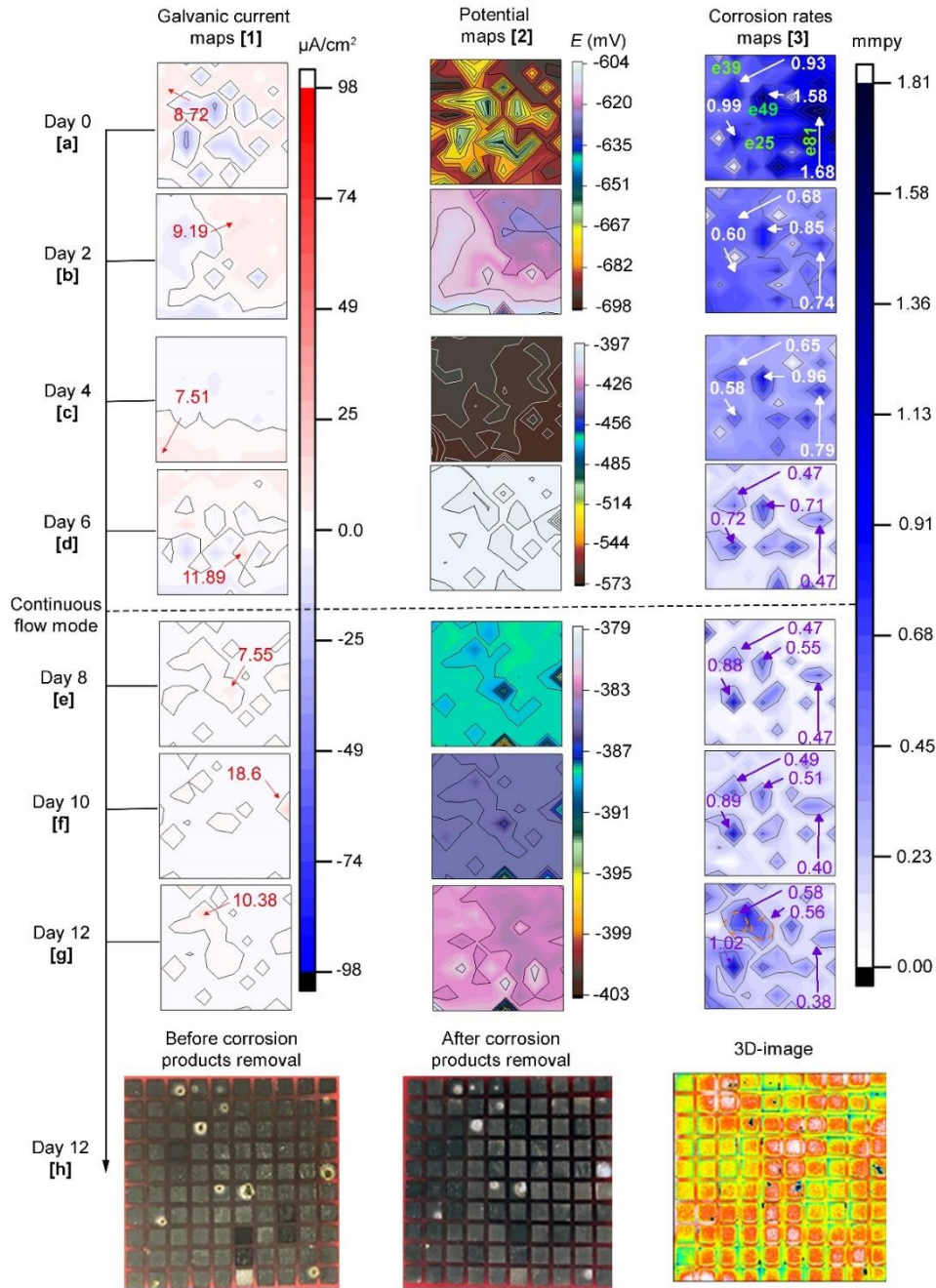
Figure 5. *Biotic test*: **5. 1a-g)** galvanic currents; **5. 2a-g)** corrosion potentials and; **5. 3a-g)** corrosion rates distribution maps of the steel WBE immersed in CO_2 saturated-ASW and *E. roggenkampii* at 40°C for 12 days. The current maps show the maximum anodic currents in red while for the corrosion rate maps high corrosion rates are shown in violet and white and electrode number in green. Photographs of the entire WBE surface **5.1h)** before and **5. 2h)** after corrosion products removal; **5. 3h)** 3D-image of WBE surface after corrosion products removal.

7.3.5 Local electrochemistry- CI test (before corrosion inhibitor addition).

Fig. 6 shows galvanic current and corrosion potential distribution maps across the WBE immersed during 18 h in CO_2/N_2 inhibited ASW before *E. roggenkampii* addition, that is during the first part of the CI test procedure. It can be seen that after 1 min of MPY contact, two (2) anodic and cathodic sites in the top right and bottom left of the WBE surface, appeared respectively (Fig. 6a). These currents are higher than the ones recorded at the WBE immersed in the abiotic test (Fig. 4a). This is probably due to the different inhibitor adsorption mechanism during film formation. Thus, resulting in different anodic and cathodic areas. However, after 6 h (Fig. 6b) and 18 h of immersion (Fig. 6c) the magnitude of these currents was considerably reduced, indicating acceptable inhibition performance of the MPY. The potential distribution maps (Fig. 6d-f) are in agreement with their respective galvanic current maps. The sites of higher negative potentials were situated in the same areas where anodic currents were recorded. After 18 h of immersion (Fig. 6f), a more uniform distribution of potential was noticed, probably related to gradual and more uniform filming of the MPY inhibitor across the WBE surface. These findings are supported by a previous study using a WBE partially covered with silica sand deposit under CO_2 conditions.
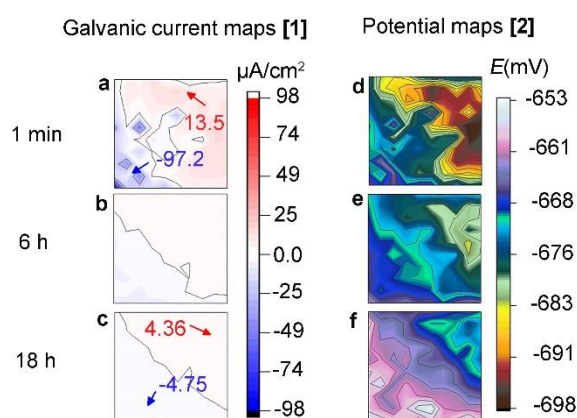
Figure 6. a-c) Galvanic currents and, **d-f)** corrosion potential distribution maps of steel WBE immersed during 18h in CO_2/N_2 inhibited-ASW (0.892 mM of 2-mercaptopyrimidine) before FeONRB addition (inhibitor pre-filming period).

7.3.6 Local electrochemistry- CI test (after corrosion inhibitor addition).

Fig. 7 displays distribution maps of galvanic currents (1st column), corrosion potentials (2nd column) and, corrosion rates (3rd column) across the WBE surface in

the CI test. The Figure also shows photos of the WBE surface before and after corrosion products removal and, a 3D- image in the last row. The height scale for the potential maps was set using the maximum and minimum values to visualise small differences in potentials at each map. Similar to the biotic test (Fig. 5), the potential maps coincided with most of the galvanic currents and corrosion rate map. Again, a trend was observed for potentials to move towards positive values in time. The potentials started with values of -687 to -625 mV on day zero (Fig. 7.a2) and finalised between -464 to -333 mV on day 12 (over 130 mV difference). (Fig. 7g.2). Based on the results in Fig.7, the sequence of events that describe corrosion inhibitor performance in the presence of bacteria is presented as follows:

Day zero (0): no significant changes were detected after FeONRB addition. Galvanic current and potentials maps remained similar to the ones at the end of the inhibitor pre-filming period (Fig. 6c and f). It can be seen in Fig. 7a.3 that corrosion rates were low on almost the entire WBE surface, except for a few areas, e.g. electrode # 16 recorded 0.56 mmpy.

Second (2nd) day: there was a reversal of galvanic currents and potentials (Fig. 7b.1-2). The reversal was accompanied by a general increase in corrosion rates corresponding to those regions of anodic currents at more negative potentials.

Fourth (4th) day: at this time, the magnitude of galvanic currents, potentials and corrosion rates increased considerably in areas previously established on the 2nd day reaching 1.68 mmpy in electrode # 26 (Fig. 7c.1-3).

Sixth (6th) day: galvanic currents and potentials reversed again, but these anodic currents diminished in magnitude (Fig. 7d.1-2). Corrosion rates decreased to some extent reaching a maximum value of 1.09 mmpy in electrode #2.

Eighth (8th) day: Fig. 7e.1 shows that after 2 days of continuous flow, the anodic currents expanded covering the top right corner of the WBE surface. It can also be noticed that there was a marked difference in potentials (120 mV) between the more negative and positive value. The more negative potential (-543 mV) was recorded at electrode #99 (Fig. 7e2), which also had the highest anodic current (Fig. 7e1), and corrosion rate (Fig. 7e3), with values of 29.47 $\mu A/cm^2$ and 0.53 mmpy, respectively. A general reduction of corrosion rate values was evident across the WBE probably due

to the replacement of corrosive metabolites by fresh solution with more inhibitor, making it possible to have a more unobstructed view of the local corrosion events.

Tenth (10th) day: It is evident in Fig. 7f.1-3 that the three (3) maps are in good agreement. At this stage, almost the total amount of the inhibited ASW (~ 2 L) was replenished. Again, potential differences on the surface continued to increase, but this time, a 132 mV difference was recorded between the maximum and minimum value. Instead, the maximum corrosion rate value was only 0.27 mmpy in electrode # 81.

Twelfth (12th) day: Similar to the maps recorded on the 10th day of immersion (Fig. 7f.1-3), the maps of the different parameters were congruent with each other (Fig. 7g.1-13). However, electrode # 81 had a higher corrosion rate, indicating a localised corrosion propagation process. Fig. 7h.1 shows a photograph of the WBE surface before corrosion products removal and after

biofilm cleaning. Similar to the biotic test, corrosion products were also found to be deposited on the WBE surface. The deposits also had mound-shaped morphology, but this time they exhibited smaller sizes compared to the deposits founded in the biotic test. After corrosion products were removed (Fig. 7h.2), pits were exposed, which were also found underneath the deposits. The 3D-image in Fig. 7h.3 revealed pits (blue-black areas) developed underneath deposits.

7.3.7. Localised corrosion results

Fig. 8 shows the results of the average and maximum pitting depths and, pitting densities from 3D-laser scanning profilometry. Average and maximum pitting depths results indicate a considerable localised attack in the presence of the bacterium with maximum pitting depth of 65 µm in the biotic test and 64 µm in the CI test; the abiotic test exhibited maximum pitting depths of 12 µm. MPY inhibited average corrosion recording 0.05 mmpy at day 12th (Fig 3.b). However, this sulphur-containing compound did not inhibit localised corrosion, which represents a significant concern in the industry (Fig. 8).

Although slightly higher average pitting depths, resulted on the WBE surface in the biotic test, the surface in the CI test still suffered considerable localised corrosion damage. In fact, the surface in this CI test showed higher depth density (1.8E+05 depth

points/m^2) compared to the biotic test (1.8E+01 depth points/m^2). The number of pits can be easily visualised on the 3D- image in Fig. 5h.3 for the biotic test and in Fig. 7h.3 for CI test. The abiotic test, on the other hand, did not show distinct pits. The WBE surface immersed in sterile conditions looked more uniform than both biotic tests, suggesting that no localised corrosion occurred in the absence of bacteria (Fig. 4d).
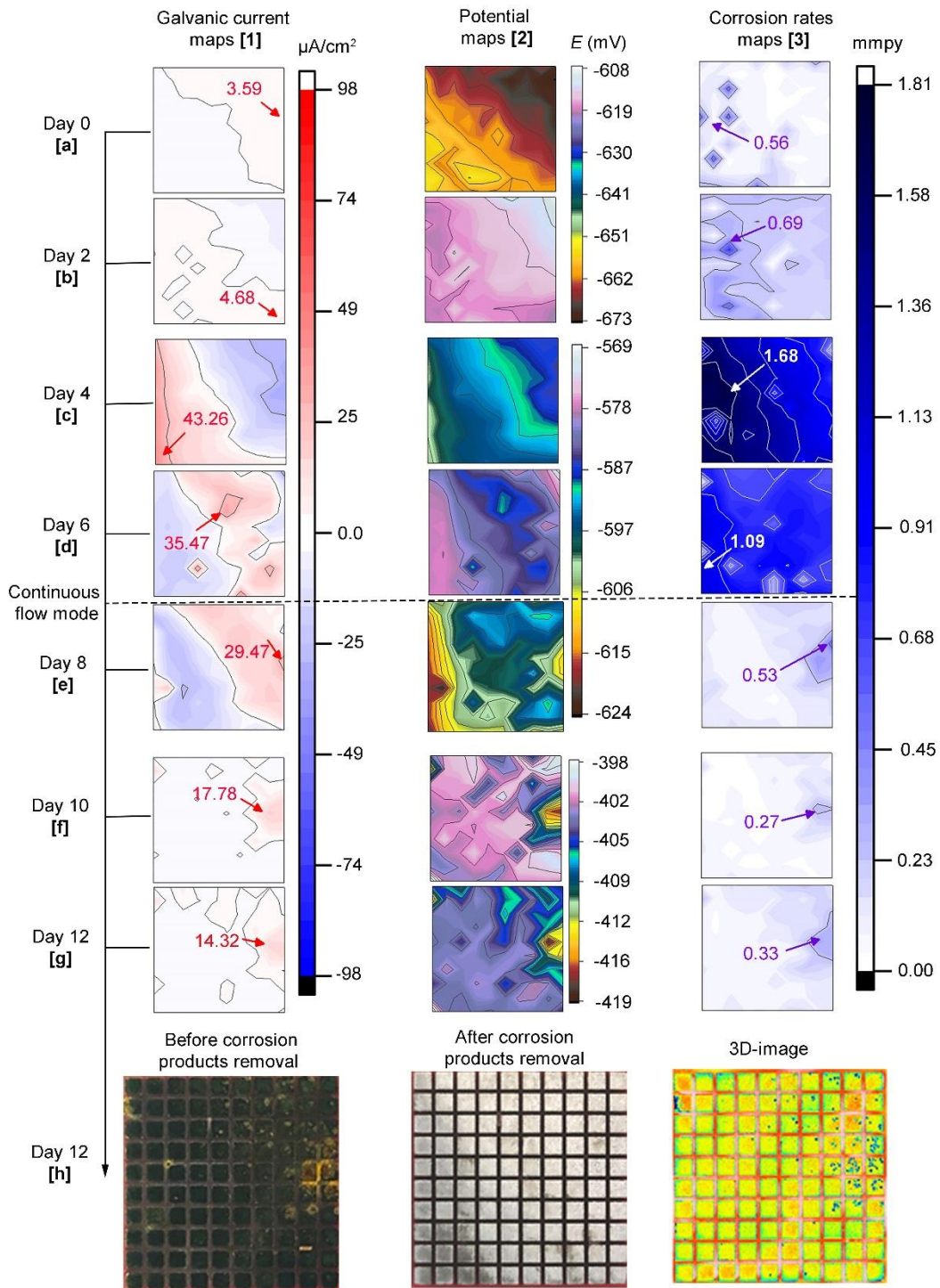
Figure 7. *CI test*: **7.1a-g)** Galvanic currents; **7.2a-g)** corrosion potentials and; **7.3a-g)** corrosion rates distribution maps of the steel WBE immersed in CO_2 saturated-ASW, *E. roggenkampii* and, corrosion inhibitor (0.892 mM 2-mercaptopyrimidine) at 40°C for 12 days. The current maps show the maximum anodic currents in red while for the corrosion rate maps high corrosion rates are shown in violet and white. Photographs of the entire WBE surface **7.1h)** before and, **7.2h)** after corrosion products removal; **7.3h)** 3D-image of WBE surface after corrosion products removal.
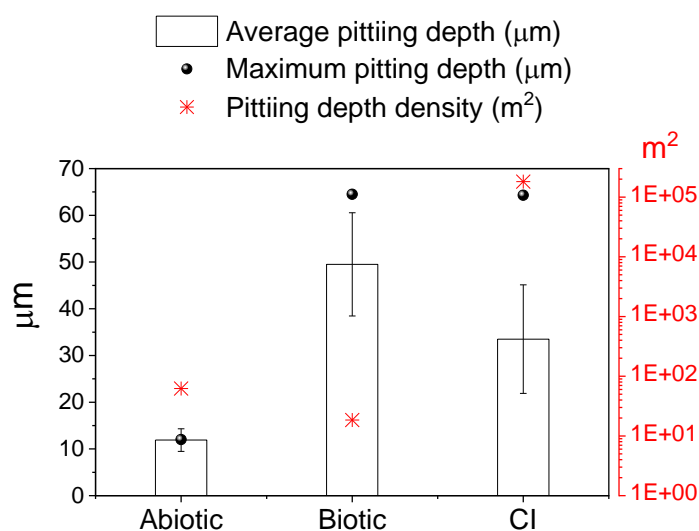
Figure 8. Localised corrosion results for all test conditions. Average, maximum pitting depths by 3D- laser scanning profilometry. The average pitting depth was obtained using all deepest points measured on each sample. Pitting depth density is the number of depth points/m^2.

7.4. Discussion

7.4.1. Under-deposit microbial corrosion (Biotic test).

This study assessed carbon steel corrosion by *Enterobacter roggenkampii*, a field bacterium capable of conducting iron oxidation coupled with nitrate reduction in anaerobic conditions. The results from this work indicate that the presence of this bacterial isolate influenced the localised corrosion process on the WBE surface. The galvanic current, potential and, corrosion rate distribution maps were in agreement with the local visual areas of metal corroded and the corresponding photographs and 3D- images. The presence of pits across the WBE surface in both biotic and CI tests (Fig. 5h.2-3 and Fig. 7h.2-3), located exactly beneath mound-shaped deposits (Fig.

5h.1 and Fig. 7h.1), indicate the occurrence of UDC in the presence of *E. roggenkampii*.

Most of the corrosion mechanisms involving FeOB have been described for oxygenic habitats, i.e. aerobic corrosion [49]. In the aerobic corrosion by FeOB, the area underneath bacterial colonies where oxygen becomes depleted acts as an anode, whereas the area outside of the colonies, where oxygen concentrations are higher than inside, support the cathodic half-reaction [50]. An electrochemical potential difference is eventually developed between the two regions, resulting in the dissolution of the underlying metal. Consequently, dissociated metal ions form ferrous hydroxides, ferric hydroxide, and iron-containing minerals [51]. Novel FeOB species from the genus *Enterobacter* have been associated with corrosion of carbon steel in aerobic conditions [52].

In the present study, *E. roggenkampii,* throughout its iron-oxidising/nitrate-reducing metabolism induced to localised corrosion of the steel underneath biogenic deposits formed under anaerobic environment. The oxidation of ferrous iron (Fe^{2+}) and the subsequent precipitation of Fe^{3+} oxides on steel surface is known to lead to UDC. Little *et al.* [53] highlighted the importance of relating biomineralisation to MIC processes, which involves either deposition of inorganic materials or removal of alloying elements from the metal substrate. The author also stated that biomineralisation that results in mineral deposition on steel surfaces could shift the corrosion potential towards either more positive or negative values, depending on the nature of the deposit.

Besides the Fe^{3+} oxides deposition as responsible for the localised corrosion process, it can also be suggested the occurrence of electrical MIC (EMIC) by this bacterium. Previous non-corrosion related works have demonstrated that some nitrate reducers can use zero-valent iron (Fe^{0}) as the only energy source. Those studies based on bioelectrochemical systems (BES) have achieved numerous advances in the understanding of extracellular electron transfer (EET) mechanisms by NRB. For instance, denitrifying biocathodes have demonstrated to be efficient in removing nitrate from contaminated waters [54-58]. Similarly, the use of nano-zero valent iron (nZVI) as co-electron donors for heterotrophic/autotrophic denitrification have found a better nitrate removal efficiency in groundwaters [59-60].

In this work, both types of dissimilar metal corrosion were assessed by the WBE system, the galvanic effects and self-corrosion or direct attack. The galvanic effects were reflected in galvanic currents distribution maps. The local self-corrosion process was represented in the corrosion rates distribution maps. Assessing the corrosion rate distribution maps in day 12 (Fig. 5g.3), the location of areas that recorded higher corrosion rates were almost the same as the ones on day zero (0), suggesting an influence of microbial deposition on localised corrosion occurrence. The presence of pits situated in similar areas identified by the corrosion rate maps confirmed these results (Fig. 5h.2-3). Perhaps the initial electrochemical heterogeneity under the biofilm can be a determining factor on MIC occurrence.

During the experimental time in the biotic test, it was noticed that in some of the labelled electrodes, the pits seemed to be formed at different times and evolved at different rates suggesting a non-uniform corrosion evolution. The electrodes started with high corrosion rate values on day zero (0), and then the values decreased during 4 or 6 days. However, after introducing flow in the system, most of the corrosion rates values gradually increased, indicating a variable local corrosion process under these conditions. Taking electrode #25 as an example, it recorded a high corrosion rate value on day zero (0), but it only evolved towards higher corrosion rates values after 6 days of immersion. Also, after 12 days of immersion (Fig. 5g. 3) there was some confluence of the corroded areas as indicated for electrodes # 39 and # 49.

Regarding the overall corrosion trend on the maps, when the WBE reactor was set to continuous flow mode (Fig. 5d.1), the areas outside of the initially affected electrodes recorded lower corrosion rates than shown in the previous maps. This is probably due to the exchange of ASW, reducing the amount of the corrosive metabolites in the bioreactor. It was also evident in the galvanic current maps from day 8 to 12 (Fig. 5e-g). In general, the tests had a low magnitude of galvanic anodic currents. However, they coincided with most of the areas of their respective corrosion rate maps demonstrating galvanic effects between deposits and underlying metal.

This work also determined the inhibition performance of 2-mercaptopyrimidine (MPY), a sulphur-containing, film-forming corrosion inhibitor, before and after the addition of bacterial cells. Similar to the biotic test, the CI test also showed considerable localised corrosion damage (maximum pitting depths were similar for both tests). These results indicate that microorganisms compromised the corrosion protection exerted by the film-forming inhibitor.

The pyrimidine derivative compound, 2-mercaptopyrimidine has been reported as high-performance CI in the presence of silica sand, aluminium oxide and calcium carbonate deposit [25]. This organic film-forming CI consists of a polar molecule with the S and N atoms with a negative and positive end of the dipole, respectively [26]. In the present study, MPY showed good performance after 18 hours contact with the steel WBE and before bacteria injection (pre-filming period). However, after 2 days of bacterial addition, the MPY performance was affected as indicated by the increase in the magnitude of galvanic currents, potentials and corrosion rates from the 2nd day to 6th day of immersion (Fig. 7b-d). Organic film-forming CIs adsorb onto the metal-solution interface. Thus, it is reasonable to suggest that the activity of *E. roggenkampii* compromised the stability of the film. Videla *et al.* [61] claimed that some organic film-forming CIs used in oil and gas systems could be affected by microbial activity. Similarly, Rajasekar *et al.* [62] demonstrated that *Bacillus cereus* ACE4 biodegraded aromatic and aliphatic hydrocarbons of a commercial corrosion inhibitor.

Another possible explanation for the observed performance of MPY could be the local accumulation of corrosive species by inducing local changes in the pH on the WBE surface by microbial activity. This can be correlated with cATP values obtained from the 2nd to the 6th day (Fig.2c) which indicate considerably high activity during that period.

Interestingly, in the presence of MPY, the maps showed a continuous reversal of galvanic currents and potentials. Considering galvanic corrosion in general (no CIs or microorganisms), Zhang *et al.* [63] stated that some galvanic couples could reverse with time. The author pointed out that the degree of passivity, the nature of the redox

couples in the solution, and the stability of the system determine the polarity and its fluctuation with time.

A favourable effect of the replenishment was evident in this CI test. From the 8th to the 12th day (Fig. 7e-g), corrosion rate values decreased in most of the areas of WBE surface probably as a result of the exchange of corrosive metabolites by fresh inhibited ASW. This fresh solution exchange made it possible to visualise affected areas in all distribution maps, which were also in agreement with photographs (Fig. 7h1-2) and 3D-image of the WBE surface (Fig. 7h.3).

In agreement with the average corrosion rate recorded at day 12, the shiny appearance of WBE surface after corrosion products removal (Fig. 7h2) indicated that the steel was protected against average corrosion by the inhibitor in most of the areas. However, some electrodes were locally affected by microbial activity. Although microorganisms impacted the WBE surfaces of both tests, there were some noticeable corrosion differences between them. In the CI test, the pit sizes are smaller than the biotic test.

In contrast, the number of pits (pitting depth density) is considerably higher when the inhibitor is present. This suggests that the inhibitor was unable to stop corrosion initiation; however, it may still be able to control the progression of corrosion as indicated by a lower average pitting depth. Curiously, the most affected area at the end of the experimental time (displayed at the top right corner by all maps and photos in Fig. 7g-h coincided with the areas that recorded anodic galvanic currents and more negative potentials in the MPY pre-filming period (Fig 6). Similar to the biotic test, this observation in the CI test suggested that the initial pattern of the electrochemistry on the steel surfaces influenced the later localised corrosion process in the presence of bacteria.

This study demonstrates that the WBE system is a suitable tool to detect, evaluate and monitor localised corrosion phenomena and the efficiency of corrosion inhibitors under MIC and UDC scenarios. These results highlight the potential for microorganisms to damage the integrity of corrosion inhibitor films, compromising the effectiveness of established mitigation strategies when conditions supporting microbial activity are present. Therefore, this work underlines the importance of

including microbial constituents in corrosion inhibition tests for preventing localised corrosion in both industrial and natural environments.

7.5. Conclusions

- This study demonstrated that *Enterobacter roggenkampii*, through its iron-oxidising capabilities coupled to nitrate reduction led to under-deposit microbial corrosion (UDMC) of carbon steel in anaerobic conditions. Local electrochemistry studied through a multi-electrode array indicated that localised corrosion occurred underneath biogenic deposits and that local events initiated and evolved differently across the carbon steel surface.

- 2-mercaptopyrimidine (MPY), an under-deposit corrosion (UDC) inhibitor, was found to inhibit average corrosion but did not prevent localised corrosion in the presence of microorganisms. Results indicate that in the presence of *Enterobacter roggenkampii,* the corrosion inhibitor film adsorbed on the metal surface was compromised, which resulted in localised corrosion.

- The ability of the WBE to locally measure the self corrosion process, galvanic effects and, corrosion potentials across the metal surface demonstrated its suitability to detect, evaluate and monitor under-deposit microbial corrosion (UDMC) as well as to investigate the efficiency of corrosion inhibitors in complex environments involving deposits and microorganisms.

7.6. References

1.   Konhauser, K. O., *Introduction to Geomicrobiology*. Wiley: 2006.

2.   Price, A.; Pearson, V. K.; Schwenzer, S. P.; Miot, J.; Olsson-Francis, K., Nitrate-Dependent Iron Oxidation: A Potential Mars Metabolism. *Frontiers in microbiology* **2018,** *9* (513).

3.   Pringsheim, Iron bacteria. *Biological Reviews* **1949,** *24* (2), 200-245.

4.   Dworkin, M.; Gutnick, D., Sergei Winogradsky: a Founder of Modern Microbiology and the First Microbial Ecologist. *FEMS Microbiology Reviews* **2012,** *36* (2), 364-379.

5.   Magot, M., Indigenous Microbial Communities in Oil Fields. In *Petroleum microbiology*, American Society of Microbiology: 2005; pp 21-34.

6.   Ollivier, B.; Cayol, J.-L., Fermentative, iron-reducing, and nitrate-reducing Microorganisms. In *Petroleum Microbiology*, American Society of Microbiology: 2005; pp 71-88.

7.   Coombe, D.; Hubert, C.; Voordou, G., Mechanistic Modelling of H_2S Souring Treatments by Application of Nitrate or Nitrite. In *Canadian International Petroleum Conference*, Petroleum Society of Canada: Calgary, Alberta, 2004; p 16.

8.   Hubert, C.; Voordouw, G., Oil Field Souring Control by Nitrate-Reducing *Sulfurospirillum* sp. that Outcompete Sulfate-Reducing Bacteria for Organic Electron Donors. *Applied and Environmental Microbiology* **2007,** *73* (8), 2644-52.

9.   Gieg, L. M.; Jack, T. R.; Foght, J. M., Biological Souring and Mitigation in Oil Reservoirs. *Applied Microbiology and Biotechnology* **2011,** *92* (2), 263-82.

10.   Bodtker, G.; Thorstenson, T.; Lillebo, B. L.; Thorbjornsen, B. E.; Ulvoen, R. H.; Sunde, E.; Torsvik, T., The Effect of Long-Term Nitrate Treatment on SRB Activity, Corrosion Rate and Bacterial Community Composition in Offshore Water Injection Systems. *Journal of Industrial Microbiology & Biotechnology* **2008,** *35* (12), 1625-36.

11.   Straub, K. L.; Schönhuber, W. A.; Buchholz-Cleven, B. E. E.; Schink, B., Diversity of Ferrous Iron-Oxidizing, Nitrate-Reducing Bacteria and their Involvement in Oxygen-Independent Iron Cycling. *Geomicrobiology Journal* **2004,** *21* (6), 371-378.

12.   Straub, K. L., Fe(II)-Oxidizing Prokaryotes. In *Encyclopedia of Earth Sciences Series*, 2011; pp 367-370.

13.   Straub, K. L.; Benz, M.; Schink, B., Iron Metabolism in Anoxic Environments at Near Neutral pH. *FEMS Microbiology Ecology* **2001,** *34* (3), 181-186.

14.   Madigan, M. T.; Martinko, J. M.; Bender, K. S.; Buckley, D. H.; Stahl, D. A., *Brock Biology of Microorganisms (14th edition)*. 2014.

15.   Hedrich, S.; Schlömann, M.; Johnson, D. B., The Iron-Oxidizing Proteobacteria. *Microbiology* **2011,** *157* (6), 1551-1564.

16.   Kappler, A.; Straub, K. L., Geomicrobiological Cycling of Iron. *Reviews in Mineralogy and Geochemistry* **2005,** *59* (1), 85-108.

17.   Miot, J.; Benzerara, K.; Morin, G.; Kappler, A.; Bernard, S.; Obst, M.; Férard, C.; Skouri-Panet, F.; Guigner, J.-M.; Posth, N.; Galvez, M.; Brown, G. E.; Guyot, F., Iron Biomineralization by Anaerobic Neutrophilic Iron-oxidizing Bacteria. *Geochimica et Cosmochimica Acta* **2009,** *73* (3), 696-711.

18.   Xu, D.; Li, Y.; Song, F.; Gu, T., Laboratory Investigation of Microbiologically Influenced Corrosion of C1018 Carbon Steel by Nitrate Reducing Bacterium *Bacillus Licheniformis*. *Corrosion Science* **2013,** *77*, 385-390.

19.   Suarez, E. M; Machuca, L.; Lepková, K., The Role of Bacteria in Under-Deposit Corrosion in Oil and Gas facilities: A Review of Mechanisms, Test Methods and Corrosion Inhibition. *Corrosion and Materials* **2019,** *44* (1), 80-87.

20.   Machuca, L. L.; Lepková, K.; Petroski, A., Corrosion of Carbon Steel in the Presence of Oilfield Deposit and Thiosulphate-Reducing Bacteria in CO_2 Environment. *Corrosion Science* **2017,** *129*, 18-25.

21.   Suarez, E. M.; Lepková, K.; Kinsella, B.; Machuca, L. L., Aggressive Corrosion of Steel by a Thermophilic Microbial Consortium in the Presence and Absence of Sand. *International Biodeterioration & Biodegradation* **2019,** *137*, 137-146.

22.   Mosher, W.; Mosher, M.; Lam, T.; Cabrera, Y.; Oliver, A.; Tsaprailis, H. In *Methodology for Accelerated Microbiologically Influenced Corrosion in Under Deposits from Crude Oil Transmission Pipelines*, NACE - International Corrosion Conference Series, 2014, 2014/5/13/; NACE International: 2014.

23.   Skovhus, T. L.; Caffrey, S. M.; Hubert, C. R. J., *Applications of Molecular Microbiological Methods*. Caister Academic Press: 2014.

24.   Esan, T.; Kapusta, S. D.; Simon-Thomas, M. J. J., Case Study: Extreme Corrosion of a 20" Oil Pipeline in the Niger Delta Region. *Paper no. 01629*, NACE International, 2001.

25.   Suarez, E. M.; Machuca, L. L.; Kinsella, B.; Lepková, K., CO_2 Corrosion Inhibitors Performance at Deposit-Covered Carbon Steel and Their Adsorption on Different Deposits. *Corrosion* **2019,** *75* (9), 1118-1127.

26.   Pandarinathan, V.; Lepková, K.; Bailey, S. I.; Gubner, R., Evaluation of Corrosion Inhibition at Sand-Deposited Carbon Steel in CO_2-Saturated Brine. *Corrosion Science* **2013,** *72*, 108-117.

27.   Pandarinathan, V.; Lepková, K.; Gubner, R., Inhibition of CO_2 Corrosion of 1030 Carbon Steel Beneath Sand-Deposits. In *Conference & Expo*, NACE International: 2011.

28.   Binks, B. P.; Fletcher, P. D. I.; Salama, I. E.; Horsup, D. I.; Moore, J. A., Quantitative Prediction of the Reduction of Corrosion Inhibitor Effectiveness Due to Parasitic Adsorption onto a Competitor Surface. *Langmuir* **2011,** *27* (1), 469-473.

29.   Tan, M. Y. J; Fwu, Y.; Bhardwaj, K., Electrochemical Evaluation of Under-deposit Corrosion and its Inhibition Using the Wire Beam Electrode Method. *Corrosion Science* **2011,** *53* (4), 1254-1261.

30.   Tan, M. Y. J; Revie, R. W., *Heterogeneous Electrode Processes and Localized Corrosion*. John Wiley & Sons: 2012; Vol. 13.

31.   Zhang, G. A.; Yu, N.; Yang, L. Y.; Guo, X. P., Galvanic Corrosion Behavior of Deposit-Covered and Uncovered Carbon Steel. *Corrosion Science* **2014,** *86*, 202-212.

32.   Sun, X.; Yang, L., Comparison of Oxidation Power Sensor With Coupled Multielectrode Array Sensor For Monitoring General Corrosion. NACE International.

33.   Tan, M.Y.J., Understanding the Effects of Electrode Inhomogeneity and Electrochemical Heterogeneity on Pitting Corrosion Initiation on Bare Electrode Surfaces. *Corrosion Science* **2011,** *53* (5), 1845-1864.

34.   Tan, M. Y. J, Sensing Electrode Inhomogeneity and Electrochemical Heterogeneity Using an Electrochemically Integrated Multielectrode Array. *Journal of The Electrochemical Society* **2009,** *156* (6), C195-C208.

35.   Tan, M. Y. J., Monitoring Localized Corrosion Processes and Estimating Localized Corrosion Rates Using a Wire-Beam Electrode. **1998**.

36.   Xu, Y.; Tan, M. Y. J, Probing the Initiation and Propagation Processes of Flow Accelerated Corrosion and Erosion Corrosion Under Simulated Turbulent Flow Conditions. *Corrosion Science* **2019,** *151*, 163-174.

37.   Xu, Y.; Tan, M. Y. J., Visualising the dynamic processes of flow accelerated corrosion and erosion-corrosion using an electrochemically integrated electrode array. *Corrosion Science* **2018,** *139*, 438-443.

38.   Mahdavi, F.; Tan, M. Y.; Forsyth, M., Communication—An Approach to Measuring Local Electrochemical Impedance for Monitoring Cathodic Disbondment of Coatings. *Journal of The Electrochemical Society* **2016,** *163* (5), C228-C231.

39.   Tan, M. Y. J.; Varela, F.; Huo, Y.; Mahdavi, F.; Forsyth, M.; Hinton, B., Monitoring Dynamic Corrosion and Coating Failure on Buried Steel Using a Multi-Electrode Array. In *Corrosion 2017*, NACE International: New Orleans, Louisiana, USA, 2017.

40.   Varela, F.; Tan, M. Y. J.; Forsyth, M., Electrochemical Method for Studying Localized Corrosion beneath Disbonded Coatings under Cathodic Protection. *Journal of The Electrochemical Society* **2015,** *162* (10), C515-C527.

41.   Turnbull, A.; Hinds, G.; Cooling, P.; Zhou, S., A Multi-Electrode Approach To Evaluating Inhibition of Underdeposit Corrosion in CO_2 Environments. NACE International: 2009.

42.   Muster, T. H.; Hughes, A. E.; Furman, S. A.; Harvey, T.; Sherman, N.; Hardin, S.; Corrigan, P.; Lau, D.; Scholes, F. H.; White, P. A.; Glenn, M.; Mardel, J.; Garcia, S. J.; Mol, J. M. C., A rapid screening multi-electrode method for the evaluation of corrosion inhibitors. *Electrochimica Acta* **2009,** *54* (12), 3402-3411.

43.   Hinds, G.; Turnbull, A., Novel Multi-Electrode Test Method for Evaluating Inhibition of Underdeposit Corrosion—Part 1: Sweet Conditions. *Corrosion* **2010,** *66* (4), 046001-046001-10.

44.   Liu, H.; Meng, G.; Li, W.; Gu, T.; Liu, H., Microbiologically Influenced Corrosion of Carbon Steel Beneath a Deposit in CO_2-Saturated Formation Water Containing Desulfotomaculum nigrificans. *Frontiers in microbiology* **2019,** *10* (1298).

45.   Dong, Z. H.; Shi, W.; Ruan, H. M.; Zhang, G. A., Heterogeneous corrosion of mild steel under SRB-biofilm characterised by electrochemical mapping technique. *Corrosion Science* **2011,** *53* (9), 2978-2987.

46.   Beech, I. B.; Zinkevich, V.; Tapper, R.; Gubner, R.; Avci, R., Study of the interaction of sulphate-reducing bacteria exopolymers with iron using X-ray photoelectron spectroscopy and time-of-flight secondary ionisation mass spectrometry. *Journal of microbiological methods* **1999,** *36* (1–2), 3-10.

47.   ASTM G1-03. Standard Practice for Preparing, Cleaning and Evaluating Corrosion Test Specimens. ASTM International, 2011.

48.   ISO 5436, S., Geometrical Product Specifications (GPS)—surface texture: profile method; measurements standards-Part 1: material measures. International Organization for Standardization: 2000.

49.   NACE TM0212, Detection, Testing, and Evaluation of Microbiologically Influenced Corrosion on Internal Surfaces of Pipelines. NACE International: 2018.

50.   Little, B.; Wagner, P.; Mansfeld, F., An overview of microbiologically influenced corrosion. *Electrochimica Acta* **1992,** *37* (12), 2185-2194.

51.   Gu, J. D.; Ford, T. E.; Mitchell, R., Microbiological Corrosion of Metallic Materials. In *Uhlig's Corrosion Handbook*, John Wiley & Sons, Inc.: 2011; pp 549-557.

52.   Ashassi-Sorkhabi, H.; Moradi-Haghighi, M.; Zarrini, G.; Javaherdashti, R., Corrosion behaviour of carbon steel in the presence of two novel iron-oxidizing bacteria isolated from sewage treatment plants. *Biodegradation* **2012,** *23* (1), 69-79.

53.   Little, B.; Wagner, P.; Hart, K.; Ray, R.; Lavoie, D.; Nealson, K.; Aguilar, C., The role of biomineralization in microbiologically influenced corrosion. *Biodegradation* **1998,** *9* (1), 1-10.

54.   Pous, N.; Koch, C.; Colprim, J.; Puig, S.; Harnisch, F., Extracellular electron transfer of biocathodes: Revealing the potentials for nitrate and nitrite reduction of denitrifying microbiomes dominated by *Thiobacillus* sp. *Electrochemistry Communications* **2014,** *49*, 93-97.

55.   Ghafari, S.; Hasan, M.; Aroua, M. K., Bio-electrochemical removal of nitrate from water and wastewater—A review. *Bioresource Technology* **2008,** *99* (10), 3965-3974.

56.   Jiang, X.; Ying, D.; Ye, D.; Zhang, R.; Guo, Q.; Wang, Y.; Jia, J., Electrochemical study of enhanced nitrate removal in wastewater treatment using biofilm electrode. *Bioresource Technology,* **2018,** *252*, 134-142.

57.   Kondaveeti, S.; Lee, S.-H.; Park, H.-D.; Min, B., Bacterial communities in a bioelectrochemical denitrification system: The effects of supplemental electron acceptors. *Water Research,* **2014,** *51*, 25-36.

58.   Molognoni, D.; Devecseri, M.; Cecconet, D.; Capodaglio, A. G., Cathodic groundwater denitrification with a bioelectrochemical system. *Journal of Water Process Engineering* **2017,** *19*, 67-73.

59.   Hu, S.; Wu, Y.; Zhang, Y.; Zhou, B.; Xu, X., Nitrate Removal from Groundwater by Heterotrophic/Autotrophic Denitrification Using Easily Degradable

Organics and Nano-Zero Valent Iron as Co-Electron Donors. *Water, Air and Soil Pollution* **2018,** *229* (3), 1-9.

60.   Biswas, S.; Bose, P., Zero-Valent Iron-Assisted Autotrophic Denitrification. *Journal of Environmental Engineering* **2005,** *131* (8), 1212-1220.

61.   Videla, H. A.; Guiawet, P. S.; Gomez Saravia, S. G.; Allegreti, P.; Furlong, J., Microbial Degradation of Film Forming Inhibitors and Its Possible Effects on Corrosion Inhibition Performance. In *Corrosion 2000*, NACE International: Orlando, Florida, 2000; p 10.

62.   Rajasekar, A.; Maruthamuthu, S.; Palaniswamy, N.; Rajendran, A., Biodegradation of corrosion inhibitors and their influence on petroleum product pipeline. *Microbiological Research* **2007,** *162* (4), 355-368.

63.   Zhang, X. G., Galvanic Corrosion. In *Uhlig's Corrosion Handbook*, John Wiley & Sons, Inc.: 2011; pp 123-143.

Chapter VIII

E.M. Suarez

Summary, Conclusions and Future work

Summary, Conclusions and Future work

8.1 Summary

The presence of biofilms and mineral deposits represent a challenge for pipeline integrity management programs [1] due to the severity of the damage and the complexity of finding an adequate treatment to mitigate both threats [2, 3]. To date, research studies related to microbial-deposit interactions towards pipeline integrity and its inhibition are minimal. However, it is undeniable the need to address the increasing concerns about the ineffectiveness of corrosion inhibitors in the presence of deposits, where MIC is also suspected. There are several procedures to accomplish UDC and MIC mitigation separately. However, an appropriate selection of procedures to mitigate under-deposit microbial corrosion (UDMC) would depend on the practicality and accessibility to implement these measures to a particular system.

Research on corrosion inhibitor performance under deposits and in the presence of microorganisms require an appropriate multidisciplinary approach to extend the lifetime of carbon steel structures associated with oilfield systems. Corrosion failures in the presence of deposits and bacteria have been reported in the oil and gas industry [4, 5]. Despite the significance and practical importance of evaluating the combined effects of microbes and deposits, research studies and programs addressing this industrial concern are not applied. This lack of knowledge has prompted this research project into the development of a multidisciplinary scientific approach for studying the complex phenomenon of UDMC.

The first part of the project allowed for identification of the existent methods and approaches to integrate UDMC research field. This part was achieved by reviewing concepts, test methods, monitoring techniques and mitigation strategies commonly used to study UDC and MIC. From this review, several methods were identified to assess MIC, UDC and their inhibition. Limited published literature was found combining these fields of corrosion research. Likewise, the integration of these corrosion fields as a single phenomenon, i.e. UDMC has not been adopted as an industry standard or recommended practice by NACE International or the American Society for Testing and Materials (ASTM). Selecting proper testing and monitoring techniques for the study of UDMC will allow linking the microbial and deposit

components to metal deterioration. Hence, it will improve mitigation strategies to extend the lifetime of production equipment.

The second part involved the evaluation of corrosion inhibitors suitable for UDC studies using a CO_2-saturated brine (NaCl 3 wt %, $NaHCO_3$ 0.01 wt %, pH ~4.8). Corrosion inhibitor adsorption on aluminium oxide (Al_2O_3), calcium carbonate $CaCO_3$, and silica sand (SiO_2) were investigated. Electrochemical tests were conducted to evaluate corrosion inhibition efficiency on both bare and deposited carbon steel surfaces. The pH of the electrolyte did not change upon addition of the corrosion inhibitors. However, pH values increased after exposure with deposits, particularly after $CaCO_3$ contact. It is believed that the presence of deposits in oil and gas assets can affect the performance of corrosion inhibitors in different ways [6]. For instance, the inhibitors penetration rate can be influenced by some features of deposits such as porosity, layer thickness, surface area, and nature of the deposit, amongst others [7]. Therefore, under certain circumstances, inhibitor concentration can be reduced as a result of its adsorption on mineral deposits [8-11].

According to the adsorption test results, two inhibitors were selected for performance testing. Both, the cationic surfactant 1-dodecylpiridinium chloride (DPC) and the sulphur-containing compound, 2-mercaptopyrimidine (MPY) showed minimal adsorption on silica sand. However, when $CaCO_3$ was present, MPY concentration was considerably reduced. These adsorption results indicated that MPY inhibitor has a high affinity for the $CaCO_3$ deposit, decreasing its concentration in the solution. Pandarinathan *et al.* [9] mentioned that MPY is oppositely charged compared to $CaCO_3$, resulting in high adsorption of this sulphur-containing compound on this deposit. The author proposed that inhibitor adsorption on mineral deposits are related to the type of corrosion inhibitor and not to the physical properties of the deposits. Although pH in the electrolyte plays an important role in CO_2 corrosion of mild steels, in this study was stated that pH in the test solution could not directly influence the corrosion process. Thereby, it was related to the nature of the deposit, which locally changed pH values beneath deposit layers. Also, it was proposed that inhibitor adsorption on mineral deposits is related to the type of corrosion inhibitor and not to the physical properties of the deposits.

Electrochemical measurements demonstrated that MPY substantially reduced the corrosion rate under all test conditions (with and without deposits). The corrosion reduction was also accompanied by a positive shift in corrosion potentials when MPY was added to the systems, particularly marked on bare steel (+110 mV). In addition, it was found that the deposits (tests without inhibitors) considerably reduced the average corrosion rates of carbon steel tested under similar conditions. The results indicated that the reduction in corrosion rate was due to the obstruction caused by the deposit, reducing the mass transfer of corrosive species (e.g. carbonic acid) to the metal surface. The overall shape of the anodic and cathodic polarisation curves for bare steel with MPY remained the same in the presence of deposits. This indicates that MPY can penetrate the deposit and influence the surface of the steel similarly to when no deposit is present. Therefore, this film-forming inhibitor was ranked as the best candidate for further UDMC experiments.

A wire-beam electrode (WBE) system was used to evaluate MPY and DPC performance at a sand-deposited steel surface. This work sought to visualise specific electrochemical events outside and underneath the deposit when corrosion inhibitors are applied. Local galvanic currents and local corrosion potentials were measured at a WBE sensor. Again, MPY demonstrated the best performance, which was related to the molecular structure of this film-forming inhibitor. Thus, proposing that the size of this small non-surfactant molecule allows a better penetration capacity through the sand layers. Besides, the sustained corrosion protection for 96 h exerted by MPY proposes a strong film persistency of this sulphur-containing molecule. Previous studies have demonstrated the MPY effectiveness against CO_2 corrosion of carbon steel fully covered with silica sand, aluminium oxide and calcium carbonate deposit [12].

Conversely, DPC did not perform efficiently underneath sand layers. The long and complex chain structure of DPC probably made this large surfactant molecule more challenging to penetrate this deposit. This configuration allowed the inhibitors comparison in terms of performance and penetration rate through the deposit layers. Based on these results, it was postulated that the effectiveness of the sulphur-containing compound was related to its molecular structure that allows its high penetration capacity through the sand layer. These molecular characteristics could be

used as a new inhibitor selection criterion of efficient molecules as corrosion inhibitors to prevent under deposit corrosion (UDC).

Under-deposit microbial corrosion (UDMC) study was carried out using a single bacterial isolate, *Shewanella oneidensis* MR-1. The corrosion effects were investigated by electrochemical measurements using a three-electrode setup, surface analysis and analytical methods. This UDCM work considered different scenarios; the first consisted of experiments in artificial seawater (ASW) containing a high concentration of soluble electron donor (59 mM Lactate) and the second scenario as in ASW lacking electron donor in the presence and absence of sand deposit. Thus, forcing *S.oneidensis* to intake electrons from the steel surface. Steel samples of the biotic test with 59 mM showed lower corrosion rates compared to samples from abiotic conditions. These results suggested that this bacterium preferred a soluble source of electrons rather than an insoluble one (metal surface). FTIR analysis revealed that lactate concentration in the solution was not significantly reduced by silica sand. This finding indicates no significant effect of the sand deposit on the penetration of this organic source through the deposit layers.

Sand-free samples immersed in biotic conditions (5 mM of lactate) recorded higher corrosion rates than the sand-deposited steel samples. However, sand-deposited samples were corroded, suggesting that this bacterium could surpass the barrier-effect presented by the sand deposit under abiotic CO_2 anaerobic conditions. This finding was also evidenced from biofilm formation beneath and between sand grains in FESEM images of cross-sectioned samples.

A second UDMC work innovatively drew a comparison between both scenarios (with and without deposits using a microbial consortium recovered from an oilfield site in Western Australia. Thus, the extent of the corrosion damage for both systems was determined under simulated oilfield conditions. The presence of the microbial consortium affected considerably both sand-deposited and sand-free carbon steel surfaces resulting in higher general and localised corrosion. Even though the sand-free samples suffered a greater corrosion affectation than sand-deposited samples; these samples covered with sand also had considerable damage when the consortium was present. Sand deposit is typically known for exerting a barrier effect under abiotic conditions [13, 14]. However, these data may suggest that sand grains on steel facilitate local precipitation of

metabolic by-products on the surface, leading to localised corrosion. The microbial metabolic groups identified by 16S rRNA gene sequencing consisted of methanogens, fermenting and sulphidogenic microorganisms. The microbial community composition and corrosion products stratification were dissimilar between sand-deposit and sand-free samples. This part of the research sought to improve our understanding of under-deposit corrosion in the presence of a microbial community which is essential to develop more effective strategies to control internal corrosion in carbon steel pipelines.

The consolidation of UDMC research comprised an in-situ study of under-deposit microbial corrosion and its inhibition using a WBE system. The bacterium selected for this work was *Enterobacter roggenkampii* recovered from a production facility in Western Australia, specifically from iron oxide deposits associated with a corrosion failure in a floating production offload facility (FPSO) [15]. This marine bacterium caused localised corrosion under deposits through its capability to oxidise iron and reduce nitrate in anaerobic conditions. Sulphur-containing organic compound MPY was selected for evaluation of this methodology since this inhibitor was effective in preventing UDC in previous studies [9, 12]. However, under biotic conditions, this compound showed less efficiency than in the abiotic test. To the best of our knowledge, it is the first time *E. roggenkampii* is associated with UDMC in anaerobic conditions. The WBE sensor in both tests with bacteria (with and without MPY) exhibited localised corrosion located exactly beneath mound-shaped deposits. This finding proved the occurrence of UDC influenced by this bacterium regardless of the presence of the corrosion inhibitor. This work also achieved a novel approach of the WBE system by measuring linear polarisation (LP) measurements at each electrode or wire. Corrosion rate distribution maps provided spatial and temporal information of self-corrosion processes at the WBE surface. Based on these results and the final location of the corroded areas or pits, it was proposed that the localised corrosion initiated and evolved differently across the steel WBE surface, i.e. corrosion rates in some electrodes increase on time. However, in some others, corrosion rate values fluctuated through testing. Therefore, this system demonstrated to be a suitable tool to detect, evaluate and monitor localised corrosion phenomena and the efficiency of corrosion inhibitors under MIC and UDC scenarios.

8.2. Conclusions

The main conclusions of this research involved the development of a multidisciplinary scientific approach to the study under-deposit microbial corrosion (UDMC) and its inhibition. The understanding of this complex phenomenon is of considerable significance to extend the lifetime of carbon steel structures in oilfield systems. In the present research, corrosion inhibitors were evaluated using different deposits in CO_2 ambience. It was demonstrated that a sulphur-containing inhibitor, MPY exhibited a superior efficiency in preventing under deposit corrosion of carbon steel. The adequate corrosion inhibitor performance of MPY was associated with its molecular characteristics that allow its penetration through the deposit layers. Localised corrosion effects were investigated at steel surfaces deposited with silica sand and biofilms formed by a bacterial isolate, *Shewanella oneidensis* and biofilms formed by a microbial consortium. From these UDMC studies, it was concluded that microorganisms could surpass the barrier-effect by deposits, leading to local damage of carbon steel surfaces.

The innovative use of the WBE system and surface analyses provided spatio-temporal information about the localised corrosion attack under deposits combined with microbial activity. It was demonstrated that microorganisms influenced under-deposit corrosion through its metabolic capability to oxidise iron. The under-deposit microbial attack could overcome the corrosion protection exerted by a film-forming inhibitor. The deficient inhibitor performance against UDMC demonstrated the importance of including the microbial component when investigating chemical treatment in the scenario where both deposits and biofilms are present.

8.3. Future work

The study of interactions and synergistic effects between corrosion inhibitors and biocides represents a potential focus of research. Another topic to explore is the possible damage to inhibitor films mediated by microorganisms. To date, there is only scarce information about corrosion inhibitors integrity in biotic environments which is an increasing concern to the industry. For instance, Duncan *et al*. [16] demonstrated a biomass 10-fold higher in coupons treated with a corrosion inhibitor compared to untreated coupons. The authors suggested that some film-forming inhibitors contain

compounds that can be potentially degraded by microorganisms leading to ineffective chemical treatments. Contrarily, Sheng *et al.* [17] reported that an organic corrosion inhibitor, 2-methylbenzimide, was also highly effective in preventing MIC occurrence.

The design of molecules with dual corrosion inhibition and biocide properties could help in inhibiting UDMC in the presence of biogenic deposits, i.e. biofilms or corrosion products formed by microbial activity. Previous studies demonstrated the biocidal properties of cationic surfactants against gram-negative and gram-positive bacteria [18, 19]. However, there is a lack of information about the efficiency of these dual-function molecules in the presence of deposits.

An unexplored aspect to consider is the possibility of biofilm reducing corrosion inhibitor concentration. Therefore, its availability to protect steel surfaces can be compromised. To our knowledge, there is no information in the literature about this topic. The application of omics-based techniques in MIC research has provided insights into the understanding of biofilms and their interaction with the metal surface [20]. Therefore, it is expected that these emerging techniques such as metagenomics, transcriptomics and metabolomics will open numerous and promising possibilities in the study of UDMC. It will help not only in elucidating biofilm-metal-deposit interactions at the molecular level but also, in combination with other techniques, will potentially facilitate the development of UDMC monitoring programs for particular operating systems.

8.4. References

1.   Videla, H. A., Prevention and Control of Biocorrosion. *International Biodeterioration & Biodegradation* **2002**, 49 (4), 259-270.

2.   Enning, D.; Venzlaff, H.; Garrelfs, J.; Dinh, H. T.; Meyer, V.; Mayrhofer, K.; Hassel, A. W.; Stratmann, M.; Widdel, F., Marine sulphate-reducing bacteria cause serious corrosion of iron under the electroconductive biogenic mineral crust. *Environmental Microbiology* **2012**, 14 (7), 1772-1787.

3.   Vigneron, A.; Alsop, E. B.; Chambers, B.; Lomans, B. P.; Head, I. M.; Tsesmetzis, N., Complementary microorganisms in highly corrosive biofilms from an

offshore oil production facility. *Applied and environmental microbiology* **2016**, 82 (8), 2545-2554.

4.	Shukla, P. K.; Naraian, S., Under-Deposit Corrosion in a Sub-Sea Water Injection Pipeline—A Case Study. NACE International: 2017.

5.	Skovhus, T. L.; Holmkvist, L.; Andersen, K.; Larsen, J.; Pedersen, H. In MIC risk assessment of the Halfdan Oil Export Spool, SPE International Conference & Workshop on Oilfield Corrosion, Society of Petroleum Engineers: 2012.

6.	Vera, J. R.; Daniels, D.; Achour, M. H., Under Deposit Corrosion (UDC) In The Oil And Gas Industry: A Review Of Mechanisms, Testing And Mitigation. NACE International: Houston, TX, 2012.

7.	De Reus, H.; Hendriksen, L. J. A.; Wilms, M.; Al-Habsi, Y. N.; Durnie, W.; Gough, M., Test Methodologies and Field Verification of Corrosion Inhibitors to Address under Deposit Corrosion in Oil and Gas Production Systems. NACE International: Houston, TX, 2005.

8.	Binks, B. P.; Fletcher, P. D. I.; Salama, I. E.; Horsup, D. I.; Moore, J. A., Quantitative Prediction of the Reduction of Corrosion Inhibitor Effectiveness Due to Parasitic Adsorption onto a Competitor Surface. *Langmui*r **2011**, 27 (1), 469-473.

9.	Pandarinathan, V.; Lepková, K.; Bailey, S. I.; Gubner, R., Evaluation of corrosion inhibition at sand-deposited carbon steel in CO_2-saturated brine. *Corrosion Science* **2013**, 72, 108-117.

10.	Pandarinathan, V.; Lepková, K.; Gubner, R., Inhibition of CO_2 corrosion of 1030 carbon steel beneath sand-deposits. In Conference & Expo, NACE International: 2011.

11.	Pandarinathan, V.; Lepková, K.; Bailey, S. I.; Gubner, R., Impact of Mineral Deposits on CO_2 Corrosion of Carbon Steel. In Conference & Expo, NACE International: 2013.

12.	Pandarinathan, V.; Lepková, K.; Bailey, S. I.; Gubner, R., Impact of Mineral Deposits on CO_2 Corrosion of Carbon Steel. NACE International: Houston, TX, 2013.

13.	Huang, J.; Brown, B.; Choi, Y.-S.; Nesic, S., Prediction of Uniform CO_2 Corrosion of Mild Steel Under Inert Solid Deposits. NACE International: 2011.

14.   Huang, J.; Brown, B.; Jiang, X.; Kinsella, B.; Nesic, S., Internal CO_2 Corrosion Of Mild Steel Pipelines Under Inert Solid Deposits. In NACE - International Corrosion Conference Series, NACE International: San Antonio, TX, 2010.

15.   Salgar-Chaparro, S. J.; Darwin, A.; Kaksonen, A. H.; Machuca, L. L., Carbon steel corrosion by bacteria from failed seal rings at an offshore facility. *Scientific Reports* **2020**, 10 (1), 1-15.

16.   Duncan, K. E.; Perez-Ibarra, B. M.; Jenneman, G.; Harris, J. B.; Webb, R.; Sublette, K., The effect of corrosion inhibitors on microbial communities associated with corrosion in a model flow cell system. *Applied microbiology and biotechnology* **2014**, 98 (2), 907-18.

17.   Sheng, X.; Ting, Y.-P.; Pehkonen, S. O., Evaluation of an Organic Corrosion Inhibitor on Abiotic Corrosion and Microbiologically Influenced Corrosion of Mild Steel. *Industrial & Engineering Chemistry Research* **2007**, 46 (22), 7117-7125.

18.   Shaban, S. M.; Aiad, I.; Fetouh, H. A.; Maher, A., Amidoamine double-tailed cationic surfactant based on dimethylaminopropylamine: Synthesis, characterization and evaluation as a biocide. *Journal of Molecular Liquids* **2015**, 212, 699-707.

19.   Shaban, S. M.; Saied, A.; Tawfik, S. M.; Abd-Elaal, A.; Aiad, I., Corrosion inhibition and Biocidal effect of some cationic surfactants based on Schiff base. *Journal of Industrial and Engineering Chemistry* **2013**, 19 (6), 2004-2009.

20.   Beale, D. J.; Karpe, A. V.; Jadhav, S.; Muster, T. H.; Palombo, E. A., Omics-based approaches and their use in the assessment of microbial-influenced corrosion of metals. *Corrosion Reviews* **2016**, 34 (1-2), 1-15.

Appendices

Appendix 1

Summary of test conditions and configurations

This appendix presents summary tables of the experimental conditions for each chapter such as steel samples, test solutions, temperatures and configurations. As could be seen throughout the thesis, some experimental conditions varied according to the requirements of the experiments. For instance, abiotic or sterile tests in which only inhibitors were involved had different test conditions than the studies designed to meet microbial needs. It is worth mentioning that some of the chapters represent published works. Thus, this appendix provides a detailed description and photographs of the setups, which were not included in the publications. It is also important to highlight that the photographs in chapters IV and VII show parts of the setups specially designed for this research project.

1.1. Steel samples

    1.1.1   One-piece carbon steel samples or coupons (1030 grade) were used as working electrodes for part of this research. Carbon steel ANSI 1030 is listed in the standard specification for seamless carbon and alloy steel mechanical tubing (ASTM A519/A519M-17) [1]. Seamless steel pipes are used for different applications within the oil and gas industry. The applications include upstream operations (OCTG pipes); midstream (transmission and distribution of fluids, as oil, gas, steam, acids, slurries); downstream (process piping to refine oil and gas in derivative products) and general plumbing applications for utility services) [2].

Table 1. Chemical composition (weight %) of 1030 carbon steel samples.

C	Mn	Si	P	S	Cr	Ni	Mo	Sn	Al	Fe
0.37	0.80	0.282	0.012	0.001	0.089	0.012	0.004	0.004	0.01	balance

1.1.2. Multi-electrode array sensor, namely, WBE sensor, were used as working electrodes. The WBE sensor was fabricated with 100 tightly packed and electrically isolated steel wires. The dimension of each wire was 2.44 mm x 2.44 mm (0.0595 cm^2) of API X65 pipeline steel with a total surface area of 5.95 cm^2. All the wires were arranged as a 10 x 10 square array and embedded in epoxy resin separated at an interval of 0.2 mm from each other.

API X65 pipeline has slightly more content of phosphorous and sulphur than carbon steel (1030 grade). It is known that steels with high P and S content can have inclusions, and thus they more susceptible to intergranular corrosion [3-4]. Therefore, in terms of research, AISI 1030 carbon steel is a good candidate for UDC-MIC testing due to its similarity to API X65 pipeline and yet fewer impurities that can lead to another type of corrosion.

1.2. Chapter III.

CO$_2$ corrosion inhibitors performance at deposit-covered carbon steel and their adsorption on different deposits.

Electrochemical tests were performed using a three-electrode test cell setup, as shown in Fig 1. Carbon steel samples were soldered to wires for electrical connection and embedded in epoxy resin. Hastelloy C and saturated Ag/AgCl fitted in a lugging capillary were used as counter and the reference electrode, respectively.

Table 2. Experimental conditions of chapter III. CO$_2$ corrosion inhibitors performance at deposit-covered carbon steel and their adsorption on different deposits

Temperature/Gas	Test solution	Stirring
30°C/ CO$_2$	Brine (3% NaCl, 0.01% NaHCO$_3$)	Stagnant conditions
Inhibitor	**Abbreviation**	**Chemical formula**
Cetylpiridinium chloride monohydrate	CPC	C$_{21}$H$_{38}$ClN · H$_2$O
2-mercaptopyrimidine- 98%	MPY	C$_4$H$_4$N$_2$S
1-dodecylpiridinium chloride hydrate −98%	DPC	C$_{17}$H$_{30}$ClN · xH$_2$O
Deposit	**Linear formula/ Deposit thickness**	**Configuration**
Silica sand	SiO$_2$ / 8 mm	Three-electrode cell
Aluminium oxide	Al$_2$O$_3$/13 mm	setup

Calcium carbonate	CaCO₃/25 mm

Samples	
Deposit-covered surfaces (no inhibitor)	Deposit-covered surfaces (inhibitor)
Bare steel surfaces (no inhibitor)	Bare steel surfaces (inhibitor)
Blank (no inhibitor/no deposits)	

Thermocouple

Hastelloy C counter electrode

Ag/AgCl reference electrode

CO₂ inlet tubing

Lugging capillary filled with 3M KCL

Electrical connection of the working electrode

Deposit-covered steel sample
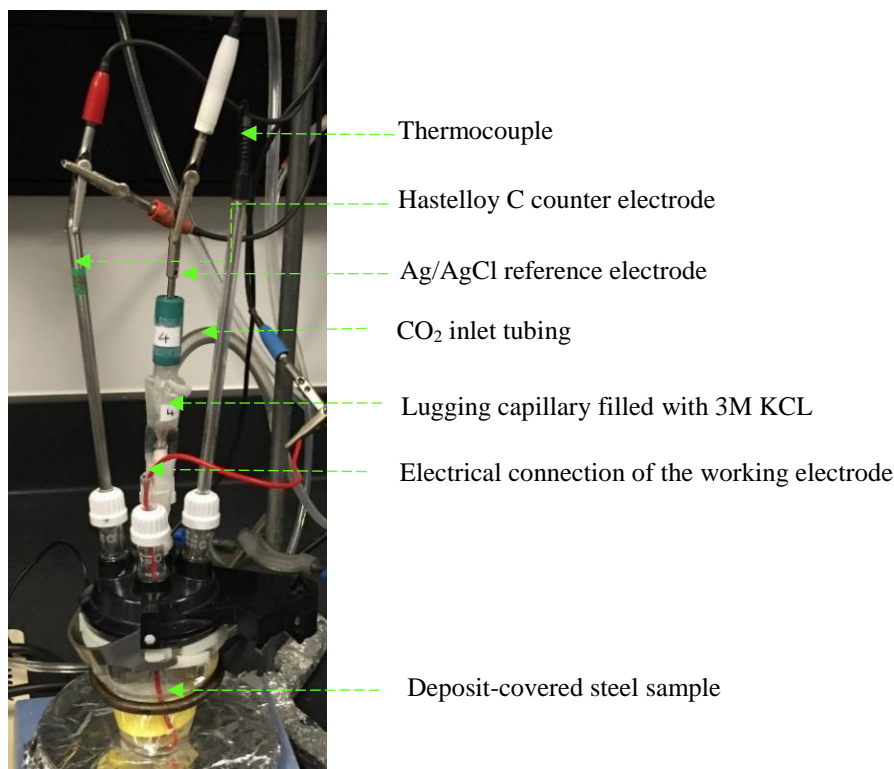
Figure 1. Image of a three-electrode setup of UDC testing and its inhibition (chapter III).

1.3. Chapter IV.

Molecular characteristics affecting the efficiency of corrosion inhibitors at sand-deposited carbon steel: A new approach using a multi-electrode array.

Local electrochemical measurements such as local galvanic currents and local corrosion potentials were carried out using a wire beam electrode (WBE) system. The polished WBE sensor was mounted face-up inside a custom-made glass cell, as shown in Fig. 2-3. A single junction Ag/AgCl reference electrode (placed into a lugging capillary filled with 3% agar and 1.5% 3M KCl). A platinum-coated titanium mesh was used as a counter electrode. The system was adapted to operate in two modes (electrochemical measurements at the entire WBE surface and each electrode or wire).

The schematic diagram of the experimental setup of UDC testing and its inhibition in a partially covered WBE and operation details are presented in chapter IV.

Table 3. Experimental conditions of chapter IV. Molecular characteristics affecting the efficiency of corrosion inhibitors at sand-deposited carbon steel: A new approach using a multi-electrode array.

Temperature/Gas	Test solution	Stirring
$30^{O}C/CO_2$	Brine (3% NaCl, 0.01% $NaHCO_3$)	None
Inhibitor	**Abbreviation**	**Chemical formula**
2-mercaptopyrimidine-	MPY	$C_4H_4N_2S$
1-dodecylpiridinium chloride hydrate	DPC	$C_{17}H_{30}ClN \cdot xH_2O$
Deposit	**Linear Formula**	**Configuration**
Silica sand	SiO_2	WBE system
Samples	**Replenishment**	**CI concentration**
Partially covered-WBE sensor	None	0.892 mM
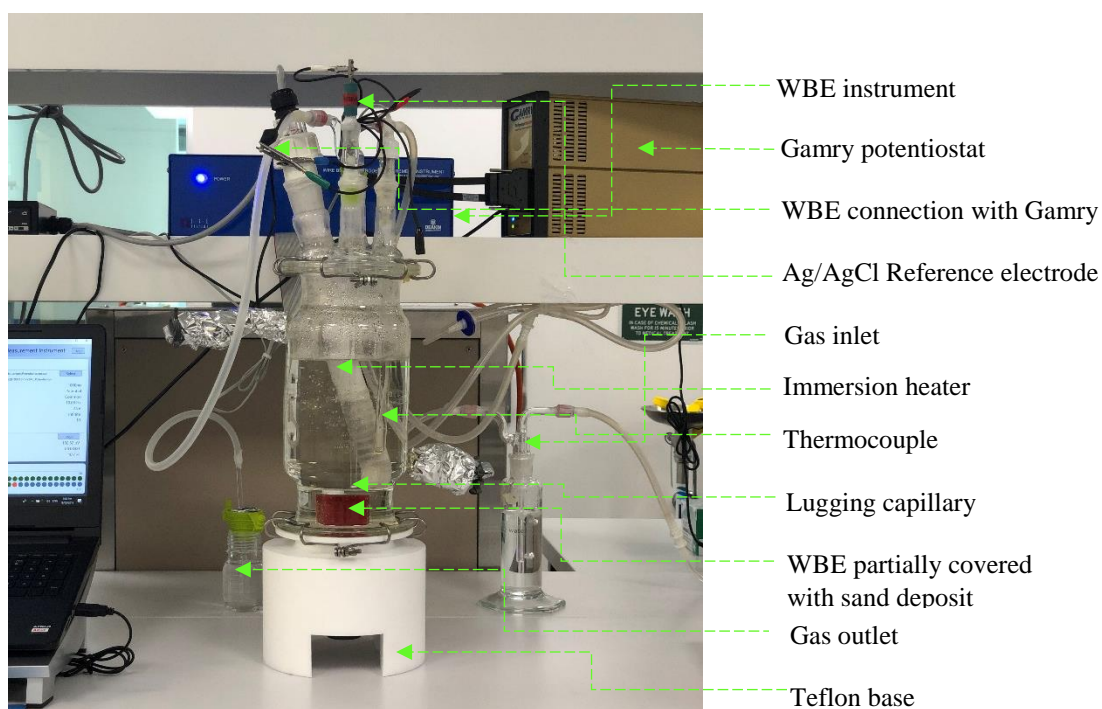
Figure 2. Experimental setup of UDC testing and its inhibition in a partially covered WBE sensor (chapter IV).
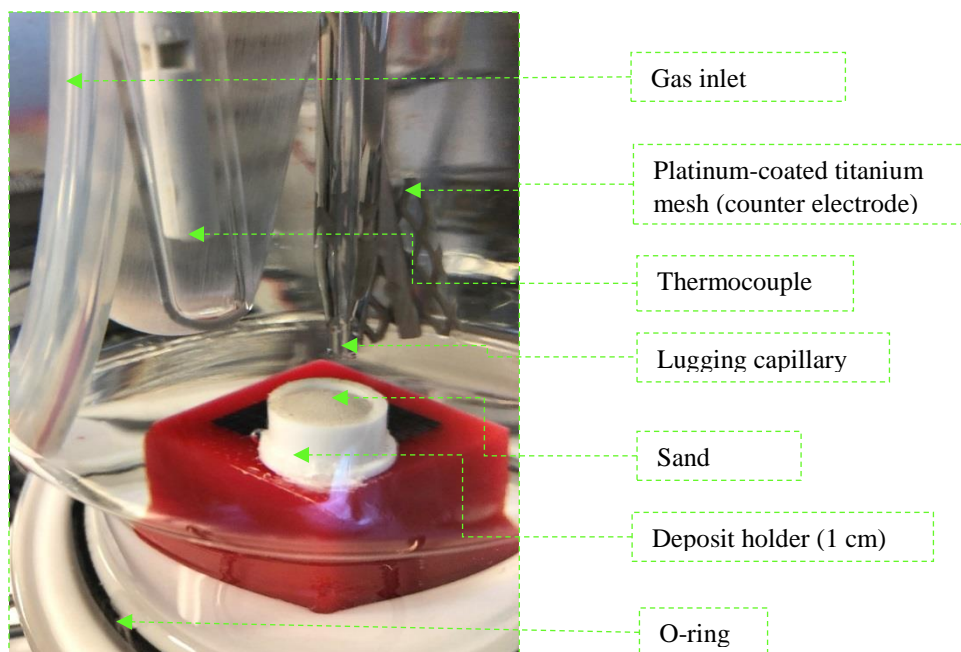
Figure 3. Close-up of the experimental setup of UDC testing and its inhibition in a partially covered WBE sensor (chapter IV).

1.4. Chapter V.

Evaluating under-deposit microbial corrosion using a bacterial isolate, Shewanella Oneidensis MR-1.

Sand-deposited and sand-free carbon steel samples were used for immersion in glass cells like-reactors. The reactors were set as a three-electrode setup, as shown in Fig 4**.** Further details can be found in chapter V.

Table 4. Experimental conditions of chapter V. Evaluating Under-deposit Microbial Corrosion using a Bacterial Isolate, *Shewanella oneidensis* MR-1

Temperature/Gas	Test solution	Stirring
30^OC/ 20% CO_2 in 80% N_2	Two culture medium	200 rpm
Microorganisms	**Deposit**	**Configuration**
Shewanella oneidensis MR-1	Silica sand (SiO_2)	Electrochemical cell (reactor)
Samples	**Replenishment**	**Methods**
Sand-free steel samples	Batch reactor (no	Electrochemical measurements, WL, 3D-
Sand-deposited steel samples	replenishment)	profilometry, FESEM, EDS analysis,
		FTIR analysis (lactate depletion by sand
		deposit)
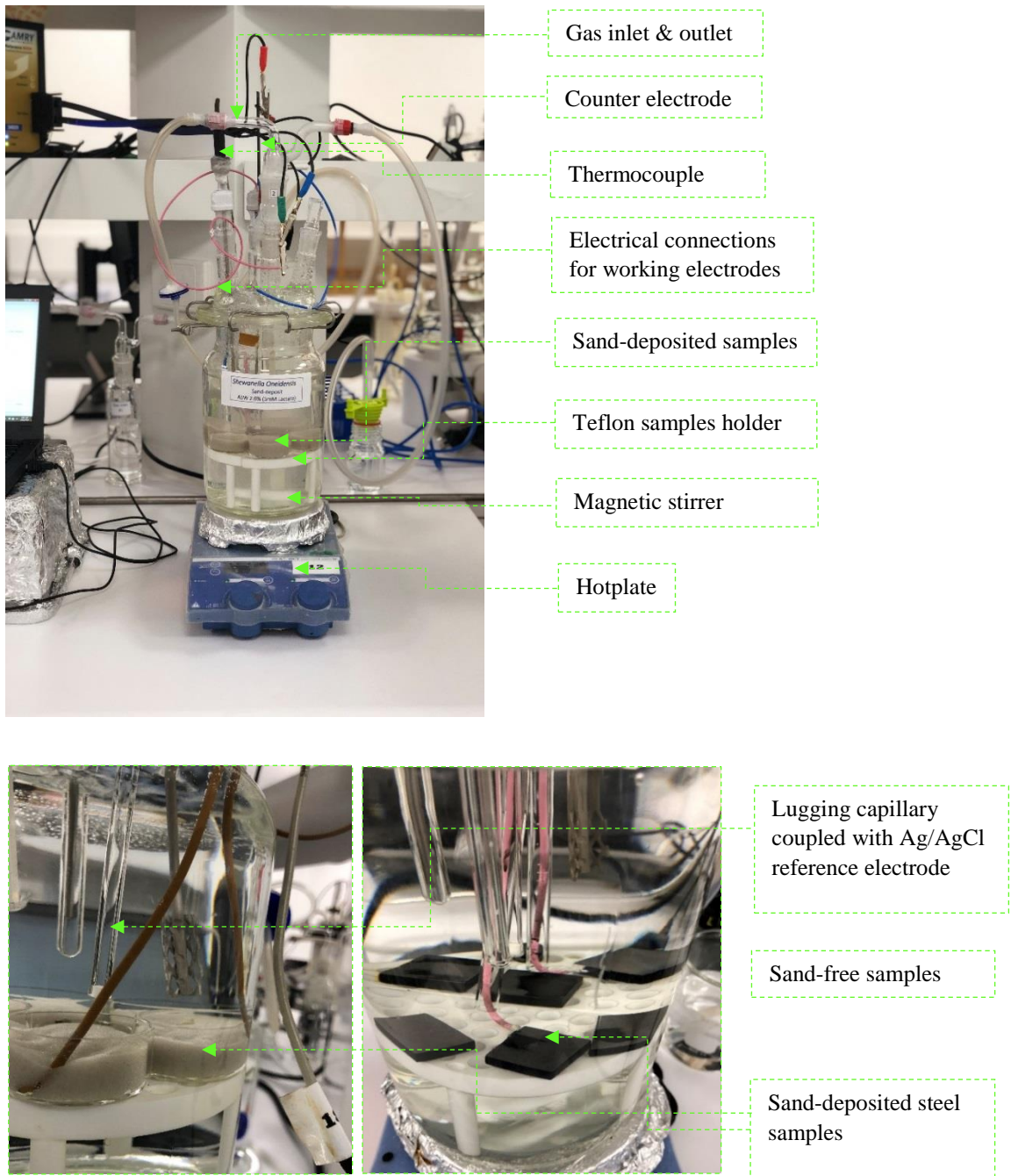
Figure 4. Top photographs: experimental setup of UDMC testing in deposit covered-steel samples. Bottom photographs: close up of UDMC setup (left) sand deposited-steel samples and sand-free steel samples (right).

1.5. Chapter VI.

Aggressive corrosion of steel by a thermophilic microbial consortium in the presence and absence of sand.

Carbon steel samples were used for immersion tests with and without sand, and their respective abiotic controls were carried out using glass cells like reactors. The reactors were also set as a three-electrode setup, as shown in Fig 5. Further details can be found in chapter VI.

Table 5. Experimental conditions of chapter VI. Aggressive corrosion of steel by a thermophilic microbial consortium in the presence and absence of sand.

Temperature/Gas	Test solution	Stirring
55°C/ 20% CO_2 in N_2	Culture medium	200 rpm
Microorganisms	**Deposit**	**Configuration**
Thermophilic microbial consortium recovered from a production facility	Silica sand (SiO_2)	Electrochemical cell (reactor)
Samples	**Replenishment**	**Methods**
Sand-deposited steel samples Sand-free steel samples	Weekly replenishment (semi-batch reactor)	16S-rRNA gene sequencing WL, 3D profilometry, FESEM, EDS mapping analysis
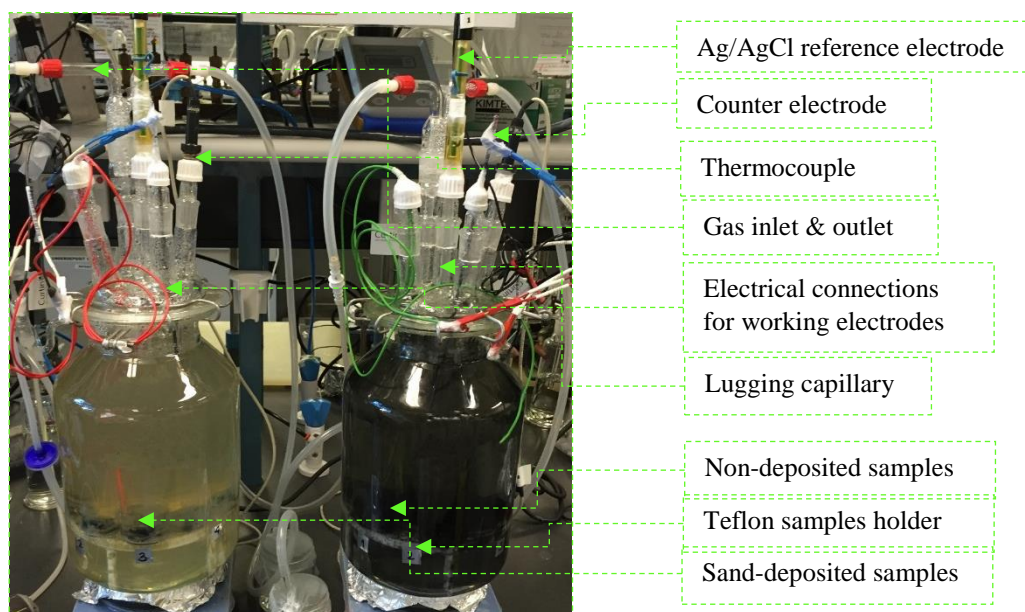
Figure 5. Experimental setup of UDMC testing in deposit covered-steel samples (chapter VI).

1.6. Chapter VII.

In situ investigation of under-deposit microbial corrosion and its inhibition using a multi-electrode array system.

Electrochemical measurements such as local galvanic currents, corrosion potentials and, corrosion rates were measured using a WBE system. The polished WBE surface was mounted an up-right inside position. The reactor was a custom-made glass cell designated to operate either in a batch or fed-batch (continuous flow mode), as shown in Fig. 6. A single junction Ag/AgCl reference electrode placed into a lugging capillary filled with sterile 3M KCl and a platinum-coated titanium mesh were used as a reference and counter electrodes, respectively. The system was adapted to operate in three (3) modes. The schematic diagram of the experimental setup of UDMC testing and its inhibition and operation details are presented in Chapter VII.

Table 5. Experimental conditions of chapter VII. *In situ* investigation of under-deposit microbial corrosion and its inhibition using a multi-electrode array system.

Temperature/Gas	Test solution	Stirring
40ºC/20% CO_2 in N_2	Artificial seawater	None
Inhibitor	**Abbreviation**	**Chemical formula**
2-mercaptopyrimidine- 98%	MPY	$C_4H_4N_2S$
Microorganism	**Microbial metabolism**	**Test configuration**
Enterobacter roggenkampii recovered from iron deposits associated with a corrosion failure.	Iron oxidising-nitrate reducing bacteria (FeONRB)	WBE reactor set in fed-batch (continuous flow mode)
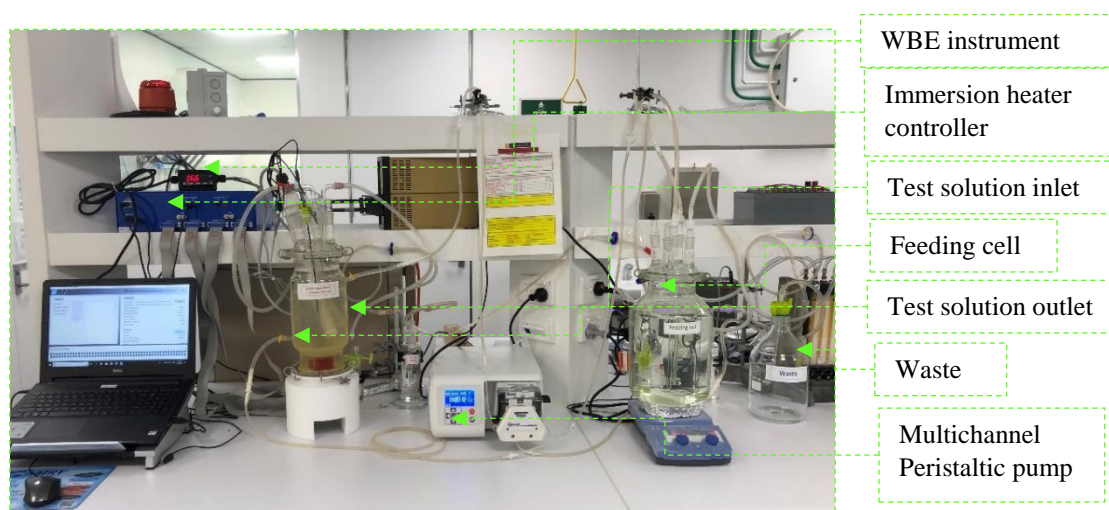
Figure 6. Experimental setup of UDMC testing and its inhibition using a WBE system. WBE reactor operated in fed-batch mode (chapter VII).

1.7. References:

1. ASTM A519/519M-17. Standard Specification for Seamless Carbon and Alloy Steel Mechanical Tubing in ASTM international, 2017.

2. Revie, R. W. (2015). Oil and gas pipelines: integrity and safety handbook, John Wiley & Sons.

3. Küpper, J., Intergranular corrosion of iron-phosphorus alloys in nitrate solutions." Corrosion Science **1981**, 21(3): 227-238.

4. Mohtadi-Bonab, M. A., Microstructural aspects of intergranular and trans granular crack propagation in an API X65 steel pipeline related to fatigue failure. *Engineering Failure Analysis,* **2018**, 94: 214-225.

Original Reprint of the Publication Chapter II

E.M. Suarez, L.L. Machuca, K. Lepková.

The Role of Bacteria in Under-Deposit Corrosion in Oil and Gas Facilities: A Review of Mechanisms, Test Methods and Corrosion Inhibition.

The Role of Bacteria in Under-Deposit Corrosion In Oil and Gas Facilities: a Review of Mechanisms, Test Methods and Corrosion Inhibition

E Suarez, L Machuca & K Lepkova

Curtin Corrosion Engineering Industry Centre (CCEIC), Curtin University, Perth, Australia

1. Introduction

Under-deposit corrosion (UDC) represents a threat to pipeline integrity. This phenomenon has been appointed as responsible for localised corrosion damage in both laboratory testing[1-2] as well as in root cause analysis of critical pipeline failures[3-4]. UDC causes localised corrosion to form beneath the deposits which occur due to chemical and physical differences between the bare and deposited-steel surfaces[5] and, in case of fully deposited surfaces, as a result of the conditions under the deposits. Typically, horizontal or inclined sections of pipelines where the flow velocity is under its minimum limit tend to accumulate (usually at 6 o'clock position) corrosion products and scales of the line leading to deep penetration of the metal surface[6]. Under-deposit corrosion can frequently take place in sub-sea injection, transmission and well-fluid pipelines. However, it can also occur in cooling water systems with scales and foulants. Solid particles can promote corrosion in two ways: 1) adsorption of inhibitors onto deposits reducing inhibitors availability and thus leading to inadequate inhibition beneath the deposits[7], and 2) producing corrosion-erosion at high low velocities by either eroding the metal wall[8] or removing layers of corrosion products and filming inhibitors[9].

In addition to the presence of mineral deposits, microorganisms are commonly present in the systems aggravating the problems in pipeline integrity management. In real life scenarios, it is unlikely to find abiotic systems due to the ubiquitous nature of the microorganisms where some of them have the capability of degrading the metal as a result of their presence or activity leading to MIC. Microbial cells thrive in between solid particles deposited on the metal surface where they could grow protected to some extent from external threats[10] (e.g., leading to less effective biocide treatment in deposited areas). After this settlement stage, further corrosion complications arise from this combination of microbes and solid particles leading to both MIC-UDC damage. In this sense, we can define "UDC-MIC occurrence" as the combination of electrochemical, physical and microbiological processes compromising pipeline integrity.

Previous work using sludge deposited on steel surfaces demonstrated that microbes living within that deposit accelerated and induced general and localised corrosion[11]. A long-term study of UDC in stagnant seawater showed that samples with a deposited mix of magnetite, calcium carbonate and sand induced more localised corrosion than the deposit-free samples[12]. The microbe-deposit combinations were also found responsible for pipeline failure in a production system[13]. Similarly, UDC in an injection water pipeline has been associated with the premature failure due to multiple factors, including the presence of microorganisms in the system 3. Wang et al.,[12, 14] proposed a synergy between MIC and UDC which led to a more severe localised corrosion at half-pipe steel covered with mixed deposits under simulated stagnant seawater conditions.

Currently, diverse testing methods have been used to assess general and localised corrosion underneath inert deposits through electrochemical measurements[15-17]. However, the intrinsic complexity of electrically conductive deposits and biofilms can impart difficulty to the interpretation of the electrochemical data. From the microbiological point of view, emerging omics based-techniques open a world of possibilities for the understanding of biofilm-deposit-metal interactions. Omics refers to a field of study in biology which involves a group of technologies used to explore the roles, relationships, and actions of the different types of molecules that make up the cells of an organism. The techniques include: 1) Metagenomics (the study of genetic material of microorganisms from environmental samples to provide information regarding diversity and ecology of a specific environment); 2) Transcriptomics (study ribonucleic acid (RNA) molecules to identify which cellular processes are active and which are dormant); 3) Proteomics (identification and quantification of protein sets produced at a specific point in time); 4) Metabolomics (the study of complete set of metabolites that are the end products of cellular processes)[18]. Furthermore, microscopy and surface chemical analysis techniques have also been employed in the study of both UDC and MIC, but usually as a separate phenomenon. For MIC, these techniques provide valuable information about the involvement of biofilms in the biocorrosion process of metals and their alloys.

Research in UDC and its inhibition has achieved understanding about the effect of diverse deposits on steel surfaces, and also some insights into the role of deposits in corrosion inhibitor performance. However, the microbial-deposit-metal relationship and how this combination impacts corrosion processes has not been investigated to a great extent. Similarly, there is a knowledge gap regarding the effect of biofilms and their extracellular polymeric substances (EPS) on inhibitor efficiency and conversely the potential biocide effect of some inhibitors on the integrity and activity of microorganisms. The following is a review of available literature regarding MIC and UDC in oil and gas pipelines. This work aims to connect these two phenomena which impact steel asset integrity. The review includes traditional and new testing techniques for both UDC-MIC as well as diverse mitigation strategies.

2. Under-Deposit Corrosion
2.1. Major factors influencing corrosion under deposits
2.1.1. Nature of deposit
The deposits found in oil and gas facilities are classified according to their nature as follows 1) inorganic deposits, e.g., sand, corrosion products, and scales. 2) organic deposits, e.g., asphaltene, wax, biofilms and, 3) mixed deposits as "schmoo" a thick black layer covering the internal wall of the pipeline[9]. A previous study showed that silica sand decreased general corrosion by a factor of 3 to 5 at both 25°C and 80°C. The authors state that the inert sand creates a mass transfer barrier for corrosive species as well as a decrease in anodic and cathodic currents due to less active available surfaces 5. However, some researchers have demonstrated that sand decreased general corrosion but also created localised attack under the sand-deposited area[19-20]. In real oil and gas scenarios, the solid particles deposited in the bottom of the pipeline have a diverse and complex composition which can determinate the type of UDC. For instance, Pandarinathan *et al.*[2] evaluated three typical constituents of pipeline deposits (sand, alumina and calcite). The authors demonstrated that general corrosion occurs depending on the type of the

deposit. The most corrosive deposit was alumina, followed by calcite and the less corrosive silica sand. Another common deposit present in pipelines is iron sulphide (FeS) which has been found to be more corrosive to X-65 carbon steel than the inert silica sand under H_2S environment[21]. Another UDC study demonstrated more severe general and localised corrosion underneath a field sludge deposit compared to a sand deposit[22].

2.1.2. Pipeline dimensions
Been *et al.*[23] mentioned that combined gravitational force in which solids settle to the bottom of the pipe and the dynamic of the fluid could lead to UDC at unusual locations in the line. The author also stated that the location, quantity and structure of the deposit layers formed could be different in large diameter lines (>500 mm) compared to small diameter lines (<250 mm).

2.1.3. Deposit features
The particle size of the deposit seems to influence the extent of the damage, with the smaller silica sand particles (diameter less than 44 μm) being less corrosive than larger sand particles (250-750μm)[24]. Results from with carbon steel under CO_2 covered with deposits of glass beads, SiO_2 powder and sand indicated that at higher deposit porosity higher corrosion rates occurred[25].

2.1.4. System conditions and chemical treatments
Undoubtedly, the presence of chemicals such as corrosion inhibitors, biocides, scale inhibitors, wax, and asphaltene amongst others will influence localised corrosion formed underneath deposits. Other determining factors include gas presence (CO_2, H_2S, O_2), electrolyte corrosiveness (pH, salinity, acetic acid, sulphur), oil/water ratio, temperature and pressure[9].

3. Microbiologically Influenced Corrosion:
It is well-known that microbial cells can either directly or indirectly influence the corrosion processes leading to metal deterioration. The indirect mechanism, also known as "chemical microbially influenced corrosion (CMIC)" occurs when microbial cells change the surrounding environment, e.g., producing corrosive species such as acids and sulphides. The direct mechanism includes 1) direct electron uptake or "electrical microbially influenced corrosion (EMIC)" [26] and 2) by biofilm deposition on the steel surfaces influencing anodic or cathodic reactions[27]. The effects of microorganisms or their activity on metals with deposits can be as follows: 1) biofilms act as organic deposits changing physically and chemically the surrounding environment even though these microorganisms are not metabolically related to corrosion; 2) microbial cells can change the properties of the solids previously deposited on the steel; 3) corrosion microbial activity leading to formation and deposition of corrosive species[28]; 4) creation of microenvironments underneath the biofilm as a result of extracellular polymeric substances (EPS) formation. The EPS mediates cell adhesion by forming a three-dimensional network that immobilizes cells within the biofilm[29]. Also, the effect of EPS on the corrosion of carbon steel has been related to the presence of acidic groups in this matrix, which increases the corrosion on steels by lowering the interfacial pH[30]; 5) microorganisms can also degrade the structure of corrosion inhibitors and coatings by utilising their constituents as carbon sources[28].

3.1. Typical metabolic groups associated with MIC
3.1.1. Sulphidogenic microorganisms
3.1.1.1. Sulphate-reducing prokaryotes (SRP)
This sulphidogenic group comprise sulphate-reducing archaea (SRA) and sulphate-reducing bacteria (SRB). SRBs have been historically associated with MIC problems because of their ability to reduce sulphate to sulphide and consequently iron sulphide (FeS) formation which can be highly corrosive[31]. Additionally, some strains of SRB can uptake electrons directly to the metal surface producing EMIC which is considered as an efficient MIC process[32].

3.1.1.2. Sulphur-reducing bacteria (S°RB)
SoRB can reduce elemental sulphur (S°) to hydrogen sulphide (H_2S) to produce energy and, iron sulphide (FeS) when Fe ions are available. S°RB can also ferment proteinous substrates, organic acids and single amino acids to produce ethanol, acetate, propionate, isovalerate/2-methyl butyrate, H_2, and CO_2[33]. *Thermovirga lienii* is one of the most representative SoRB related to MIC process both experimentally as well as in case studies of failure, where it was classified as high-risk microorganism due to its predominance within deposits covering highly corroded steel surfaces[34].

3.1.1.3. Thiosulphate-reducing bacteria (TRB)
TRBs disproportionate thiosulphate to produce sulphate and sulphide which eventually form iron sulphide (FeS)[35]. This microbial metabolic group has been cited numerously in MIC literature, especially *Thermoanaerobacter* genus. A recent MIC-UDC work showed that fermenting-TRB considerably enhanced localised attack underneath an oilfield deposit[36]. *Thermoanaerobacter* species can also use diverse fermentation pathways producing hexoses, ethanol, acetate, lactate, H_2, and CO_2[37].

3.1.2. Fermentative microorganisms
This metabolic group obtain energy from a wide range of organic compounds, including sugars, peptides, amino acids, or organic acids. Some can also use inorganic sulphur compounds, ferric iron, and nitrate as electron acceptors to oxidise their substrates[38]. Thus, those who use sulphur compounds as an electron sink during fermentation can contribute to H_2S production. Fermenters influence corrosion by producing different volatile fatty acids such as acetate formic and lactic, with acetate being the most common end product formed. The high corrosivity of acetic acid has been largely studied[39] and the widespread distribution of acetogens in oilfield CO_2 environment make these type of fermenters as a fundamental group involved in MIC problems. Typically, acetogenic bacteria ferment carbohydrates and oil hydrocarbons producing acetic acid which can precipitate on steel surfaces creating a local acid environment[40]. Acetogenics can also produce acetic acid using H_2 and CO_2 to synthesise acetyl-CoA[41]. Recently, Kato *et al.*[42] proposed the link acetogenesis-MIC with a *Sporomusa* sp. strain cultured acetogenetically using Fe^0 as a sole electron donor. Additionally, the organic acids produced by fermenters can be metabolised by SRB growth, nitrate- and/or iron-reducing bacteria inhabiting oil reservoirs establishing cooperation between these metabolic groups[38].

3.1.3. Iron-oxidizing bacteria
These microorganisms generate energy oxidising ferrous ions to ferric ions which precipitate as ferric oxides[43]. Starosvetsky *et al.*,[44] demonstrated that localised corrosion occurred in the presence of IOB, which resulted in a crevice effect caused by biogenic ferric oxides deposited on stainless steel surfaces. Anaerobically, some IOBs can reduce nitrate (NO_3^-) and oxidise ferrous iron (Fe^{2+}) [45] this efficient denitrification performance can potentially affect nitrate-based corrosion inhibitors. The EPS produced by IOB has been found to accelerate corrosion on carbon steel surfaces[46].

3.1.4. Iron/manganese reducing bacteria (IRB/MRB)

IRB/MRB reduce solid Fe^{+3} and Mn^{+4} oxides to soluble Fe^{+2} and Mn^{+2} ions. *Geobacter* and *Shewanella* genera have frequently been linked to corrosion and metal reduction. The role of metal-reducing bacteria towards steel corrosion is related to the removal of passivating layers of Fe^{+3}/Mn^{+4} oxides, which leads to localised corrosion by the exposure of metal surfaces to corrosive species.

3.1.5. Methanogens

Methanogenic archaea have become an important microbial group in the MIC field. They use molecular hydrogen (H_2) to reduce CO_2 and produce methane (CH4)[47]. These hydrogenotrophic microorganisms consume cathodic hydrogen in a process called "cathodic depolarisation" which contribute to steel corrosion[48]. Methanogens have also been identified as electromethanogenic microorganisms able to induce EMIC by extracellular electron transfer (EET) uptaking electrons directly from the steel and hence accelerate corrosion[49].

3.1.6. Syntrophic relationships

The interest for microbial syntrophic (cross-feeding) associations in MIC has grown in the recent years. These associations are not referred only to the transfer of reducing agents such as hydrogen or formate; they can also include the exchange of organic, sulphur and nitrogen compounds as well as the removal of toxic agents[50]. Although it is difficult to interpret the precise mechanism(s) in which microbial associations contribute to MIC, it is expected a metabolic interaction between microbial partners could thrive and eventually affect metal integrity in oil fields. The most cited syntrophy in MIC research is between sulphate-reducing prokaryotes (SRP) and methanogens in which SRB convert lactate into acetate and hydrogen, both of which are subsequently utilised by methanogens for the production of methane[51-53]. Another biocorrosion study associated the presence of hydrogen-utilising methanogens, sulphur and thiosulphate reducing bacteria, fermenting bacteria and iron reducing bacteria, with important corrosion problems in Alaskan North Slope Oil Facilities[54].

4. UDC-MIC Testing Methods
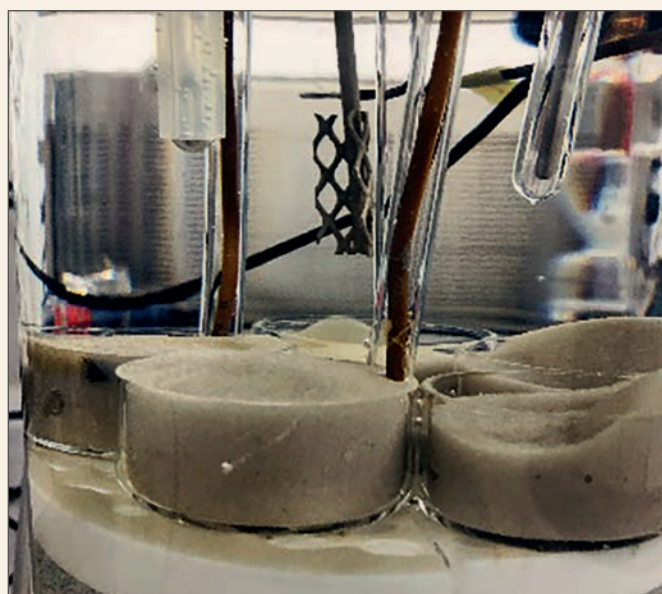
Figure 1. Sand-deposited carbon steel samples immersed under biotic conditions in CO_2/N_2 containing solution. Suarez et al, (unpublished results).
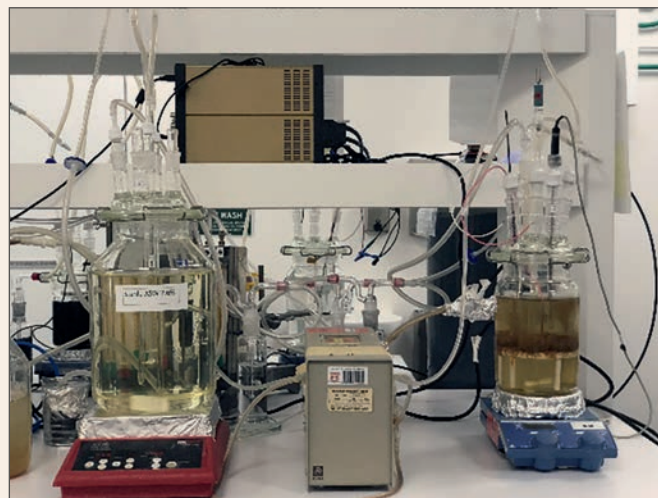
Figure 2. Three electrode set-up for UDC-MIC testing after 4 weeks of immersion under biotic conditions Suarez et al, (unpublished results).

Selecting appropriate techniques to determine electrochemical reactions involved in UDC-MIC is challenging because of the multiple and complex variables involved in a deposited system. For UDC, several laboratory techniques that simulate field conditions have been adapted. Vera *et al.*[9] listed and compared testing methods in their UDC review. Other methods, such as scanning probes, radiography, ultrasonic testing, field signature and electrical resistance probes, amongst others can be suitable techniques to evaluate UDC although some of them possess limitations[55].

Testing methodologies using test reactors have been used to assess both general and localised corrosion underneath deposits and in the presence of inhibitors by electrochemical measurements[15, 56]. Additionally, the susceptibility to localised corrosion of deposited surfaces can be assessed through accelerated electrochemical tests using this configuration[1]. This test methodology also allowed the study of UDC using different types of mineral deposits, e.g., sand, calcite, and alumina[2] as well as different coatings, biofilms and/or field deposits collected from industrial operations such as sludge, mixed mineral and oil deposits[36]. Recently, we studied the MIC-UDC phenomenon using a three-electrode test set-up (Figures 1 and 2) covering the samples with silica sand. The test solution was continuously replenished to keep microorganism active during the experiment. After the immersion period, the samples were maintained under continuous injection of N_2 to ensure complete drying before surface analysis (Data unpublished). The set-up was shown to provide a suitable method to evaluate the interactions between microorganisms and sand-deposits on corroding steel. Likewise, we have recently assessed biocide and inhibitor efficiency in the presence of sand deposits containing a microbial consortium (data unpublished). This study showed that deposits significantly decreased biocide efficiency and resulted in a faster re-establishment of injured biofilms.

Moreover, some techniques such as multi-electrode arrays can provide insights into the galvanic effects beneath the deposits and can be used for biofilms. Solid particles can provide different chemical and physical conditions underneath the deposit than those conditions on the bare steel resulting in galvanic cells forming between the two areas leading to localised corrosion. Various multi-electrode arrays has been used to investigate UDC. For instance, Turnbull *et al.*[57] developed an electrode array of 24 electrodes designed

for evaluating UDC inhibition. Tan *et al*.[58], Zhang et al.[59], Hinds *et al*.[60] and, Xu et al.[61] amongst others have also used microelectrode arrays with deposits to study UDC and/or its inhibition. Dong *et al*.[62] assessed the heterogeneous corrosion processes underneath SRB-biofilm.

Figure 3. Image of a cross-section through a sand deposited-metal surface in the presence of a microbial consortium. Suarez et al, (unpublished results).

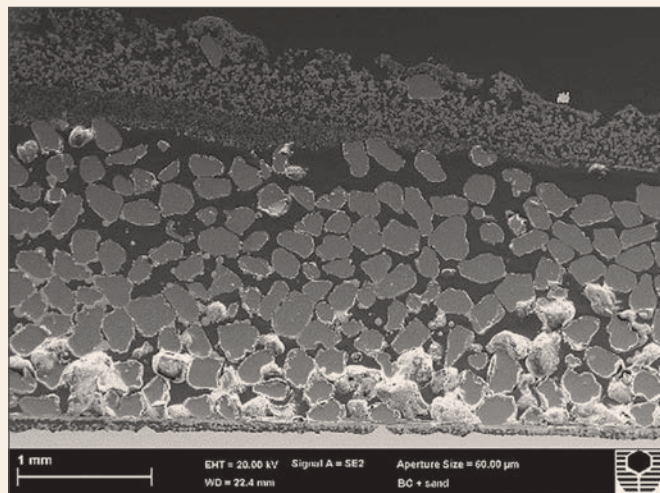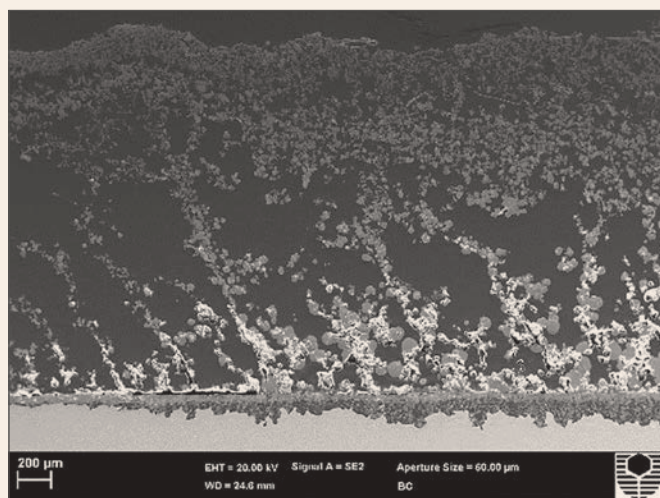*Figure 4. Image of a cross section through a sand-free metal surface in the presence of microbial consortium. Suarez et al, (unpublished results).*

In regards to the microbiological component, several techniques have been developed to study microbe-metal interaction and how it influences corrosion of metals. Table 1 shows some MIC traditional and emerging methods, some of these methods can be suitable to study corrosion under deposits. Particularly, microscopy and surface chemical analysis are important tools for studying biofilm/metal interaction. Microscopy has been widely used to investigate the contribution of microorganisms to metallic corrosion. These techniques involved Field Emission Scanning electron microscopy (FESEM), 3D-profilometry, Atomic force microscopy (AFM), and Transmission electron microscopy (TEM)[63]. Microscopy can provide information about: 1) Biofilm contribution to corrosion, e.g., changes in the microstructure of the metal after cleaning of corrosion products 2) Biofilm development, distribution, adhesion and relation substratum/corrosion products; 3) Morphology of microorganisms and colony formation and distribution on the metal 4) SEM of

cross-sectional- images reveal the profile of the damage[64] e.g., as presented in Figure 3 and 4 (steels covered and uncovered with sand deposits respectively). These SEM images of corroded steel specimens exposed to microorganisms showed corrosion products/deposits distribution, metal penetration and morphology of the damage under the deposits, and microbial cells (data unpublished). Surface analysis techniques, on the other hand, can provide surface chemical characterization, nano-scale analysis, and/or thin film characterisation[65-66]. The information about chemical composition of corrosion products, biodeposits and underlying layers formed (in cross-sectional images) contribute to the understanding of electrochemical mechanisms that take place as a result of microbial presence/activity towards steel corrosion.

Although some traditional microbiological techniques provide insight into microbial activity and corrosion processes, identification and role of the whole microbial community related to UDC and its inhibition has not been widely addressed. Gaining information about microbial community activity is probably a milestone in the understanding of corrosion mechanisms on deposited-steel surfaces. An Accelerated Low-Water Corrosion (ALWC) study in a European harbour determined diversity, distribution, abundance and activity of sulphate-reducing bacteria (SRB) within deposits obtained from carbon steel sheet piles[67]. The results showed that SRBs were more active in the inner and intermediate layers of the deposits and related to the presence of FeS in these layers. Emerging omics-based techniques can contribute to determining MIC microbial populations regarding diversity and metabolisms. These techniques have achieved significant progress in health sciences, and recently it has gained attention in MIC research. Beale et al.[18] stated that the bioinformatic approaches to MIC research provide information about microbial respiratory processes, metabolic reactions, corrosion mechanisms, pathways, microbial community structure and its activity. For example, the use of metabolomics techniques identified critical metabolomics biomarkers to predict MIC in copper pipes[68] as well as differentiation of samples due to the reduction of carboxylic acids produced by microorganisms with the potential to cause MIC problems[69]. It is expected that in the near future the exponential growth of the omics discipline will improve the understanding of microbe-metal-deposit interactions resulting in metal deterioration. For instance, transcriptomics could serve to establish differences in metabolic pathways of microorganisms between the surfaces of steels with deposits and those with no deposits. Similarly, metagenomics would be able to reveal differences in composition and structure of the microbial population in the presence and the absence of deposits and relate them to the development of corrosion.

From the practical point of view, it is essential to consider the sensitivity of microbial molecules (DNA, RNA, proteins) to degradation and change which requires strict preservation methods for accurate detection and quantification. In this way, it is important to highlight that to generate meaningful and reliable data, experiments should be ideally designed in the way to control aspects such as critical temperatures, sample replicates, samples handling, solution for molecules preservation, and processing times among others. Collecting and processing samples on-site, on the other hand, make these conditions more difficult to achieve. It is necessary to take extra effort on sampling to preserve molecules to be analysed as well as the deposit-steel interface for further characterisation and visualisation of the layers formed. It is also relevant to mention that to help diagnose MIC as part of UDC, analysis should target identification of microbial cells in such deposits.

Due to the complexity of a system containing deposits and microorganisms, interdisciplinary participation is essential when defining the laboratory test methodology. Ideally, a combination of methodologies should undoubtedly aid better understanding of a problem hypothesised in the laboratory or a problem faced in oilfield facilities. For instance, Been et al.,[23] described a testing protocol developed to evaluate the effectiveness of five inhibitors to mitigate UDC in the presence of bacteria at large diameter pipeline deposited with a sludge (oil, water, sand and microorganisms). The protocol included inhibitors filming effectiveness, partitioning studies, sludge corrosivity, and bacterial kill tests.

5. UDC-MIC Mitigation

Corrosion management programs in pipelines involve pigging and inhibitors treatment to mitigate internal corrosion. Chemical treatment is commonly used to mitigate UDC. Nonetheless, it is a challenging strategy because some inhibitors cannot penetrate the deposit, leading to unprotected areas underneath of the deposit. In fact, some inhibitors have been shown to enhance localised corrosion in the presence of deposits[58, 92]. Pandarinathan et al.[20] showed that some inhibitors such as thiobenzamide inhibited general corrosion (>90%) on steel with and without sand deposits, but could not provide protection against localized corrosion. Also, pyrimidine derivates have shown to be highly protective under sand deposits 15. It is important to mention that some mitigation strategies typically included in UDC programs can potentially serve to prevent or mitigate MIC (e.g., mechanical cleaning, use of coatings and adequate facilities design). Table 2 lists strategies commonly used for MIC mitigation in oil and gas facilities. It is relevant to mention that the majority of methods have limitations and some of them are not long-term effective[93] (e.g., chemical methods). Moreover, there is a lack of information regarding the effectiveness of some MIC mitigation methods in the presence of deposits (e.g., biocide treatments) which need to be addressed to cover both aspects.

Table 1. MIC testing methods and monitoring

	Description	References
Microbial culture testing	Cultivating microorganisms allows detection and semi-quantitative enumeration of corrosion-related microorganisms. Limitation: underestimate microbial population	NACE-TM0212.[70] NACE-TM0194.[71]
Biochemical assays	Measure compounds and enzymes of cells to estimate microbial population related to MIC. Adenosine triphosphate (ATP), Adenosine Phosphosulfate reductase (APS), Hydrogenase.	Little et al.[72], Beech et al.[64]
Physiological activity	Techniques to detect microbial activity by transformation of radiolabelled metabolic precursors.14C-labeled compounds have been used to quantify catabolic and anabolic activities linked to corrosion tubercles	Phelps et al.[73]
Traditional MMM techniques	Molecular microbiological methods (MMMs) are genetic techniques which are culture-independent such as PCR and qPCR to detection and/or quantification of microorganisms by DNA amplification.	Whitby et al.[74]
Omics-based techniques	Metagenomic techniques (identification and characterisation of the complete microbial population); Transcriptomics (gene expression-activity); Proteomics (proteins production) and, Metabolomics (metabolism)	Beale et al.,[18] Beech et al.[29] Machuca et al.[75]
Microscopy	Field Emission Scanning electron microscopy (FESEM), 3D-Profilometry, Atomic force microscopy (AFM), Transmission electron microscopy (TEM)	Beech et al.[76], Sheng et al.[77], Yves et al.[78], Fang et al.[79] Wikiel et al.[80]
Fluorescence microscopy	Examination of samples treated with dyes that fluoresce under specific wavelength. Biological stains such as acridine orange which permeates cells to attach to DNA and RNA. Fluorescent in situ hybridisation (FISH) probes used to identify and quantify species and groups of corrosion-related microorganisms. 4', 6-diamidino-2-phenylindole (DAPI) is a fluorescent dye that binds to DNA allowing detection/quantification of live and dead cells. Confocal laser scanning microscopy (CLSM) create three-dimensional images using fluorescent dyes, to determine surface contour and measure critical dimensions such as biofilm thickness.	Chen et al.[81], Mudali et al.[82]
Surface chemical analysis	Elemental composition of corrosion products and deposits originated from microbial activity. X-ray diffraction (XRD), energy dispersive X-ray (EDS), X-ray emission spectroscopy (PIXE), attenuated total reflectance Fourier transform infrared spectroscopy (ATR/FT-IR), X-ray photoelectron spectroscopy, time-of-flight secondary ionisation mass spectrometry (TOF-SIMS), Auger electron spectroscopy (AES), X-ray photoelectron spectroscopy (XPS)	Beech et al.[83], Boxer et al.[84], Ding et al.[85], Seyeux et al.
Isotope Fractionation	Sulphur isotopes (^{32}S and ^{34}S) present in the sulphate which is reduced resulting in ^{32}S rich sulphide as a result of microbial metabolism within the biofilm	Little et al.[86],
Electrochemical techniques to measure and monitoring MIC	No external polarization: galvanic couples, open circuit potential (OCP), electrochemical noise (ECN), Multielectrode array systems (WBE) Small external polarization: Linear polarization technique (LPR), Electrochemical impedance spectroscopy (EIS), Electrochemical frequency modulation (EFM) Large external polarization: potentiostat or potentiodynamic polarization curves and pitting scans.	Angell et al.[87], Little et al.[72], Dominguez et al.[88], Mansfeld et al.[89], Beese et al.[90], Ben-Yoav et al.[91], Hue et al.[62]

160

Table 2. Strategies for MIC-prevention/mitigation

Physical Methods

Description	References
Mechanical cleaning Brushing in production and injection lines, rubbing spheres for heat exchangers, blasting with sand, grit or water. Removal of sludge, scale, encrustations and biomass. Pipeline inspection gauge (pig) is also efficient in removing deposits, and it can record information about corrosion problems, metal loss and curvatures in the pipe wall.	Videla *et al.*[94]
Filtration /UV-radiation/ These methods can use an alternative to the traditional chemical treatments which sometimes are toxic, expensive and non- biodegradables. A combination of filtration and UV disinfection of seawater has been shown to decrease localised corrosion of susceptible alloys. Membrane filtration systems are commonly used to control biofouling. These systems use a wide range of anti-adhesion and anti-microbial strategies on the membranes. Sand screens which mechanically filter out sand while fluids flow.	Machuca *et al.*[95] Mansouri *et al.*

Chemical Methods (Biocides/Biocide enhancers, biofilm dispersants and corrosion inhibitors)

	Description	References
Non-oxidizing biocides		
Glutaraldehyde	A traditional biocide used against fungi, algae and bacteria including SRBs biofilms. The functional group of glutaraldehyde acts against proteins of the cell wall and cytoplasm. It has large-scale application, a broad spectrum efficiency, biodegradability and safety profile.	Ganzer *et.al.*[97] Wen *et al.* Greene *et al.*[98]
Quaternary ammonium compounds (QUATS)	These form cationic compounds which act as biocides and corrosion inhibitors. Their detergent property dissolves lipids on the cell. QUATS also avoid the formation of polysaccharides.	Cloete *et al.*
Organo-sulphur compounds	These prevent energy transfer mechanisms critical for microbial growth. Some are pH sensitive suffering rapid hydrolysis which makes them not suitable for cooling water systems at pH > 8.	Londry *et al.*[99]
Tetrakis hydroxymethyl phosphonium sulphate (THPs)	This has biocidal properties against bacteria, fungi and algae. It has good compatibility with other chemicals. Dissolve iron sulphides. It has large-scale application, broad spectrum efficiency, biodegradability and, safety profile.	Talbot *et al.*,[100]. Wen *et al.*[101].
Biocides- new approaches		
D-Amino acids as (biocide enhancers)	These are biofilm dispersal agents which convert sessile cells to planktonic cells which are more susceptible to biocides. D-amino acids are enhancers of THPs and alkyldimethylbenzylammonium chloride but not for Glutaraldehyde.	Kolding *et al.*[102]. Xu *et al.* Jia *et al.*[103] Xu *et al.*
Chelators (biocide enhancers)	Ethylene-diamine tetraacetic acid (EDTA) is slowly biodegradable. Ethylene-diamine disuccinate (EDDS) is more biodegradable and not hazardous. EDSS enhances the effects of THPs and Glutaraldehyde. It also cuts down biocide dosages in SRBs biofilm treatment.	Wen *et al.* , Xu *et al.*
Norspermidine (biofilm dispersant)	This polyamine inhibits biofilm formation. The combination of D-tyrosine and Norspermidine reduces the EPS content and modify the matrix structure in microbial aggregates, converting sessile to planktonic cells.	Hobley *et al.*[104] Si *et al.*[105] Xu *et al.*
Bacteriophages for biofilm treatment	Bacteriophages can prevent biofilm formation, biofilm eradication. Phages are host specific thus phage cocktails are expensive but necessary field applications at large scales.	Gutierrez *et al.*[106] Eydal *et al.*[107]. Motlagh *et al.*[108]
Antimicrobial stainless steels	304L-Cu antibacterial stainless steel has strong MIC resistance against *E.coli*. Copper-containing 2205 duplex stainless steels (2205-Cu DSS) have shown high antibacterial efficiency and localised corrosion resistance under biotic conditions.	Lin *et al.*[109] Nan *et al.*[110], Xia *et al.*[111] Machuca *et al.*[112]

Other Methods

Description	References
Design	
Selecting the design of the appropriate pipeline is critical to minimize UDC-MIC occurrence. These strategies are focused on UDC but may help to mitigate MIC simultaneously. The strategies include; selecting corrosion resistance alloys, increase flow rates, avoid dead legs as well as low parts in the pipes as a preventive measure for deposits accumulation 9 and similarly, potential microbial accumulation.	

6. Conclusions and Future Prospects

Corrosion observed under deposits on steels in the presence of microorganisms is the result of synergistic effects of different microbial groups that act as a consortium and alter the metal surfaces, directly or indirectly 113. It is possible to describe "UDC-MIC" as the combination of electrochemical, physical and microbiological processes towards metal integrity.

This paper reviews some concepts, testing methods and monitoring techniques for UDC and MIC, and discusses MIC mitigation strategies. Future research is required to fill knowledge gaps. These include the effect of the microorganisms on inhibitor efficiency and inhibitor performance in the presence of microbial cells and deposits. MIC research should also focus on mechanisms of how syntrophic relationships relate to corrosion and, specific interactions between deposits and microorganisms which lead to metal corrosion.

It is clear that understanding microbial-deposit-metal interactions entirely is very ambitious. However, information obtained by traditional and emerging techniques suited to provide both UDC and MIC insights should surely aid in the understanding of this combination, and in the development of more effective strategies to mitigate this aggressive form of corrosion. The contribution of omics-based techniques applied to MIC-UDC opens numerous and promising possibilities in this field. For instance, elucidating biofilm–metal-deposit interactions at the molecular level will aid in the understanding of the contribution of the UDC-MIC mechanism, and will potentially facilitate the development of UDC-MIC monitoring programs for particular operating systems.

The complexity of deposited-systems, which makes more difficult the assessment of localised metal corrosion under organic/inorganic deposit layers, should promote the application of more suitable techniques/configurations able to study localised electrochemical processes. In this way, it would facilitate future research focus on the study of corrosion inhibitor performance under deposits and in the presence of microorganisms.

A broad consensus in regards to experience and knowledge of a particular system, is critical for selecting testing methods as well as for designing mitigation programs. An appropriate multidisciplinary approach is crucial to extend the lifetime of oil and gas pipelines potentially exposed to deposits and microorganisms.

References

[1.] Pandarinathan, V.; Lepková, K.; van Bronswijk, W., Chukanovite (Fe₂(OH)₂CO₃) identified as a corrosion product at sand-deposited carbon steel in CO₂-saturated brine. Corrosion Science:2014, 85, pp 26-32.

[2.] Pandarinathan, V.; Lepková, K.; Bailey, S. I.; Gubner, R., Impact of Mineral Deposits on CO₂ Corrosion of Carbon Steel. NACE International: 2013, pp 5118-5132.

[3.] Shukla, P. K.; Naraian, S., Under-Deposit Corrosion in a Sub-Sea Water Injection Pipeline—A Case Study. NACE International: 2017, pp 2296-2306.

[4.] Nelson, D.; Edwards, M. A.; Kovash, P. Monitoring and controlling corrosion in an aging sour gas gathering system A nine-year case history, CORROSION 2007, NACE International: 2007, pp 076681-0766821

[5.] Huang, J.; Brown, B.; Choi, Y.-S.; Ne; ic, S., Prediction of Uniform CO₂ Corrosion of Mild Steel Under Inert Solid Deposits. NACE - International Corrosion Conference Series:2011.

[6.] Papavinasam, S., Chapter 4 - The Main Environmental Factors Influencing Corrosion. In Corrosion Control in the Oil and Gas Industry, Gulf Professional Publishing: Boston: 2014; pp 179-247.

[7.] Binks, B. P.; Fletcher, P. D. I.; Salama, I. E.; Horsup, D. I.; Moore, J. A., Quantitative Prediction of the Reduction of Corrosion Inhibitor Effectiveness Due to Parasitic Adsorption onto a Competitor Surface. Langmuir : the ACS journal of surfaces and colloids :2011, 27 (1), pp 469-473.

[8.] Guo, H. X.; Lu, B. T.; Luo, J. L., Interaction of mechanical and electrochemical factors in erosion–corrosion of carbon steel. Electrochimica Acta: 2005, 51 (2), pp 315-323.

[9.] Vera, J. R.; Daniels, D.; Achour, M. H., Under Deposit Corrosion (UDC) In The Oil And Gas Industry: A Review Of Mechanisms, Testing And Mitigation. NACE International: 2012, pp 3028-3040.

[10.] Skovhus, T. L.; Enning, D.; Lee, J. S., Microbiologically Influenced Corrosion in the Upstream Oil and Gas Industry. CRC Press: 2017, pp 1-559.

[11.] Mosher, W.; Mosher, M.; Lam, T.; Cabrera, Y.; Oliver, A.; Tsaprailis, H. Methodology for Accelerated Microbiologically Influenced Corrosion in Under Deposits from Crude Oil Transmission Pipelines. NACE - International Corrosion Conference Series: 2014.

[12.] Wang, X.; Melchers, R. E. In Long-term Under-deposit Corrosion of Carbon Steel Pipelines under Stagnant Seawater, The 26th International Ocean and Polar Engineering Conference, International Society of Offshore and Polar Engineers: 2016.

[13.] Esan, T.; Kapusta, S. D.; Simon-Thomas, M. J. J., Case Study: Extreme Corrosion of a 20" Oil Pipeline in the Niger Delta Region. In NACE International, NACE International: 2001.

[14.] Wang, X.; Melchers, R. E., Corrosion of carbon steel in presence of mixed deposits under stagnant seawater conditions. Journal of Loss Prevention in the Process Industries: 2017, 45, pp 29-42.

[15.] Pandarinathan, V.; Lepková, K.; Bailey, S. I.; Gubner, R., Evaluation of corrosion inhibition at sand-deposited carbon steel in CO2-saturated brine. Corrosion Science: 2013, 72, pp 108-117.

[16.] Lepková, K.; Gubner, R., Development of standard test method for investigation of under-deposit corrosion in carbon dioxide environment and its application in oil and gas industry. In NACE - International Corrosion Conference Series: 2010.

[17.] Lepková, K.; Tan, Y.; Gubner, R. In Electrochemical study of under-deposit carbon dioxide corrosion and its inhibition, 49th Annual Conference of the Australasian Corrosion Association 2009: Corrosion and Prevention: 2009; pp 336-344.

[18.] Beale, D. J.; Karpe, A. V.; Jadhav, S.; Muster, T. H.; Palombo, E. A., Omics-based approaches and their use in the assessment of microbial-influenced corrosion of metals. Corrosion Reviews:2016, 34 (1-2), pp 1-15.

[19.] Mohammed, M., Assessment of Underdeposit Corrosion and Mitigation Using Chemicals. In CORROSION 2016, NACE International: Vancouver, British Columbia, Canada :2016, pp 3412-3424.

[20.] Pandarinathan, V.; Lepkova, K.; Bailey, S. I.; Gubner, R., Inhibition of Under-Deposit Corrosion of Carbon Steel by Thiobenzamide. Journal of the Electrochemical Society:2013, 160 (9), pp, 432-440.

[21.] Standlee, S.; Efird, K. D.; Spiller, D., Under Deposit Corrosion From Iron Sulfide. In Conference & Expo, NACE International: 2011.

[22.] Alanazi, N. M., Investigation of Under-Deposit Corrosion on X-60 using Multielectrode System. NACE International: 2017, 8, pp 5321-533.

[23.] Been, J.; Place, T. D.; Crozier, B.; Mosher, M.; Ignacz, T.; Soderberg, J.; Cathrea, C.; Holm, M.; Archibald, D., Development Of A Test Protocol For The Evaluation Of Underdeposit Corrosion Inhibitors In Large Diameter Crude Oil Pipelines. NACE - International Corrosion Conference Series: 2011.

[24.] Hassani, S.; Huang, J.; Victor, A. C.; Brown, B.; Singer, M., Inhibited Under-Deposit CO₂ Corrosion: Small Particle Silica Sand and Eicosane Paraffin Deposits. In CORROSION, NACE International: New Orleans, Louisiana, USA: 2017, 4 , pp 2340-2351.

[25.] Huang, J.; Brown, B.; Jiang, X.; Kinsella, B.; Nesic, S., Internal CO₂ Corrosion Of Mild Steel Pipelines Under Inert Solid Deposits. NACE - International Corrosion Conference Series: 2010.

[26.] Kato, S., Microbial extracellular electron transfer and its relevance to iron corrosion. Microbial Biotechnology:2016, 9 (2), pp 141-148.

[27.] Gu, J. D.; Ford, T. E.; Mitchell, R., Microbiological Corrosion of Metallic Materials. In Uhlig's Corrosion Handbook, John Wiley & Sons, Inc: 2011; pp 549-557.

[28.] Stott, J. F. D., 2.20 - Corrosion in Microbial Environments. In Shreir's Corrosion, Elsevier: Oxford, 2010; pp 1169-1190.

[29.] Beech, I. B.; Sztyler, M.; Gaylarde, C. C.; Smith, W. L.; Sunner, J., 2 - Biofilms and biocorrosion. In Understanding Biocorrosion, Woodhead Publishing: Oxford, 2014; pp 33-56.

[30.] Chongdar, S.; Gunasekaran, G.; Kumar, P., Corrosion inhibition of mild steel by aerobic biofilm. Electrochimica Acta 2005, 50 (24), pp 4655-4665.

[31.] Beech, I. B.; Gaylarde, C. C., Recent advances in the study of biocorrosion: an overview. Revista de Microbiologia 1999, 30, pp 117-190.

[32.] Enning, D.; Venzlaff, H.; Garrelfs, J.; Dinh, H. T.; Meyer, V.; Mayrhofer, K.; Hassel, A. W.; Stratmann, M.; Widdel, F., Marine sulfate-reducing bacteria cause serious corrosion of iron under electroconductive biogenic mineral crust. Environmental microbiology 2012, 14 (7), pp 1772-1787.

[33.] Dahle, H.; Birkeland, N.-K., Thermovirga lienii gen. nov., sp. nov., a novel moderately thermophilic, anaerobic, amino-acid-degrading bacterium isolated from a North Sea oil well. International Journal of Systematic and Evolutionary Microbiology 2006, 56 (7), pp 1539-1545.

[34.] Skovhus, S. M. C. T. L., Applications of molecular microbiological methods. Caister Academic Press: 2014.

[35.] Madigan, M. T; Martinko, J. M.; Bender, K. S.; Buckley, D. H.; Stahl, D. A., Brock biology of microorganisms (14th edition). 2014.

[36.] Machuca, L. L.; Lepkova, K.; Petroski, A., Corrosion of carbon steel in the presence of oilfield deposit and thiosulphate-reducing bacteria in CO₂ environment. Corrosion Science 2017, 129, pp 18-25.

[37.] Vos, P.; Garrity, G.; Jones, D.; Krieg, N. R.; Ludwig, W.; Rainey, F. A.; Schleifer, K.-H.; Whitman, W. B., Bergey's manual of systematic bacteriology: Volume 3: The Firmicutes. Springer Science & Business Media: 2011; Vol. 3.

[38.] Ollivier, B.; Magot, M., Fermentative, Iron-Reducing, and Nitrate-Reducing Microorganisms. In Petroleum Microbiology, American Society for Microbiology (ASM) 2005, 5, pp 71-88

[39.] Liu, D.; Chen, Z.; Guo, X., The effect of acetic acid and acetate on CO2 corrosion of carbon steel. Anti-Corrosion Methods and Materials 2008, 55 (3), pp 130-134.

[40.] Suflita, J. M.; Phelps, T. J.; Little, B., Carbon Dioxide Corrosion and Acetate: A Hypothesis on the Influence of Microorganisms. Corrosion 2008, 64 (11), pp 854-859.

[41.] Schiel-Bengelsdorf, B.; Dürre, P., Pathway engineering and synthetic biology using acetogens. FEBS letters 2012, 586 (15), pp 2191-2198.

[42.] Kato, S.; Yumoto, I; Kamagata, Y., Isolation of Acetogenic Bacteria That Induce Biocorrosion by Utilizing Metallic Iron as the Sole Electron Donor. Applied and environmental microbiology 2015, 81 (1), pp 67-73.

[43.] Starosvetsky, D.; Armon, R.; Yahalom, J.; Starosvetsky, J., Pitting corrosion of carbon steel caused by iron bacteria. International Biodeterioration & Biodegradation 2001, 47 (2), pp 79-87.

[44.] Starosvetsky, J.; Starosvetsky, D.; Pokroy, B.; Hilel, T.; Armon, R., Electrochemical behaviour of stainless steels in media containing iron-oxidizing bacteria (IOB) by corrosion process modeling. Corrosion Science 2008, 50 (2), pp 540-547.

[45.] feng Su, J.; cheng Shao, S.; lin Huang, T.; Ma, F.; fei Yang, S.; ming Zhou, Z.; chen Zheng, S., Anaerobic nitrate-dependent iron (II) oxidation by a novel autotrophic bacterium, Pseudomonas sp. SZF15. Journal of environmental chemical engineering 2015, 3 (3), pp 2187-2193.

[46.] Liu, H.; Gu, T.; Asif, M.; Zhang, G.; Liu, H., The corrosion behavior and mechanism of carbon steel induced by extracellular polymeric substances of iron-oxidizing bacteria. Corrosion Science 2017, 114, pp 102-111.

[47.] Ozuolmez, D.; Na, H.; Lever, M. A.; Kjeldsen, K. U.; Jørgensen, B. B.; Plugge, C. M., Methanogenic archaea and sulfate reducing bacteria co-cultured on acetate: teamwork or coexistence? Frontiers in microbiology 2015, 6, pp 492.

[48.] Davidova, I. A.; Duncan, K. E.; Perez-Ibarra, B. M.; Suflita, J. M., Involvement of thermophilic archaea in the biocorrosion of oil pipelines. Environmental microbiology 2012, 14 (7), pp 1762-1771.

[49.] Hara, M.; Onaka, Y.; Kobayashi, H.; Fu, Q.; Kawaguchi, H.; Vilcaez, J.; Sato, K., Mechanism of Electromethanogenic Reduction of CO2 by a Thermophilic Methanogen. Energy Procedia 2013, 37 (Supplement C), pp 7021-7028.

[50.] Morris, B. E. L.; Henneberger, R.; Huber, H.; Moissl Eichinger, C., Microbial syntrophy: interaction for the common good. FEMS Microbiology Reviews 2013, 37 (3), pp 384-406.

[51.] Zhang, T.; Fang, H.; Ko, B., Methanogen population in a marine biofilm corrosive to mild steel. Applied microbiology and biotechnology 2003, 63 (1), pp 101-106.

[52.] Mand, J.; Park, H. S.; Jack, T. R.; Voordouw, G., The role of acetogens in microbially influenced corrosion of steel. Frontiers in microbiology 2014, 5 pp 268.

[53.] Lohner, S. T.; Deutzmann, J. S.; Logan, B. E.; Leigh, J.; Spormann, A. M., Hydrogenase-independent uptake and metabolism of electrons by the archaeon Methanococcus maripaludis. The ISME Journal 2014, 8 (8), pp 1673-1681.

[54.] Duncan, K. E., Biocorrosive Thermophilic Microbial Communities in Alaskan North Slope Oil Facilities. Environmental Science & Technology 2010, 43 (20), pp 7977–7984.

[55.] Tan, Y. M.; Revie, R. W., Heterogeneous electrode processes and localized corrosion. John Wiley & Sons: 2012; Vol. 13.

[56.] Pandarinathan, V.; Lepková, K.; ina; Gubner, R., Inhibition Of CO₂ Corrosion Of 1030 Carbon Steel Beneath Sand-Deposits. NACE - International Corrosion Conference Series, 2011.

[57.] Turnbull, A.; Hinds, G.; Cooling, P.; Zhou, S., A Multi-Electrode Approach To Evaluating Inhibition Of Underdeposit Corrosion In CO2 Environments. NACE - International Corrosion Conference Series 2009.

[58.] Tan, Y.; Fwu, Y.; Bhardwaj, K., Electrochemical evaluation of under-deposit corrosion and its inhibition using the wire beam electrode method. Corrosion Science 2011, 53 (4), pp 1254-1261.

[59.] Zhang, G. A.; Yu, N.; Yang, L. Y.; Guo, X. P., Galvanic corrosion behavior of deposit-covered and uncovered carbon steel. Corrosion Science 2014, 86, pp 202-212.

[60.] Hinds, G.; Turnbull, A., Novel Multi-Electrode Test Method for Evaluating Inhibition of Underdeposit Corrosion—Part 1: Sweet Conditions. CORROSION 2010, 66 (4), 046001-046001-10.

[61.] Xu, Y. Z.; Zhu, Y. S.; Liu, L.; He, L. M.; Wang, X. N.; Huang, Y., The study of the localized corrosion caused by mineral deposit using novel designed multi-electrode sensor system. Materials and Corrosion 2017, 68 (6), pp 632-644.

[62.] Dong, Z. H.; Shi, W.; Ruan, H. M.; Zhang, G. A., Heterogeneous corrosion of mild steel under SRB-biofilm characterised by electrochemical mapping technique. Corrosion Science 2011, 53 (9), pp 2978-2987.

[63.] Beech, I. B.; Tapper, R. C.; Gubner, R. J., Microscopy methods for studying biofilms. Biofilms: Recent advances in their study and control 2000, pp 51-70.

[64.] Beech, I. B., Corrosion of technical materials in the presence of biofilms—current understanding and state-of-the art methods of study. International Biodeterioration & Biodegradation 2004, 53 (3), pp 177-183.

[65.] Seyeux, A.; Zanna, S.; Marcus, P., 8 - Surface analysis techniques for investigating biocorrosion. In Understanding Biocorrosion, Woodhead Publishing: Oxford, 2014; pp 197-212.

[66.] Seyeux, A.; Marcus, P., Analysis of the chemical or bacterial origin of iron sulfides on steel by time of flight secondary ion mass spectrometry (ToF-SIMS). Corrosion Science 2016, pp 112, 728-733.

[67.] Païssé, S.; Ghiglione, J.-F.; Marty, F.; Abbas, B.; Gueuné, H.; Amaya, J. M. S.; Muyzer, G.; Quillet, L., Sulfate-reducing bacteria inhabiting natural corrosion deposits from marine steel structures. Applied microbiology and biotechnology 2013, 97 (16), pp 7493-7504.

[68.] Beale, D. J.; Dunn, M. S.; Marney, D., Application of GC–MS metabolic profiling to 'blue-green water'from microbial influenced corrosion in copper pipes. Corrosion Science 2010, 52 (9), pp 3140-3145.

[69.] Beale, D. J.; Dunn, M. S.; Morrison, P. D.; Porter, N. A.; Marlow, D. R., Characterisation of bulk water samples from copper pipes undergoing microbially influenced corrosion by diagnostic metabolomic profiling. Corrosion Science 2012, 55, pp 272-279.

[70.] International, N., Detection, Testing, and Evaluation of Microbiologically Influenced Corrosion on Internal Surfaces of Pipelines. NACE International: 2018.

[71.] International, N., Field Monitoring of Bacterial Growth in Oil and Gas Systems. NACE International: 2014.

[72.] Little, B. J.; Ray, R. I.; Lee, J. S., Diagnosing, Measuring, and Monitoring Microbiologically Influenced Corrosion. In Uhlig's Corrosion Handbook, John Wiley & Sons, Inc.: 2011; pp 1203-1216.

[73.] Phelps, T.; Schram, R.; Ringelberg, D.; Dowling, N.; White, D., Anaerobic microbial activities including hydrogen mediated acetogenesis within natural gas transmission lines. Biofouling 1991, 3 (4), pp 265-276.

[74.] Whitby, C.; Skovhus, T. L., Applied microbiology and molecular biology in oilfield systems. Springer: 2011.

[75.] Machuca, L.; Jeffrey, R.; Melchers, R. E., Microorganisms associated with corrosion of structural steel in diverse atmospheres. International Biodeterioration and Biodegradation 2016, 114, pp 234-243.

[76.] Beech, I. B.; Smith, J. R.; Steele, A. A.; Penegar, I.; Campbell, S. A., The use of atomic force microscopy for studying interactions of bacterial biofilms with surfaces. Colloids and Surfaces B: Biointerfaces 2002, 23 (2–3), pp 231-247.

[77.] Sheng, X.; Ting, Y. P.; Pehkonen, S. O., Force measurements of bacterial adhesion on metals using a cell probe atomic force microscope. Journal of Colloid and Interface Science 2007, 310 (2), pp 661-669.

[78.] Dufrêne, Y. F., Atomic force microscopy, a powerful tool in microbiology. Journal of bacteriology 2002, 184 (19), pp 5205-5213.

[79.] Fang, H. H. P.; Chan, K.-Y.; Xu, L.-C., Quantification of bacterial adhesion forces using atomic force microscopy (AFM). Journal of microbiological methods 2000, 40 (1), pp 89-97.

[80.] Wikieł, A. J.; Datsenko, I.; Vera, M.; Sand, W., Impact of Desulfovibrio alaskensis biofilms on corrosion behaviour of carbon steel in marine environment. Bioelectrochemistry 2014, 97, pp 52-60.

[81.] Chen, Y.; Tang, Q.; Senko, J. M.; Cheng, G.; Zhang Newby, B.-m.; Castaneda, H.; Ju, L.-K., Long-term survival of Desulfovibrio vulgaris on carbon steel and associated pitting corrosion. Corrosion Science 2015, 90, pp 89-100.

[82.] Mudali, U. K.; George, R. P.; Anandkumar, B., Metal-Microbe Synergy in Pitting Corrosion of Stainless Steels. NACE - International Corrosion Conference Series 2016.

[83.] Beech, I. B.; Zinkevich, V.; Tapper, R.; Gubner, R.; Avci, R., Study of the interaction of sulphate-reducing bacteria exopolymers with iron using X-ray photoelectron spectroscopy and time-of-flight secondary ionisation mass spectrometry. Journal of microbiological methods 1999, 36 (1–2), pp 3-10.

[84.] Boxer, S. G.; Kraft, M. L.; Weber, P. K., Advances in imaging secondary ion mass spectrometry for biological samples. Annual review of biophysics 2009, 38, 53-74.

[85.] Ding, Y.; Zhou, Y.; Yao, J.; Szymanski, C.; Fredrickson, J.; Shi, L.; Cao, B.; Zhu, Z.; Yu, X.-Y., In Situ Molecular Imaging of the Biofilm and Its Matrix. Analytical Chemistry 2016, 88 (22), pp 11244-11252.

[86.] Little, B. J.; Wagner, P.; Jones-Meehan, J., Sulfur Isotope Fractionation in Sulfide Corrosion Products as an Indicator for Microbiologically Influenced Corrosion (MIC). In Microbiologically Influenced Corrosion Testing, ASTM International 1994.

[87.] Angell, P.; Luo, J.; White, D., Studies of the reproducible pitting of 304 stainless steel by a consortium containing sulphate-reducing bacteria. International conference on Microbially Influence Corrosion, NACE - International Corrosion Conference Series 1995.

[88.] Dominguez-Benetton, X.; Sevda, S.; Vanbroekhoven, K.; Pant, D., The accurate use of impedance analysis for the study of microbial electrochemical systems. Chemical Society Reviews 2012, 41 (21), pp 7228-7246.

[89.] Mansfeld, F., The use of electrochemical techniques for the investigation and monitoring of microbiologically influenced corrosion and its inhibition – a review. Materials and Corrosion 2003, 54 (7), pp 489-502.

[90.] Beese, P.; Venzlaff, H.; Srinivasan, J.; Garrelfs, J.; Stratmann, M.; Mayrhofer, K. J. J., Monitoring of anaerobic microbially influenced corrosion via electrochemical frequency modulation. Electrochimica Acta 2013, 105, pp 239-247.

[91.] Ben-Yoav, H.; Freeman, A.; Sternheim, M.; Shacham-Diamand, Y., An electrochemical impedance model for integrated bacterial biofilms. Electrochimica Acta 2011, 56 (23), pp 7780-7786.

[92.] Huang, J.; Brown, B.; Nesic, S.; Papavinasam, S.; Gould, D., Localized Corrosion of Mild Steel under Silica Deposits in Inhibited Aqueous CO2 solutions. NACE - International Corrosion Conference Series, 2013.

[93.] Machuca, L. L. In Microbiologically influenced corrosion: A review focused on hydrotest fluids in subsea pipelines, Annual Conference of the Australasian Corrosion Association: Corrosion and Prevention, 2014.

[94.] Videla, H. A., Prevention and control of biocorrosion. International Biodeterioration & Biodegradation 2002, 49 (4), pp 259-270.

[95.] Machuca, L. L.; Jeffrey, R.; Bailey, S. I.; Gubner, R.; Watkin, E. L. J.; Ginige, M. P.; Kaksonen, A. H.; Heidersbach, K., Filtration-UV irradiation as an option for mitigating the risk of microbiologically influenced corrosion of subsea construction alloys in seawater. Corrosion Science 2014, 79, pp 89-99.

[96.] Mansouri, J.; Harrisson, S.; Chen, V., Strategies for controlling biofouling in membrane filtration systems: challenges and opportunities. Journal of Materials Chemistry 2010, 20 (22), pp 4567-4586.

[97.] Ganzer, G.; McIlwaine, D.; Diemer, J.; Freid, M.; Russo, M., Applications of Glutaraldehyde in the Control of MIC. In CORROSION 2001, NACE International: Houston, Texas, 2001.

[98.] Greene, E. A.; Brunelle, V.; Jenneman, G. E.; Voordouw, G., Synergistic Inhibition of Microbial Sulfide Production by Combinations of the Metabolic Inhibitor Nitrite and Biocides. Applied and environmental microbiology 2006, 72 (12), pp 7897-7901.

[99.] L., L. K.; M., S. J., Toxicity effects of organosulfur compounds on anaerobic microbial metabolism. Environmental Toxicology and Chemistry 1998, 17 (7), pp 1199-1206.

[100.]Talbot, R. E.; Larsen, J.; Sanders, P. F., Experience With the Use of Tetrakishydroxymethylphosphonium Sulfate (THPS) for the Control of Downhole Hydrogen Sulfide. In CORROSION 2000, NACE International: Orlando, Florida, 2000.

[101.]Wen, J.; Xu, D.; Gu, T.; Raad, I., A green triple biocide cocktail consisting of a biocide, EDDS and methanol for the mitigation of planktonic and sessile sulfate-reducing bacteria. World journal of microbiology & biotechnology 2012, 28 (2), pp 431-5.

[102.]Kolodkin-Gal, I.; Romero, D.; Cao, S.; Clardy, J.; Kolter, R.; Losick, R., D-Amino Acids Trigger Biofilm Disassembly. Science 2010, 328 (5978), pp 627-629.

[103.]Jia, R.; Yang, D.; Li, Y.; Xu, D.; Gu, T., Mitigation of the Desulfovibrio vulgaris biofilm using alkyldimethylbenzylammonium chloride enhanced by D-amino acids. International Biodeterioration & Biodegradation 2017, 117, pp 97-104.

[104.]Hobley, L.; Kim, S. H.; Maezato, Y.; Wyllie, S.; Fairlamb, A. H.; Stanley-Wall, N. R.; Michael, A. J., Norspermidine is not a self-produced trigger for biofilm disassembly. Cell 2014, 156 (4), pp 844-854.

[105.]Si, X.; Quan, X.; Li, Q.; Wu, Y., Effects of D-amino acids and norspermidine on the disassembly of large, cold-aged microbial aggregates. Water research 2015, 75, pp 247-253.

[106.]Gutiérrez, D.; Rodríguez-Rubio, L.; Martínez, B.; Rodríguez, A.; García, P., Bacteriophages as weapons against bacterial biofilms in the food industry. Frontiers in microbiology 2016, 7, pp 825.

[107.]Eydal, H. S.; Jägevall, S.; Hermansson, M.; Pedersen, K., Bacteriophage lytic to Desulfovibrio aespoeensis isolated from deep groundwater. The ISME journal 2009, 3 (10), pp 1139.

[108.]Motlagh, A. M.; Bhattacharjee, A. S.; Goel, R., Biofilm control with natural and genetically-modified phages. World Journal of Microbiology and Biotechnology 2016, 32 (4), pp 67.

[109.]Lin, H.; Yin, Y.; Wang, X.; ZHAO, R.-d.; ZHANG, W.-q., Structure and properties of Cu-contained antibacterial martensitic stainless steel. Metall. Funct. Mater 2007, 14, pp 14-17.

[110.]Nan, L.; Xu, D.; Gu, T.; Song, X.; Yang, K., Microbiological influenced corrosion resistance characteristics of a 304L-Cu stainless steel against Escherichia coli. Materials Science and Engineering: C 2015, 48, pp 228-234.

[111.]Xia, J.; Yang, C.; Xu, D.; Sun, D.; Nan, L.; Sun, Z.; Li, Q.; Gu, T.; Yang, K., Laboratory investigation of the microbiologically influenced corrosion (MIC) resistance of a novel Cu-bearing 2205 duplex stainless steel in the presence of an aerobic marine Pseudomonas aeruginosa biofilm. Biofouling 2015, 31 (6), pp 481-492.

[112.]Machuca, L. L.; Bailey, S. I.; Gubner, R.; Watkin, E.; Kaksonen, A. H., Microbiologically influenced corrosion of high resistance alloys in seawater. In NACE - International Corrosion Conference Series, 2011.

[113.]AlAbbas, F. M.; Williamson, C.; Bhola, S. M.; Spear, J. R.; Olson, D. L.; Mishra, B.; Kakpovbia, A. E., Influence of sulfate reducing bacterial biofilm on corrosion behavior of low-alloy, high-strength steel (API-5L X80). International Biodeterioration & Biodegradation 2013, 78, pp 34-42.

Original Reprint of the Publication Chapter III

E.M. Suarez, L.L. Machuca, B. Kinsella, K. Lepková.

CO_2 Corrosion Inhibitors Performance at Deposited-Carbon Steel and their Adsorption on Different Deposits.

Corrosion, 75 (9):1118-1127 (2019).

CO$_2$ Corrosion Inhibitors Performance at Deposit-Covered Carbon Steel and Their Adsorption on Different Deposits

Erika M. Suarez,* Laura L. Machuca,* Brian Kinsella,* and Kateřina Lepková‡,*

The efficiency of inhibitors to prevent under deposit corrosion of carbon steel and their adsorption on aluminum oxide, calcium carbonate, and silica sand deposits have been evaluated using electrochemical measurements and UV-visible spectroscopy. 2-Mercaptopyrimidine provided the highest corrosion protection on both bare and deposit-covered steels. In contrast, 1-Dodecylpiridinium chloride had minimal adsorption on all deposits, but it exhibited insufficient performance. Inhibitors adsorption tended to be related to the inhibitor type and not notably to the physical properties of the deposits. Deposit porosity, layers thickness, and depletion of the inhibitor by adsorption on deposits could not be linked entirely to corrosivity and inhibitors performance.

KEY WORDS: carbon steel, CO$_2$ corrosion, corrosion inhibitors, under-deposit corrosion

INTRODUCTION

Several oil and gas systems which operate in CO$_2$ conditions can contain mineral deposits which are transported throughout pipelines. As a result, it can cause corrosion problems to occur, such as under-deposit corrosion (UDC).[1-2] This phenomenon is usually related to a localized form of attack underneath the deposits which may be present in oil and gas transportation pipelines.[3-4] The variety of different deposit materials that can occur in pipelines makes the mechanism of UDC quite complex. In general, the deposits can be of inorganic and organic nature. Inorganic deposits like sand, scales, and corrosion products and organic like wax, asphaltene, and inhibitor residues.[5] Sometimes complex mixtures of organic and inorganic deposits are formed such as "schmoo" found in production water facilities[6-9] or more adverse combinations like biofilms and minerals deposits leading to UDC-microbiologically influenced corrosion.[10]

Regarding mineral deposits, silica sand (SiO$_2$) is often the most abundant mineral found in petroleum pipelines in volumetric concentrations from 1% to 40%.[11] SiO$_2$ is found in the formation and transported through the pipelines. Other inorganic deposits include corrosion products such as iron carbonates, iron sulphides, iron oxides, among others.[12] Scales are also common inorganic deposits which precipitate from produced water like calcium carbonate (CaCO$_3$), calcium sulphate, and barite sulphate (barite).[13]

One of the most common strategies for UDC mitigation is the use of chemical treatment to extend the lifetime of pipelines. Corrosion inhibitors play an essential role in the protection of carbon steel containing settled particles.[14] Inhibitor molecules are absorbed on metal surfaces, developing a protective barrier against corrosion. For instance, cationic-surfactants such as Cetyl pyridinium chloride monohydrate (CPC) and 1-Dodecyl pyridinium chloride hydrate (DPC) have been investigated to prevent UDC. DPC inhibitor particularly decreases corrosion dissolution by adsorbing at the bare metal surface creating a corrosion protective layer.[15] The increase of DPC concentration is known to alter the adsorbed aggregate morphology from hemispherical to cylindrical which lower corrosion rates at carbon steel surfaces.[16] Other groups of UDC inhibitors are the pyrimidine derivatives compounds such as 2-mercaptopyrimidine (MPY) which have been reported as highly effective in preventing corrosion at deposit-covered steel surfaces. MPY is a polar molecule with the S and N atoms being the negative and positive end of the dipole, respectively.[17] Reznik, et al.,[18] suggested that the performance of pyrimidine derivatives is related to the creation of strong surface complexes with the metal, modifying the cathodic and anodic reactions. The inhibition performance involves many factors that determine the ability of inhibitors to pass through the deposit layers. Thus, it is crucial to evaluate both inhibitor and deposit properties. The inhibitors' properties include the mechanism of inhibitor adsorption on steels, solubility in water and hydrocarbon phases, and inhibitors' adsorption on the different type of deposits or mixtures. The properties of a deposit determine the ability of inhibitors to penetrate to the steel surface include surface area, deposit thickness, and surface charge.[19] It is commonly believed that in optimal conditions an appropriate amount of inhibitor could be enough to provide corrosion protection. However, the presence of deposits can affect the efficiency of a corrosion inhibitor by reducing its availability at the steel surface. Indeed, Binks, et al.,[20] pointed out the importance of predicting the parasitic adsorption of inhibitors onto deposits which can lead to a decrease in inhibitor performance on the underlying metal surface.

Table 1. *Names, Abbreviation, Formulas, and Concentrations of Corrosion Inhibitors*

Inhibitor	Abbreviation	Chemical Formula	Concentration (mg/L)	Molar Concentration (mM)	CMC (mM)
Cetylpiridinium chloride monohydrate	CPC	$C_{21}H_{38}ClN \cdot H_2O$	100	0.279	0.006[A]
2-Mercaptopyrimidine 98%	MPY	$C_4H_4N_2S$	100	0.892	NA
1-Dodecylpiridinium chloride hydrate 98%	DPC	$C_{17}H_{30}ClN \cdot xH_2O$	100	0.352	0.211[A]

[A] CMC: Critical micelle concentration (CMC) determined by the pendant drop method. These results compare favorably to CMCs for CPC and DPC of 0.006 mM, and 0.211 mM, respectively, reported elsewhere.[16-17]

Table 2. *Properties of the Evaluated Deposits*

Deposit	Linear Formula	Supplier	Grain Size (µm)[A]	Bulk Density (g/cm³)[B]	Porosity (%)[C]	Thickness (mm)[D]
Silica sand	SiO_2	Sigma-Aldrich	300	1.45	27	8
Aluminum oxide	Al_2O_3	Sigma-Aldrich	24	0.89	67	13
Calcium carbonate (light)	$CaCO_3$	Chem-supply	3	0.32	80	25

[A] Grain size determined elsewhere.[17]
[B] Bulk density: the mass of deposit particles divided by the volume they occupy.
[C] Porosity: volume of the pores or interstices of the deposit, to the total volume of the mass.
[D] Thickness of 8 g of deposit above the steel and placed it into a holder.

Previous studies conducted by Pandarinathan, et al.,[17] evaluated the effect of silica sand on the performance of MPY and DPC on carbon steel surfaces. In the present study, the work has been extended to determine if the presence of Al_2O_3 and $CaCO_3$ can affect corrosion inhibitor efficiency on carbon steel surfaces under a CO_2 environment. The adsorption properties of CPC were also evaluated, but this inhibitor was excluded from further corrosion tests due to its strong adsorption on the deposit materials. UV spectroscopy was used to measure inhibitor adsorption onto these materials. This technique has been proven in previous studies as a simple but robust tool to determine inhibitor residuals after adsorption on minerals.[17,21] In this work, results from adsorption test were linked to corrosion inhibition efficiency assessed by potentiodynamic polarization measurements. This research aimed to gain insight into the understanding of inhibitors performance on carbon steel surfaces covered with deposits of different properties, such as mineral type, surface charge, porosity, and particle size.

EXPERIMENTAL

2.1 | Test Materials

The inhibited solutions were prepared in a brine that consisted of 3% sodium chloride NaCl (Chem-supply[†] analytical grade, 99.9%) and 0.01% sodium hydrogen carbonate $NaHCO_3$ (Chem-supply[†], analytical grade 99.7%). These salts were dissolved in ultra-pure water Milli-Q[†] system with resistivity 18.2 MΩ·cm. Subsequently, the brine was saturated with dissolved CO_2 by sparging for 2 h and adding a corrosion inhibitor. Corrosion inhibitors were supplied from Sigma-Aldrich[†]; their information is displayed in Table 1. The properties and general information of the deposits tested are shown in Table 2. The particle size porosity and bulk density of each deposit were measured elsewhere.[12,22] The chemical composition of the carbon steel (1030) used for the tests is as follows (wt%):

C (0.37%), Mn (0.80%), Si (0.282%), P (0.012%), S (0.001%), Cr (0.089%), Ni (0.012%), Mo (0.004%), Sn (0.004%), Al (0.01%), and Fe (balance).

2.2 | UV-Spectrophotometry

UV-spectrophotometry was used to evaluate the adsorption of corrosion inhibitors on deposits. Initially, a calibration curve was created using inhibited solutions over a concentration range of 10 ppm through 200 ppm. The correlation coefficient (R^2) values were as a follows 0.9999, 0.9934, and 0.9998 for MPY, DPC, and CPC, respectively, showing an acceptable calibration. Inhibitor adsorption was performed by mixing 8 g of a mineral with 100 mL of inhibited test solutions (100 mg/L) in glass bottles. The bottles were then sparged with CO_2 for 2 h, capped and kept at 30°C with stirring for 24 h or 48 h to allow inhibitor adsorption to occur. Stirring and temperature were achieved using a Ratek[†] orbital shaker-incubator at 150 rpm. After each adsorption period, the total content was centrifuged twice at 3260× g for 40 min to remove mineral particles from the solution before UV analysis. The pH of the inhibited solutions was measured before and, after deposits addition (for each adsorption period). The absorbances were recorded at a wavelength range of 230 nm through 300 nm using a JASCO V-670 UV-Vis[†] spectrophotometer. The amount of corrosion inhibitor adsorbed after each adsorption time was determined from the calibration curve. The reduction of inhibitor concentration corresponded to the amount of inhibitor adsorbed in mg/g (q_{ads}) on the mineral and was calculated using the following equation:[23]

$$q_{ads} = \frac{(C_i - C_f) \times V}{M} \qquad (1)$$

where C_i corresponds to the inhibitor concentration before deposit addition in mg/L = 100 mg/L, C_f is the final inhibitor concentration in the solution after contact with deposits, V is the volume of the test solution in liters = 0.1 L, and M is the mass of the deposits in grams = 8 g.
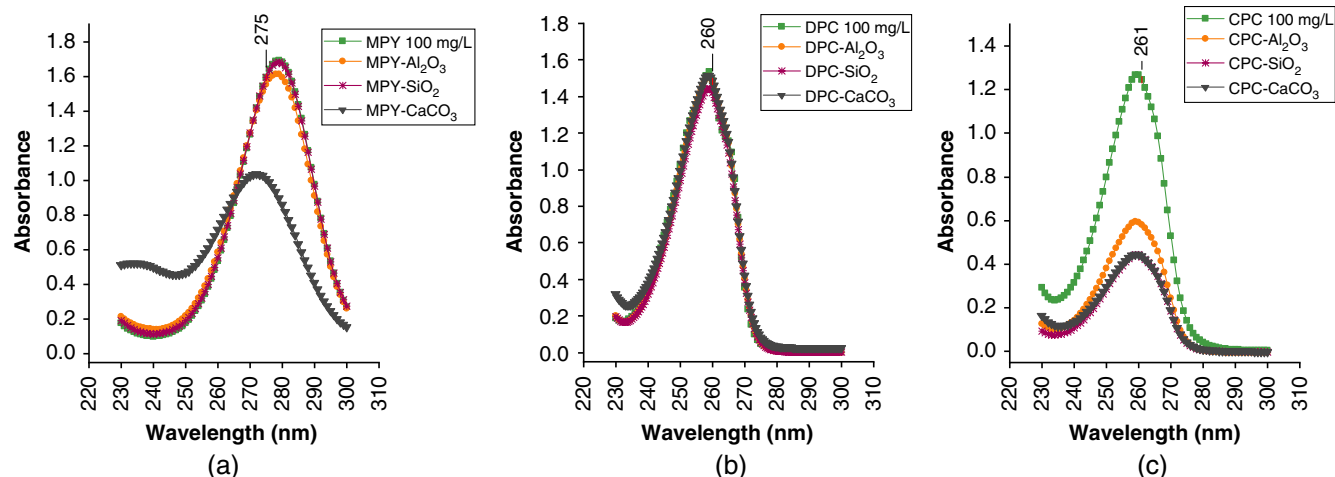
† Trade name.

FIGURE 1. *UV absorbance spectra of inhibited solutions after 48 h adsorption period on mineral deposits at 30°C in a CO₂ environment. Each set of the test includes the spectrum for the inhibited solutions (without deposit present) at 100 mg/L.*

The CMC of the surfactant corrosion inhibitors CPC and DPC was determined by the pendant drop method using KSV CAM 200 goniometer and is included in Table 1.

2.3 | Electrochemical Measurements

Carbon steel samples were prepared as working electrodes by electro-coating with Powercron 6000cx[†] and embedding in epoxy resin (Epofix[†]), leaving 0.785 cm[2] of the steel surface exposed. Subsequently, the surface area was ground to 1200 grit finish (SiC paper), washed with ethanol and dried with N₂. The sample mounted in the resin was coupled with a holder which was filled with 8 g of each deposit and, thus covering the entire sample surface with a uniform deposit layer. The reference electrode was a single junction Ag/AgCl electrode placed into a capillary with a porous ceramic tip (filled with 3 M KCl), and a 3.5-mm diameter rod of Hastelloy C[†] was used as a counter electrode. The capillary and the tip of the capillary was placed in close proximity to the steel surface within the deposit layer in order to minimize errors due to IR drop.[17] The assembled electrochemical cells were deoxygenated using N₂ gas for 15 min before contact with the solution. The inhibited solutions containing 100 mg/L of each inhibitor were sparged with CO₂ for 2 h. Then, dissolved oxygen was measured to ensure <20 ppb oxygen in the inhibited solutions before their transfer into the test cell. Afterward, 100 mL of the solution was pumped into the deaerated cell, using a low gas permeability TYGON®[†] tubing. The test temperature was set at 30°C using an IKA RTC[†] digital hotplate under thermocouple control and, the CO₂ flow was maintained for the total immersion period.

Electrochemical measurements were performed using a Gamry Reference 600[†] potentiostat (Gamry Instruments, Inc.). Ten linear polarization resistance (LPR) measurements were recorded within the 24 h of immersion period. The LPR measurements were performed using a potential perturbation of ±10 mV$_{OCP}$ and a scan rate of 0.1667 mV/s with an initial potential of −10 mV. The corrosion rates from LPR measurements were calculated assuming the Stern-Geary constant of 26 mV.[24] Potentiodynamic curves were recorded after 24 h of immersion and LPR measurements had been completed. They were performed with an initial potential of −0.25 V scanning through to + 0.25 V$_{OCP}$ at a scan rate of 0.1667 mV/s.

A total of 12 electrochemical tests, that included the LPR measurements followed by potentiodynamic scans, were performed to investigate UDC and the performance of MPY and DPC corrosion inhibitors. Tests conditions were as follows: (1) a blank, bare steel in un-inhibited test solution; (2) SiO₂, Al₂O₃, and CaCO₃ deposit-covered steel in uninhibited test solution; (3) bare steel in MPY and DPC inhibitor test solutions; and (4) SiO₂, Al₂O₃, and CaCO₃ deposit-covered steel in MPY and DPC test solutions. During the test period, the solutions were continuously sparged with CO₂ gas.

RESULTS AND DISCUSSION

3.1 | Inhibitors Adsorption on Mineral Deposits by UV-Spectrophotometry

Figures 1(a), (b), and (c) display the UV spectra of inhibited solutions, MPY, DPC, and CPC, respectively, after 48 h adsorption on Al₂O₃, SiO₂, and CaCO₃ mineral deposits. Spectra of each inhibitor solution (100 mg/L), without the deposit, is also included in these figures. The wavelength of maximum adsorption for the inhibitors was MPY 275 nm, DPC 260 nm, and CPC 261 nm. Table 3 shows the amount of inhibitor absorbed (q$_{ads}$), as a function of contact time (24 h and 48 h), for each mineral, obtained from UV absorbance intensities, measured at the maximum absorbance wavelength (λ$_{max}$). Figure 2 shows the final inhibitors concentrations after contact with deposits. DPC results revealed minimal adsorption of this inhibitor on all deposits. After 48 h of the contact period, DPC concentration in the presence of Al₂O₃ and CaCO₃ was 97.41 mg/L and 97.66 mg/L, respectively.

The concentration of MPY only slightly decreased in the presence of SiO₂ and Al₂O₃. However, in the presence of CaCO₃, the inhibitor concentration was significantly reduced resulting in 60.07 mg/L at 24 h and 59.25 mg/L at 48 h contact periods. These results indicate that the MPY inhibitor has a high affinity for the CaCO₃ deposit reducing its amount considerably in the solution. A possible explanation for this high adsorption of MPY on CaCO₃ is that MPY is oppositely charged compared to CaCO₃. Pandarinathan, et al.,[17] stated that MPY had a strong electronegative sulphur atom (absorption center) which had less attraction to surfaces charged negatively like silica sand. Calcium carbonate surface, on the other hand, carries a stable positive charge in this acidic environment.[25] It is worth mentioning that the spectrum of MPY inhibitor with CaCO₃ deposit had a slight

Table 3. *Adsorption of Corrosion Inhibitors on Mineral Deposits After 24 h and 48 h Assessed by UV-Visible Spectrophotometry*[A]

Initial Inhibitor Concentration (C$_i$) (mg/L)	Exposure Time (h)	pH	Absorbance (λ$_{max}$)	Inhibitor Absorbed (q$_{ads}$) (mg/g)[B]	Percentage Adsorption (%)
CPC 100 ppm (λ$_{max}$ 1.27) pH: 4.78	Al$_2$O$_3$-24 h	4.85	0.60	0.66	53.0
	Al$_2$O$_3$-48 h	4.84	0.59	0.67	53.5
	CaCO$_3$-24 h	6.52	0.41	0.85	68.3
	CaCO$_3$-48 h	6.45	0.41	0.85	68.3
	SiO$_2$-24 h	4.92	0.48	0.78	62.6
	SiO2-48 h	4.95	0.44	0.82	65.4
DPC 100 ppm (λ$_{max}$ 1.69) pH: 4.81	Al$_2$O$_3$-24 h	4.93	1.53	0.01	0.8
	Al$_2$O$_3$-48 h	4.99	1.51	0.03	2.6
	CaCO$_3$-24 h	6.79	1.53	0.02	1.3
	CaCO$_3$-48 h	6.19	1.51	0.03	2.3
	SiO$_2$-24 h	4.84	1.49	0.05	3.6
	SiO2-48 h	4.87	1.45	0.09	6.9
MPY 100 ppm (λ$_{max}$ 1.69) pH: 4.77	Al$_2$O$_3$-24 h	4.91	1.65	0.08	6.7
	Al$_2$O$_3$-48 h	4.86	1.65	0.08	6.8
	CaCO$_3$-24 h	6.14	1.07	0.50	39.9
	CaCO$_3$-48 h	6.26	1.05	0.51	40.7
	SiO$_2$-24 h	4.91	1.69	0.06	4.5
	SiO2-48 h	4.86	1.66	0.07	6.0

[A] The table also includes pH values of the inhibited solutions before and after 24 h and 48 h contact with deposits.
[B] q$_{ads}$ amount of inhibitor absorbed in mg/g of mineral.
Equation: (C$_i$-C$_f$) x V/M Ci initial inhibitor concentration,
C$_f$ final inhibitor concentration = volume of solution in L,
M = mass of mineral.
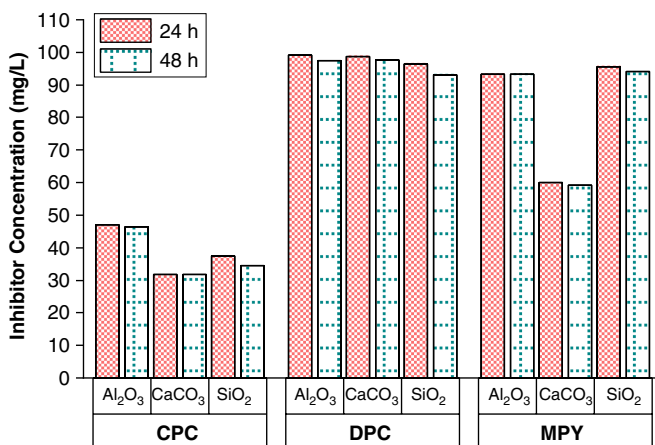
FIGURE 2. *Final inhibitors concentration after 24 h and 48 h adsorption period on mineral deposits at 30°C in a CO$_2$ environment. The initial concentration of the inhibited solution (100 mg/L).*

shift in wavelength (Figure 1[a]). A possible explanation for this shift is that the supernatant in the inhibited solution remained slightly turbid after contact with CaCO$_3$. This observation suggests that there was an incomplete separation of the mineral from the test solution even after the high-speed centrifugation.

CPC was the inhibitor which was most adsorbed onto all of the deposits at both contact times. Whereas the other surfactant molecule, DPC was not significantly adsorbed. The reason for the different adsorption could be related to the difference in the alkyl chain length between the DPC (C$_{12}$) and CPC (C$_{16}$). The length of the alkyl chain has a significant influence on their critical micelle concentration (CMC). The CMC for CPC is about thirty times less than DPC in the test solution used in this investigation. This means there would be an appreciably greater number of CPC micelles compared to DPC micelles in solution. It is generally recognized that micelles or agglomerated molecules are more easily adsorbed on to solid materials than single molecules. It is postulated that the greater adsorption of CPC is due to the larger number of micelles present and their greater affinity to adsorb to mineral surfaces. CPC was not investigated for preventing UDC because of its strong adsorbance to the mineral deposits and similar chemical molecular properties to DPC. This inhibitor also has shown poor performance on sand deposit-covered carbon steel recording corrosion rate of 0.43 mm/y after 72 h contact with this cationic surfactant.[17] Therefore, the authors selected the best performing inhibitors compounds for further evaluation in the presence of different deposits.

Regarding the effect of pH in the bulk solution, it is known to be an important influential parameter in the corrosion process of bare carbon steel surfaces under CO$_2$ conditions.[26-27] However, previous studies demonstrated that the bulk solution pH did not affect the CO$_2$ corrosion of mild steel in the presence of mineral deposits. The authors also founded higher surface pH values beneath the silica sand, SiO$_2$ powder and glass beads than the bulk solution suggesting different water chemistry within
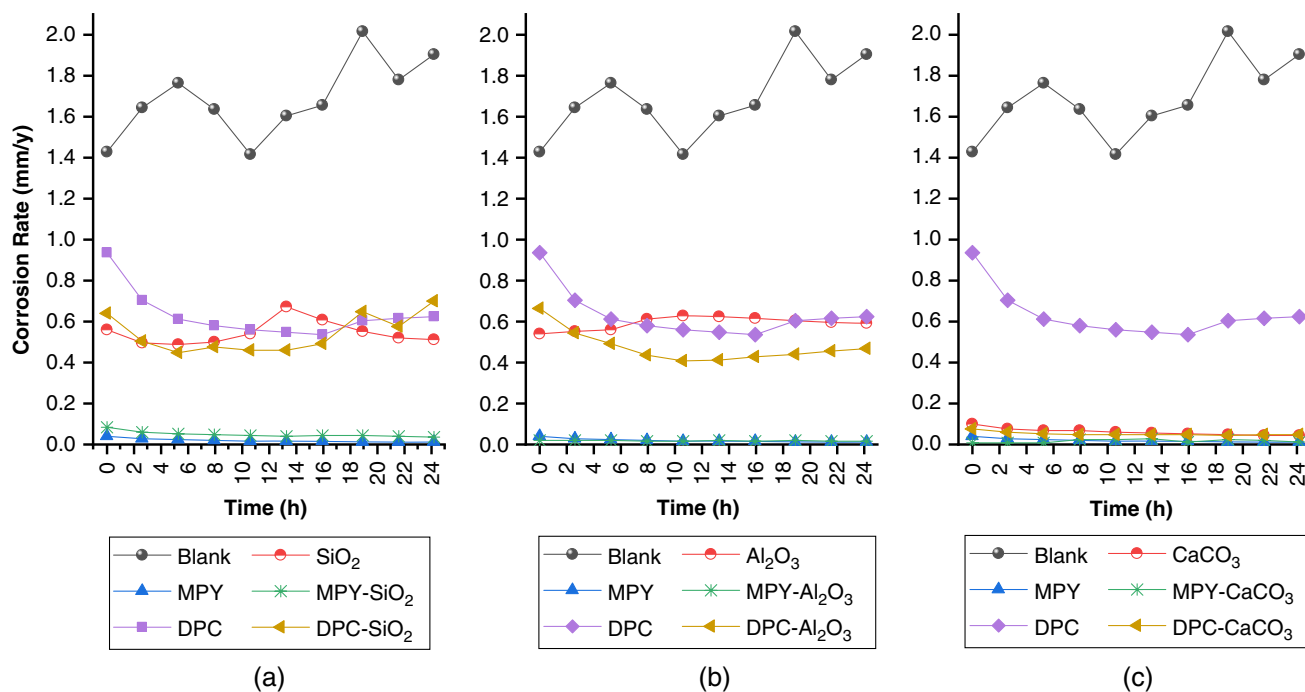
FIGURE 3. *Corrosion rates of deposit-covered carbon steel surfaces determined by LPR measurements during 24 h immersion in CO_2-inhibited and uninhibited solutions. Deposits: silica sand (SiO_2), aluminum oxide (Al_2O_3), and calcium carbonate ($CaCO_3$). Blank is a specimen of bare or nondeposited steel in uninhibited test solution (3% NaCl, 0.01% $NaHCO_3$, saturated with CO_2).*

or underneath the deposit layers.[22] Although, in the present study, the pH of the inhibited test solutions in contact with $CaCO_3$ had a higher pH >6 when compared to the pH values <5 in the presence of SiO_2 and Al_2O_3 (Table 3). It is not possible to infer that the pH in bulk could directly affect the corrosion process in the underlying steel surfaces covered with these mineral deposits.

3.2 | Corrosion Monitoring by Linear Polarization Resistance Measurements

Figure 3 shows corrosion rates monitored over 10 LPR measurements taking during 24 h immersion for all of the 12 experimental conditions. Figure 3(a) gives the results for (1) the blank or bare steel in an uninhibited test solution, (2) DPC and bare steel, (3) MPY and bare steel, (4) SiO_2 deposit-covered steel, (5) MPY and SiO_2 deposit-covered steel, and (6) DPC and SiO_2 deposit-covered steel. Figure 3(b) shows the results for (1) the blank or bare steel in an uninhibited test solution, (2) DPC and bare steel, (3) MPY and bare steel, (4) Al_2O_3 deposit-covered steel, (5) MPY and Al_2O_3 deposit-covered steel, and (6) DPC and Al_2O_3 deposit covered steel. Figure 3(c) shows the results for (1) the blank or bare steel in an uninhibited test solution, (2) DPC and bare steel, (3) MPY and bare steel, (4) $CaCO_3$ deposit covered steel, (5) MPY and $CaCO_3$ deposit-covered steel, and (6) DPC and $CaCO_3$ deposit-covered steel.

In general, the corrosion rates remained reasonably constant throughout the experimental period (24 h) except for the DPC test without a deposit. The first LPR measurement (1 h immersion) recorded a corrosion rate of 0.94 mm/y and the last measurement (24 h) a corrosion rate of 0.62 mm/y. This indicates that a minimum of 6 h contact of DPC is needed to protect the bare steel against corrosion. It is also a good indication of the low rate at which this cationic surfactant adsorbs onto bare steel surfaces to form an assembled protective film. The reduction of the uninhibited corrosion rate from 1.5 mm/y to 2 mm/y for the blank

solution to 0.62 mm/y in the presence of DPC demonstrates the relatively poor performance of DPC as a corrosion inhibitor.

DPC did not demonstrate good performance in preventing UDC at Al_2O_3 (Figure 3[b]) and SiO_2 (Figure 3[a]) deposit-covered surfaces. Under these deposits, DPC solutions achieved maximum inhibition after 6 h immersion, followed by a steady-state inhibition period until approximately the 16th hour. Afterward, the corrosion rates increased reaching values of 0.47 mm/y for Al_2O_3 and 0.70 mm/y for SiO_2 after 24 h of immersion. The $CaCO_3$-deposit-covered steel surface recorded the least corrosion rates <0.1 mm/y in DPC-test solution.

In contrast, MPY was shown to be highly efficient on the bare surface with corrosion rate values below 0.04 mm/y during the immersion period. MPY was also very effective in reducing UDC as can be seen in Figures 3(a) through (c) where the corrosion rates for all of the deposits was below 0.05 mm/y after 6 h. At 24 h the corrosion rates reached 0.037 mm/y, 0.015 mm/y, and 0.012 mm/y, respectively, under SiO_2, Al_2O_3, and $CaCO_3$ deposits demonstrating the superior performance of this heterocyclic molecule.

Concerning the effect of the deposits on carbon steel corrosion, it can be seen that all deposit-covered steel surfaces, in the absence of inhibitor, had lower corrosion rates when compared with the bare steel (Figures 3[a] through [c]). Al_2O_3 had the highest average corrosion rates (0.59 mm/y) Figure 3(b) followed very close by SiO_2 (0.51 mm/y) Figure 3(a). The least corrosive was $CaCO_3$ deposit with corrosion rates values <0.1 mm/y Figure 3(c).

3.3 | Potentiodynamic Polarization Measurements (Tafel Plots)

As mentioned earlier, only DPC and MPY inhibitors were selected for electrochemical measurements due to their low adsorption on most mineral deposits (inhibitors adsorption

results). Figures 4(a) through (f) display the potentiodynamic curves recorded after 24 h of immersion for each experimental condition described in the Experimental section (Electrochemical Measurements). The diagrams in the figures are arranged as follows: Figures 4(a), (c), and (e) show the performance of MPY in the presence and absence of SiO₂, Al₂O₃, and CaCO₃ deposits. Figures 4(b), (d), and (f) give corresponding potentiodynamic

curves for DPC. Curves for SiO_2, Al_2O_3, and $CaCO_3$ deposits without inhibitor present are also provided in respective, applicable figures. The blank curve recorded for bare steel exposed in the uninhibited test solution (CO_2 saturated 3% NaCl, 0.01% $NaHCO_3$) is also provided in each figure. This enables the relevant effect of the inhibitor and the deposit on the corrosion process to be observed or compared. Table 4 shows the
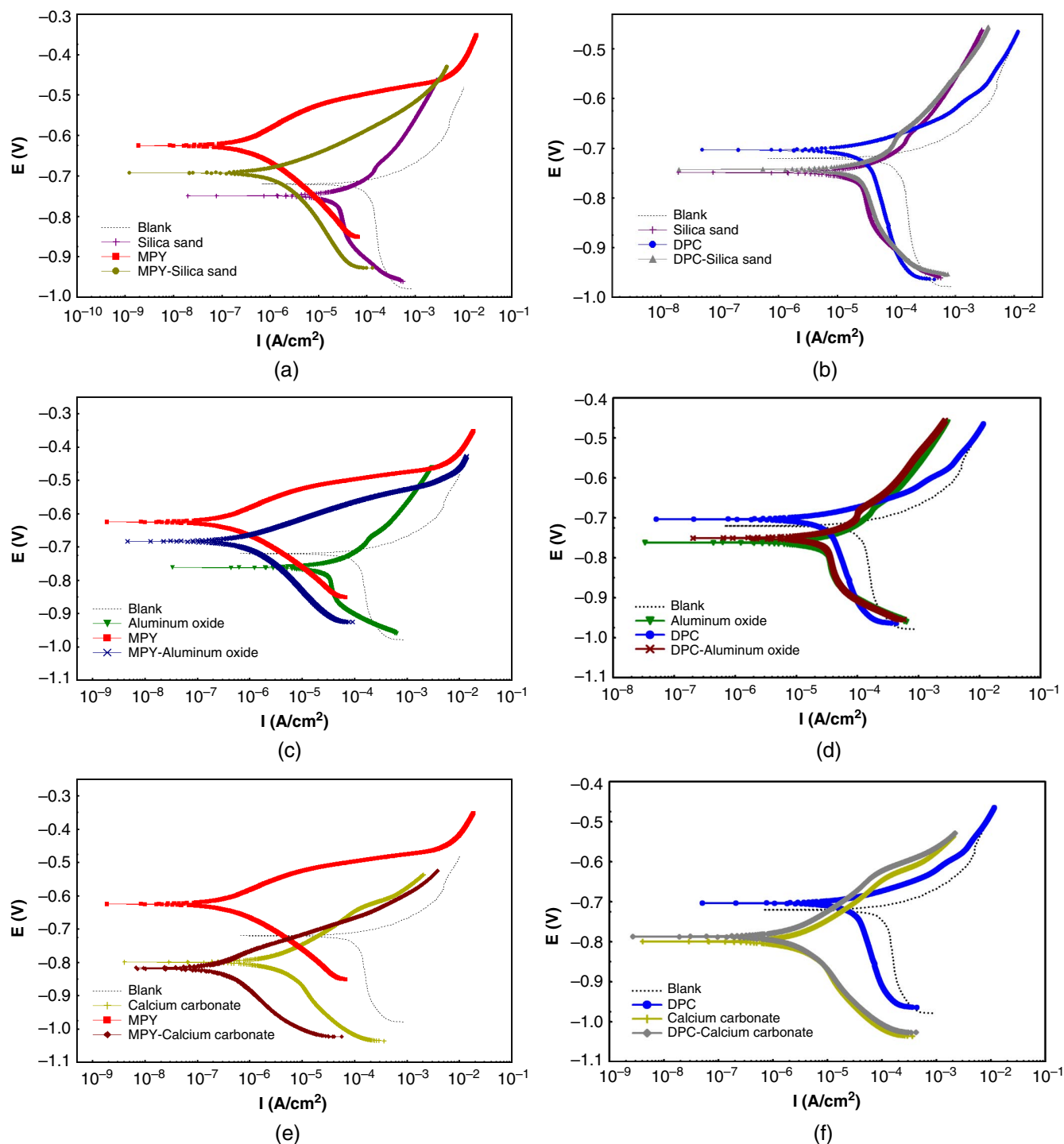
FIGURE 4. *Potentiodynamic polarization curves recorded at bare and deposit-covered-steel surfaces in uninhibited and inhibited solutions (100 mg/L) at 30°C after 24 h immersion period under CO_2 environment. Combinations of (a) silica sand and MPY, (b) silica sand and DPC, (c) aluminum oxide and MPY, (d) aluminum oxide and DPC, (e) calcium carbonate and MPY, and (f) calcium carbonate and DPC. In each figure, a blank, the potentiodynamic curve recorded for bare steel exposed in uninhibited test solution has been included for a comparative purpose.*

Table 4. *Electrochemical Parameters of the Carbon Steel Derivated from Potentiodynamic Polarization Measurements in Figure 4*

Test	βa (V/dec)	−βc (V/dec)	E_{corr} ($V_{Ag/AgCl}$)	i_{corr} ($\mu A/cm^2$)	v_{corr} (mm/y)
Blank[A]	0.08	0.92	−0.73	122.53	1.42
SiO_2	0.11	0.47	−0.75	24.68	0.29
Al_2O_3	0.12	0.50	−0.77	28.98	0.34
$CaCO_3$	0.10	0.18	−0.79	3.41	0.04
MPY	0.06	0.07	−0.62	0.22	<0.01
MPY-SiO_2	0.05	0.12	−0.69	1.23	0.01
MPY-Al_2O_3	0.05	0.09	−0.68	0.51	<0.01
MPY-$CaCO_3$	0.06	0.14	−0.81	0.32	<0.01
DPC	0.05	0.41	−0.70	31.25	0.36
DPC-SiO_2	0.11	0.32	−0.75	23.72	0.28
DPC-Al_2O_3	0.12	0.44	−0.76	27.92	0.32
DPC-$CaCO_3$	0.09	0.14	−0.78	2.10	0.02

[A] Blank is bare steel electrode exposed to the uninhibited test solution.
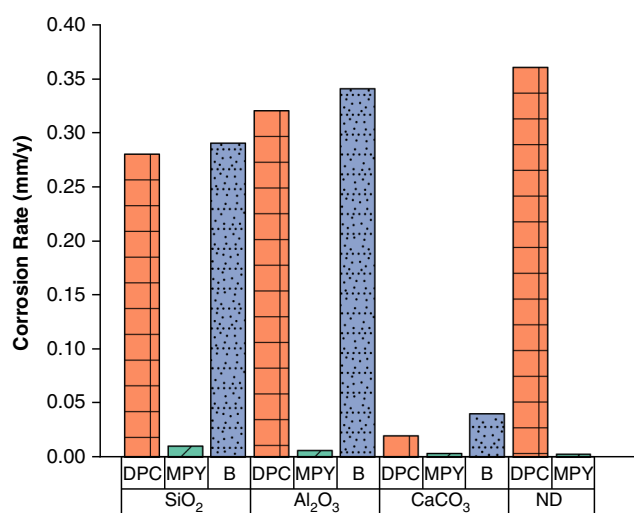
FIGURE 5. *Corrosion rates calculated from potentiodynamic measurements after 24 h of immersion period. B: deposit-covered steel in uninhibited solution. ND: no deposits.*

electrochemical parameters, such as corrosion potential (E_{corr}), corrosion current density (i_{corr}), and Tafel constants (βa, βc) obtained from the potentiodynamic polarization measurements.

3.4 | Effect of Deposits on Corrosion of Carbon Steel (Tests in Uninhibited Solutions)

It can be seen in Figures 4(a), (c), and (e), Table 4 and Figure 5 that the deposits had a favorable effect on reducing i_{corr} and the average corrosion rate. Compared to the blank or undeposited or bare steel, the corrosion rate was reduced from 1.42 mm/y to 0.29 mm/y, 0.34 mm/y, and 0.04 mm/y in the presence of SiO_2, Al_2O_3, and $CaCO_3$, respectively (Table 4). The deposits also shifted the corrosion potential to more negative values in the order of −20 mV, −40 mV, and, −60 mV for SiO_2, Al_2O_3, and $CaCO_3$, respectively. Generally speaking the overall shapes of the anodic and cathodic curves for SiO_2 and Al_2O_3

deposit-covered steel remained similar to the blank. In the case of $CaCO_3$, there was a more noticeable change in the shape of the cathodic curve (Figure 4[e]) and reduction in corrosion rate (Figure 4[e] and Table 4). This can be attributed to the alkaline nature of the $CaCO_3$ resulting in an increase in pH at the surface and the electrolyte in the pores of this deposit resulting in a dramatic reduction in the average corrosion rate to 0.04 mm/y. The surface pH and the electrolyte in the pores of the $CaCO_3$ deposit would be higher than the bulk solution (pH 6.65) which was buffered by the continual sparge of CO_2 gas. These results are in general agreement with the deposits having a blocking effect in reducing the rate of mass transfer of corroding species (H_2CO_3 and H^+) to the steel surface. This reduction in mass transfer can also cause the interfacial pH to increase resulting in a negative shift in the corrosion potential and reduction in corrosion rate. Huang, et al.,[22] and Pandarinathan, et al.,[12] stated that inert deposits provide a barrier to the mass transfer of corrosive species and a reduction in average corrosion rates. The cathodic and anodic curves recorded for bare steel in Figure 4 are typical for CO_2 corrosion of steel. In the case of the cathodic reaction, the reaction goes from kinetic or charge transfer control to mixed control and mass transfer control as the polarization increases negatively from the corrosion potential. It is difficult to obtain a Tafel slope measurement as there is no extended Tafel region. Nevertheless, the β_c values given in Table 4 provide a guide to the macroscopic changes in Tafel behavior. Drawing a comparison between oxygen and CO_2 corrosion is interesting. In the case of oxygen corrosion, the area under a deposit (deoxygenated region) behaves as the anode while the area outside of the deposit (oxygen-rich region) behaves as the cathode. CO_2 corrosion of steel has the opposite effect, at least early in the corrosion process. The areas under the deposit behave as the cathode (shifted to a more negative potential) while areas of bare steel outside the deposit undergoes a greater rate of corrosion. It is, however, emphasized, that with time, localized anodes and cathodes can develop under deposits resulting in pitting or localized forms of corrosion.

In relation to the corrosive behavior under each deposit, values given in Table 4 and Table 5 indicate that Al_2O_3 produced

the highest average corrosion rate of 0.34 mm/y followed by SiO_2 with 0.29 mm/y and $CaCO_3$ with only 0.04 mm/y. These corrosion rates are lower than those obtained from LPR measurements, namely 0.59 mm/y for Al_2O_3, 0.51 mm/y for SiO_2 and <0.1 mm/y for $CaCO_3$. The difference is probably due to errors incurred extrapolating the Tafel region back to the corrosion potential. The corrosiveness of Al_2O_3 deposit under CO_2 ambience has been previously associated with a low pH developing underneath of the deposit as a result of its hydrolysis.[12] Huang, et al.,[22] on the other hand, correlated high deposit porosity with high corrosion rates. In the present study, porosities of Al_2O_3 (67%) and, SiO_2 (27%) cannot be associated with an order of corrosivity as $CaCO_3$ had the highest porosity (80%) and yet it was the least corrosive. As discussed earlier, the most likely reason for the low corrosion rates measured in the presence of calcium carbonate (Table 4) is the alkaline nature of this mineral. Naturally, calcium carbonate precipitates in the crystalline forms of calcite, aragonite, vaterite, calcium carbonate monohydrate, and calcium carbonate hexahydrate. However, calcite is the only thermodynamically stable form under normal conditions.[28] Patra, et al.,[25] stated that the surface Ca^{2+} and CO_3^- ions could undergo hydrolysis in acidic solutions making the mineral more positive and the solution more alkaline. The pH of calcite is approximately 9.9, and it and other crystalline forms of $CaCO_3$ would, therefore, increase the pH at the steel surface. In the presence of CO_2 the solubility of $CaCO_3$ can increase due to the formation of more soluble calcium bicarbonate by the following reaction:

$$CaCO_3 + H_2O + CO_2 \rightarrow Ca(HCO_3)_2 \rightarrow Ca^{2+} + 2HCO_3^- \quad (2)$$

The overall effect would be for the carbonate and bicarbonate to increase pH at the steel surface.

3.5 | Corrosion Inhibitors Performance on Bare and Deposit-Covered Steel Surfaces (Tests with Inhibited Solutions)

It is acknowledged that there are several testing methods to evaluate inhibitors performance in the presence of deposits. Each model differs in the design and thus, assess this UDC phenomenon and its mitigation in different ways.[29] For instance, multielectrode arrays systems have been used the study inhibitor efficiency at the bare and deposit-covered steel surfaces allowing to visualize electrochemical differences beneath and outside the deposit[30] or in precorroded systems.[31] In this study, however, the inhibition performance was evaluated at carbon steel surfaces completely covered with a sand deposit. Previous studies have used this configuration to evaluate UDC inhibition, where it was founded electrochemical differences compared to bare steel surfaces.[17] It can be seen in Table 4 that the inhibitors, when there was no deposit present, caused the corrosion potential to shift positively. This was particularly noticeable with MPY where the corrosion potential changed from −0.73 V to −0.62 V or +110 mV (Table 4). The shift in corrosion potential with DPC was less positive, i.e., from −0.73 mV to −0.70 mV or +30 mV.

In the presence of silica sand and aluminum oxide, MPY still caused the corrosion potential to shift positively. However, this was not the case with calcium carbonate where the potential was negative relative to the corrosion potential of bare steel in uninhibited solution. With DPC the corrosion potential was negative relative to the blank in all cases when there was deposit present.

As discussed in the Section Effect of Deposits on Corrosion of Carbon Steel (Tests in Uninhibited Solutions), the mass transfer limited region of the cathodic curve for CO_2 corrosion of steel (blank Figures 4[a] through [f]) is classical of CO_2 corrosion of carbon steel. In the presence of MPY, the corrosion process became more kinetically or charge transfer controlled. This can be seen in Figures 4(a), (c), and (e), whereby comparison to the blank, the mass transfer region of the cathodic curve has disappeared to demonstrate greater Tafel behavior or a better linear relationship between the logarithm of current and voltage. The influence of DPC on the cathodic curve for CO_2 corrosion, however, was not marked. In the presence of SiO_2 and Al_2O_3 deposits, the mass transfer cathodic region was still evident. However, as outlined in Table 4, it was a slight decrease in βc values from 0.41 V/dec in the DPC test to 0.32 V/dec in DPC-SiO_2 test. Similarly, a small change was observed in the presence of Al_2O_3 deposit where the βc values increase from 0.41 V/dec in DPC test to 0.44 V/dec in DPC-Al_2O_3 test. Calcium carbonate, due to its alkaline nature reflected in the bulk pH 6.79 (Table 3), affected the kinetics of both the anodic and cathodic reactions as can be observed in Figures 4(e) and (f) with the changes in Tafel slopes.

All tests with MPY present exhibited the lowest corrosion rate of ≤0.01 mm/y (Table 4) indicating that this inhibitor provides the highest corrosion protection at bare and deposit-covered carbon steel. It can be seen in Figures 4(a), (c), and (e) and Table 4 that at surfaces covered with SiO_2 and Al_2O_3, the addition of MPY shifted the corrosion potential more positively by +40 mV and +0.50 mV respectively compared to the blank. For $CaCO_3$, on the other hand, the potentials shifted more negatively by −0.80 mV compared to the blank. With MPY the overall shape of the anodic and cathodic polarization curves for bare steel remained the same in the presence of a deposit (Figures 4[a], [c], and [e]). This indicates that MPY can penetrate the deposit and influence the surface of the steel similarly to when no material was present.

On the contrary, DPC had little influence on the overall shape of the anodic and cathodic curves compared to the blank and those recorded in the presence of SiO_2 and Al_2O_3 deposits (Figures 4[b] and [d]). $CaCO_3$ however, due to its alkalinity had a marked effect on the shape of the anodic and cathodic curves (Figure 4[f]). As mentioned earlier, DPC caused the corrosion potential of bare steel (blank) to shift positively by only 30 mV (Table 4). The influence of the deposits on the corrosion potential was dominant over the inhibitor. In the presence of DPC, SiO_2 shifted the corrosion potential negative by −20 mV, Al_2O_3 by −30 mV and $CaCO_3$ by −50 mV (Figures 4[b], [d], and [f] and Table 4). It can be seen in Table 4 that DPC was not effective in reducing the corrosion of bare steel and deposit covered steel surfaces compared to MPY.

3.6 | Correlation Between Inhibitors Adsorption and Corrosion Inhibition Performance

The presence of mineral deposits in a system can affect the corrosion inhibitors effectiveness in different ways. De Reus, et al.,[19] suggested that the inhibitors penetration or diffusion rate of inhibitors to go through deposits layers can be influenced by some features of deposits e.g., porosity, layer thickness, surface area, and nature of the deposit including surface charge of the particles. In addition, the concentration of can be depleted by adsorption on mineral deposits.[20] In this study, the low percentage adsorption of DPC on the deposits shown in

172

Table 5. *Sequences of Inhibitor Adsorption on Deposits, Deposit Corrosivity and Porosity, and Corrosion Inhibition Efficiency at Carbon Steel Surfaces Under CO_2 Conditions*

Inhibitors Adsorption	Most Adsorbed → Least Adsorbed								
	$CPC\text{-}CaCO_3$	$CPC\text{-}SiO_2$	$CPC\text{-}Al_2O_3$	$MPY\text{-}CaCO_3$	$MPY\text{-}Al_2O_3$	$DPC\text{-}SiO_2$	$MPY\text{-}SiO_2$	$DPC\text{-}CaCO_3$	$DPC\text{-}Al_2O_3$
Corrosion Inhibition Efficiency	Highest → Lowest								
	$MPY\text{-}CaCO_3 = MPY\text{-}Al_2O_3$			$MPY\text{-}SiO_2$	$DPC\text{-}CaCO_3$	$DPC\text{-}SiO_2$	$DPC\text{-}Al_2O_3$		
Deposit Corrosivity	Highest → Lowest								
	Al_2O_3	SiO_2	$CaCO_3$						
Deposit Porosity	Highest → Lowest								
	$CaCO_3$	Al_2O_3	SiO_2						

Table 3 indicates that these deposits would have little impact on the concentration of DPC. The corrosion rate recorded at the bare surface with DPC was 0.36 mm/y compared to the surfaces covered SiO_2, Al_2O_3, and $CaCO_3$ with values of 0.28 mm/y, 0.32 mm/y, and 0.02 mm/y respectively. That is, in the case of silica and aluminum oxide deposits the corrosion rates were not significantly different from bare steel. In the case of calcium carbonate, the significant reduction in corrosion rate is due to the nature and inherent inhibitor properties of this material. According to these results, the depletion of DPC by absorption on to the deposits was not the critical reason for its relatively poor performance in preventing UDC.

In contrast, MPY provided superior inhibition efficacy in all tests (≤0.01 mm/y). In the test with $CaCO_3$, due to the alkaline nature of this material, the uninhibited corrosion rate was particularly low, i.e., 0.04 mm/y (Table 4). However, MPY was still able to lower the corrosion rate significantly to <0.01 mm/y, despite it being appreciably adsorbed (40.7% depletion) by $CaCO_3$. Results from this work indicate that MPY is as a good candidate for UDC mitigation despite the depletion that can occur in the presence of $CaCO_3$. However, it is worth pointing out that in terms of average corrosion rates, $CaCO_3$ was proven essentially no corrosive in this investigation. Reznik, et al.,[18] demonstrated high inhibition activity of pyrimidine compounds like MPY even in low concentrations (0.02 mg/L to 5 mg/L) suggesting that the efficiency is most probably connected with the chemisorption of inhibitor not on the whole surface but only on active centers. Evidently, the remaining MPY was able to effectively penetrate the settled deposit layers protecting the underlying steel surfaces. Durnie, et al.,[32] mentioned that the affinity of the inhibitor for the deposits and its ability to penetrate the deposit layers are determining parameters for inhibitors performance evaluation. Indeed, the author demonstrated that sulphur species were able to penetrate faster than some quaternary amines and imidazoline compounds. Different factors can influence inhibitors performance, and this includes the presence of deposits. For instance, Pandarinathan, et al., showed that inhibition mechanism of Thiobenzamide changed in the presence of sand deposit.[28] If deposits are present, it is recommended that UDC tests similar to those used in this study are integrated into the test program.

Table 5 summarizes the sequences of adsorption and inhibition performance tests as well as corrosivity of each deposit. Corrosion rates from polarization measurements follow the same order than the ones calculated from LPR measurements (last measurement at approximately 24 h immersion).

CONCLUSIONS

➢ Inhibitor adsorption measurements on Al_2O_3, SiO_2, and $CaCO_3$ mineral deposits using UV spectroscopy revealed that of the two surfactant corrosion inhibitors evaluated, CPC adsorbed substantially greater, from 53% to 68%, on these deposits at the concentration of 100 mg/L tested. On the other hand, DPC adsorbed only 0.8% to 6.9% (Table 3). It is postulated that the greater adsorption of CPC is related to its larger alkyl chain length (C16 as opposed to C12) and lower CMC.

➢ Adsorption of MPY on Al_2O_3 and SiO_2 was only 6.8% and 6.0%, respectively, however, in the presence of $CaCO_3$, it was about 41%. Despite the relatively high percentage adsorption on $CaCO_3$, MPY was shown to be a good inhibitor in preventing UDC with all three mineral deposits investigated. It appears to be a good candidate for preventing this type of corrosion.

➢ In uninhibited solution, the presence of a deposit significantly reduced the baseline corrosion rate measured for bare steel tested under similar conditions, for instance, in the presence of SiO_2, Al_2O_3, and $CaCO_3$ the corrosion rate was reduced from 1.42 mm/y to 0.29 mm/y, 0.34 mm/y, and 0.04 mm/y (Table 4). This reduction in corrosion rate is attributed to the obstruction caused by the deposit and reduction in the mass transfer of corrosive species to the metal surface. The dramatic reduction in corrosion rate caused by $CaCO_3$ (0.04 mm/y) is ascribed to the alkaline nature of this material increasing the pH on the steel surface and, in the bulk from pH ~4.8 to pH >6.1 before and after $CaCO_3$ addition, respectively.

➢ The influence of DPC in reducing the average corrosion rate under deposits was noticeably not much greater than the blockage caused by the deposit itself by diminishing the rate of mass transfer. In the presence of DPC the corrosion rates under, SiO_2, Al_2O_3, and $CaCO_3$ were 0.28 mm/y, 0.32 mm/y, and 0.02 mm/y, respectively. These results can be compared to the aforementioned values of 0.29 mm/y, 0.34 mm/y, and 0.04 mm/y, for deposit-covered steel without inhibitor present (Table 4).

➢ In contrast, MPY substantially reduced the corrosion rate under all of the deposits investigated, for example, in the presence of SiO_2, Al_2O_3, and $CaCO_3$ the corrosion rate was reduced from 0.29 mm/y to 0.01 mm/y, 0.28 mm/y to <0.01 mm/y and 0.04 mm/y to <0.01 mm/y, respectively.

➢ The influence of the deposits on UDC of the steel surface did not appear to be significantly related to their physical properties (Table 2). In the case of $CaCO_3$, the reduction in corrosion rate is most probably related to the chemical properties and alkaline nature of this material.

➢ A test protocol to prevent UDC is worth incorporating into a program to evaluate the effectiveness of inhibitors for controlling

CO$_2$ corrosion during oil and gas production when sand and deposits are present.

References

1. T. Esan, S.D. Kapusta, M.J.J. Simon-Thomas, "Case Study: Extreme Corrosion of a 20"-Oil Pipeline in the Niger Delta Region," CORROSION 2001, paper no. 01629 (Houston, TX: NACE, 2001).
2. A. Jenkins, D. MacDougall, "Mitigation of Under-Deposit and Weldment Corrosion with an Environmentally Acceptable Corrosion Inhibitor," CORROSION 2013, paper no. 2508 (Houston, TX: NACE, 2013).
3. Z. Liu, T. Jackson, P. Kearns, "Mechanistic Studies of Sour Underdeposit Corrosion in the Presence of Chemical Inhibition," CORROSION 2015, paper no. 5781 (Houston, TX: NACE, 2015).
4. R. Nelson, M.A. Edwards, P. Kovash, "Monitoring and Controlling Corrosion in an Aging Sour Gas Gathering System a Nine-Year Case History," CORROSION 2007, paper no. 07668 (Houston, TX: NACE, 2007).
5. J. Huang, B. Brown, Y.-S. Choi, S. Nešić, "Prediction of Uniform CO$_2$ Corrosion of Mild Steel Under Inert Solid Deposits," CORROSION 2011, paper no. 11260 (Houston, TX: NACE, 2011).
6. Y. Zhang, J. Moloney, S. Mancuso, "Understanding Factors Affecting Corrosion Inhibitor Performance in Under-Deposit Testing with Sand," CORROSION 2013, paper no. 2575 (Houston, TX: NACE, 2013).
7. W. Mosher, M. Mosher, T. Lam, Y. Cabrera, A. Oliver, H. Tsaprailis, "Methodology for Accelerated Microbiologically Influenced Corrosion in Under Deposits from Crude Oil Transmission Pipelines," CORROSION 2014, paper no. 4254 (Houston, TX: NACE, 2014).
8. K.T. Ly, D.J. Blumer, W.M. Bohon, A. Chan, "Novel Chemical Dispersant for Removal of Organic/Inorganic Schmoo Scale in Produced Water Injection Systems," CORROSION 1998 (Houston, TX: NACE, 1998).
9. J.R. Vera, D. Daniels, M.H. Achour, "Under Deposit Corrosion (UDC) in the Oil and Gas Industry: A Review of Mechanisms, Testing and Mitigation," CORROSION 2012 (Houston, TX: NACE, 2012), p. 3028-3040.
10. E.M. Suarez, K. Lepková, B. Kinsella, L.L. Machuca, *Int. Biodeteriorat. Biodegrad.* 137 (2019): p. 137-146.
11. Z. Zhenjin, W. Keith, J.T. Patrick, "Solid Deposition in Liquids Petroleum (Oil) and Wet-Gas Pipelines for Internal Corrosion Predictive Modeling (ICPM)," NACE Northern Area Western Conference (Houston, TX: NACE, 2010).
12. V. Pandarinathan, K. Lepková, S.I. Bailey, R. Gubner, "Impact of Mineral Deposits on CO$_2$ Corrosion of Carbon Steel," CORROSION 2013 (Houston, TX: NACE, 2013).
13. Z. Amjad, K.D. Demadis, *Mineral Scales and Deposits: Scientific and Technological Approaches* (Amsterdam, NL: Elsevier, 2015).
14. S. Papavinasam, *Corrosion Inhibitors* (Hoboken, NJ: John Wiley & Sons, Inc., 2011), p. 1021-1032.
15. K. Lepková, W. Van Bronswijk, V. Pandarinathan, R. Gubner, *Vib. Spectrosc.* 68 (2013): p. 204-211.
16. V. Pandarinathan, K. Lepková, S.I. Bailey, T. Becker, R. Gubner, *Ind. Eng. Chem. Res.* 53, 14 (2014): p. 5858-5865.
17. V. Pandarinathan, K. Lepková, S.I. Bailey, R. Gubner, *Corros. Sci.* 72 (2013): p. 108-117.
18. V.S. Reznik, V.D. Akamsin, Y.P. Khodyrev, R.M. Galiakberov, Y.Y. Efremov, L. Tiwari, *Corros. Sci.* 50, 2 (2008): p. 392-403.
19. H. De Reus, L.J.A. Hendriksen, M. Wilms, Y.N. Al-Habsi, W. Durnie, M. Gough, "Test Methodologies and Field Verification of Corrosion Inhibitors to Address Under Deposit Corrosion in Oil and Gas Production Systems," CORROSION 2005 (Houston, TX: NACE, 2005).
20. B.P. Binks, P.D.I. Fletcher, I.E. Salama, D.I. Horsup, J.A. Moore, *Langmuir: ACS J. Surf. Colloids* 27, 1 (2011): p. 469-473.
21. D. Doležal, T. Bolanca, Š.C. Stefanović, *Materialwiss. Werkst.* 42, 3 (2011): p. 229-233.
22. J. Huang, B. Brown, X. Jiang, B. Kinsella, S. Nešić, "Internal CO$_2$ Corrosion of Mild Steel Pipelines Under Inert Solid Deposits," CORROSION 2010, paper no. 10379 (Houston, TX: NACE, 2010).
23. C. Blachier, L. Michot, I. Bihannic, O. Barrès, A. Jacquet, M. Mosquet, *J. Colloid Interf. Sci.* 336, 2 (2009): p. 599-606.
24. V. Pandarinathan, K. Lepková, S.I. Bailey, R. Gubner, *J. Electrochem. Soc.* 160, 9 (2013): p. C432-C440.
25. P. Patra, P. Somasundaran, C. Lo, *Impact of Calcium Carbonate Mineral Scales in Industries* (Boca Raton, FL: CRC Press, 2013), p. 309-324.
26. S. Nešić, J. Postlethwaite, S. Olsen, *Corrosion* 52, 4 (1996): p. 280-294.
27. S. Nešić, *Carbon Dioxide Corrosion of Mild Steel* (Hoboken, NJ: John Wiley & Sons, Inc., 2011), p. 229-245.
28. R. Gaur, N. Abbas, *Characterization of Oil-Field Calcium Carbonate Scales* (Boca Raton, FL: CRC Press, 2013), p. 407-422.
29. NACE TG380-24253 "Underdeposit Corrosion (UDC) Testing and Mitigation Methods in the Oil and Gas Industry" NACE International publication 61114 (Houston, TX: NACE, 2014).
30. Y. Tan, Y. Fwu, K. Bhardwaj, *Corros. Sci.* 53, 4 (2011): p. 1254-1261.
31. G. Hinds, A. Turnbull, *Corrosion* 66, 4 (2010): p. 046001-01 to 046010-10.
32. W. Durnie, M. Gough, H. De Reus, "Development of Corrosion Inhibitors to Address Under Deposit Corrosion in Oil and Gas Production Systems," CORROSION 2005 (Houston, TX: NACE, 2005).
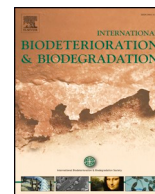
Original Reprint of the Publication Chapter VI

E.M. Suarez, K. Lepková, B. Kinsella, L.L. Machuca.

Aggressive Corrosion of Steel by a Thermophilic Microbial Consortium in the Presence and Absence of Sand.

Aggressive corrosion of steel by a thermophilic microbial consortium in the presence and absence of sand

Erika M. Suarez, Katerina Lepkova, Brian Kinsella, Laura L. Machuca*

Curtin Corrosion Centre (CCC), Western Australia School of Mines: Minerals, Energy and Chemical Engineering (WASM-MECE), Curtin University, Bentley, WA, 6102, Australia

ARTICLE INFO

ABSTRACT

Microbiologically influenced corrosion of carbon steel by a thermophilic microbial consortium was investigated in the presence and absence of sand using surface analysis techniques and 16S rRNA gene sequencing. The activity of the consortium, involving methanogens, fermenting and sulphidogenic microorganisms, significantly increased average and localised corrosion regardless of the presence of sand deposit. Microbial metabolisms and syntrophic relationships of the consortium species contributing to accelerated corrosion were discussed. Electrochemical reactions are proposed based on the layers of corrosion products deposited on the metal surface. Differences in the microbial community composition and corrosion products stratification were identified between steel samples covered and uncovered with sand. This work is closely related to industrial applications highlighting the importance of conducting tests for under deposit corrosion incorporating microbial consortia isolated from the field environment. Otherwise, the severity of localised corrosion could be severely underestimated.

1. Introduction

Corrosion of metal structures severely affects the oil and gas sector resulting in health, safety, economic and environmental problems (Duret-Thual, 2014; Kruger, 2011). Under deposit corrosion (UDC) is a critical topic of interest which has been designated as responsible for many operation failures, representing a threat for hydrocarbon transporting pipelines and seawater injection systems (De Reus et al., 2005; Nelson et al., 2007; Shukla and Naraian, 2017). UDC is often associated with a localised form of corrosion as a result of deposits settlement on metal surfaces. Deposits can make steel surfaces more vulnerable to localised forms of corrosion by facilitating the formation of anodes and cathodes locally (Pandarinathan et al., 2013a, 2014). The mechanism of UDC is affected by the nature of the deposit, material type (e.g., carbon steel, stainless steel) and the environmental conditions surrounding the metal (presence and amount of corrosive species such as oxygen, carbon dioxide, hydrogen sulphide and hydrogen ions (H+), among others) (Vera et al., 2012). In particular, UDC is influenced by components of the deposits which can include organic matter, minerals or their mixtures, typically found in oil production pipelines (Ly et al., 1998). The presence of oxygen is also a significant factor because the fundamental corrosion mechanism is different. It is important to distinguish that in the presence of oxygen deposits can lead to the classical formation of differential aeration cells. The area under the deposit becomes depleted of oxygen (anode) and corrodes whereas the cathodic oxygen reduction reaction takes place on the steel surface outside of the deposit. A previous UDC study in stagnant seawater showed that steel samples covered by mixed deposits of magnetite, calcium carbonate and silica sand, exhibited higher localised corrosion attack than deposits-free samples (Wang and Melchers, 2016). In that study, oxygen was present. In oxygen-free CO_2 environments, however the presence of a deposit have been shown to have a blocking effect as it can reduce the mass transfer of dissolved CO_2 species to the steel surface. Studies under these conditions using silica sand have shown a decrease in the general corrosion rate under the deposit due to a barrier effect exerted by the sand grains reducing the mass transfer of corrosive species to the metal surface (Huang et al., 2011; Pandarinathan et al., 2013b). The work by Pandarinathan et al. (2013c), extended to using alumina (Al_2O_3) and calcite ($CaCO_3$) deposits and although the average corrosion rate determined by weight loss decreased, localised pitting corrosion developed in all cases. UDC tests of carbon steel under ambient sour gas (H_2S) conditions demonstrated that samples deposited with a field sludge had both higher general and localised corrosion affectation compared to sand-deposited samples (Alanazi, 2017). Most UDC investigations have focused on determining the effect of various types of deposits on corrosion and its inhibition. However, the role of

---

Table 1
Microorganisms identified in the thermophilic consortium, their reported metabolisms and reactions potentially contributing to MIC.

Genus	Metabolism type	Metabolic Substrates	Metabolic End products	Potential MIC Reactions	References
Thermovirga sp.	Fermentative*	Proteinous substrates, organic acids and single amino acids	Acetate, ethanol, propionate, isovalerate/2-methyl butyrate, H_2, and CO_2	Anodic reaction (iron oxidation) $Fe \rightarrow Fe^{2+} + 2e^-$ Cathodic reaction (proton reduction) $2H^+ + 2e- \rightarrow H_2$ Chemical reaction $Fe(s) + 2HAc \rightarrow Fe^{2+} + 2Ac- + H_2$	Duncan (2010); Madigan et al. (2014); Dahle and Birkeland (2006); Li et al. (2018).
		Coupled fermentative metabolism with elemental sulphur (S^0) reduction		$S^0 + H_2 \rightarrow HS- + H^+ \rightarrow H_2S$ $H_2S + Fe^0 \rightarrow FeS + H_2$	
Methanothermobacter sp. (archaea)	Hydrogenotrophic methanogenic	H_2, formate, some alcohols	CO_2	Methanogenesis (cathodic depolarisation) $4H_2 + CO_2 \rightarrow CH_4 + 2H_2O$	Madigan et al. (2014); Mand et al. (2014); Hara et al. (2013)
		Fe^0	CO_2	Electromethanogenesis $4Fe^0 \rightarrow 4Fe2+ + 8e^-$ $8H^+ + 8e^- \rightarrow 4H_2$ $4H_2 + CO_2 \rightarrow CH_4 + 2H_2O$	
Thermoanaerobacter sp.	Fermentative*	Glucose, xylose, amino acids	Acetate, ethanol, lactate, H_2, and CO_2	Anodic reaction (iron oxidation) $Fe \rightarrow Fe^{2+} + 2e^-$ Cathodic reaction (proton reduction) $2H^+ + 2e- \rightarrow H_2$ Chemical reaction $Fe(s) + 2HAc \rightarrow Fe^{2+} + 2Ac- + H_2$	Scully and Orlygsson (2015); Feng et al., 2009; Jørgensen and Bak (1991); Madigan et al. (2014); Vos et al. (2011); Li et al. (2018)
		Coupled fermentative metabolism with the use of hydrogen scavengers (thiosulphate and hydrogenotrophic methanogens)	Thiosulphate disproportionation $S-SO_3^{2-} + H_2O \rightarrow SO_4^{2-} + HS^- + H^+$ $HS- + H+ \rightarrow H_2S$ $H_2S + Fe^0 \rightarrow FeS$		
Limnochordales ord.	Fermentative*	Organic compounds	organic acids, H_2	Anodic reaction (iron oxidation) $Fe \rightarrow Fe^{2+} + 2e^-$ Cathodic reaction (proton reduction) $2H^+ + 2e- \rightarrow H_2$ Chemical reaction $Fe(s) + 2HAc \rightarrow Fe^{2+} + 2Ac- + H_2$	Watanabe et al. (2015); Li et al. (2018)

microorganisms under these conditions has not been extensively addressed. (see Table 1)

Understanding the effect of microbes on UDC is essential because microbial cells typically thrive in deposits present in oil and gas production systems resulting in an adverse combination "UDC-Microbiologically Influenced Corrosion (MIC)" for pipelines integrity (Skovhus et al., 2017). Mosher et al. (2014), reported that microorganisms living within sludge deposits could increase uniform corrosion and also induce a localised attack on steel surfaces. Previous corrosion failure analyses of oil and gas production systems have shown the co-existence of deposits and microorganisms on corroded steel where, presumably, bacterial activity was the primary cause of the pipeline failure (Esan et al., 2001). Microorganisms are known to actively interact with the surrounding environment making it more aggressive towards carbon steel. At deposited steel surfaces, microbial activity can result in formation of a biofilms with the production of enzymes and extracellular polymeric substances (EPS) that create a complex array of microenvironments on the surfaces which can changes the properties of the deposits, e.g., making them more electroactive and can cause local deposition of new corrosive species on the steel surface (Machuca et al., 2011). The participation of microorganisms in corrosion is widely known to be either indirectly creating aggressive microenvironments, e.g., production of acidic species and sulphide amongst others (Alasvand Zarasvand and Rai, 2014; Beech, 2004) or directly, via influencing the anodic or cathodic reactions (Gu et al., 2011). The

deposits generated by microbial activity can modify the corrosion behaviour of metal surfaces leading to localised attack (Videla, 2002). It has been previously reported that biofilms formed within sludge deposits (a mixture of hydrocarbons, sand, clays corrosion products, microorganisms, and water) can rapidly increase corrosion of steel as well as induce localised corrosion under this deposited environment (Mosher et al., 2014). Wang et al. (Wang and Melchers, 2016), demonstrated that steel samples covered with deposits (magnetite, calcium carbonate, and sand) had markedly more pitting corrosion than bare steel samples in the presence of microorganisms. Sulphate-reducing bacteria (SRB) have been traditionally targeted to assess the risk of MIC in a system (Chen et al., 2016; Enning and Garrelfs, 2014; Javed et al., 2017; Lee et al., 1995; Little and Lee, 2007b). However, there are many other microorganisms frequently identified in oil and gas facilities which have the potential to cause MIC. For instance, Machuca et al., recently demonstrated that localised corrosion underneath a complex oilfield deposit was greatly accelerated by fermenting, thiosulphate-reducing bacteria (Machuca et al., 2017).

Furthermore, the inherent aggressiveness of MIC is thought to be due to the synergistic and syntrophic activities of microorganisms within a consortium. For decades, microbial syntrophic (cross-feeding) associations have been a topic of interest in the field of MIC. For instance, the relationship between sulphate reducing microorganisms and methanogens has been identified as an essential mechanism for corrosion (Conlette, 2016; Deutzmann et al., 2015; Ozuolmez et al., 2015). In

177

this way, the coexistence of different corrosion related-microbial species on corroding surfaces could suggest the existence of syntrophic associations which can accelerate corrosion through interspecies metabolic collaboration (Li et al., 2017; Little and Lee, 2014; Morris et al., 2013; Stams and Plugge, 2009; Valentine, 2002). This study investigates the effect of sand deposit and a thermophilic microbial consortium recovered from an oilfield facility in Western Australia. Thermophilic microorganisms have been found to be predominant in Western Australian oil fields where temperatures of 50 °C–80 °C are encountered in production facilities. Microbial consortia recovered at these temperatures range usually come from reservoirs, and they have been frequently associated with corrosion problems (Magot, 2005). Despite the well-known barrier effect exerted by sand on carbon steel surfaces under abiotic conditions (Pandarinathan et al., 2013c), it was hypothesised that the presence of sand deposit on steel would facilitate local precipitation of microbial metabolites on steel and formation of concentration radiation cells leading to localised corrosion. This research seeks to improve the understanding of under-deposit corrosion mechanisms in the oil and gas production environment which is essential to develop more effective strategies to control internal corrosion in carbon steel pipelines.

2. Materials and methods

2.1. Microbial consortium and growth conditions

The microbial consortium used in this study was recovered from an oil production facility in Western Australia. The consortium was maintained using an enriched medium containing diverse electron donors and electron acceptors. The medium composition was as follows: NaCl 85 mM, K_2HPO_4 0.8 mM, NH_4Cl 4.7 mM, KCL 4.6 mM, $MgSO_4 \cdot 7H_2O$ 18 mM, $FeSO_4 \cdot 7H_2O$ 1.8 mM, D-glucose 6.1 mM, $Na_2S_2O_3 \cdot 5H_2O$ 7.5 mM, Na-formate 147 mM, Na-lactate 59 mM, Na-acetate 24 mM, and 1 L of ultrapure water (Milli-Q system, resistivity 18.2 MΩ cm). The compounds were mixed and sterilised by filtering through 0.2 μm membrane filters, followed by addition of 1 mL of Wolfe's mineral elixir and 10 mL of vitamins solution (Zinkevich and Beech, 2000). Finally, the solution was saturated with a gas mixture of 20% CO_2 in N_2 for 2 h followed by pH adjustment to 7.0 ± 0.2 using deoxygenated $NaHCO_3$ solution 60 mM. Cultures were maintained at 55 °C (to simulate in situ field temperature) in anaerobic glass bottles. For corrosion testing, the microbial consortium was first inoculated at 10% into anaerobic growth medium and incubated at 55 °C. After three days of incubation (during exponential phase ≈ 10^8 cells/mL) the culture was centrifuged twice at 1100 × g for 3 min to remove precipitates formed in the medium by bacterial activity. The supernatant was then inoculated directly into the reactors.

2.2. Metal coupons and immersion tests

Carbon steel coupons (AISI 1030) of 6.25 cm^2 exposed surface area were used for immersion tests. Their chemical composition by weight % was: C (0.37), Mn (0.80), Si (0.282), P (0.012), S (0.001), Cr (0.089), Ni (0.012), Mo (0.004), Sn (0.004), Al (0.01), and Fe (balance). The steel coupons were painted twice (Belzona 1111® epoxy) and wet ground up to 600 grit finish. Ground metal coupons were immersed in ethanol 70% for 5 min, dried with nitrogen and finally exposed to ultraviolet (UV) radiation for 10 min each side before testing. Four different immersion tests were conducted using fed-batch reactors. 1) Biotic reactor with sand, 2) Biotic reactor without sand, 3) Abiotic reactor with sand and 4) Abiotic reactor without sand. All the materials for the test set-up were sterilised by autoclaving followed by UV radiation. Steel coupons were placed horizontally and individually in glass holders as described previously (Machuca et al., 2017). For test using deposits, silica sand (Sigma-Aldrich) with a grain size of ≈ 300 μm (Pandarinathan et al., 2011) was used to cover the steel surfaces. The sand was acid washed

and dried before testing (Pandarinathan et al., 2013b). After placing the coupons on the glass holders, the sand was added covering the total coupons surface. All deposited samples had the same thickness of the sand layer (≈ 5 mm). Subsequently, reactors were sealed and saturated with filtered-sterilised 20% CO_2 in N_2 gas mixture. The solution used for the corrosion tests was the same growth medium (Section 2.1). The test temperature and agitation were controlled at 55 ± 1 °C and 200 rpm using an IKA RTC digital hotplate with a thermocouple. The test solution was replenished weekly (30% of total volume) with fresh test solution (adjusted pH to 7.0 ± 0.2) and active bacterial cells prepared using the same procedure described in the inoculum preparation part (Section 2.1.1). Replenishment was done to maintain microbial activity throughout the exposure. Tests were completed after 36 days exposure. At the completion of the tests, the reactors were dismantled inside an anaerobic (N_2) glove box to prevent oxygen exposure of the tested coupons. Steel coupons were processed in duplicate for the analyses described in the following sections.

2.3. Weight loss measurements and 3D-profilometry

After the immersion period, three samples were cleaned removing corrosion products and/or biofilm. Subsequently, weight loss was determined according to the ASTM standard for cleaning and evaluating corrosion test samples (ASTM, 2017). Two of the cleaned samples were imaged to determine the average and the maximum intrusion depth at each sample using a 3D optical profilometer (Alicona imaging infinite focus microscope IFM G4 3.5). The average intrusion depth was obtained using the 10 deepest points measured on each sample.

2.3.1. Microscopy and chemical surface analysis

Field-Emission Scanning Electron Microscopy (FESEM) was performed to visualise cross-sectional features of the damage from top to bottom (metal base). These images were also used to generate elemental composition maps of the corrosion products using energy-dispersive X-ray spectroscopy (EDS) analysis. After the immersion period, one coupon from each experiment was placed in a sealed glass cell under continuous injection of N_2 for two weeks to ensure complete drying of the sample before surface analysis. Subsequently, samples were mounted in Epofix® resin and cut to reveal the cross-section profile of the corroded steel. FESEM analysis of the cross-section images was performed using a Zeiss NEON high-resolution scanning electron microscope. The microscope was coupled with an energy dispersive X-ray detector for EDS-mapping analysis to determine the distribution of the elements within the surface layers. Aztec® 3.0 software (Oxford Instruments NanoAnalysis) was used for FESEM/EDS data analysis.

2.3.2. Structure and composition of the microbial community in the samples

Microbial communities in the biotic tests (with and without sand) were identified using 16S next-generation sequencing. For each test, sessile (biofilms attached to the steel) and planktonic (in the test fluid) microorganisms were analysed separately. Sessile populations are known to be the main culprits of metal deterioration. However, the planktonic community was also examined to establish differences in the structure of the planktonic and the biofilm consortium. The initial consortium used to inoculate the reactors was also analysed to determine changes in the consortium after the immersion period.

2.3.2.1. DNA extraction from planktonic microorganisms.
60 mL of the test solution (in duplicate) was filtered using polycarbonate membrane filters with pore size 0.2 μm to harvest microbial cells from the bulk solution. The filters were stored at −20 °C until DNA extraction. The genomic DNA was extracted directly from the membrane filters using the PowerWater® DNA Isolation Kit (MO-BIO Laboratories Inc.) following the manufacturer's instructions. NanoDrop spectrophotometer (NanoDrop® Technologies) and 1% agarose gels were used to quantify and check the quality of the DNA extracted,
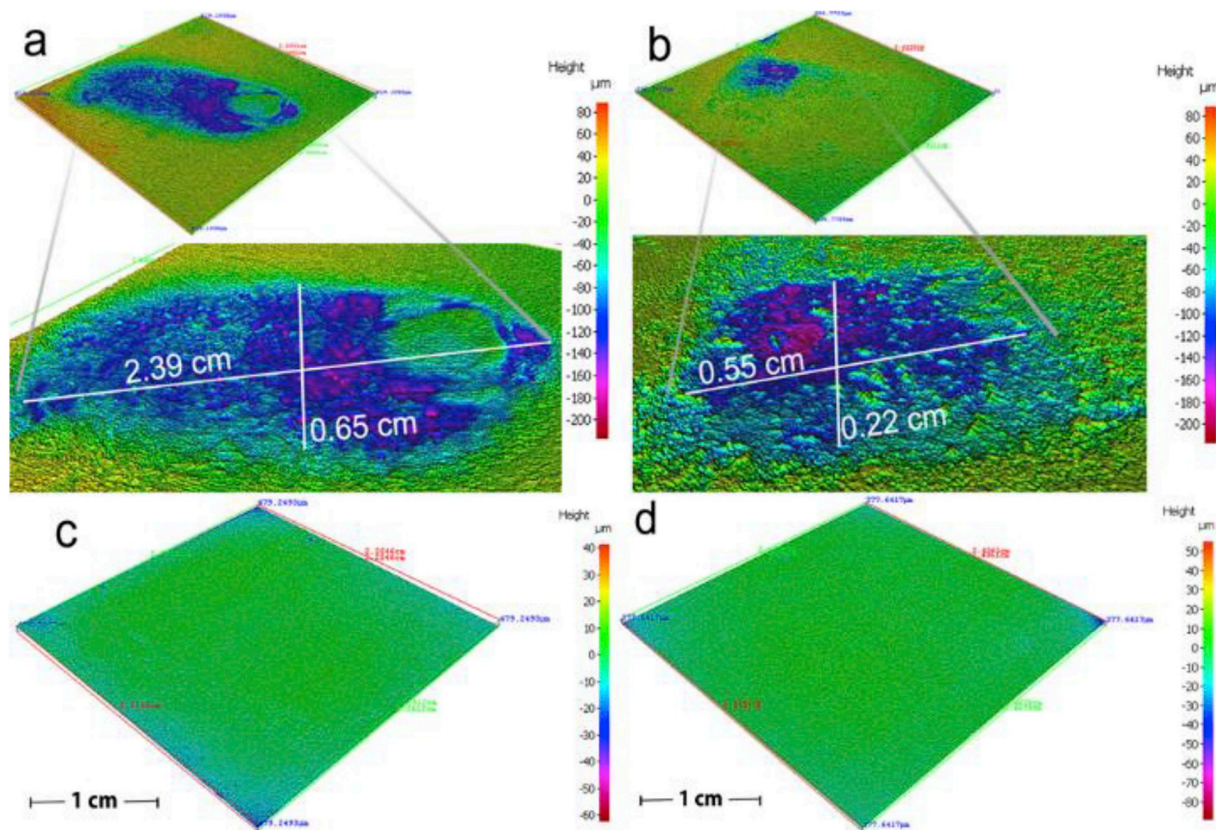
178

Fig. 1. Visible light microscopy 3D-images of the entire carbon steel surfaces. Biotic tests (top images): a) sand-free and b) sand-deposited steel surface. Abiotic experiments (lower images): c) sand-free and, d) sand-deposited steel surface.

respectively.

2.3.2.2. DNA extraction from biofilms on steel coupons (sessile microorganisms). Sessile microorganisms in the test without sand deposit refer to those attached and recovered from the metal surfaces. In the case of test with sand deposit, sessile communities were recovered from both sand grains and steel surfaces due to the sand being firmly adhered to the metal surface at the end of the tests. Before DNA extraction, carbon steel coupons in duplicate were immersed in anaerobic phosphate-buffered saline (PBS) and subjected to biofilm detachment procedure using sonication as previously described (Machuca et al., 2014). Sonicated solutions were collected and centrifuged at $1100 \times g$ for 3 min at 25 °C to remove corrosion products and/or sand followed by high-speed centrifugation at $3600 \times g$ for 30 min at 25 °C to concentrate biomass. Finally, the pellet was suspended in 50 mL of anaerobic Phosphate Buffered Saline (PBS) solution and filtered using 0.2 μm membrane filters. Membrane filters were stored at −20 °C. Afterwards, DNA was extracted from membrane filters using the PowerWater® DNA Isolation kit (MO-BIO Laboratories Inc.)

2.3.2.3. 16S rRNA gene sequencing. The microbial community present in the initial consortium, planktonic and sessile communities were identified using Illumina next-generation sequencing (NGS). Both Polymerase chain reaction (PCR) and sequencing were performed by the Australian Genome Research Facility (AGRF), Australia. The Region V3−V4 of the 16S ribosomal RNA was amplified using universal primers 341F (5′ CCTAYGGGRBGCASCAG 3′) – 806R (5′ GGACTACNNGGGTATCTAAT 3′) which are known to amplify a vast range of bacteria and archaea (Bai et al., 2012; Bates et al., 2011; Cardoso et al., 2017; Huws et al., 2007). A primary PCR was performed using AmpliTaq Gold 360 master-mix (Life Technologies, Australia) and

a second PCR reaction was run to index the amplicons with TaKaRa Taq DNA Polymerase (Clontech). The PCR products were measured by fluorometry (Invitrogen Picogreen) and normalised. Target PCR products were pooled in equimolar concentrations and quantified by qPCR (KAPA) followed by sequencing on Illumina MiSeq (Buermans and den Dunnen, 2014) with 2x300bp Paired End Chemistry. The illumine bcl2fastq 2.17.1.14 pipeline was used to generate the sequence data. Subsequently, bioinformatic analysis was performed as a follows: paired-end reads were assembled by merging the forward and reverse reads using PEAR (version 0.9.10) (Zhang et al., 2014). After that, sequences were processed and analysed using Quantitative Insights into Microbial Ecology (QIIME version 1.8) software package (Caporaso et al., 2010). Primers were identified and trimmed with Cutadapt using default settings. Then, the sequences were size filtered; the full-length duplicate sequences were removed and sorted by abundance by USEARCH tools (USEARCH version 9.2). After the dereplication process, USEARCH: UNOISE algorithm was used for clustering to determine the zOTUs (zero-radius operational taxonomic units). Chimeric sequences were removed using UCHIME (Edgar et al., 2011) with SILVA as reference database (SILVA version 128) (Quast et al., 2013). Abundances were calculated after denoising, and the OTU table was generated. Taxonomic classification of the reference sequences (zOTUs) was performed by similarity searches using BLAST against the same database. Raw data files were deposited in NCBI Sequence Read Archive (SRA) with accession number SRP130173 (Bioproject Accession Number: PRJNA430026, Biosamples accession numbers: SAMN08364894, SAMN08364895, SAMN08364896, SAMN08364897, SAMN08364898, SAMN08364899, SAMN08364900, SAMN08364901, SAMN08364902, SAMN08364903 Release date 31-07-2018).
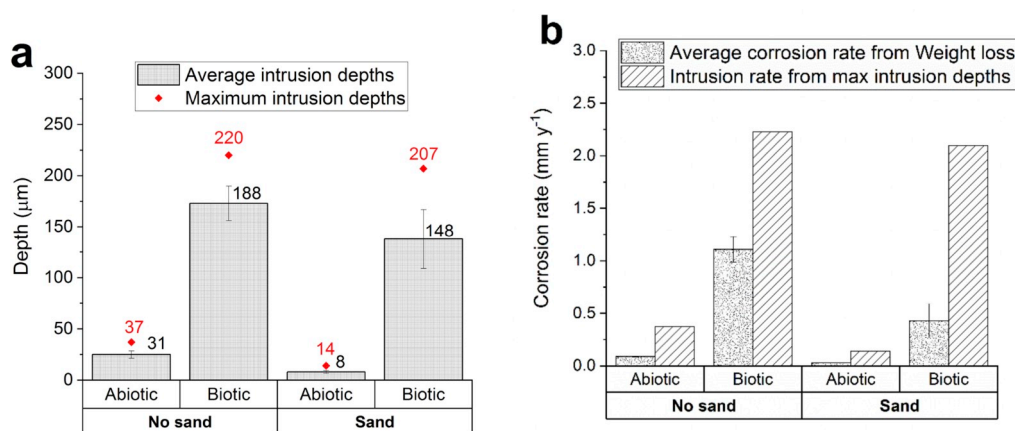
Fig. 2. Results of under deposit corrosion tests in CO2/N2 sparged solutions at 55 °C for 36 days: (a) average and maximum intrusion depths by visible light 3D profilometry. The average intrusion depth was obtained using the 10 deepest points measured on each sample; (b) average corrosion rates from weight loss measurements and intrusion rates calculated from maximum intrusion depth measurements.

3. Results

3.1. The surface area affected

3D-optical surface images of the total exposed area of carbon steel coupons revealed damaged areas at each steel sample (Fig. 1). Carbon steel exposed to biotic conditions (Fig. 1a and b) exhibited greater corroded area than surfaces under abiotic conditions (Fig. 1c and d). The effect of sand in biotic tests can be seen from a comparison of images in Fig. 1a and b. Notably, the sand-free surface exhibited a much larger corroded area (close-up shown in Fig. 1a) compared to the sand-deposited surface (Fig. 1b). However, both surfaces covered and uncovered with sand deposit had similar maximum penetration depths as shown by the height scale in Fig. 1.

3.2. Average and localised corrosion damage

Fig. 2 gives the average corrosion rate from weight loss measurements together with the intrusion rates and depths from visible light 3D profilometry on the carbon steel samples under abiotic and biotic conditions. Average and maximum intrusion depths results (Fig. 2a) shows considerably localised attack in the presence of microorganisms with maximum intrusion depths of 220 μm in sand-free samples and, 207 μm in sand-deposited samples compared to the abiotic counterparts with only 37 μm and 14 μm respectively. Fig. 2b provides a comparison between the average corrosion rates calculated by weight loss data and projected intrusion rates calculated from maximum intrusion depth values. The measurements assume that the localised corrosion measured over 36 days initiated from day 1 and propagated at the same rate throughout testing. Furthermore, that this rate would continue over the extended period of time for 1 year or more. Although sand-free samples had higher average corrosion and intrusion rates than sand-deposited samples, these samples covered with sand also suffered an immense damage when microorganisms are present.

3.3. Cross-sectional features of corroded steel and its chemical composition

Fig. 3 presents FESEM from cross-sectioned corroded steel specimens exposed to biotic and abiotic conditions. It can be seen that the steel exposed to the microbial consortium with and without a sand deposit (Fig. 3a and b) exhibited profound surface attack. The damage can also be seen in the form of large cavities in Fig. 1a and b. Such an extent of localised corrosion was not observed at samples immersed in abiotic environments (supplementary material). The electron image of the sand-free surface under biotic conditions (Fig. 3a) shows the

following components (from top to bottom): a thin top surface layer covering corrosion products [4], a membrane [3], a corroded area or cavity [2] and the base metal [1]. The top surface layer is covering corrosion products deposited on the membrane. This layer, which appears to be continuous and compact, is separating corrosion products deposited on top of the surface and corrosion products contained in the corroded area or cavity. Below the corrosion products formed inside the cavity there is an uneven corroded floor (base metal). In the sand deposited-sample (Fig. 3b), it is evident that the presence of sand grains altered the structure of corrosion layers observed in the sand-free sample (Fig. 3a). Similar to the test without sand, this sample covered with sand also presents a cavity or corroded area between surface layers and the base metal. It also has a membrane separating corrosion products in the cavity from those deposited on the surface. The structure and distribution of corrosion products on the surface above the membrane are altered by the deposition of sand grains on the surface. No corroded cavity was found in steel exposed to abiotic conditions, with and without sand.

SEM/EDS analysis in Fig. 4 revealed differences in the composition of corrosion layers between biotic tests. For the sand-free surface, the top surface layer is comprised of Fe and O which could indicate an iron oxide on this area. The corrosion products below the top surface layer and deposited on the delimiting membrane are comprised mostly of Fe and S (Fig. 4b and c), suggesting the presence of iron sulphide in direct contact with this membrane. Underneath the membrane, the corrosion products are also composed mainly of Fe and O (Fig. 4b and d). Differently, in the sand-deposited sample, this membrane seems to be a single layer composed mainly of Fe and O (Fig. 4f and h). The sand grains (Si and O) are deposited on top of the steel surface and became coated with Fe and S which can be also be observed accumulated in areas among sand grains. Although some oxygen is present in parts of this layer; it provides evidence that this phase mostly comprises by Fe and S.

For samples under abiotic environments (supplementary material), Fe and S can be seen scattered and surrounding the sand grains. EDS data indicates that FeS was formed under abiotic conditions. Previous research has shown that thiosulphate can react to form H_2S abiotically when in contact with carbon steel which results in localised corrosion (Tsujikawa et al., 1993). Thiosulfate is also thermodynamically stable only in neutral and alkaline solutions and undergoes chemical decomposition even under mild acidic conditions (Choudhary et al., 2015). In the presence of acid, thiosulphate can disproportionate to form sulphur and unstable thiosulphuric acid which decomposes almost immediately into water, SO_2 and S according to the following reaction: $S_2O_3^{2-} + 2H^+ \rightarrow H_2O + SO_2 + S$. In the presence of electrolyte the S can reacts
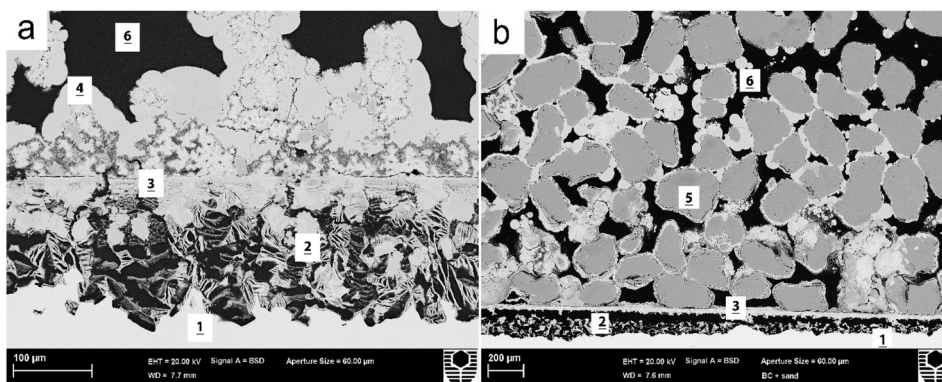
180

Fig. 3. FESEM images from cross-sectioned carbon steel samples after immersion under biotic conditions in CO2/N2 containing solution at 55 °C for 36 days. a) sand-free and b) sand-deposited steel surface. [1] Metal; [2] corroded area "cavity"; [3] delimiting layer; [4] top surface layer; [5] sand grain and [6] resin.

quickly to oxidise iron with the formation of FeS according to this reaction: $Fe + S \rightarrow FeS$ (Kappes, 2011). Additionally, in these samples, carbon is detected among iron sulphide precipitates which is likely to correspond to the Epoxy resin which displaced Fe and S from the surface. This indicates that corrosion layers in abiotic tests were very friable, less compacted onto the surface compared to corrosion layers formed under biotic conditions. Also, no corroded area or cavity is observed under abiotic conditions with or without sand. For both abiotic and abiotic tests, the samples were covered with a black deposit suggesting the presence of sulphide.

3.4. Microbial community composition by 16S rRNA gene sequencing

A total of 223,281 sequences were obtained from biotic tests. The distribution of was as a follows: 33,216 for the initial inoculum, planktonic microorganisms in the test with no sand (28,367) and with sand (44,646). Sessile communities in tests without sand (56,438) and with sand (60,615). Clustering of these reads at 100% similarity threshold resulted in bacteria 89% and archaea 11%. Fig. 5 displays the taxonomic distribution of planktonic and sessile populations and their percentage of relative abundance in the consortium. The four first categories represent taxonomic units with an average of relative abundance > 1%. The "Others" category represents populations with a relative abundance of less than 1%. Microorganisms constituting the initial consortium were identified as follows: *Thermovirga* sp. 52.8%, *Methanothermobacter* sp. 24.8%, uncultured members of the order Limnochordales ord. 15.8% and *Thermoanaerobacter* sp. 6.6%. Interestingly, *Thermovirga* sp. and Limnochordales ord. were found to be the
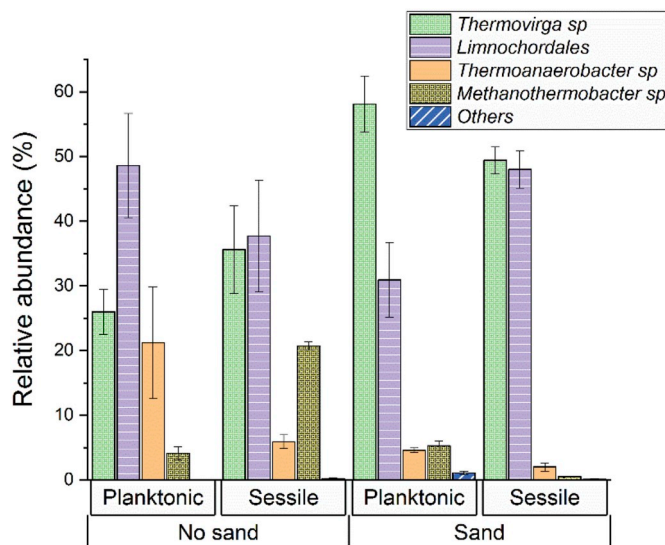
Fig. 5. Taxonomic distribution of abundant microorganisms from planktonic and sessile communities in tests with and without sand. Identification at the order level (unculturedLimnochordales) and, at the genus level (*Thermoanaerobacter*, *Thermovirga* and *Methanothermobacter*). Labels show the taxonomic units with average relative abundance > 1%. "Others" category represents the relative abundance < 1%.
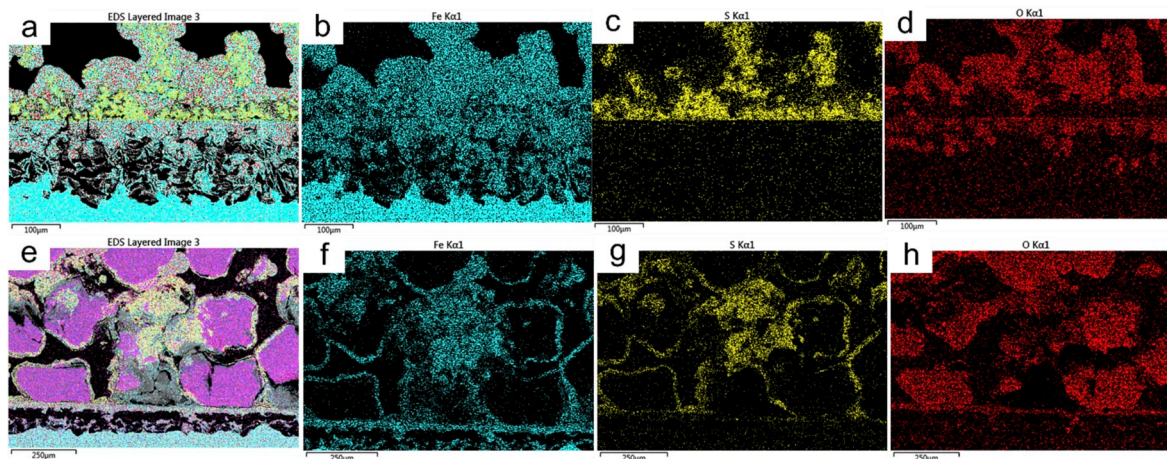
Fig. 4. EDS-elemental mapping of cross-sectioned carbon steel after immersion under biotic conditions in CO2/N2 containing solution at 55 °C for 36 days. From left to right: combined elemental map, iron, sulphur and, oxygen map. a-d) Sand-free steel surface and, e-h) Sand deposited steel surface.

dominant species in the consortium but after immersion for both tests (with and without sand).

3.4.1. Planktonic versus biofilm (sessile) communities

Fig. 5 shows differences between planktonic and sessile communities in both tests (with and without sand). Although *Thermovirga* sp. and Limnochordales ord. remained the dominant species of the consortium across all tests, changes in the proportion of all species were observed in biofilms. In the sand-free corroded surface, the most notorious difference between biofilm and the planktonic community was the higher proportion of *Methanothermobacter* sp. and *Thermovirga* sp. in biofilms when compared to the planktonic microorganisms. On the other hand, biofilms formed on the sand-deposited surface had a lower proportion of *Methanothermobacter* sp. and *Thermovirga* sp. as compared to their planktonic counterparts. Similarly, the high relative proportion of *Thermovirga* sp. and Limnochordales ord. was always observed in biofilms.

3.4.2. Effect of sand deposits on biofilm community structure\

Thermovirga sp. and Limnochorda ord. were the most abundant groups in both tests with sand (49.4% and 48%) and without sand (35.6% and 37.7%), respectively. Notably, *Methanothermobacter* sp. is more abundant in sand-free samples (20.7%) as compared to the sand-deposited ones (0.5%) showing that the methanogenic population thrived preferentially in sand-free surfaces. Similarly, the proportion of sessile *Thermoanaerobacter* sp was higher in sand-free than sand-deposited steel surfaces.

4. Discussion

This study assessed carbon steel corrosion by a thermophilic microbial consortium in a CO_2 environment and the effect that sand deposit exerted on this process. Despite the greater corrosion affectation (average corrosion) in the sand-free samples, the sand-deposited ones also showed considerable damage in contact with the consortium. These results suggest that microbial cells and/or their activity could surpass the barrier effect commonly observed by sand deposit in abiotic CO_2 anaerobic conditions. Similarly, the surface analysis also revealed aggressive localised corrosion caused by the microbial consortium on the steel surfaces. Although average and localised corrosion information followed the same pattern, the average corrosion rate from weight loss measurements does not adequately represent the extent of the damage caused by microbial attack. This is because it underestimates the degree of localised attack and wall penetration caused by the microbes.

The presence of a cavity underneath the corrosion products formed in the presence of the microbial consortium suggests a more direct interaction between the metal and the corrosive species formed by microbial activity (e.g., FeS) and precipitated on the steel surface. These results point out the importance of conducting tests with deposits using microbial consortia isolated from the system. If microorganisms that cause corrosion are present in the field environment, they should be incorporated into laboratory tests when assessing the severity of UDC and mitigation treatment.

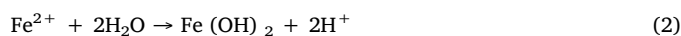### 4.1. Electrochemical and chemical reactions

Electrochemical and chemical reactions are proposed according to the structure of corrosion products layers and their composition. Carbon steel corrosion under carbon dioxide environments was described by (Nešić, 2011) and (Kahyarian et al., 2017). Assuming the anodic reactions occurred at the corroded cavity and cathodic reactions at the surface layers, the possible reactions can be as a follows:

Reactions in the anodic region:
anodic reaction:

$$Fe \rightarrow Fe^{2+} + 2e^- \tag{1}$$

chemical reaction:

$$Fe^{2+} + 2H_2O \rightarrow Fe(OH)_2 + 2H^+ \tag{2}$$

Reactions in the cathodic region
cathodic reaction:

$$2H^+ + 2e^- \rightarrow H_2 \tag{3}$$

chemical reaction:

$$H_2S + Fe^{2+} \rightarrow FeS + 2H^+ \tag{4}$$

chemical reaction:

$$Fe^{2+} + 2(OH)\text{-} \rightarrow Fe(OH)_2 \tag{5}$$

Electrochemical iron dissolution of the steel (oxidation of iron, Equation (1)) and acidification due to hydrolysis (Equation (2)) may have taken place in the anodic region of localised corrosion. The local low pH in the anodic area will tend to prevent precipitation of insoluble salts.

Regarding reactions in the cathodic region, hydrogen evolution in CO_2 solutions can result from the reduction of the dissociated (free) hydrogen ions (Equation (3)). This reaction could have happened in two different ways: by reduction of H_2S and/or by the presence of organic acids formed as a result of microbial activity. Microorganisms can generate H_2S as a result of the reduction of sulphur compounds. This dissolved H_2S is a weak acid acting as a reservoir of H^+ ions. The net result is that the sulphide generated (S^{2-}) will immediately undergo a chemical reaction with the dissolved ferrous ions from the metal surface and also from the test solution to produce insoluble iron sulphide (Equation (4)). In the present study, the rich layer of Fe and S formed on the metal surface (Fig. 4) suggest the presence of iron sulphide. The role of biogenic H_2S on carbon steel has been a controversial topic. Previous research has indicated that certain parameters such as the presence of specific sulfidogenic microorganisms, initial pH, the dissolved iron concentration, the type of electron donor and the free sulphide concentration determine the corrosive characteristics of the iron sulphide that can be formed from the biogenic H_2S (Enning and Garrelfs, 2014; Zhou et al., 2014). Some others authors, linked the activity of sulphate-reducing bacteria to the type of corrosion products, e.g., in biotic tests at 60 °C mackinawite ($Fe_{1+x}S$) was preferentially formed whereas greigite (Fe_3S_4) was present under abiotic conditions (Gramp et al., 2010). Recently, Jia et al. (2018), investigated carbon steel corrosion in the presence of SRB using culture medium. The authors concluded that biogenic H_2S corrosion is not a significant contributor to carbon steel corrosion by *Desulfovibrio vulgaris*. Instead, corrosion affectation was attributed to a larger headspace in the culture vial which allowed more H_2S to escape, lower dissolved H_2S, higher planktonic and sessile microorganism, and higher culture medium pH leading to more severe general and localised corrosion.

Another potential reaction in the cathodic region is the presence of iron oxides rich corrosion products. In this study, Fe and O layers were identified at the top surface area and the areas within the cavity in contact with the metal. A possible explanation for this is that the cathodic areas become alkaline because this reaction consumes protons or hydrogen ions. The build-up of alkalinity leads to the formation of insoluble oxides (Equation (5)). A concentration of Fe^{2+} originated by the anodic reaction inside the vast corroded area and diffusion of these ferrous ions (movement under a concentration gradient) to the alkaline rich region will lead to the formation of iron oxides. The reason why this reaction seems to occur also in the areas inside the cavity is not apparent. In addition, the presence of organic acids as a product of fermentation reactions by microorganisms can contribute to the cathodic part by being another source of hydrogen ions. Acid producing bacteria (APB) has been shown to accelerate corrosion due to the

formation of acids such as acetic acid (Jain et al., 2013). The mechanism for acetic acid on carbon steel corrosion consists of acceleration of the cathodic reaction (Tran et al., 2013). In the presence of microorganisms, the role of acetic acid in enhancing CO_2 corrosion is critical when net production of this organic acid, exceeds its consumption, e.g., when acetate-consuming bacteria are inhibited or stressed (Suflita et al., 2008) thus a large amount of acetic acid formed is accumulated on the metal surface. It is interesting to see that cathodic and anodic regions appear to be separated physically by a membrane (Fig. 3a and b). It is suggested that such a membrane could act as a conductive or semi-conductive membrane that facilitates electron flow thus resulting in accelerated corrosion.

4.2. Microbial activities associated with corrosion

The results from this study demonstrate that microbial activity was the primary cause of the aggressive localised corrosion observed on steel surfaces under conditions that would otherwise be considered not aggressive (abiotic tests). The key metabolic activities of the consortium can include fermentation, sulfidogenesis, and methanogenesis. Sulphidogenesis and formation of FeS are likely attributed to the activity of Thermovirga and Thermoanaerobacter populations. These populations have been recovered from oil and gas facilities and have been previously associated with severe corrosion problems (Duncan, 2010; Lan et al., 2012; Lenhart et al., 2014; Stevenson et al., 2011).

The first metabolic activity associated with corrosion is fermentation linked to sulphur reduction. It is known that some sulphur reducers, e.g., *Desulfuromonas acetoxidans* can oxidise acetate or ethanol to CO_2 coupled with the reduction of S^0 to H_2S (Madigan et al., 2014). The electrons for sulphur reduction come from H_2 or any of some organic compounds. In this study, the microorganism isolated with these capabilities was *Thermovirga* sp. This thermophilic microbe can ferment proteinous substrates, organic acids and single amino acids producing ethanol, acetate, propionate, isovalerate/2-methyl butyrate, H_2, and CO_2. *Thermovirga* sp can also couple fermentation with the reduction of elemental sulphur (S^0) to hydrogen sulphide (H_2S) (Dahle and Birkeland, 2006; Duncan, 2010). In particular, *Thermovirga lienii* has been associated with MIC processes in laboratory experiments (De Paula et al., 2014; Stipanicev et al., 2014) and also involved in case studies. For instance, a case study in West Africa, *Thermovirga* sp was reported as a high-risk bacterium due to its predominance in solids deposited on separation vessels exhibiting corrosion rates of 150–200 mpy (30 times more than the expected range). In united states, *T. lienii* was predominant in coupons located in production separators that had experienced corrosion problems (Skovhus, 2014).

Thermoanaerobacter sp. is also a thermophilic microorganism. All species can grow organoheterotrophically using various fermentation pathways including the homoacetogenic route. Generally, fermentation end products from hexoses are ethanol, acetate, lactate, H_2, and CO_2; Some Thermoanaerobacter strains are also able to grow chemolithoheterotrophically by coupling H_2 oxidation to growth. Additionally, others are facultative chemolithoautotrophs, growing with $H_2 + CO_2$ or Fe(III) + H_2 + CO_2 (Vos et al., 2011). Some strains of Thermoanaerobacter are also able to degrade amino acids but in the presence of a hydrogen-scavenging system (thiosulphate and coculture with hydrogenotrophic methanogens) with the formation of acetate as a dominant end product (Fardeau et al., 1996; Scully and Orlygsson, 2015). In this way, thiosulphate can be reduced to hydrogen sulphide with subsequent iron sulphide formation (Jørgensen and Bak, 1991). The ability of microorganisms to reduce thiosulphate and generate sulphide has received increasing attention among microbial corrosion researchers. Recently, Machuca et al. (2017), demonstrated that oilfield deposits containing thiosulphate reducing-bacteria (TRB) exhibited very high corrosion rates. Likewise, the activity of TRB on carbon steel corrosion was shown to increase corrosion rates almost six (6) times compared to abiotic control experiments (Liang et al., 2014).

Fermentation represents a dominant form of energy conservation. In this metabolism, organic substrates are catabolized by microbes producing organic acidic metabolic by-products. These organic acids, e.g., acetate, can decrease the pH beneath the biofilm and accelerate corrosion (Little and Lee, 2007a) leading to metabolite-MIC (M-MIC). This type of MIC involves an electrochemical process in which the acidic pH underneath the biofilm lead to proton reduction coupled with iron oxidation to yield a thermodynamically favourable corrosion process (Li et al., 2018). Some authors have highlighted the microbial acid production as an essential MIC mechanism for steel surfaces (Machuca et al., 2016). Apart from *Thermovirga* sp. and *Thermoanaerobacter* sp. as a possible fermenter microbe, a member of the Limnochordales order was also identified. In fact, Limnochordales ord. was one of the dominant groups identified in the consortium. Despite the lack of information about Limnochordales in the literature and even less about its relation to corrosion, previous studies described *Limnochorda pilosa* species as a fermenting microorganism, with pleomorphic filamentous cells that grow in a temperature range of 30–55 °C and a salinity range of 0.5–4% using glucose and other sugars to produce fatty acids (Watanabe et al., 2015). The high abundance of this species in the biofilm consortium on carbon steel suggest that this group contributed to the activities of the consortium and possibly to the corrosion of carbon steel.

Methanogenesis is other metabolic activity associate with corrosion. The methanogenic archaea *Methanothermobacter* sp. was also identified in the consortium. They typically use molecular hydrogen (H_2) while reducing carbon dioxide (CO_2) to produce methane (CH_4) (Ozuolmez et al., 2015). Methanogens can consume hydrogen produced during the corrosion of steel in a phenomenon known as cathodic depolarisation (Davidova et al., 2012). Also, this archaeon has been identified as an electromethanogenic (Hara et al., 2013) organism with the ability to conduct extracellular electron transfer (EET) uptaking electrons directly from the steel. In this EET-MIC, the zero valent iron (Fe^0) is used as an electron donor for metabolic energy activities stimulating cathodic reaction and hence iron corrosion (Kato, 2016; Xu and Gu, 2014). EET mechanism on steel surfaces can result in greater corrosion affectation compared to the processes involved in metabolite-MIC (M-MIC) (Enning et al., 2012; Li et al., 2018).

4.2.1. Syntrophic associations

Syntrophic is a metabolic link between dependent microbial partners with mutual benefits from the degradation of complex substrates (Morris et al., 2013). The microorganisms identified in the consortium used in this study are known to be metabolically diverse with capabilities for fermentation as well as being able to use diverse electron donors and acceptors. In some fermentations, oxidation-reduction balance is facilitated by H_2 production which is a strong electron donor and can be oxidised by various microorganisms such as methanogens stablishing syntrophic relationships (Madigan et al., 2014). Results from this work suggest the coexistence of fermenting species (Limnochordales ord., *Thermoanaerobacter* sp and *Thermovirga* sp) with methanogens with potential syntrophic activities within the consortium. H_2 produced by fermentation can be consumed by *Methanothermobacter* sp. constituting a crucial modular feeding web. Acetate produced by fermentation can also be transferred among species. Suflita et al. (Warikoo et al., 1996), stated that numerous metabolic pathways of anaerobes result in acetate formation. The authors mentioned that some bacterial syntrophic associations could be based on interspecies acetate utilisation as well as hydrogen consumption. In oilfields, both CO_2 and acetate are produced and consumed by microorganisms during the anaerobic biodegradation of organic matter including hydrocarbons. However, no potential acetate consuming (acetotrophic) microorganisms were detected by 16S rRNA gene sequencing suggesting an imbalance acetate production-consumption, leading to acetate accumulation on metal surfaces. Previously, a thermophilic microbial consortium, similar to the one used in the present study, involving

hydrogen-utilising methanogens, sulphur and thiosulphate reducing bacteria, fermenting bacteria and iron reducing bacteria was associated with severe corrosion problems (Duncan, 2010). However, based on the results obtained from this study it is not possible to determine the specific metabolic interactions of the consortium species and how these accelerate the corrosion process.

4.3. Sand-deposit

Previous studies in abiotic ambience CO_2 environments have shown that inert sand-deposits under abiotic conditions decrease average corrosion rates for carbon steel, but sand-deposited surfaces can be more susceptible to the localised attack (Pandarinathan et al., 2013c). In this work, sand-free samples exposed to the consortium had higher corrosion values than sand-deposited ones. However, this difference was not marked considering the barrier that the sand layers could exert on the surfaces. DNA sequencing analysis indicates that the microbial consortium structure exhibited slight variation as a result of the presence of sand on the steel surface (Fig. 4). *Methanothermobacter* sp. was more abundant in the sand-free metal surfaces than the sand-deposited ones. Based on the results from this study, it is not possible to conclude whether the consortium structure and activity were directly affected by the deposition of sand or indirectly, by the distinct corrosion process developed in the steel surface with and without sand deposits. Regardless, these results suggest that the methanogens played an essential role in the accelerated corrosion observed in sand-free surfaces. It is likely that in the absence of sand, a direct contact between methanogens and the metal surface facilitated both cathodic depolarisation and direct electron transfer (oxidation of Fe^0 to Fe^{2+}) (Daniels et al., 1987; Deutzmann et al., 2015; Lohner et al., 2014; Mand et al., 2014; Zhang et al., 2003) which is known to result in corrosion propagation.

5. Conclusions

The presence of the microbial consortium affected considerably both sand-deposited and sand-free carbon steel surfaces resulting in higher average and localised corrosion. In contrast to abiotic tests, the barrier effect of the sand deposit was not as pronounced in the presence of the microbial consortium. The microbial community structure of the microbial consortium and corrosion products stratification on carbon steel surfaces were different between tests with and without sand.

Funding

Declaration of interest

None.

Data availability

The raw/processed data required to reproduce these findings cannot be shared at this time due to technical or time limitations.

Acknowledgments

Appendix A. Supplementary data

References

Alanazi, N.M., 2017. Investigation of under-Deposit Corrosion on X-60 Using Multielcetrode System.

Alasvand Zarasvand, K., Rai, V.R., 2014. Microorganisms: induction and inhibition of corrosion in metals. Int. Biodeterior. Biodegrad. 87, 66–74.

ASTM, G., 2017. Standard Practice for Preparing, Cleaning, and Evaluating Corrosion Test Specimens.

Bai, Y., Sun, Q., Wen, D., Tang, X., 2012. Abundance of ammonia-oxidizing bacteria and archaea in industrial and domestic wastewater treatment systems. FEMS Microbiol. Ecol. 80, 323–330.

Bates, S.T., Berg-Lyons, D., Caporaso, J.G., Walters, W.A., Knight, R., Fierer, N., 2011. Examining the global distribution of dominant archaeal populations in soil. ISME J. 5, 908–917.

Beech, I.B., 2004. Corrosion of technical materials in the presence of biofilms-current understanding and state-of-the art methods of study. Int. Biodeterior. Biodegrad. 53, 177–183.

Buermans, H.P.J., den Dunnen, J.T., 2014. Next generation sequencing technology: advances and applications. Biochim. Biophys. Acta (BBA) - Mol. Basis Dis. 1842, 1932–1941.

Caporaso, J.G., Kuczynski, J., Stombaugh, J., Bittinger, K., Bushman, F.D., Costello, E.K., Fierer, N., Peña, A.G., Goodrich, J.K., Gordon, J.I., 2010. QIIME allows analysis of high-throughput community sequencing data. Nat. Methods 335–336.

Cardoso, D.C., Sandionigi, A., Cretoiu, M.S., Casiraghi, M., Stal, L., Bolhuis, H., 2017. Comparison of the active and resident community of a coastal microbial mat. Sci. Rep. 7.

Chen, Y., Torres, J., Castaneda, H., Ju, L.-K., 2016. Quantitative comparison of anaerobic pitting patterns and damage risks by chloride versus *Desulfovibrio vulgaris* using a fast pitting-characterization method. Int. Biodeterior. Biodegrad. 109, 119–131.

Choudhary, L., Macdonald, D.D., Alfantazi, A., 2015. Role of thiosulfate in the corrosion of steels: a review. Corrosion 71, 1147–1168.

Conlette, O.C., 2016. Microbial communities of light crude from Nigeria and potential for in situ biodegradation, souring, and corrosion. Petrol. Sci. Technol. 34, 71–77.

Dahle, H., Birkeland, N.-K., 2006. *Thermovirga lienii* gen. nov., sp. nov., a novel moderately thermophilic, anaerobic, amino-acid-degrading bacterium isolated from a North Sea oil well. Int. J. Syst. Evol. Microbiol. 56, 1539–1545.

Daniels, L., Belay, N., Rajagopal, B.S., Weimer, P.J., 1987. Bacterial methanogenesis and growth from CO_2 with elemental iron as the sole source of electrons. Science 237, 509–511.

Davidova, I.A., Duncan, K.E., Perez-Ibarra, B.M., Suflita, J.M., 2012. Involvement of thermophilic archaea in the biocorrosion of oil pipelines. Environ. Microbiol. 14, 1762–1771.

De Paula, R.M., Keasler, V.V., Bennett, B., Clark, J.C., Cloud, R., 2014. On-site Evaluation of Microbiologically Induced Corrosion and the Effects of Continuous Low Dosage Corrosion Inhibitor Application. Proceedings of the CORROSION 2014, San Antonio, Texas, USA.

De Reus, H., Hendriksen, L.J.A., Wilms, M., Al-Habsi, Y.N., Durnie, W., Gough, M., 2005. Test Methodologies and Field Verification of Corrosion Inhibitors to Address under Deposit Corrosion in Oil and Gas Production Systems.

Deutzmann, J.S., Sahin, M., Spormann, A.M., 2015. Extracellular enzymes facilitate electron uptake in biocorrosion and bioelectrosynthesis. mBio 6.

Duncan, K.E., 2010. Biocorrosive thermophilic microbial communities in alaskan north slope oil facilities. Environ. Sci. Technol. 43, 7977–7984.

Duret-Thual, C., 2014. 1 - Understanding Corrosion: Basic Principles, Understanding Biocorrosion. Woodhead Publishing, Oxford, pp. 3–32.

Edgar, R.C., Haas, B.J., Clemente, J.C., Quince, C., Knight, R., 2011. UCHIME improves sensitivity and speed of chimera detection. Bioinformatics 27, 2194–2200.

Enning, D., Garrelfs, J., 2014. Corrosion of iron by sulfate-reducing bacteria: new views of an old problem. Appl. Environ. Microbiol. 80, 1226–1236.

Enning, D., Venzlaff, H., Garrelfs, J., Dinh, H.T., Meyer, V., Mayrhofer, K., Hassel, A.W., Stratmann, M., Widdel, F., 2012. Marine sulfate-reducing bacteria cause serious corrosion of iron under electroconductive biogenic mineral crust. Environ. Microbiol. 14, 1772–1787.

Esan, T., Kapusta, S.D., Simon-Thomas, M.J.J., 2001. Case study: extreme corrosion of a 20 oil pipeline in the Niger Delta Region. In: Proceedings of the NACE International.

Fardeau, M.-L., Faudon, C., Cayol, J.-L., Magot, M., Patel, B., Ollivier, B., 1996. Effect of thiosulphate as electron acceptor on glucose and xylose oxidation by *Thermoanaerobacter finnii* and a *Thermoanaerobacter* sp. isolated from oil field water. Res. Microbiol. 147, 159–165.

Feng, X., Mouttaki, H., Lin, L., Huang, R., Wu, B., Hemme, C.L., He, Z., Zhang, B., Hicks, L.M., Xu, J., 2009. Characterization of the central metabolic pathways in Thermoanaerobacter sp. strain X514 via isotopomer-assisted metabolite analysis. Appl. Environ. Microbiol. 75, 5001–5008.

Gramp, J.P., Bigham, J.M., Jones, F.S., Tuovinen, O.H., 2010. Formation of Fe-sulfides in cultures of sulfate-reducing bacteria. J. Hazard Mater. 175, 1062–1067.

Gu, J.D., Ford, T.E., Mitchell, R., 2011. Microbiological Corrosion of Metallic Materials, Uhlig's Corrosion Handbook. John Wiley & Sons, Inc., pp. 549–557.

Hara, M., Onaka, Y., Kobayashi, H., Fu, Q., Kawaguchi, H., Vilcaez, J., Sato, K., 2013. Mechanism of electromethanogenic reduction of CO2 by a thermophilic methanogen.

Energy Procedia 37, 7021–7028.

Huang, J., Brown, B., Choi, Y.-S., Nešić, S., 2011. Prediction of Uniform CO2 Corrosion of Mild Steel under Inert Solid Deposits.

Huws, S.A., Edwards, J.E., Kim, E.J., Scollan, N.D., 2007. Specificity and sensitivity of eubacterial primers utilized for molecular profiling of bacteria within complex microbial ecosystems. J. Microbiol. Methods 70, 565–569.

Jain, L.A., Williamson, C., Spear, J.R., Olson, D.L., Mishra, B., Kane, R.D., 2013. Microbiologically Influenced Corrosion of Linepipe Steels in Ethanol and Acetic Acid Solutions. Proceedings of the CORROSION 2013, Orlando, Florida.

Javed, M.A., Neil, W.C., McAdam, G., Wade, S.A., 2017. Effect of sulphate-reducing bacteria on the microbiologically influenced corrosion of ten different metals using constant test conditions. Int. Biodeterior. Biodegrad. 125, 73–85.

Jia, R., Tan, J.L., Jin, P., Blackwood, D.J., Xu, D., Gu, T., 2018. Effects of biogenic H2S on the microbiologically influenced corrosion of C1018 carbon steel by sulfate reducing Desulfovibrio vulgaris biofilm. Corrosion Sci. 130, 1–11.

Jorgensen, B.B., Bak, F., 1991. Pathways and microbiology of thiosulfate transformations and sulfate reduction in a marine sediment (kattegat, Denmark). Appl. Environ. Microbiol. 57, 847–856.

Kahyarian, A., Achour, M., Nesic, S., 2017. CO2 Corrosion of Mild Steel, Trends in Oil and Gas Corrosion Research and Technologies. pp. 149–190.

Kappes, M.A., 2011. Evaluation of Thiosulfate as a Substitute for Hydrogen Sulfide in Sour Corrosion Fatigue Studies. Ph.D., The Ohio State University, Ann Arbor.

Kato, S., 2016. Microbial extracellular electron transfer and its relevance to iron corrosion. Microb. Biotechnol. 9, 141–148.

Kruger, J., 2011. Cost of Metallic Corrosion, Uhlig's Corrosion Handbook. John Wiley & Sons, Inc., pp. 15–20.

Lan, G., Hong, H., Qing, D., Wu, Y., Tan, H., 2012. Identification and bio-corrosion behavior of Thermoanaerobacter CF1, a thiosulfate reducing bacterium isolated from Dagang oil field. Afr. J. Microbiol. Res. 6, 3065–3071.

Lee, W., Lewandowski, Z., Nielsen, P.H., Hamilton, W.A., 1995. Role of sulfate-reducing bacteria in corrosion of mild steel: a review. Biofouling 8, 165–194.

Lenhart, T.R., Duncan, K.E., Beech, I.B., Sunner, J.A., Smith, W., Bonifay, V., Biri, B., Suflita, J.M., 2014. Identification and characterization of microbial biofilm communities associated with corroded oil pipeline surfaces. Biofouling 30, 823–835.

Li, X.-X., Yang, T., Mbadinga, S.M., Liu, J.-F., Yang, S.-Z., Gu, J.-D., Mu, B.-Z., 2017. Responses of microbial community composition to temperature gradient and carbon steel corrosion in production water of petroleum reservoir. Front. Microbiol. 8.

Li, Y., Xu, D., Chen, C., Li, X., Jia, R., Zhang, D., Sand, W., Wang, F., Gu, T., 2018. Anaerobic microbiologically influenced corrosion mechanisms interpreted using bioenergetics and bioelectrochemistry: a review. J. Mater. Sci. Technol. 34, 1713–1718.

Liang, R., Grizzle, R.S., Duncan, K.E., McInerney, M.J., Suflita, J.M., 2014. Roles of thermophilic thiosulfate-reducing bacteria and methanogenic archaea in the biocorrosion of oil pipelines. Front. Microbiol. 5, 89.

Little, B.J., Lee, J.S., 2007a. Microbiologically Influenced Corrosion. John Wiley & Sons.

Little, B.J., Lee, J.S., 2007b. Microbiologically Influenced Corrosion, 1 ed. Wiley, Hoboken.

Little, B.J., Lee, J.S., 2014. Microbiologically influenced corrosion: an update. Int. Mater. Rev. 59, 384–393.

Lohner, S.T., Deutzmann, J.S., Logan, B.E., Leigh, J., Spormann, A.M., 2014. Hydrogenase-independent uptake and metabolism of electrons by the archaeon Methanococcus maripaludis. ISME J. 8, 1673–1681.

Ly, K.T., Blumer, D.J., Bohon, W.M., Chan, A., 1998. Novel Chemical Dispersant for Removal of Organic/Inorganic "Schmoo"; Scale in Produced Water Injection Systems.

Machuca, L.L., Bailey, S.I., Gubner, R., Watkin, E., Kaksonen, A.H., 2011. Microbiologically Influenced Corrosion of High Resistance Alloys in Seawater. NACE - International Corrosion Conference Series.

Machuca, L.L., Jeffrey, R., Bailey, S.I., Gubner, R., Watkin, E.L.J., Ginige, M.P., Kaksonen, A.H., Heidersbach, K., 2014. Filtration-UV irradiation as an option for mitigating the risk of microbiologically influenced corrosion of subsea construction alloys in seawater. Corrosion Sci. 79, 89–99.

Machuca, L.L., Jeffrey, R., Melchers, R.E., 2016. Microorganisms associated with corrosion of structural steel in diverse atmospheres. Int. Biodeterior. Biodegrad. 114, 234–243.

Machuca, L.L., Lepkova, K., Petroski, A., 2017. Corrosion of carbon steel in the presence of oilfield deposit and thiosulphate-reducing bacteria in CO2 environment. Corrosion Sci. 129, 16–25.

Madigan, M.T., Martinko, J.M., Bender, K.S., Buckley, D.H., Stahl, D.A., 2014. Brock Biology of Microorganisms, fourteenth ed. .

Magot, M., 2005. Indigenous Microbial Communities in Oil Fields, Petroleum Microbiology. American Society of Microbiology, pp. 21–34.

Mand, J., Park, H.S., Jack, T.R., Voordouw, G., 2014. The role of acetogens in microbially influenced corrosion of steel. Front. Microbiol. 5.

Morris, B.E.L., Henneberger, R., Huber, H., Moissl-Eichinger, C., 2013. Microbial syntrophy: interaction for the common good. FEMS (Fed. Eur. Microbiol. Soc.) Microbiol. Rev. 37, 384–406.

Mosher, W., Mosher, M., Lam, T., Cabrera, Y., Oliver, A., Tsaprailis, H., 2014. Methodology for Accelerated Microbiologically Influenced Corrosion in under Deposits from Crude Oil Transmission Pipelines.

Nelson, R., Edwards, M.A., Kovash, P., 2007. Monitoring and Controlling Corrosion in an Aging Sour Gas Gathering System a Nine-year Case History, CORROSION 2007.

NACE International.

Nešić, S., 2011. Carbon Dioxide Corrosion of Mild Steel, Uhlig's Corrosion Handbook. John Wiley & Sons, Inc., pp. 229–245.

Ozuolmez, D., Na, H., Lever, M.A., Kjeldsen, K.U., Jørgensen, B.B., Plugge, C.M., 2015. Methanogenic archaea and sulfate reducing bacteria co-cultured on acetate: teamwork or coexistence? Front. Microbiol. 6, 492.

Pandarinathan, V., Lepkova, K., Bailey, S.I., Gubner, R., 2013a. Inhibition of under-deposit corrosion of carbon steel by thiobenzamide. J. Electrochem. Soc. 160, C432–C440.

Pandarinathan, V., Lepková, K., Bailey, S.I., Gubner, R., 2013b. Evaluation of corrosion inhibition at sand-deposited carbon steel in CO2-saturated brine. Corrosion Sci. 72, 108–117.

Pandarinathan, V., Lepková, K., Bailey, S.I., Gubner, R., 2013c. Impact of Mineral Deposits on CO2 Corrosion of Carbon Steel.

Pandarinathan, V., Lepková, K., Gubner, R., 2011. Inhibition of CO2 corrosion of 1030 carbon steel beneath sand-deposits. In: Proceedings of the Conference & Expo.

Pandarinathan, V., Lepková, K., van Bronswijk, W., 2014. Chukanovite (Fe2(OH)2CO3) identified as a corrosion product at sand-deposited carbon steel in CO2-saturated brine. Corrosion Sci. 85, 26–32.

Quast, C., Pruesse, E., Yilmaz, P., Gerken, J., Schweer, T., Yarza, P., Peplies, J., Glöckner, F.O., 2013. The SILVA ribosomal RNA gene database project: improved data processing and web-based tools. Nucleic Acids Res. 41, D590–D596.

Scully, S.M., Orlygsson, J., 2015. Amino acid metabolism of Thermoanaerobacter strain AK90: the role of electron-scavenging systems in end product formation. J. Amino Acids 2015.

Shukla, P.K., Naraian, S., 2017. Under-Deposit Corrosion in a Sub-sea Water Injection Pipeline—A Case Study.

Skovhus, S.M.C.T.L., 2014. Applications of Molecular Microbiological Methods. Caister Academic Press.

Skovhus, T.L., Enning, D., Lee, J.S., 2017. Microbiologically Influenced Corrosion in the Upstream Oil and Gas Industry. CRC Press.

Stams, A.J., Plugge, C.M., 2009. Electron transfer in syntrophic communities of anaerobic bacteria and archaea. Nat. Rev. Microbiol. 7, 568–577.

Stevenson, B.S., Drilling, H.S., Lawson, P.A., Duncan, K.E., Parisi, V.A., Suflita, J.M., 2011. Microbial communities in bulk fluids and biofilms of an oil facility have similar composition but different structure. Environ. Microbiol. 13, 1078–1090.

Stipanicev, M., Turcu, F., Esnault, L., Rosas, O., Basseguy, R., Sztyler, M., Beech, I.B., 2014. Corrosion of carbon steel by bacteria from North Sea offshore seawater injection systems: laboratory investigation. Bioelectrochemistry 97, 76–88.

Suflita, J.M., Phelps, T.J., Little, B., 2008. Carbon dioxide corrosion and acetate: a hypothesis on the influence of microorganisms. Corrosion 64, 854–859.

Tran, T., Brown, B., Nesic, S., Tribollet, B., 2013. Investigation of the Mechanism for Acetic Acid Corrosion of Mild Steel. Proceedings of the CORROSION 2013, Orlando, Florida.

Tsujikawa, S., Miyasaka, A., Ueda, M., Ando, S., Shibata, T., Haruna, T., Katahira, M., Yamane, Y., Aoki, T., Yamada, T., 1993. Alternative for evaluating sour gas resistance of low-alloy steels and corrosion-resistant alloys. Corrosion 49, 409–419.

Valentine, D.L., 2002. Thermodynamic Ecology of hydrogen-based syntrophy. In: Seckbach, J. (Ed.), Symbiosis: Mechanisms and Model Systems. Springer Netherlands, Dordrecht, pp. 147–161.

Vera, J.R., Daniels, D., Achour, M.H., 2012. Under deposit corrosion (UDC) in the oil and gas industry: a review of mechanisms, testing and mitigation. In: Proceedings of the NACE 2012 Conference & Expo.

Videla, H.A., 2002. Prevention and control of biocorrosion. Int. Biodeterior. Biodegrad. 49, 259–270.

Vos, P., Garrity, G., Jones, D., Krieg, N.R., Ludwig, W., Rainey, F.A., Schleifer, K.-H., Whitman, W.B., 2011. Bergey's Manual of Systematic Bacteriology: Volume 3: the Firmicutes. Springer Science & Business Media.

Wang, X., Melchers, R.E., 2016. Long-term under-deposit corrosion of carbon steel pipelines under stagnant seawater. In: The 26th International Ocean and Polar Engineering Conference. International Society of Offshore and Polar Engineers.

Warikoo, V., McInerney, M.J., Robinson, J.A., Suflita, J.M., 1996. Interspecies acetate transfer influences the extent of anaerobic benzoate degradation by syntrophic consortia. Appl. Environ. Microbiol. 62, 26–32.

Watanabe, M., Kojima, H., Fukui, M., 2015. Limnochorda pilosa gen. nov., sp. nov., a moderately thermophilic, facultatively anaerobic, pleomorphic bacterium and proposal of Limnochordaceae fam. nov., Limnochordales ord. nov. and Limnochordia classis nov. in the phylum Firmicutes. Int. J. Syst. Evol. Microbiol. 65, 2378–2384.

Xu, D., Gu, T., 2014. Carbon source starvation triggered more aggressive corrosion against carbon steel by the Desulfovibrio vulgaris biofilm. Int. Biodeterior. Biodegrad. 91, 74–81.

Zhang, J., Kobert, K., Flouri, T., Stamatakis, A., 2014. PEAR: a fast and accurate Illumina Paired-End reAd mergeR. Bioinformatics 30, 614–620.

Zhang, T., Fang, H., Ko, B., 2003. Methanogen population in a marine biofilm corrosive to mild steel. Appl. Microbiol. Biotechnol. 63, 101–106.

Zhou, C., Vannela, R., Hayes, K.F., Rittmann, B.E., 2014. Effect of growth conditions on microbial activity and iron-sulfide production by Desulfovibrio vulgaris. J. Hazard Mater. 272, 28–35.

Zinkevich, V., Beech, I.B., 2000. Screening of sulfate-reducing bacteria in colonoscopy samples from healthy and colitic human gut mucosa. FEMS Microbiol. Ecol. 34, 147–155.

185

Appendix 5
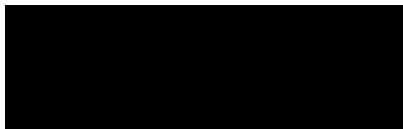
Written Statements from Co-authors of the Publications and Manuscripts Submitted.

1. Written statements from co-authors of the publication entitled "*The Role of Bacteria in Under-Deposit Corrosion in Oil and Gas Facilities: a Review of Mechanisms, Test Methods and Corrosion Inhibition.*"

2. Written statements from co-authors of the publication entitled *"CO_2 Corrosion Inhibitors Performance at Deposited-Carbon Steel and their Adsorption on Different Deposits."*

3. Written statements from co-authors of the manuscript submitted entitled "*Molecular Characteristics Affecting The Efficiency of Corrosion Inhibitors at Sand-Deposited Carbon Steel: a New Approach Using a Multi-Electrode Array.*"

4. Written statements from co-authors of the publication entitled "*Aggressive Corrosion of Steel by a Thermophilic Microbial Consortium in the Presence and Absence of Sand.*"

5. Written statements from co-authors of the manuscript submitted entitled "*In Situ Investigation of Under-Deposit Microbial Corrosion and Its Inhibition Using A Multi-Electrode Array System.*"

Appendix 5. Written Statements from Co-authors of the Publications

To Whom It May Concern,

I, Erika Suarez-Rodriguez, contributed by conducting the research, interpreting the obtained data and writing up contents reported in the publication entitled **"The Role of Bacteria in Under-deposit Corrosion in Oil and Gas Facilities: A Review of Mechanisms, Test Methods and Corrosion inhibition".**

Signature of Candidate

I, as Co-Author, endorse that this level of contribution by the candidate indicated above is appropriate.

Kateřina Lepková
_____   _____
Full Name of Co-author 1   Signature of Co-author 1
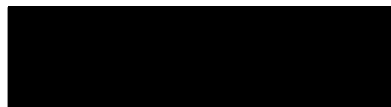
Laura.L. Machuca-Suarez
_____
Full Name of Co-author 2

To Whom It May Concern,

I, Erika Suarez-Rodriguez, contributed by conducting the research, interpreting the obtained data and writing up contents reported in the publication entitled **"CO$_2$ Corrosion Inhibitors Performance at Deposited-Carbon Steel and their Adsorption on Different Deposits".**

_____

Signature of Candidate

I, as Co-Author, endorse that this level of contribution by the candidate indicated above is appropriate.

Kateřina Lepková

_____
Full Name of Co-author 1   Signature of Co-author 1
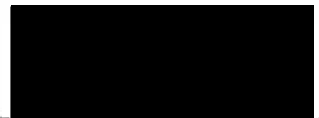
Laura.L. Machuca-Suarez

_____
Full Name of Co-author 2   2
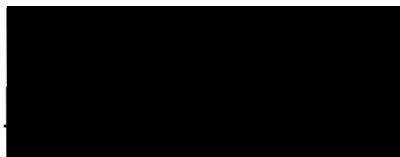
Brian Kinsella

_____
Full Name of Co-author 3   Signature of Co-author 3

To Whom It May Concern,

I, Erika Suarez-Rodriguez, contributed by conducting the research, interpreting the obtained data and writing up contents reported in the publication entitled **"Molecular Characteristics Affecting the Efficiency of Corrosion Inhibitors at Sand-Deposited Carbon Steel: A New Approach Using a Multi-Electrode Array"**.

Signature of Candidate

I, as Co-Author, endorse that this level of contribution by the candidate indicated above is appropriate.

Kateřina Lepková

Full Name of Co-author 1   Signature of Co-author 1

Laura.L. Machuca-Suarez

Full Name of Co-author 2   Signature of Co-author 2

Brian Kinsella

Full Name of Co-author 3   Signature of Co-author 3

Maria Forsyth
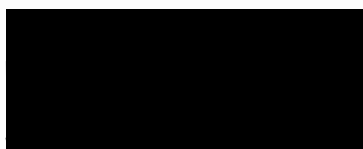
Full Name of Co-author 4   Signature of Co-author 4

To Whom It May Concern,

I, Erika Suarez-Rodriguez, contributed by conducting the research, interpreting the obtained data and writing up contents reported in the publication entitled **"Aggressive Corrosion of Steel by a Thermophilic Microbial Consortium in the Presence and Absence of Sand, International Biodeterioration & Biodegradation".**

█████████████

Signature of Candidate

I, as Co-Author, endorse that this level of contribution by the candidate indicated above is appropriate.

Kateřina Lepková

█████████████

Full Name of Co-author 1
Signature of Co-author 1

Laura.L. Machuca-Suarez

█████████████

Full Name of Co-author 2
Signature of Co-author 2

Brian Kinsella

█████████████

Full Name of Co-author 3
Signature of Co-author 3

To Whom It May Concern,

I, Erika Suarez-Rodriguez, contributed by conducting the research, interpreting the obtained data and writing up contents reported in the publication entitled *"In Situ* **Investigation of Under-Deposit Microbial Corrosion and Its Inhibition Using a Multi-Electrode Array System".**

Signature of Candidate

I, as Co-Author, endorse that this level of contribution by the candidate indicated above is appropriate.

Kateřina Lepková

Full Name of Co-author 1   Signature of Co-author 1

Laura.L. Machuca-Suarez

Full Name of Co-author 2   Signature of Co-author 2

Brian Kinsella

Full Name of Co-author 3   Signature of Co-author 3

Maria Forsyth

Full Name of Co-author 4   Signature of Co-author 4

Mike Yongjun Tan

Full Name of Co-author 5   Signature of Co-author 5

Appendix 6

Copyrights statements
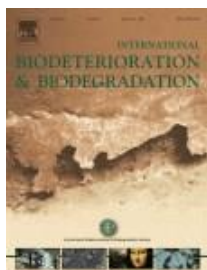
RightsLink

Title: Aggressive corrosion of steel by a thermophilic microbial consortium in the presence and absence of sand

Author: Erika M. Suarez, Katerina Lepkova, Brian Kinsella, Laura L. Machuca

Publication: International Biodeterioration & Biodegradation **Publisher:** Elsevier

Date: February 2019

LOGIN

If you're a copyright.com user, you can login to RightsLink using your copyright.com credentials.

Already **a RightsLink user** or want to learn more?

Please note that, as the author of this Elsevier article, you retain the right to include it in a thesis or dissertation, provided it is not published commercially. Permission is not required, but please ensure that you reference the journal as the original source. For more information on this and on your other retained rights, please visit: https://www.elsevier.com/about/our-business/policies/copyright#Authorrights

BACK   CLOSE WINDOW

From: Erika Suarez Rodriguez <erika.suarezro@postgrad.curtin.edu.au>
Sent: Tuesday, July 23, 2019 9:59 AM
To: Rights and Permissions (ELS) <Permissions@elsevier.com>
Subject: Copyright permission

*** External email: use caution ***

Dear Sir/Madam,

I would like to request copyright permission to use an article journal for my doctoral thesis and to store it in a central repository. Please see the permission letter attached.

Kind regards,

Erika M. Suarez
Ph.D candidate | Curtin Corrosion Centre (CCC)
Faculty of Science and Engineering
Western Australian School of Mines-Minerals, Energy and Chem Eng (WASM-MECE)
Curtin University
Tel | +61 8 9266 0000
Fax | +61 8 9266 7221
Mobile | 0410865471

Email | erika.suarezro@postgrad. curtin.edu.au
Web | http://curtin.edu.au

ELSEVIER

Dear Erika Suarez Rodriguez

We hereby grant you permission to reprint the material below at no charge **in your thesis** subject to the following conditions:

1. If any part of the material to be used (for example, figures) has appeared in our publication with credit or acknowledgement to another source, permission must also be sought from that source. If such permission is not obtained then that material may not be included in your publication/copies.

2. Suitable acknowledgment to the source must be made, either as a footnote or in a reference list at the end of your publication, as follows:

   "This article was published in Publication title, Vol number, Author(s), Title of article, Page Nos, Copyright Elsevier (or appropriate Society name) (Year)."

3. Your thesis may be submitted to your institution in either print or electronic form.

4. Reproduction of this material is confined to the purpose for which permission is hereby given.

5. This permission is granted for non-exclusive world **English** rights only. For other languages please reapply separately for each one required. Permission excludes use in an electronic form other than submission. Should you have a specific electronic project in mind please reapply for permission.

6. Should your thesis be published commercially, please reapply for permission.

Kind regards
Anita

Anita Mercy

Senior Copyrights Coordinator – Global Rights

Elsevier | Health Content Operations
(A division of Reed Elsevier India Pvt. Ltd.)

Ascendas International Tech Park, Crest – 12th Floor|Taramani, Chennai 600113 · India|
Tel: +91 42994696
a.vethakkan@elsevier.com

Permissions Helpdesk no - +1 215 239 3867

Join the Elsevier Connect Community
www.elsevier.com
Twitter | Facebook | LinkedIn | Google+

Copyright Clearance Center

Note: Copyright.com supplies permissions but not the copyrighted content itself.

1	2	3
PAYMENT	REVIEW	CONFIRMATION

Step 3: Order Confirmation

Thank you for your order! A confirmation for your order will be sent to your account email address. If you have questions about your order, you can call us 24 hrs/day, M-F at +1.855.239.3415 Toll Free, or write to us at info@copyright.com. This is not an invoice.

Confirmation Number: 11834150
Order Date: 07/22/2019

If you paid by credit card, your order will be finalized and your card will be charged within 24 hours. If you choose to be invoiced, you can change or cancel your order until the invoice is generated.

Payment Information

Erika Suarez- Rodriguez
erika.suarezro@postgrad.curtin.edu.au
+61 (4)10865471
Payment Method: n/a

Order Details

International biodeterioration & biodegradation

Order detail ID:	71952550	
Order License Id:	4634550312033	
ISSN:	0964-8305	
Publication Type:	Journal	
Volume:		
Issue:		
Start page:		
Publisher:	ELSEVIER LTD.	
Author/Editor:	INTERNATIONAL BIODETERIORATION ASSOCIATION ; BIODETERIORATION SOCIETY	

Permission Status: ✓ Granted

Permission type: Republish or display content
Type of use: Thesis/Dissertation

Requestor type	Academic institution
Format	Electronic
Portion	chapter/article
Number of pages in chapter/article	10
The requesting person/organization	Erika Suarez-Rodriguez
Title or numeric reference of the portion(s)	Aggressive corrosion of steel by a thermophilic microbial consortium in the presence and absence of sand
Title of the article or chapter the portion is from	Aggressive corrosion of steel by a thermophilic microbial consortium in the presence and absence of sand
Editor of portion(s)	N/A
Author of portion(s)	N/A

197

Volume of serial or monograph		137
Page range of portion		137-146
Publication date of portion		February, 2019
Rights for		Main product
Duration of use		Life of current edition
Creation of copies for the disabled		no
With minor editing privileges		no
For distribution to		Worldwide
In the following language(s)		Original language of publication
With incidental promotional use		yes
Lifetime unit quantity of new product		Up to 4,999
Title		Aggressive corrosion of steel by a thermophilic microbial consortium in the presence and absence of sand
Institution name		Curtin University
Expected presentation date		Sep 2019

Note: This item will be invoiced or charged separately through CCC's **RightsLink** service. More info $ 0.00

This is not an invoice.

Total order items: 1   **Order Total: 0.00 USD**

198

Confirmation Number: 11834150

Special Rightsholder Terms & Conditions
The following terms & conditions apply to the specific publication under which they are listed

International biodeterioration & biodegradation
Permission type: Republish or display content
Type of use: Thesis/Dissertation

TERMS AND CONDITIONS

The following terms are individual to this publisher:

None

Other Terms and Conditions:

STANDARD TERMS AND CONDITIONS

1. Description of Service; Defined Terms. This Republication License enables the User to obtain licenses for republication of one or more copyrighted works as described in detail on the relevant Order Confirmation (the "Work(s)"). Copyright Clearance Center, Inc. ("CCC") grants licenses through the Service on behalf of the rightsholder identified on the Order Confirmation (the "Rightsholder"). "Republication", as used herein, generally means the inclusion of a Work, in whole or in part, in a new work or works, also as described on the Order Confirmation. "User", as used herein, means the person or entity making such republication.

2. The terms set forth in the relevant Order Confirmation, and any terms set by the Rightsholder with respect to a particular Work, govern the terms of use of Works in connection with the Service. By using the Service, the person transacting for a republication license on behalf of the User represents and warrants that he/she/it (a) has been duly authorized by the User to accept, and hereby does accept, all such terms and conditions on behalf of User, and (b) shall inform User of all such terms and conditions. In the event such person is a "freelancer" or other third party independent of User and CCC, such party shall be deemed jointly a "User" for purposes of these terms and conditions. In any event, User shall be deemed to have accepted and agreed to all such terms and conditions if User republishes the Work in any fashion.

3. Scope of License; Limitations and Obligations.

3.1 All Works and all rights therein, including copyright rights, remain the sole and exclusive property of the Rightsholder. The license created by the exchange of an Order Confirmation (and/or any invoice) and payment by User of the full amount set forth on that document includes only those rights expressly set forth in the Order Confirmation and in these terms and conditions, and conveys no other rights in the Work(s) to User. All rights not expressly granted are hereby reserved.

3.2 General Payment Terms: You may pay by credit card or through an account with us payable at the end of the month. If you and we agree that you may establish a standing account with CCC, then the following terms apply: Remit Payment to: Copyright Clearance Center, 29118 Network Place, Chicago, IL 60673-1291. Payments Due: Invoices are payable upon their delivery to you (or upon our notice to you that they are available to you for downloading). After 30 days, outstanding amounts will be subject to a service charge of 1-1/2% per month or, if less, the maximum rate allowed by applicable law. Unless otherwise specifically set forth in the Order Confirmation or in a separate written agreement signed by CCC, invoices are due and payable on "net 30" terms. While User may exercise the rights licensed immediately upon issuance of the Order Confirmation, the license is automatically revoked and is null and void, as if it had never been issued, if complete payment for the license is not received on a timely basis either from User directly or through a payment agent, such as a credit card company.

3.3 Unless otherwise provided in the Order Confirmation, any grant of rights to User (i) is "one-time" (including the editions and product family specified in the license), (ii) is non-exclusive and non-transferable and (iii) is subject to any and all limitations and restrictions (such as, but not limited to, limitations on duration of use or circulation) included in the Order Confirmation or invoice and/or in these terms and conditions. Upon completion of the licensed use, User shall either secure a new permission for further use of the Work(s) or immediately cease any new use of the Work(s) and shall render inaccessible (such as by deleting or by removing or severing links or other locators) any further copies of the Work (except for copies printed on paper in accordance with this license and still in User's stock at the end of such period).

3.4 In the event that the material for which a republication license is sought includes third party materials (such as photographs, illustrations, graphs, inserts and similar materials) which are identified in such material as having been used by permission, User is responsible for identifying, and seeking separate licenses (under this Service or otherwise) for, any of such third party materials; without a separate license, such third party materials may not be used.

3.5 Use of proper copyright notice for a Work is required as a condition of any license granted under the Service. Unless otherwise provided in the Order Confirmation, a proper copyright notice will read substantially as follows: "Republished with permission of [Rightsholder's name], from [Work's title, author, volume, edition number and year of copyright]; permission conveyed through Copyright Clearance Center, Inc. " Such notice must be provided in a reasonably legible font size and must be placed either immediately adjacent to the Work as used (for example, as part of a by-line or footnote but not as a separate electronic link) or in the place where substantially all other credits or notices for the new work containing the republished Work are located. Failure to include the required notice results in loss to the Rightsholder and CCC, and the User shall be liable to pay liquidated damages for each such failure equal to twice the use fee specified in the Order Confirmation, in addition to the use fee itself and any other fees and charges specified.

3.6 User may only make alterations to the Work if and as expressly set forth in the Order Confirmation. No Work may be used in any way that is defamatory, violates the rights of third parties (including such third parties' rights of copyright, privacy, publicity, or other tangible or intangible property), or is otherwise illegal, sexually explicit or obscene. In

199

addition, User may not conjoin a Work with any other material that may result in damage to the reputation of the Rightsholder. User agrees to inform CCC if it becomes aware of any infringement of any rights in a Work and to cooperate with any reasonable request of CCC or the Rightsholder in connection therewith.

4. Indemnity. User hereby indemnifies and agrees to defend the Rightsholder and CCC, and their respective employees and directors, against all claims, liability, damages, costs and expenses, including legal fees and expenses, arising out of any use of a Work beyond the scope of the rights granted herein, or any use of a Work which has been altered in any unauthorized way by User, including claims of defamation or infringement of rights of copyright, publicity, privacy or other tangible or intangible property.

5. Limitation of Liability. UNDER NO CIRCUMSTANCES WILL CCC OR THE RIGHTSHOLDER BE LIABLE FOR ANY DIRECT, INDIRECT, CONSEQUENTIAL OR INCIDENTAL DAMAGES (INCLUDING WITHOUT LIMITATION DAMAGES FOR LOSS OF BUSINESS PROFITS OR INFORMATION, OR FOR BUSINESS INTERRUPTION) ARISING OUT OF THE USE OR INABILITY TO USE A WORK, EVEN IF ONE OF THEM HAS BEEN ADVISED OF THE POSSIBILITY OF SUCH DAMAGES. In any event, the total liability of the Rightsholder and CCC (including their respective employees and directors) shall not exceed the total amount actually paid by User for this license. User assumes full liability for the actions and omissions of its principals, employees, agents, affiliates, successors and assigns.

6. Limited Warranties. THE WORK(S) AND RIGHT(S) ARE PROVIDED "AS IS". CCC HAS THE RIGHT TO GRANT TO USER THE RIGHTS GRANTED IN THE ORDER CONFIRMATION DOCUMENT. CCC AND THE RIGHTSHOLDER DISCLAIM ALL OTHER WARRANTIES RELATING TO THE WORK(S) AND RIGHT(S), EITHER EXPRESS OR IMPLIED, INCLUDING WITHOUT LIMITATION IMPLIED WARRANTIES OF MERCHANTABILITY OR FITNESS FOR A PARTICULAR PURPOSE. ADDITIONAL RIGHTS MAY BE REQUIRED TO USE ILLUSTRATIONS, GRAPHS, PHOTOGRAPHS, ABSTRACTS, INSERTS OR OTHER PORTIONS OF THE WORK (AS OPPOSED TO THE ENTIRE WORK) IN A MANNER CONTEMPLATED BY USER; USER UNDERSTANDS AND AGREES THAT NEITHER CCC NOR THE RIGHTSHOLDER MAY HAVE SUCH ADDITIONAL RIGHTS TO GRANT.

7. Effect of Breach. Any failure by User to pay any amount when due, or any use by User of a Work beyond the scope of the license set forth in the Order Confirmation and/or these terms and conditions, shall be a material breach of the license created by the Order Confirmation and these terms and conditions. Any breach not cured within 30 days of written notice thereof shall result in immediate termination of such license without further notice. Any unauthorized (but licensable) use of a Work that is terminated immediately upon notice thereof may be liquidated by payment of the Rightsholder's ordinary license price therefor; any unauthorized (and unlicensable) use that is not terminated immediately for any reason (including, for example, because materials containing the Work cannot reasonably be recalled) will be subject to all remedies available at law or in equity, but in no event to a payment of less than three times the Rightsholder's ordinary license price for the most closely analogous licensable use plus Rightsholder's and/or CCC's costs and expenses incurred in collecting such payment.

8. **Miscellaneous.**

8.1 User acknowledges that CCC may, from time to time, make changes or additions to the Service or to these terms and conditions, and CCC reserves the right to send notice to the User by electronic mail or otherwise for the purposes of notifying User of such changes or additions; provided that any such changes or additions shall not apply to permissions already secured and paid for.

8.2 Use of User-related information collected through the Service is governed by CCC's privacy policy, available online here: http://www.copyright.com/content/cc3/en/tools/footer/privacypolicy.html.

8.3 The licensing transaction described in the Order Confirmation is personal to User. Therefore, User may not assign or transfer to any other person (whether a natural person or an organization of any kind) the license created by the Order Confirmation and these terms and conditions or any rights granted hereunder; provided, however, that User may assign such license in its entirety on written notice to CCC in the event of a transfer of all or substantially all of User's rights in the new material which includes the Work(s) licensed under this Service.

8.4 No amendment or waiver of any terms is binding unless set forth in writing and signed by the parties. The Rightsholder and CCC hereby object to any terms contained in any writing prepared by the User or its principals, employees, agents or affiliates and purporting to govern or otherwise relate to the licensing transaction described in the Order Confirmation, which terms are in any way inconsistent with any terms set forth in the Order Confirmation and/or in these terms and conditions or CCC's standard operating procedures, whether such writing is prepared prior to, simultaneously with or subsequent to the Order Confirmation, and whether such writing appears on a copy of the Order Confirmation or in a separate instrument.

8.5 The licensing transaction described in the Order Confirmation document shall be governed by and construed under the law of the State of New York, USA, without regard to the principles thereof of conflicts of law. Any case, controversy, suit, action, or proceeding arising out of, in connection with, or related to such licensing transaction shall be brought, at CCC's sole discretion, in any federal or state court located in the County of New York, State of New York, USA, or in any federal or state court whose geographical jurisdiction covers the location of the Rightsholder set forth in the Order Confirmation. The parties expressly submit to the personal jurisdiction and venue of each such federal or state court.If you have any comments or questions about the Service or Copyright Clearance Center, please contact us at 978-750-8400 or send an e-mail to info@copyright.com.

v 1.1

Close

200

Confirmation Number: 11834150

Citation Information

Order Detail ID: 71952550

International biodeterioration & biodegradation by INTERNATIONAL BIODETERIORATION ASSOCIATION ; BIODETERIORATION SOCIETY Reproduced with permission of ELSEVIER LTD. in the format Thesis/Dissertation via Copyright Clearance Center.

Close

201

NACE International - Corrosion Society LICENSE
TERMS AND CONDITIONS

Nov 13, 2019

This is a License Agreement between Mrs. Erika Suarez- Rodriguez ("You") and NACE
International - Corrosion Society ("NACE International - Corrosion Society") provided by
Copyright Clearance Center ("CCC"). The license consists of your order details, the terms
and conditions provided by NACE International - Corrosion Society, and the payment terms
and conditions.

**All payments must be made in full to CCC. For payment instructions, please see
information listed at the bottom of this form.**

License Number	4707280111404
License date	Jul 23, 2019
Licensed content publisher	NACE International - Corrosion Society
Licensed content title	Corrosion
Licensed content date	Jan 1, 1945
Type of Use	Thesis/Dissertation
Requestor type	Academic institution
Format	Print, Electronic
Portion	chapter/article
The requesting person/organization is:	Erika Suarez-Rodriguez

202

Title or numeric reference of the portion(s)	CO2 Corrosion Inhibitors Performance at Deposited-Carbon Steel and their Adsorption in Different Deposits
Title of the article or chapter the portion is from	CO2 Corrosion Inhibitors Performance at Deposited-Carbon Steel and their Adsorption in Different Deposits
Editor of portion(s)	N/A
Author of portion(s)	N/A
Volume of serial or monograph.	75
Issue, if republishing an article from a serial	6
Page range of the portion	
Publication date of portion	June, 2019
Rights for	Main product
Duration of use	Life of current edition
Creation of copies for the disabled	no
With minor editing privileges	no
For distribution to	Worldwide
In the following language(s)	Original language of publication
With incidental promotional use	no
The lifetime unit quantity of new product	Up to 4,999
Title	

203

	Aggressive corrosion of steel by a thermophilic microbial consortium in the presence and absence of sand
Institution name	Curtin University
Expected presentation date	Sep 2019
Billing Type	Invoice
Billing Address	Mrs. Erika Suarez- Rodriguez 5 de Laeter Way, Technology Park CCEIC buildling 614, Bentley Perth, Australia 6102 Attn: Mrs. Erika Suarez- Rodriguez
Total (may include CCC user fee)	0.00 USD

Terms and Conditions

TERMS AND CONDITIONS

The following terms are individual to this publisher:

None

Other Terms and Conditions:

STANDARD TERMS AND CONDITIONS

1. Description of Service; Defined Terms. This Republication License enables the User to obtain licenses for republication of one or more copyrighted works as described in detail on the relevant Order Confirmation (the "Work(s)"). Copyright Clearance Center, Inc. ("CCC") grants licenses through the Service on behalf of the rightsholder identified on the Order Confirmation (the "Rightsholder"). "Republication", as used herein, generally means the inclusion of a Work, in whole or in part, in a new work or works, also as described on the Order Confirmation. "User", as used herein, means the person or entity making such republication.

2. The terms set forth in the relevant Order Confirmation, and any terms set by the Rightsholder with respect to a particular Work, govern the terms of use of Works in connection with the Service. By using the Service, the person transacting for a republication license on behalf of the User represents and warrants that he/she/it (a) has been duly authorized by the User to accept, and hereby does accept, all such terms and conditions on behalf of User, and (b) shall inform User of all such terms and conditions. In the event such person is a "freelancer" or other third party independent of User and CCC, such party shall

be deemed jointly a "User" for purposes of these terms and conditions. In any event, User shall be deemed to have accepted and agreed to all such terms and conditions if User republishes the Work in any fashion.

3. Scope of License; Limitations and Obligations.

3.1 All Works and all rights therein, including copyright rights, remain the sole and exclusive property of the Rightsholder. The license created by the exchange of an Order Confirmation (and/or any invoice) and payment by User of the full amount set forth on that document includes only those rights expressly set forth in the Order Confirmation and in these terms and conditions, and conveys no other rights in the Work(s) to User. All rights not expressly granted are hereby reserved.

3.2 General Payment Terms: You may pay by credit card or through an account with us payable at the end of the month. If you and we agree that you may establish a standing account with CCC, then the following terms apply: Remit Payment to: Copyright Clearance Center, 29118 Network Place, Chicago, IL 60673-1291. Payments Due: Invoices are payable upon their delivery to you (or upon our notice to you that they are available to you for downloading). After 30 days, outstanding amounts will be subject to a service charge of 1-1/2% per month or, if less, the maximum rate allowed by applicable law. Unless otherwise specifically set forth in the Order Confirmation or in a separate written agreement signed by CCC, invoices are due and payable on "net 30" terms. While User may exercise the rights licensed immediately upon issuance of the Order Confirmation, the license is automatically revoked and is null and void, as if it had never been issued, if complete payment for the license is not received on a timely basis either from User directly or through a payment agent, such as a credit card company.

3.3 Unless otherwise provided in the Order Confirmation, any grant of rights to User (i) is "one-time" (including the editions and product family specified in the license), (ii) is non-exclusive and non-transferable and (iii) is subject to any and all limitations and restrictions (such as, but not limited to, limitations on duration of use or circulation) included in the Order Confirmation or invoice and/or in these terms and conditions. Upon completion of the licensed use, User shall either secure a new permission for further use of the Work(s) or immediately cease any new use of the Work(s) and shall render inaccessible (such as by deleting or by removing or severing links or other locators) any further copies of the Work (except for copies printed on paper in accordance with this license and still in User's stock at the end of such period).

3.4 In the event that the material for which a republication license is sought includes third party materials (such as photographs, illustrations, graphs, inserts and similar materials) which are identified in such material as having been used by permission, User is responsible for identifying, and seeking separate licenses (under this Service or otherwise) for, any of such third party materials; without a separate license, such third party materials may not be used.

3.5 Use of proper copyright notice for a Work is required as a condition of any license granted under the Service. Unless otherwise provided in the Order Confirmation, a proper copyright notice will read substantially as follows: "Republished with permission of [Rightsholder's name], from [Work's title, author, volume, edition number and year of copyright]; permission conveyed through Copyright Clearance Center, Inc. " Such notice must be provided in a reasonably legible font size and must be placed either immediately adjacent to the Work as used (for example, as part of a by-line or footnote but not as a separate electronic link) or in the place where substantially all other credits or notices for the

new work containing the republished Work are located. Failure to include the required notice results in loss to the Rightsholder and CCC, and the User shall be liable to pay liquidated damages for each such failure equal to twice the use fee specified in the Order Confirmation, in addition to the use fee itself and any other fees and charges specified.

3.6 User may only make alterations to the Work if and as expressly set forth in the Order Confirmation. No Work may be used in any way that is defamatory, violates the rights of third parties (including such third parties' rights of copyright, privacy, publicity, or other tangible or intangible property), or is otherwise illegal, sexually explicit or obscene. In addition, User may not conjoin a Work with any other material that may result in damage to the reputation of the Rightsholder. User agrees to inform CCC if it becomes aware of any infringement of any rights in a Work and to cooperate with any reasonable request of CCC or the Rightsholder in connection therewith.

4. Indemnity. User hereby indemnifies and agrees to defend the Rightsholder and CCC, and their respective employees and directors, against all claims, liability, damages, costs and expenses, including legal fees and expenses, arising out of any use of a Work beyond the scope of the rights granted herein, or any use of a Work which has been altered in any unauthorized way by User, including claims of defamation or infringement of rights of copyright, publicity, privacy or other tangible or intangible property.

5. Limitation of Liability. UNDER NO CIRCUMSTANCES WILL CCC OR THE RIGHTSHOLDER BE LIABLE FOR ANY DIRECT, INDIRECT, CONSEQUENTIAL OR INCIDENTAL DAMAGES (INCLUDING WITHOUT LIMITATION DAMAGES FOR LOSS OF BUSINESS PROFITS OR INFORMATION, OR FOR BUSINESS INTERRUPTION) ARISING OUT OF THE USE OR INABILITY TO USE A WORK, EVEN IF ONE OF THEM HAS BEEN ADVISED OF THE POSSIBILITY OF SUCH DAMAGES. In any event, the total liability of the Rightsholder and CCC (including their respective employees and directors) shall not exceed the total amount actually paid by User for this license. User assumes full liability for the actions and omissions of its principals, employees, agents, affiliates, successors and assigns.

6. Limited Warranties. THE WORK(S) AND RIGHT(S) ARE PROVIDED "AS IS". CCC HAS THE RIGHT TO GRANT TO USER THE RIGHTS GRANTED IN THE ORDER CONFIRMATION DOCUMENT. CCC AND THE RIGHTSHOLDER DISCLAIM ALL OTHER WARRANTIES RELATING TO THE WORK(S) AND RIGHT(S), EITHER EXPRESS OR IMPLIED, INCLUDING WITHOUT LIMITATION IMPLIED WARRANTIES OF MERCHANTABILITY OR FITNESS FOR A PARTICULAR PURPOSE. ADDITIONAL RIGHTS MAY BE REQUIRED TO USE ILLUSTRATIONS, GRAPHS, PHOTOGRAPHS, ABSTRACTS, INSERTS OR OTHER PORTIONS OF THE WORK (AS OPPOSED TO THE ENTIRE WORK) IN A MANNER CONTEMPLATED BY USER; USER UNDERSTANDS AND AGREES THAT NEITHER CCC NOR THE RIGHTSHOLDER MAY HAVE SUCH ADDITIONAL RIGHTS TO GRANT.

7. Effect of Breach. Any failure by User to pay any amount when due, or any use by User of a Work beyond the scope of the license set forth in the Order Confirmation and/or these terms and conditions, shall be a material breach of the license created by the Order Confirmation and these terms and conditions. Any breach not cured within 30 days of written notice thereof shall result in immediate termination of such license without further notice. Any unauthorized (but licensable) use of a Work that is terminated immediately upon notice thereof may be liquidated by payment of the Rightsholder's ordinary license price therefor; any unauthorized (and unlicensable) use that is not terminated immediately for any reason (including, for example, because materials containing the Work cannot reasonably be

206

recalled) will be subject to all remedies available at law or in equity, but in no event to a payment of less than three times the Rightsholder's ordinary license price for the most closely analogous licensable use plus Rightsholder's and/or CCC's costs and expenses incurred in collecting such payment.

8. **Miscellaneous.**

8.1 User acknowledges that CCC may, from time to time, make changes or additions to the Service or to these terms and conditions, and CCC reserves the right to send notice to the User by electronic mail or otherwise for the purposes of notifying User of such changes or additions; provided that any such changes or additions shall not apply to permissions already secured and paid for.

8.2 Use of User-related information collected through the Service is governed by CCC's privacy policy, available online here:
http://www.copyright.com/content/cc3/en/tools/footer/privacypolicy.html.

8.3 The licensing transaction described in the Order Confirmation is personal to User. Therefore, User may not assign or transfer to any other person (whether a natural person or an organization of any kind) the license created by the Order Confirmation and these terms and conditions or any rights granted hereunder; provided, however, that User may assign such license in its entirety on written notice to CCC in the event of a transfer of all or substantially all of User's rights in the new material which includes the Work(s) licensed under this Service.

8.4 No amendment or waiver of any terms is binding unless set forth in writing and signed by the parties. The Rightsholder and CCC hereby object to any terms contained in any writing prepared by the User or its principals, employees, agents or affiliates and purporting to govern or otherwise relate to the licensing transaction described in the Order Confirmation, which terms are in any way inconsistent with any terms set forth in the Order Confirmation and/or in these terms and conditions or CCC's standard operating procedures, whether such writing is prepared prior to, simultaneously with or subsequent to the Order Confirmation, and whether such writing appears on a copy of the Order Confirmation or in a separate instrument.

8.5 The licensing transaction described in the Order Confirmation document shall be governed by and construed under the law of the State of New York, USA, without regard to the principles thereof of conflicts of law. Any case, controversy, suit, action, or proceeding arising out of, in connection with, or related to such licensing transaction shall be brought, at CCC's sole discretion, in any federal or state court located in the County of New York, State of New York, USA, or in any federal or state court whose geographical jurisdiction covers the location of the Rightsholder set forth in the Order Confirmation. The parties expressly submit to the personal jurisdiction and venue of each such federal or state court.If you have any comments or questions about the Service or Copyright Clearance Center, please contact us at 978-750-8400 or send an e-mail to info@copyright.com.

v 1.1

Questions? customercare@copyright.com or +1-855-239-3415 (toll free in the US) or +1-978-646-2777.

207

NACE
INTERNATIONAL
The Worldwide Corrosion Authority

Permission to Reproduce Figures, Photos, and Tables from Copyrighted Works

Date: 23/07/2019

Name: Erika Magali Suarez-Rodriguez   Title: Mrs.

Company ("Publisher"): Curtin University

Address: 5 de Laeter Way, Technology Park, Biulding 614, Bentley 6102, Perth, Western Australia.

Tel: +61 410865471   Fax:

Email: erika.suarezro@postgrad.curtin.edu.au

Material to be Reproduced ("Work"): Please provide a complete description of the material involved. Include the following elements where applicable: publication name, issue date, page number, figure/photo/table number, paper number, conference name, etc.

CO2 Corrosion Inhibitors Performance at Deposited-Carbon Steel and their Adsorption

in Different deposits. CORROSION the Journal of Science and Engineering

Issue date 06/28/2019, ISSN 0010-9312. Volume 75, Issue 6, https://doi.org/10.5006/3223

Reproduction Method ("Publication Media"): Please provide a complete description of how and where the Work will be used. Include the following elements as applicable: publication name, issue, circulation, print run, web site address, conference name, presentation time and place, etc.

PhD Thesis. The thesis will be made available in online form via Curtin University's Institutional

Repository e-space (http://espace.curtin.edu.au).

The material will be provided strictly for educational purposes and on a non-commercial basis

NACE International ("NACE") hereby grants to "Publisher" the right to publish the Work utilizing the Publication Media described above. The publication right granted herein is limited the specific Publication Media described above. To the extent the publication of the Work is to occur by an above-specified date, such as in a particular periodical or at a particular conference, the right granted herein shall automatically terminate upon the date of such occurrence, whether or not the Work is actually published. To the extent the Publication Media is a web site, the publication right is limited to publication at the specific web site URL identified above. Any right granted herein is a limited, non-transferable, non-exclusive right. No other rights in the Work are granted herein.

Publisher shall not edit or modify the Work except to meet the style and graphic requirements of the individual media involved.

The Publisher shall include the following notation with any publication of the Work:*

   A. Conference Paper
   Reproduced with permission from NACE International, Houston, TX. All rights reserved. Author(s), Paper NUMBER presented at CORROSION/YEAR, City, State. © NACE International FIRST YEAR OF PUBLICATION.

   B. Journal Article
   Reproduced with permission from NACE International, Houston, TX. All rights reserved. Author(s) name, Article title, Journal title, Vol. no., Issue no., and publication year. © NACE International FIRST YEAR OF PUBLICATION.

   C. Magazine Article
   Reproduced with permission from NACE International, Houston, TX. All rights reserved. Author(s) name, Article title, Magazine title, Vol. no., Issue no., and publication year. © NACE International FIRST YEAR OF PUBLICATION.

   D. Standards
   STANDARDS/TECHNICAL COMMITTEE REPORT NAME. © NACE International YEAR. All rights reserved by NACE. Reprinted with permission. NACE standards are revised periodically. Users are cautioned to obtain the latest edition; information in an outdated version of the standard may not be accurate.

* Modifications to Notations: Other reference wording can be used, but must be approved by NACE in writing *in advance*.

The Publisher shall include full bibliographic citations of or references to the original NACE source, where applicable.

Publisher shall obtain a copy of the original Work directly from NACE International and shall not utilize copies of the Work from other sources, including the author(s).

To the extent the Work is published on a web site as authorized herein, the Work shall be posted in a file format that does not allow the content of the Work to be easily copied from the Web Site or changed.

As between NACE and Publisher, Publisher acknowledges that NACE owns all rights in the Works.

Publisher shall not be entitled to any compensation for its efforts in promoting the Work.

THE WORK IS PROVIDED "AS IS." ALL EXPRESS OR IMPLIED COVENANTS, CONDITIONS, REPRESENTATIONS OR WARRANTIES, INCLUDING ANY IMPLIED WARRANTY OF MERCHANTABILITY OR FITNESS FOR A PARTICULAR PURPOSE OR CONDITIONS OF ACCURACY, COMPLETENESS OR QUALITY AND THOSE ARISING BY STATUTE OR OTHERWISE IN LAW, ARE HEREBY DISCLAIMED.

IN NO EVENT WILL NACE BE LIABLE FOR ANY DIRECT, INDIRECT, PUNITIVE, SPECIAL, INCIDENTAL OR CONSEQUENTIAL DAMAGES IN CONNECTION WITH OR RELATED TO THIS AGREEMENT (INCLUDING LOSS OF PROFITS, USE, DATA, OR OTHER ECONOMIC ADVANTAGE), HOWSOEVER ARISING.

This Agreement and the rights granted herein may be terminated immediately by NACE upon breach of this Agreement by Publisher. Unless earlier terminated, this Agreement and the rights granted herein will automatically terminate 6 months from the Date set forth above. If the Work has not been published within that time period, a new Agreement must be obtained.

Publisher may not, directly or indirectly, sell, assign, sublicense, lease, rent, distribute, or otherwise transfer this Agreement or any rights granted herein, without the prior written consent of NACE.

If any provision of this Agreement is found to be unenforceable, then this Agreement shall be deemed to be amended by modifying such provision to the extent necessary to make it legal and enforceable while preserving its intent. The remainder of this Agreement shall not be affected by such modification.

This Agreement does not create, and shall not be construed to create, any employer-employee, joint venture or partnership relationship between the parties. No officer, employee, agent, servant or independent contractor of either party shall at any time be deemed to be an employee, servant, agent or contractor of any other party for any purpose whatsoever.

This Agreement shall be governed by, and construed and enforced in accordance with, the laws of the State of Texas, without regard to the choice of law provisions of that State.

This Agreement shall only be effective if signed by authorized representatives of both parties. This Agreement constitutes the entire Agreement between the parties with respect to the subject matter of this Agreement. Any change, modification or waiver hereto must be in writing and signed by authorized representatives of both parties.

Other Terms & Conditions: _____

_____

Publisher hereby requests permission to publish the Work described above and agrees to comply with all Terms and Conditions listed above.

Request submitted by:
Erika M. Suarez-Rodriguez
Printed Name
Erika Suarez Rodriguez
Title
Mrs.

Date
23/07/2019

Request agreed to by:
Erika Suarez-Rodriguez
Lead Author Printed Name
Erika Suarez-Rodriguez
Lead Author Title
Erika Suarez-Rodriguez

Date
23/07/2019

Request approved by NACE:

Printed Name
Lauren Reyes
Title
Publications Copyright Specialist
Signature
Lauren Reyes
Date
September 5, 2019

209

23/07/2019

Australasian Corrosion Association INC.

Dear **Australasian Corrosion Association**

It is my understanding that you/your organisation are the copyright holder for the following material:

Journal article (The role of bacteria in under-deposit corrosion in oil and gas facilities: A review of mechanisms, test methods and corrosion inhibition, published in Corrosion & Materials journal, ISSN 1326-1932, volume 44, February, 2019)

I would like to reproduce an extract of this work in a doctoral thesis which I am currently undertaking at Curtin University in Perth, Western Australia. The subject of my research is **corrosion inhibition of deposited-carbon steels in the presence of microorganisms**. I am carrying out this research in my own right and have no association with any commercial organisation or sponsor.

The specific material that I would like to use for the purposes of the thesis is **the full article**

Once completed, the thesis will be made available in online form via Curtin University's Institutional Repository e-space (http://espace.curtin.edu.au). The material will be provided strictly for educational purposes and on a non-commercial basis.

I would be most grateful for your consent to the copying and communication of the work as proposed. If you are willing to grant this consent, please complete and sign the attached approval slip and return it to me at the address shown. Full acknowledgement of the ownership of the copyright and the source of the material will be provided with the material.

If you are not the copyright owner of the material in question, I would be grateful for any information you can provide as to who is likely to hold the copyright.

I look forward to hearing from you and thank you in advance for your consideration of my request.

Yours sincerely

Erika Suarez-Rodriguez
Ph.D. candidate | Curtin Corrosion Centre (CCC)
Faculty of Science and Engineering
Western Australian School of Mines-Minerals, Energy and Chem Eng. (WASM-MECE)
Curtin University

PERMISSION TO USE COPYRIGHT MATERIAL AS SPECIFIED BELOW:

[Specify material and source, as per cover letter]

I hereby give permission for **[The role of bacteria in under-deposit corrosion in oil and gas facilities: A review of mechanisms, test methods and corrosion inhibition]** to include the abovementioned material in her higher degree thesis for Curtin University, and to communicate this material via the e-space institutional repository. This permission is granted on a non-exclusive basis and for an indefinite period.
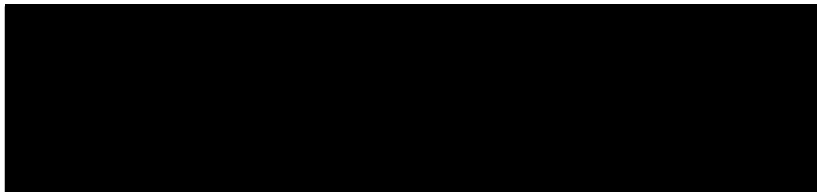
I confirm that I am the copyright owner of the specified material.

Signed:

Name:

Position: Marketing Manager

Date: 22/7/19

Please return signed form to **[Erika Suarez, email: erika.suarezro@postgrad.curtin.edu.au]**

211